MYOCARDIAL PROTECTION AND THERAPEUTIC ANGIOGENESIS USING PEPTIDE AND EMBRYONIC STEM CELL TRANSPLANTATION

RUFAIHAH BINTE ABDUL JALIL
(B. Appl. Sci. (Hons), NUS)

A THESIS SUBMITTED

FOR THE DEGREE OF DOCTOR OF PHILOSOPHY

DEPARTMENT OF SURGERY

NATIONAL UNIVERSITY OF SINGAPORE

2006

ACKNOWLEDGEMENT

I wish to express my sincere gratitude and appreciation to my supervisors, **Associate Professor Eugene Sim Kwang Wei**, MBBS FRCS, Department of Surgery, Yong Loo Lin School of Medicine, National University of Singapore (NUS), **Dr Cao Tong**, PhD, Faculty of Dentistry, NUS and **Dr Khawaja Husnain Haider**, BSc MPharm PhD, Research Scientist, Laboratory of Pathology and Medicine, University of Cincinnati, Ohio, USA for their invaluable guidance, advice and constant support throughout the course of my study.

My special thanks go to **Associate Professor Ge Ruowen**, Department of Biological Sciences, NUS for providing the adenoviral vector carrying angiogenic growth factor and **Associate Professor Sim Meng Kwoon** for providing his patented peptide, des-aspartate-angiotensin-I for my research work; **Dr Tan Rusan, Dr Ding Zee Pin** and **Ms Lili Beth Ramos** from National Heart Centre, Singapore for their assistance in rat heart echocardiography.

I am mostly grateful to **Dr Ye Lei**, National University Medical Institutes and **Dr Alexis Heng Boon Chin,** Faculty of Dentistry, NUS for their generous assistance in reviewing my dissertation and their helpful advice, constant patience and support throughout the development of the research.

I am thankful to the staff members of Animal Holding Unit, NUS, **Dr Leslie Ratnam, Dr Lu Juntang, Mr Shawn Tay, Mr Jeremy Loo** and **Mr James Low** for their help in assisting with the preparation of animal studies and maintenance of the animals.

I will be failing in my duty if I do not acknowledge my lab members from Surgery Laboratory; **Dr Jiang Shujia, Dr Guo Chang Fa, Miss Niagara Muhd Idris, Miss Wahidah Esa, Mr Toh Wee Chi** and from Stem Cell Laboratory, **Dr Liu Hua, Dr Tian Xianfeng, Dr Vinoth J Kumar** and **Mr Toh Wei Seong** for their invaluable help and strong support throughout my work in the laboratories.

I would like to thank **National University of Singapore** for supporting me with a research scholarship and **National Medical Research Council** for providing grant to conduct this research. My sincere thanks also goes out to **Muslimin Trust Fund Association (MTFA)** and **Islamic Religious Council of Singapore (MUIS)** for all the bursary awards and travel grants that they provided me during the course of my study.

Last but not least my utmost and sincere appreciation and gratitude to **Allah (SWT)** for his Benevolence, my beloved parents, **Mr Abdul Jalil Marzuki and Madam Faridah Osman**, my beloved sister**, Miss Raudhah Abdul Jalil**, my best friend, **Nurul Huda Hassan** and lastly my wonderful fiancé **Mr Muhd Isa Mitzcavitch** for their unfailing support, encouragement and love that kept me going at the most difficult and testing periods of my study.

TABLE OF CONTENT

SUMMARY

Ischemic coronary heart disease is one of the leading causes of morbidity and mortality in many countries worldwide. The main contributor to the development of this condition is myocardial infarction where the blood vessels are narrowed or blocked due to atherosclerosis. Over time, deficient oxygenation and nutrient supply to the heart muscle occurs leading to massive damage and death of the cardiomyocytes. This permanent deficit in the number of functioning cardiomyocytes results in an increase in loading conditions that induces a unique pattern of left ventricular remodeling, which is a major contributor to the progression of heart failure.

This study has chosen to focus on preservation of cardiomyocytes and maintenance of ventricle integrity via the influence of a novel peptide on expression of pro-inflammatory cytokines, as well as on the transplantation of human embryonic stem cell-derived $CD133^+$ cells for enhanced neovascularization in the ischemic myocardium. Both studies showed positive effects in controlling the size of the myocardial infarct and improving cardiac function.

The first part of the study demonstrated that des-aspartate-angiotensin-I therapy downregulated critical pro-inflammatory cytokines and growth factors implicated in the pathophysiology of heart failure. The gene expression levels of IL-6, TNF-α, TGF-β and GM-CSF in des-aspartate-angiotensin-I-treated animals were significantly reduced after 3 days of treatment as compared to saline-treated animals. Reduced infiltration of immune cells into the infarct area during the acute phase of infarction was also observed in des-aspartate-angiotensin-I-treated animals. These results were significant since these immune cells together with pro-inflammatory cytokines initiate necrotic and apoptotic

death of the cardiomyocytes during the inflammatory process upon infarction. The cardioprotective effect exerted by des-aspartate-angiotensin-I during the acute phase of myocardial infarction is crucial since it reduces the extent of cardiac muscle damage leading to better morphology and enhanced function of the infarcted myocardium.

The second part of this study assessed the efficacy of transplanting human embryonic stem cell derived $CD133^+$ endothelial progenitor cells in treating ischemic heart disease. $CD133^+$ endothelial progenitor cells were differentiated from human embryonic stem cells by transduction with adenoviral expressing human vascular endothelial growth factor-165. The results demonstrated that ad-$hVEGF_{165}$ was capable of efficient delivery and stable expression of VEGF into differentiating human embryonic stem cells. This was accompanied by enhanced endothelial-lineage differentiation as confirmed by increased numbers of both progenitor and mature endothelial-positive cells detected through immunofluorescent staining and real time PCR. Gene expression of mature endothelial markers such as CD31, Ve-cadherin and von-Willebrand factor together with endothelial progenitor markers such as Flk-1 and CD133 were also significantly upregulated as observed in RT-PCR studies.

Transplantation of purified human embryonic stem cell derived $CD133^+$ cells into the infarcted myocardium led to significant increase in the number of functional blood vessels. This stable collateral enhancement improved the microvascular network which led to enhanced myocardial perfusion and hence provision of oxygen and nutrients to the starved cardiomyocytes. The results demonstrated that $CD133^+$ endothelial progenitor cells derived from ad-$VEGF_{165}$ transduced differentiating human embryonic stem cells were effective and safe for heart regeneration in a rat model of myocardial infarction.

LIST OF TABLES

LIST OF FIGURES

ABBREVIATIONS

ACE	Angiotensin converting enzyme
ad-hVEGF$_{165}$	Adenoviral expressing human vascular endothelial growth factor-165
ad-Null	Null adenoviral vector
Ang-1	Angiopoietin-1
bFGF	Basic fibroblast growth factor
CABG	Coronary artery bypass graft
cDNA	Complementary deoxyribonucleic acid
CT-1	Cardiotrophin-1
DAA-I	Des-aspartate-angiotensin-I
DAPI	4',6-Diamidino-2-phenylindole
EB	Embryoid body
EC	Endothelial cell
ELISA	Enzyme Linked Immunoabsorbent Sandwich Assay
EPC	Endothelial progenitor cell
ESC	Embryonic stem cell
FBS	Fetal bovine serum
FGF	Fibroblast growth factor
Flt-1	Fms-related tyrosine kinase
Flk-1	Fetal liver kinase-1
GAPDH	Glyceraldehyde-3-phosphate dehydrogenase
GM-CSF	Granulocyte-macrophage colony stimulating factor
gp130	Glycoprotein 130

HEK	Human embryonic kidney
HESC	Human embryonic stem cell
HIF-1	Hypoxia-inducible factor-1
HUVEC	Human umbilical vein endothelial cells
IL-1α	Interleukin-1α
IL-1β	Interleukin-1β
IL-6	Interleukin-6
IL-11	Interleukin-11
LAD	Left anterior descending
LIF	Leukemia inhibitory factor
LVEF	Left ventricular ejection fraction
MAP	Mitogen-activated protein
MEF	Mouse embryonic fibroblasts
MI	Myocardial infarction
MMP	Matrix metalloproteinase
MPCR	Multiplex polymerase chain reaction
MRI	Magnetic resonance imaging
mRNA	Messenger ribonucleic acid
PBS	Phosphate-buffered saline
PDGF-B	Platelet derived growth factor-B
pfu	Plaque-forming units
RNA	Ribonucleic acid
RTK	Receptor tyrosine kinases

RT-PCR	Reverse transcription polymerase chain reaction
SPECT	Single photo emission computed tomography
TGF-β	Transforming growth factor-β
TNF-α	Tumour necrosis factor-α
TTC	Triphenyl tetrazolium chloride
VEGF	Vascular endothelial growth factor

PUBLICATIONS, PRESENTATIONS AND AWARDS

Research Publications

Rufaihah AJ, Khawaja Husnain Haider, Heng Boon Chin, Toh Wei Seong, Tian Xianfeng, Ge Ruowen, CaoTong, Eugene Sim Kwang Wei.
Directing endothelial differentiation of human embryonic stem cells via transduction with an adenoviral vector expressing $VEGF_{165}$ gene (in press; *Journal of Gene Medicine*)

Rufaihah AJ, Haider Kh Husnain, Sim MK, Ding ZP, LiLi RB, Jiang S, Lei Y, Sim EKW. Cardiopotective effect of Des-aspartate angiotensin-I (DAA-I) on cytokine gene expression profile in ligation model of myocardial infarction. *Life Sci*. 2006; 78:1341-1351

Heng BC, Ye CP, Liu H, Toh WS, **Rufaihah AJ**, Yang Z, Bay BH, Ge Z, Ouyang HW, Lee EH, Cao T. Loss of viability during freeze-thaw of intact and adherent human embryonic stem cells with conventional slow-cooling protocols is predominantly due to apoptosis rather than cellular necrosis. *J Biomed Sci* 2005; 23: 1-13

Toh WS, Liu H, Heng BC, **Rufaihah AJ**, Ye CP, Cao T
Combined effects of TGF-β1 and BMP-2 in serum free chondrogenic differentiation of mesenchymal stem cells induced hyaline-like cartilage formation. *Growth Factors* 2005; 23(4): 313-321

Boon Chin Heng, Tong Cao, Hua Liu, **Rufaihah Abdul Jalil**
Reduced mitotic activity at the periphery of human embryonic stem cell colonies cultured in vitro with mitotically inactivated murine embryonic fibroblast feeder cells. *Cell Biochem Func* 2004; 22: 1-6

Boon Chin Heng, Tong Cao, Husnain Khawaja Haider, **Rufaihah Abdul Jalil**, Eugene Kwang Wei Sim
Utilizing stem cells for myocardial repair- to differentiate or not to differentiate prior to transplantation. *Scand Cardiovasc J* 2003; 39: 0-00 (editorial)

Shujia J, Khawaja Husnain Haider, Lei Y, Niagara MI, **Rufaihah AJ**, Sim EKW. Allogenic stem cells transplantation in rabbit myocardial infarction. *Ann Acad Med Singapore* 2003; 32(5): S60-2

Lei Y, Husnain Kh Haider, Shujia J, His LL, Niagara MI, **Rufaihah AJ**, Law PK, Sim EKW. Angiogenesis using human myoblast carrying human $VEGF_{165}$ for injured heart. *Ann Acad Med Singapore* 2003; 32(5): S21-23

Published Abstracts

Rufaihah AJ, Husnain Kh Haider, Sim MK, Ding ZP, Shujia J, Lei Y, Sim KWE. Cardioprotective effect of Des-aspartate-angiotensin-I (DAA-I) therapy on cytokine gene expression profile in myocardial infarction. *Ann Acad Med Singapore* 2004; 33(5): S162

Rufaihah AJ, Husnain Kh Haider, Shujia J, Ding ZP, Sim MK, Lei Y, Niagara MI, Sim KWE. Effect of Des-aspartate-angiotensin-I (DAA-I) therapy on the cytokine gene expression profile in a rodent model of myocardial infarction. *J Heart and Lung Transplant*. 2004: 23 (2S): S101

Lei Y, Husnain Kh Haider, Ge R, Law PK, Niagara MI, **Rufaihah AJ**, Aziz S, Sim EKW. In vitro functional assessment of human skeletal myoblast after transduction with adenoviral bicistronic vector carrying human $VEGF_{165}$ and Ang-1. *J Heart and Lung Transplant*. 2004; 23 (2S): S102

Lei Y, Husnain Kh Haider, Shujia J, Niagara MI, **Rufaihah AJ**, Law PK, Sim EKW. Angiomyogenesis in a rodent heart using myoblasts carrying $VEGF_{165}$. *Int J Medical Implants & Devices* 2003, 1: 100-155

Conference Presentations

Oral Presentations

World Congress of Cardiology organized by European Society of Cardiology, Barcelona, Spain 2nd-6th September 2006

Singapore Cardiac Society Annual Meeting, Singapore, 25th -26th March 2006

First Conference on Cardiovascular Clinical Trials and Pharmacotherapy incorporating the 2nd WHF Global Conference on Cardiovascular Clinical Trials and 13th International Society of Cardiovascular Pharmacotherapy Congress, Hong Kong, 1st-3rd October 2004

16th Biennial Congress of Association of Thoracic and Cardiovascular Surgeons of Asia, Bangkok, Thailand, 16th-19th November 2003

5th Combined Annual Scientific Meeting (CASM) incorporating the 4th Graduate Student Society- Faculty of Medicine, Singapore, 12th -14th May 2004

Poster Presentations

International Society for Stem Cell Research 4th Annual Meeting, Toronto, Canada, 29th - 1st July 2006

International Symposium on Germ Cells, Epigenetics, Reprogramming and Embryonic Stem Cells, Kyoto University, Kyoto, Japan, 15th-18th November 2005

Combined Scientific Meeting (CSM) 2005 organized by SingHealth, National Healthcare Group and National University of Singapore, Singapore, 4th-6th November 2005

International Society for Stem Cell Research 3rd Annual Meeting, San Francisco, California, USA, 23rd- 25th June 2005

National Healthcare Group Annual Scientific Congress 2004, Singapore, 9th-10th October 2004

The International Society for Heart and Lung Transplantation 24th Annual Meeting and Scientific Sessions, San Francisco, California, USA, April 21st -24th 2004

Cardiovascular Cell & Gene Therapy Conference II, Boston, Massachusetts, USA, 13th-16th April 2004,

Singapore Cardiac Society Annual Meeting, Singapore, 21st March 2004

7th NUS-NUH Annual Scientific meeting in conjunction with Institute of Molecular & Cell Biology & John Hopkins Singapore, 2nd-3rd October 2003

16th Meeting European Association for Cardiothoracic Surgery (EACTS) Monte Carlo, September 2002

6th NUS-NUH Annual Scientific meeting in conjuction with Institute of Molecular & Cell Biology & John Hopkins Singapore, 16th & 17th August 2002

Attended

The Second International Conference on Cell Therapy for Cardiovascular Diseases organized by Cell Therapy Foundation. New York Academy of Science, New York, USA, 19th -21st January 2006

International Stem Cell Conference, Singapore, 28th-30th October 2003

Awards

Muslimin Trust Fund Association Bursary Award	August 2005
MUIS Postgraduate Research Travel Financial Grant	July 2005
NUS Research Scholarship	July 2002 – July 2006
Muslimin Trust Fund Association Bursary Award	December 2004
Muslimin Trust Fund Association Bursary Award	August 2002

CHAPTER 1

GENERAL INTRODUCTION AND LITERATURE REVIEW

TABLE OF CONTENT

1.1 Ischemic coronary heart disease

1.1.1 Prevalence

Cardiovascular disease is the leading cause of morbidity and mortality in many countries world wide. It is estimated that this will constitute the largest healthcare burden globally by the year 2015 (www.who.int/whr/en, WHO report). Cardiovascular diseases accounted for 30% of global deaths and 10% of the total number of main causes of global burden of disease in 2005 (www.who.int/whr/en,WHO report). Ischemic coronary heart disease is one of the most frequent cardiovascular diseases that cause death globally. It is caused by narrowing of the blood vessels in the heart (atherosclerosis) which over time results in gradual loss of heart muscle leading to ineffective pumping of the heart. Although it was known for centuries to be very common in high income countries, the epidemics have now spread worldwide.

In the United States of America, it was reported that coronary heart disease is the single largest killer of American males and females, accounting for 53% of deaths from cardiovascular diseases in 2003 (www.americanheart.org). It caused one out of every five deaths in United States and myocardial infarction (MI) as an underlying or contributing cause of death constitutes 46.1% of the total deaths related to coronary heart disease. In Singapore, ischemic heart disease is the second major cause of death, accounting for 18.8% of the total number of deaths and was the third highest cause of hospitalization (3.8%) in 2004 (www.moh.gov.sg).

1.1.2 Development and progression of heart failure upon coronary ischemic insult

Ischemic coronary heart disease is a condition that affects the supply of blood to the heart. The main contributor to the development of this condition is MI where the

blood vessels are narrowed or blocked due to the deposition of cholesterol plaques on their wall; a process known as atherosclerosis. Over time, deficient oxygenation and nutrient supply to the heart muscle occurs and this will then lead to massive damage and death of the cardiomyocytes. This permanent deficit in the number of functioning cardiomyocytes is a key factor in the development and progression of heart failure.

The resultant loss of cardiomyocytes results in an abrupt increase in loading conditions of the heart that induces a unique change in structure and function of the left ventricular myocardium that involves the infarcted border zone and the remote non-infarcted zone of the myocardium. This process is known as left ventricular remodeling (Cohn 1995; Pfeffer et al, 1990).

Left ventricular remodeling is a normal feature during maturation and may be a useful adaptation to increased demand such as during athletic training in the adult. However when it occurs in response to pathologic stimuli, it is usually adaptive in the short term but maladaptive in the long term and often results in further myocardial dysfunction.

Post infarction left ventricular remodeling is divided into an early and late phase. The early phase of remodeling involves the expansion of the infarct while the late phase of remodeling involves the left ventricle globally and is associated with dilatation and distortion of ventricle shape.

The death of cardiomyocytes and resultant increase in load following an ischemic insult usually triggers a cascade of biochemical intracellular signaling processes that initiates and subsequently modulates reparative genetic, molecular and cellular changes leading to ventricular remodeling. Important mediators that are involved in remodeling

include wall stress, neurohormonal activation, renin-angiotensin system, inflammatory cytokines and oxidative stress. These mediators often act in concert and are linked to one another. The effects of these mediators result in to pathological consequences such as cardiomyocyte hypertrophy, apoptosis and necrosis, ventricular dilatation, fibrosis formation and collagen degradation. These changes over time lead to abnormalities in myocardial contractility and relaxation, to declined heart pumping capacity, and to dilatation and increased sphericity of the heart; progressive alterations which finally result in systolic and diastolic heart dysfunction: the basis of heart failure and death.

1.2 Overview on the pathophysiology of left ventricular remodeling

Left ventricular remodeling is a central feature in the progression of heart failure. This process involves a variety of cellular and molecular events that eventually lead to significant changes in heart structure and function (Figure 1).

1.2.1 Cellular events involved in left ventricular remodeling

1.2.1.1 Cardiomyocyte hypertrophy

Increased wall stress is a powerful stimulus for cardiomyocyte hypertrophy, an adaptive response to offset increased load, attenuate progressive dilatation and stabilize contractile function. Cardiomyocyte hypertrophy is initiated by neurohormonal activation, activation of myocardial renin-angiotensin system (RAS) and myocardial stretch.

1.2.1.2 Cardiomyocyte necrosis and apoptosis

Progressive left ventricular dysfunction occurs in part as a result of continuing loss of viable cardiomyocytes via two death mechanisms; necrosis and apoptosis. Following abrupt coronary occlusion, ischemic necrosis takes place which is

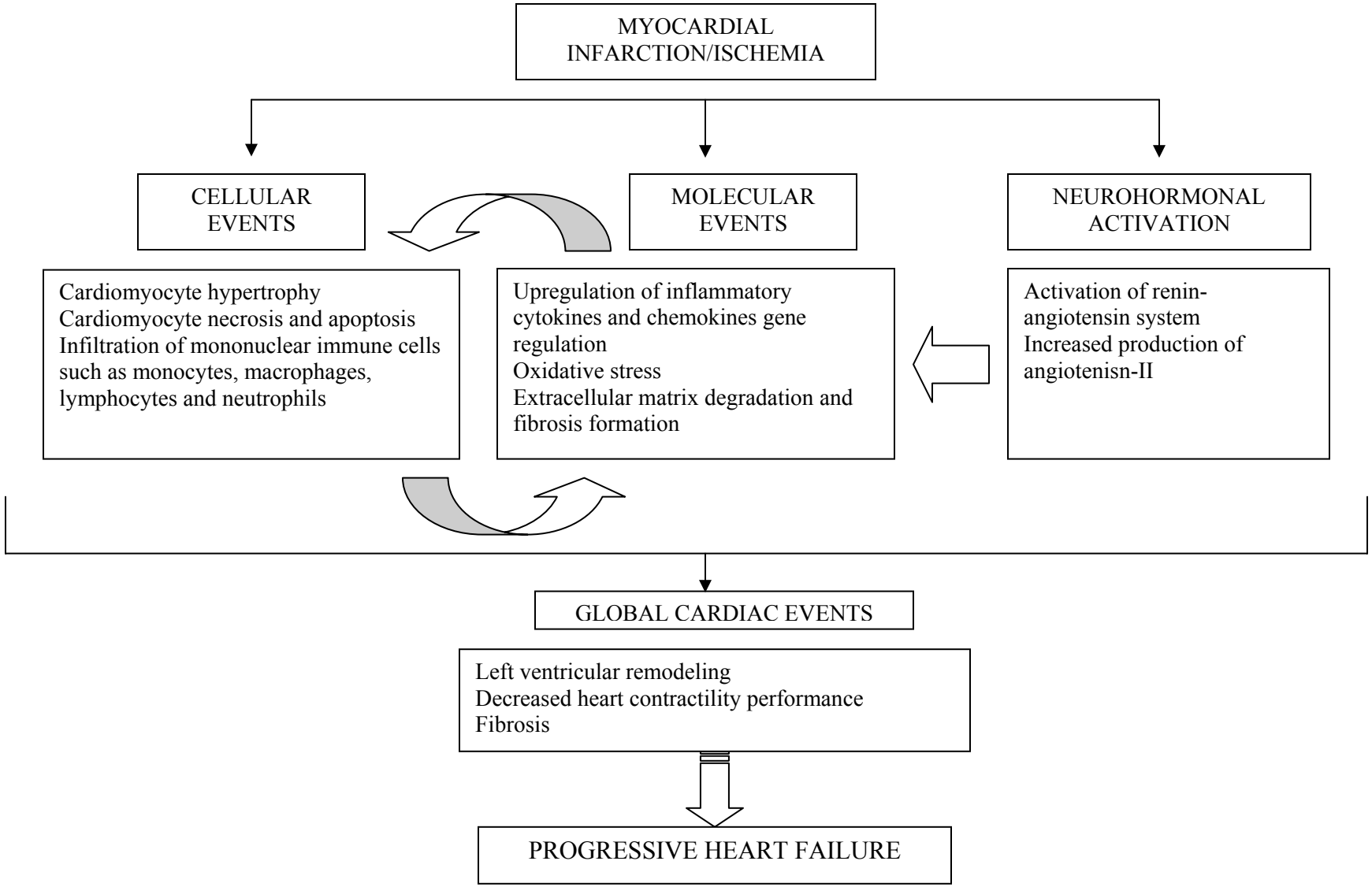

Figure 1: **Pathophysiology of heart failure.** Myocardial infarction triggers a cascade of cellular and molecular events, including neurohormanal system which lead to ventricular remodeling. The vicious cycle of all these events are believed to cause progressive worsening of the heart failure syndrome over time.

characterized by rapid loss of cellular homeostasis, rapid swelling as a result of accumulation of water and electrolytes that result in early plasma membrane rupture and disruption of cellular organelles (Krijnen et al, 2002; Majno et al, 1995). These in turn induce an inflammatory response involving inflammatory cells such as neutrophils, macrophages that infiltrate into the ischemic site (Fishbein et al, 1978). While necrosis is associated with abrupt onset, apoptosis which is also known as programmed cell death cause silent but persistent death of the cardiomyocytes.

Apoptosis is an active, precisely regulated series of energy dependent molecular and biochemical events that appears to be orchestrated by a genetic program. Cardiomyocytes undergoing apoptosis is characterized by shrinkage of the cell and the nucleus. The nuclear chromatin then condenses and eventually breaks up and the cell dissociates itself from the tissue and forms apoptotic bodies containing condensed cellular organelles and nuclear fragments. These apoptotic bodies are either phagocytosed by neighbouring cells or undergo degradation (Krijnen et al, 2002; Saraste et al, 2000; Majno et al, 1995). Apoptosis however does not provoke inflammatory response unlike necrosis.

Ongoing loss of cardiomyocytes leads to thinning of the left ventricular wall and over time results in alteration in left ventricular chamber geometry through increased sphericity and dilatation of the left ventricular wall and progressive loss of contractile function- all of which leads to left ventricular dysfunction which is the hallmark of a failing heart.

1.2.2 Molecular events involved in left ventricular remodeling

1.2.2.1 Myocardial stretch

Small mechanical strains induced by elevated wall stresses lead to small mechanical stretches in cardiomyocytes. These mechanical stretches results in the secretion of angiotensin II from cytoplasmic granules and the stretch-induced hypertrophic response is mediated by G-protein-coupled receptor known as the AT1 receptors (Yamazaki et al, 1995; Sadoshima et al, 1993). Activation of AT1 receptors in turn activates multiple downstream signaling pathways such as the calcium dependent activation of tyrosine kinase and activation of protein kinase C (PKC) via inositide signaling (phospholipase Cβ), mitogen-activated protein (MAP) kinase and S6 kinase (Ju et al, 1998) as well as induction of early gene response such as jun, fos and myc and fetal gene program such as β-MyHC and ANP. Activation of phospholipase Cβ via Gαq protein leads to production of 1,2 diacylglycerol and activation of PKC (Ju et al, 1998). PKC further induces secretion of angiotensin II and by paracrine and autocrine action, secreted angiotensin II amplifies the signals evoked by mechanical stress. Growth factors such as epidermal growth factor, insulin-like growth factor and fibroblast growth factor activate receptor tyrosine kinase, p21 ras and MAP kinase. It has been reported that activation of MAP kinase is a prerequisite for transcriptional and morphological changes of cardiomyocyte hypertrophy (Glennon et al, 1996)

1.2.2.2 Neurohormonal activation

The sympathetic nervous system activation in the heart increases tremendously upon infarction (Esler et al, 1988). Enhanced expression of the primary sympathetic neurotransmitter, norepinephrine contributes directly and indirectly to the hypertrophic

response of the cardiomyocytes via α-1 and β-1 receptors respectively. Direct stimulation of α-1 adrenergic receptors by norepinephrine leads to hypertrophy via the Gαq-dependent signaling pathway (Ju et al, 1998). Gαq expression has been shown to increase in viable, border and scar area of the myocardium after a myocardial infarct (Ju et al, 1998). Gαq-dependent signaling pathway is known to be a main contributor to pathological conditions following myocardial infarction. β-1 adrenergic receptors are activated in the juxtaglomerular apparatus and they induce release of renin which enhances production of angiotensin II. Increased production of angiotensin II promotes presynaptic release of norepinephrine and blocks its reuptake, increasing catecholamine synthesis and potentiating the postsynaptic action of norepinephrine (Ball 1989).

1.2.2.3 Renin-angiotensin system

The renin-angiotensin system contributes to cardiomyoycte hypertrophy by upregulation of angiotensin-converting enzyme activity which leads to increased production of angiotensin II and subsequent stimulation of the angiotensin II type I receptor which follows a similar pathway as α-1 adrenergic activation in cardiomyocytes via Gαq stimulation (Hirsch et al, 1991; Meggs et al, 1993). Angiotensin II also increases DNA and protein synthesis in both cardiomyocytes and fibroblast and hence is a major player in hypertrophy and fibrosis (Sadoshima et al, 1993).

Norepinephrine and angiotensin II may also augment release of endothelins. Endothelins are potent vasoconstrictor peptides acting through coupling to their receptors. Activation of endothelin A leads to cardiomyocytes hypertrophy which is also mediated by Gαq stimulation.

1.2.2.4 Inflammatory cytokines

Over the last decade, there is growing evidence that cytokine-mediated immunologic responses play an important role in the pathophysiology of heart failure (Frangogiannis et al 2002; Parissis et al, 2002; Blum et al, 2001; Blum et al, 1998; Frangogiannis et al, 1998; Pulkki et al, 1997). Cytokines mediate cell-to-cell interactions via specific cell-surface receptors and regulate activation, differentiation, growth, death and acquisition of effector function of various cell types.

Cytokines affect the cardiovascular system in many ways including cardiomyocyte and endothelial apoptosis, promotion of inflammation, intravascular coagulation, cardiac structural and functional abnormalities, endothelial injury and oxidative stress (Parissis et al, 2002). Cytokines are not only secreted by immune cells but also by structural cells of the cardiovascular system. The activation of inflammatory cytokine cascade is triggered by initial myocardial injury, mechanical overloading or abnormal left ventricular end-diastolic wall stress which will then result in abnormal cardiac contractile performance and promotes maladaptive left ventricular remodeling. Two of the most well studied inflammatory cytokines in heart failure are interleukin-6 (IL-6) and tumour necrosis factor-α (TNF-α).

IL-6

IL-6 is a multifunctional cytokine produced by activated T-cells, mononuclear phagocytes, fibroblasts and vascular endothelial cells. IL-6 is a member of a larger family of structurally-related cytokines which have overlapping biological effects. The other IL-6 related cytokines include cardiotrophin-1 (CT-1), leukemia inhibitory factor (LIF) and IL-11. These IL-6 related cytokines signal through multisubunit receptor complexes that

share the transmembrane glycoprotein 130 (gp130), which explains the redundancy of these cytokines (Taga et al, 1997). Intracellular signaling takes place either via homodimerization of gp130 in the case of IL-6 and IL-11 systems or a structurally related protein in the case of other systems like LIF and CT-1.

Several experiments and clinical studies have shown the elevation of IL-6 expression in the myocardium and circulation in the event of a heart failure (Deten et al, 2002; Plenz et al, 2001; Wollert et al, 2001; MacGowan et al, 1997; Torre-Amione et al, 1996a). Circulating levels of gp130 also increased in patients with left ventricular dysfunction (Aukrust et al, 1999). Observation has been made that there is close relation between the expression level of IL-6 and gp130 and cardiac performance. Ventricular expression of IL-6 and gp130 correlated positively with reduced left ventricular ejection fraction and cardiac index, elevated pulmonary capillary wedge pressure, right atrial pressure and heart rate. The mechanism of elevated levels of IL-6 in heart failure is still unknown but the ability of TNF-α to induce IL-6 expression in various cell types suggested the possibility of cytokine cascade in heart failure (Gwechenberger et al, 1999).

IL-6 mRNA expression levels are also elevated in the non-infarcted myocardium and CT-1 expression has been shown to be increased in dogs pacing-induced chronic heart failure. These studies showed that the failing heart itself is also a source of IL-6 and CT-1. In vitro studies have shown that cardiac myocytes and fibroblasts also release IL-6 related cytokines.

IL-6 related cytokines are potent inducers of cardiomyocytes hypertrophy and inhibitors of cardiomyocyte apoptosis (Wollert et al, 2001). Similarly, CT-1 and LIF induce overlapping set of immediate early genes, induce and increase in cell size and

display sarcomeric organization as well as activate gene transcription and secretion of atrial natriuretic peptide (Pennica et al, 1995). In the case of IL-6, hypertrophic response in cardiomyocytes requires substantially elevated IL-6R (Wollert et al, 1996, Hirota et al, 1995). The hypertrophic response triggered by IL-6 and related cytokines takes place via the activation of Janus kinase (JAK)- signal transducer and activator of transcription (STAT) and mitogen (MAP) kinase pathways (Kodoma et al, 1997; Kunisada et al, 1996,). The significant role of IL-6 related cytokines is the protection of cardiomyocytes from apoptosis and enhancement of their survival (Sheng et al, 1997). In another study, it was shown that CT-1 protected cultured myocytes from ischemia-induced apoptosis (Stephanou et al, 1998).

Tumour necrosis factor-α

TNF-α is a proinflammatory cytokine identified primarily for its potent anti-tumor activity have highlighted its role in the pathogenesis of many cardiovascular diseases such as acute myocardial infarction, chronic heart failure, artherosclerosis, viral myocarditis, cardiac allograft rejection and sepsis associated cardiac dysfunction (Irwin et al, 1999; Meldrum et al, 1998; Oral et al, 1997; Neumann et al, 1995;). TNF is a 157-amino acid polypeptide which exists as either a secreted molecule (type I) or a membrane bound form (type II). The propensity of activities and effects of TNF-α have been attributed to the widespread distribution of TNF-α receptors TNF-R1 and TNF-R2 on almost all the nucleated cells in the body (Bolger et al, 2000). Binding affinity of TNF-α to both receptors is the same but the inotropic effects of TNF-α are mediated by its interaction with TNF-R1 alone. The dynamic interaction between TNF-α and its receptors is responsible for the pathophysiological effects of TNF-α to the heart. The

soluble forms of TNF-R1 and TNF-R2 have been documented to increase in heart failure patients. They are capable of binding to TNF-α, thus neutralizing the biological effects of circulating TNF-α on cell-bound receptors (Ferrari et al, 1995; Kapadia et al, 1995).

Besides other cell types that produced TNF-α, cardiomyocytes are also capable of producing TNF-α in response to LPS induction (Comstock et al, 1998; Kapadia et al, 1995a; Vassali 1992;) or ischemia (Meldrum et al, 1998; Gurevitch et al, 1996;). The role of TNF-α is mediated through activation of multiple transduction pathways and suppression or induction of a wide variety of genes encoding the production of other inflammatory cytokines, adhesion molecules and inducible nitric oxide synthase (iNOS) (Kelly et al, 1997).

The role of TNF-α in cardiovascular diseases was first reported by Levine in patients with cardiac cachexia (Levine et al, 1990). Subsequent studies confirmed a correlation between the circulating levels of TNF-α and the severity of the disease (Torre-Amione et al, 1996b; Katz et al. 1994). TNF-α has a dual biological effect on the heart, being either a killer or a protector to the heart depending on the amount and duration of its expression. A short-term expression is an adaptive response to any stress that takes place while long-term expression is maladaptive and results in cardiomyopathy, left ventricular dysfunction and progression of heart failure. These effects are multifactorial and involve cardiomyocyte hyperthrophy through generation of reactive oxygen intermediates in the cardiomyocytes (Bozkurt et al, 1998; Bryant et al, 1998; Ferrari 1998; Kubota et al, 1997; Yokoyama et al, 1997), ventricular remodeling by extracellular matrix protein formation, cardiomyocyte death by apoptosis and necrosis (Comstock et al, 1998; Krown et al, 1996,) and production of negative inotropic leading

to suppressed cardiac function through sphingomyelinase and nitric-oxide dependent pathways (Oral et al, 1997; Habib et al, 1996; Haywood et al, 1996; Kelly et al, 1996; Yokoyama et al, 1993).

1.2.2.5 Oxidative stress

Oxidative stress, a situation where there is an imbalance between the production of oxygen free radicals and the endogenous anti-oxidant defense mechanisms occur in the progression of heart failure (Grieve et al, 2004; Byrne et al, 2003). Mechanical stress and exposure to inflammatory cytokines such as TNF-α are important stimulus for increased oxidative stress (Aikawa et al, 2001). Both stimuli induce free radical production which can cause cardiomyocyte apoptosis by activating the expression of immediate early genes associated with cardiomyocytes growth and apoptosis (Webster et al, 1994). Free radicals can also stimulate fibroblast proliferation, collagen synthesis, matrix metalloproteinases (MMP) expression and activation (Spinale 2002; Murrell et al, 1990).

1.2.2.6 Extracellular matrix degradation and fibrosis formation

Cardiomyocytes and other cell types found in the heart such as endothelial cells are interconnected by a complex of connective tissue and extracellular matrix. The extracellular matrix is important for the structural characteristics of the heart. It consists of collagen, proteoglycans, glycoproteins and peptide growth factors. Upon infarction, collagen breakdown occurs which is induced by activated myocardial MMPs, serine proteases, MMP8 released by neutrophils (Thomas et al, 1998; Cleutjens et al, 1995). Digestion of the collagen will lead to mural alignment (slippage) of myocyte bundles or individual cardiomyocytes that is responsible for infarct expansion and thinning of the left ventricular wall (Olivettiet al, 1990). Excessive deposition of fibrillar collagen will

also occur following the death of cardiomyocytes resulting in a stiffer and less compliant ventricle.

1.3 Overview of current surgical and pharmacological treatments for heart failure

Currently there are various pharmacological and surgical interventional treatment options for patients with coronary ischemic heart disease. These include pharmacological modulation using angiotensin-converting enzyme (ACE) inhibitors (SOLVD Investigators, 1991), beta-blocking agents (Packer et al, 2002) and cytokine antagonists; device implantation such as the left ventricular assist devices (LVADs) (Rose et al, 2001), implantable cardioverter-defibrillators (ICDs) and cardiac resynchronization therapy (Bristow et al, 2004; St John Sutton et al, 2003) and surgical treatments such as coronary revascularization, angioplasty, coronary artery bypass graft (CABG) and heart transplantation.

However, despite the various effective treatments available, coronary ischemic heart disease remains the predominant cause of death. Even when heart transplantation is the best solution out of all the options available for end-stage heart failure, the donor supply never matches the demand for heart replacement therapy. Patients continue to experience progressively worsening symptoms, frequent admission to hospitals and premature death. The prevalence of the disease imposes enormous financial strain on the health care system, calling for new approaches in the treatment of coronary heart disease.

1.4 Molecular and cellular approaches for heart failure

Recent advances in understanding the molecular and cellular mechanisms of cardiovascular diseases have led to much interest in genetic and cellular therapy for treatment of ischemic heart disease (Melo et al, 2004; Mayer et al, 1997). Gene and cell-based cardiac repair offers a revolutionary approach for treating heart diseases. Gene therapy is a strategy to replace or augment the function of either defective or under-compensating genes that are involved in progression of the disease while cell therapy is a strategy focusing on repair and regeneration of cardiac muscles and vascular tissues in the heart.

1.5 Therapeutic angiogenesis

1.5.1 Vascular endothelial growth factor

Vascular endothelial growth factor (VEGF) is an extensively studied growth factor and considered as one of the more critical factors involved in angiogenesis during embryonic development and during adult life.

1.5.1.1 Functions of VEGF

For over a decade, there have been intense investigations on functions of VEGF *in vitro* and *in vivo*. As an angiogenic growth factor, VEGF is known for its ability to induce mobilization and proliferation of endothelial progenitor cells (EPCs) (Asahara et al, 1999). It promotes growth of vascular endothelial cells (EC) derived from arteries, veins and lymphatics (Ferrara et al, 1997) and also acts as a survival factor for ECs both *in vitro* and *in vivo*. It prevents apoptosis via phosphatidylinositol (PI) - kinase-Akt pathway and also upregulate expression of anti-apoptotic proteins Bcl-2 and A1 in ECs (Gerber et

al, 1998a and b). VEGF also known as a vascular permeability exerts it effects by promoting vasculature leakage and permeability (Dvorak et al, 1995; Keck et al, 1989). It also induces vasodilation *in vitro* in a dose-dependent manner as a result of EC derived nitric oxide actions (Selke et al, 1996; Ku et al, 1993). Finally, VEGF is capable of inducing integrin expression and MMPs secretion (Wang et al, 1998; Senger et al, 1997)

1.5.1.2 VEGF ligands and receptors

VEGF is a 40-45 kDa heparin-binding homodimeric glycoprotein released by a variety of cell types including endothelial and smooth muscle cells. The human VEGF-A (the prototype VEGF species) gene is organized as eight exons separated by seven introns (Tischer et al, 1991). Alternative splicing of the mRNA results in five different VEGF isoforms; $VEGF_{121}$, $VEGF_{145}$, $VEGF_{165}$, $VEGF_{189}$, $VEGF_{206}$. $VEGF_{165}$ is the most predominant isoform, lacking exon 6. It displays intermediate diffusion characteristics with a significant portion remaining bound to the cell surface and extracellular matrix (Park et al, 1993). These VEGF isoforms play a pivotal role in vascular development and it has been reported that the loss of a single VEGF-A allele disrupted the development of normal embryonic vasculature system leading to fatal outcomes (Carmeliet et al, 1996; Ferrara et al, 1996).

The biological activity of VEGF-A is mediated by interaction with two types of high affinity receptor tyrosine kinases (RTKs) expressed mostly on ECs. They are identified as VEGF receptor 1 (VEGFR-1/Flt-1) and VEGF receptor 2 (VEGFR-2/KDR/Flk-1). Another receptor known as VEGFR-3 (Flt-4) also belongs to the same family of RTKs but it binds to VEGF-C and VEGF-D (Karkkainen et al, 2002). It is restricted predominantly to ECs lining the lymphatic channels. These receptors have

seven immunoglobulin-like domains in the extracellular domain of a single transmembrane region and a consensus tyrosine kinase sequence that is interrupted by a kinase-insert domain (Terman et al, 1991; Shibuya et al, 1990).

Flt-1 though expressed primarily on ECs is also present on smooth muscle cells and monocytes (Neufeld et al, 1999). Activation of Flt-1 results in cell migration and contributes directly to migration of primitive vascular buds through extracellular matrix by enhancing production of MMPs by ECs and associated smooth muscle cells (Sato et al, 2000; Esser et al, 1998). Binding of VEGF to Flt-1 also results in monocyte recruitment and expression of tissue factor by both monocytes and ECs (Barleon et al, 1996; Clauss et al, 1996).

Flk-1 is essential for embryonic vasculogenesis and definitive hematopoiesis. This is evidenced by the failure of Flk1-null mice to develop blood islands and form organized blood vessels resulting in death *in utero* between days 8.5 and 9.5 (Shalaby et al, 1995). Flk-1 is exclusively expressed in both EPCs and primitive hematopoietic stem cells and plays a critical role in EC differentiation, proliferation, vasculogenesis and angiogenesis (Millauer et al, 1993; Terman et al, 1992).

VEGF has also been reported to bind to neuropilins, a family of co-receptors. Binding of $VEGF_{165}$ to neuropilin-1 receptor enhances $VEGF_{165}$ binding to Flk-1 and $VEGF_{165}$-mediated chemotaxis (Soker et al, 1998).

1.5.1.3 Regulation of VEGF gene expression

VEGF mRNA expression has been shown to be induced by exposure to low oxygen concentration under a variety of pathophysiological conditions, therefore enhancing angiogenesis in such conditions (Dor et al, 2001; Shweiki et al, 1992).

Hypoxia-inducible factor-1 (HIF-1) plays a key role in embryonic and tumour vascularization (Ryan et al, 1998). HIF-1α and HIF-2α are required for VEGF release during hypoxic conditions and inhibition of these two factors during hypoxia suppresses VEGF induction (Mie Lee et al, 2003). Both transcription factors bind to the hypoxia-response element (HRE) in the VEGF promoter in order to upregulate VEGF expression (Semenza et al, 2000). Hypoxia not only increases the transcriptional rate of VEGF but also enhances the half-life of VEGF mRNA (Levy 1998). *In vivo* hypoxic conditions also showed an upregulation in VEGF expression with enhanced neovascularization observed (Banai et al, 1994).

Several major growth factors and inflammatory cytokines such as TGF-β, PDGF, TNF-α, IL-1α and IL-6 serve as indirect angiogenic factors (Cohen et al, 1996; Brogi et al, 1994). They stimulate VEGF expression in several cell types. This suggests that paracrine or autocrine release of such molecules cooperates with the local hypoxia condition in regulating VEGF release (Ferrara et al, 1997; Neufeld et al, 1999).

1.6 Therapeutic angiogenesis: molecular and cellular approach

1.6.1 Therapeutic angiogenesis: molecular approach

Angiogenic cytokines used for therapeutic angiogenesis can be administered in the form of recombinant human protein or by gene therapy (Khan et al, 2003). Protein and gene-based approaches using selected isoforms of VEGF-A ($VEGF_{121}$, $VEGF_{165}$) and FGF (FGF-1, FGF-2 and FGF-4) have been extensively studied. Recombinant protein therapy usually shows a precise dose-response relationship than gene transfer therapy. One limitation of using recombinant protein is its very short half-life which ranges from

minutes to few hours. Hence, it has to be administered in a repeated fashion to maintain the plasma serum level within the therapeutic window. As it is usually administered systematically, it tends to result in potential adverse effects of high plasma concentrations required to achieve sufficient myocardial uptake. Such adverse effects include hypotension and edema when VEGF is used (Baumgartner et al, 2000; Hariawala et al, 1996) and anemia, thrombocytopenia and renal toxicity when FGF is used (Mazue et al, 1991).

Gene-based approaches use vectors to incorporate the angiogenic gene into a target host cell and induce production of the encoded angiogenic protein. The expression of these genes can be maintained from days to weeks when using adenoviral vectors or for months when using retroviral or lentiviral vectors. This helps to overcome the problem of short half-life of recombinant proteins. However, one of the major limitations in using such vectors is the stimulation of immune and inflammatory response in humans via circulating antibodies to the viruses (Gilgenkrantz et al, 1995). Naked plasmid DNA can also be used but its efficiency is limited by the amount of plasmid DNA that actually enters the target cell nucleus. The advantages and disadvantages of using various viral vectors and non-viral vectors are listed in Table 1.

1.6.1.1 Protein-based angiogenesis

Pre-clinical studies

Protein-based therapy was one of the earliest forms of therapy used. The effect of recombinant human $VEGF_{165}$ protein has been studied in dog and porcine models of myocardial ischemia which were created by gradual occlusion of the circumflex coronary artery. Pre clinical experience with VEGF has mainly involved its $VEGF_{121}$ and $VEGF_{165}$

Table 1: Gene Therapy Vectors

Viral vector	Gene	Advantages	Disadvantages
Adenovirus	DNA	High transfection efficiency	Limited duration of transgene expression Strong inflammatory reaction
Adeno-associated virus	DNA	High transfection efficiency Sustained transgene expression	Limited transgene size Random nuclear incorporation Complex technology for production
Lentivirus	RNA	High transfection efficiency even for non-dividing cells	Limited transgene size Danger of reversion to replication competitive virus
Retrovirus	RNA	Sustained transgene expression	Low rate of transfection Effective only in replicating cells Random nuclear incorporation
Non-viral vector			
Cell	Vectors carrying DNA or RNA	Sustained and localized transgene expression Multiple transgene expression possible	Difficulty in production and scale up
Liposome	DNA	Unlimited transgene size Safe to use	Low transduction efficiency
Plasmid DNA	DNA, RNA, oligonucleotide	Unlimited transgene size Safe to use Episomal location	Low transduction efficiency

isoforms, derived from splicing of the VEGF-A gene. The studies demonstrated a dose-response relationship and evidence of enhanced angiogenesis after treatment. Lower dosage of administered protein over an extended period of time shows better prognosis with fewer side effects as compared to higher dosage for a shorter period of time. Banai and colleagues (Banai et al, 2004) showed marked augmentation of collateral blood flow to the ischemic myocardium in a dog heart model of MI using 45μg of VEGF daily for 4 weeks. Another study done by Lopez and colleagues (Lopez et al, 1998) also showed that treatment of recombinant VEGF protein at 20μg daily for 3 weeks in porcine model of MI was still able to induce significant angiogenesis with improved regional perfusion. Administration of 2μg recombinant VEGF for 4 weeks has also been shown to be effective in improving regional coronary flow as well as fractional left ventricular shortening of porcine ischemic myocardial model (Harada et al, 1996). On the other hand, administration of 0.72mg to 2mg recombinant VEGF protein for 7 days did not increase collateral formation but instead, it significantly exacerbated neointimal proliferation and also resulted to severe hypotension in 50% of the animals (Hariawala et al, 1996; Lazarous et al, 1996).

The effectiveness of angiogenic protein based therapy is also influenced by the route of administration. Single intracoronary doses were effective in the porcine model (Hariawala et al, 1996) as were a series of two local injections via balloon catheter, 3 to 4 week periadventitial infusions via minipump (Hariawala et al, 1996; Harada et al, 1996), intramyocardial injection (Biswas et al, 2004) and 28-day intracoronary injections in the dog model (Banai et al, 1994). Intravenous administration however was ineffective (Sato et al, 2001).

Clinical studies

Given the positive results from animal studies in inducing collateral formation to improve blood flow, protein-based therapy was then brought into the realm of clinical trials to test its feasibility in a wide range of patients. Clinical trials using angiogenic proteins until today is still in its infancy and no Phase III trials have been initiated. However, limited efficacy data were obtained from ongoing and completed Phase I/II trials.

Two small Phase I trials using intracoronary (n=16) and intravenous (n=14) administration of $VEGF_{165}$ demonstrated significant improvement in exercise capacity, perfusion and symptoms; defined as angina class (Hendel et al, 2000; Henry et al, 2001). These promising results became the basis for Phase II trial. The VIVA trial is a randomized, double-blinded, placebo-controlled Phase II trial (Henry et al, 2003). The VIVA trial assessed the safety and efficacy of intracoronary and intravenous infusions of $VEGF_{165}$ in 178 patients with two different doses (low dose: 17ng/kg/min; high dose: 50ng/kg/min) administered. Results were discouraging since an improvement in angina class and exercise time were observed only in the high dose receiving group at only 120 days after treatment. The summary of clinical studies using VEGF protein therapy for cardiac repair is listed in Table 2.

1.6.1.2 Gene-based angiogenesis

Plasmid: Pre-clinical

Studies investigating the efficacy and safety of VEGF gene therapy for treatment of ischemic heart disease using animal models have been conducted with increasing frequency.

Table 2: Clinical studies using VEGF recombinant protein

Reference	Dose	Patient Selection	Number of patients	Study phase	Study design	Route of administration	End point of measurement	Results
Hendel et al, 2000	Low dose: 0.005 and 0.017μg/kg High dose: 0.05 and 0.167μg/kg	Coronary artery disease	14	I	Safety and Tolerability, Blinded	Intra-coronary injection	ETT, Rest/Stress SPECT at 30 and 60 days after procedure	10 out of 14 patients showed SPECT improvement especially in high dose group. Improved collateral count in 7 patients who had angiography
Henry et al, 2001	Low dose: 0.005 and 0.017μg/kg High dose: 0.05 and 0.167μg/kg	Coronary artery disease	15	I	Safety and Tolerability, Blinded	Intra-coronary injection	Rest/Stress SPECT at 30 and 60 days after procedure	Myocardial perfusion imaging was improved in 7 of 15 patients at 60 days. All 7 patients with follow-up angiograms had improvements in the collateral density score.
Henry et al, 2003	Low dose: 17ng/kg High dose: 50ng/kg	Coronary artery disease	178	II	Safety and Efficacy, Double blinded, placebo-controlled	Intra-coronary injection and intra-venous injection	ETT and Angiography	Improved angina and quality of life within all groups at day 60, however with no significant intra-group difference. Placebo group showed no difference with low dose group by day 120, but high dose group showed significant improvement in angina class

Genes encoding $VEGF_{165}$, $VEGF_{121}$ and VEGF-2 have been transfected in a number of animal studies using either naked plasmid DNA or adenoviral vectors. Studies that involved intra-myocardial injections of naked DNA have shown the safety of using these approaches.

Tio and colleagues demonstrated increased left circumflex blood flow when performing four injections delivering a total of 200μg of plasmid vector encoding $VEGF_{165}$ in porcine ameroid model of stress-induced regional myocardial ischemia (Tio et al, 1999). Another group used intramyocardial injection of a total of 300μg plasmid $VEGF_{165}$ in conjunction with transmyocardial laser revascularization in a porcine model of myocardial ischemia. Their results showed improved wall motion compared to the ischemic controls (Sayeed-Shah et al, 1998). However, one study which injected one single dose of plasmid $VEGF_{165}$ at a single site in a rodent model of MI induced both angiogenesis and angioma formation, without enhanced regional blood flow (Schwartz et al, 2000). Subsequent study indicated that this was a dose-related event since a 50% reduction in the dose of plasmid DNA did not induce angioma formation (Kloner et al, 2000).

Recently, a study injected 3.8mg of plasmid-$VEGF_{165}$ intramyocardially in porcine model of infarction and demonstrated significant increase in mature blood vessels and improved myocardial perfusion (Crottogini et al, 2003). The same group did a similar study with adult sheep (Vera et al, 2006). A reduction in infarct size was reported and was accompanied by an increase in early angiogenesis and arteriogenesis, decrease in peri-infarct fibrosis and myofibroblast proliferation and enhanced cardiomyoblast proliferation.

Plasmid: Clinical

Losordo and colleagues were the first to study the feasibility and safety of intra-myocardial injection of plasmid human VEGF in patients (Losordo et al, 1998). Five patients with inoperable coronary artery disease and symptomatic myocardial ischemia received 125μg of plasmid $VEGF_{165}$. The treatment caused no changes in heart rate, systolic or diastolic pressure. Perfusion scans showed fewer abnormally perfused segments and decreased segments with fixed defects while coronary angiography showed improved blood flow. The same group did a follow-up study on a larger sample size with the same clinical symptoms (Symes et al, 1999). Either 125μg or 250μg of plasmid $VEGF_{165}$ was administered directly into the myocardium of the patients. A reduction in the ischemic defects was observed in 13 of the 16 patients that were followed for 90 days. This improvement was observed to be more consistent with the high dose rather than the low dose.

The feasibility of intra-myocardial administration of plasmid VEGF was assessed using an electromechanical left ventricular mapping system (NOGA) in 13 patients (Vale et al, 2000). Results were encouraging showing improved left ventricular ejection fraction after treatment and a marked reduction in the area of ischemic myocardium after 60 days. A study using percutaneous, catheter-based myocardial plasmid VEGF transfer in 6 patients showed improvement in angina frequency, perfusion defect and electromechanical function (Vale et al, 2001). This study then led to a multicentre randomized, double-blinded, placebo-controlled trial of catheter-based plasmid VEGF-2 gene transfer in 19 patients (Losordo et al, 2002). End-point analysis at 12 weeks disclosed significantly improved angina class and myocardial perfusion and decreased

focal ischemia on electromechanical mapping compared to the placebo group. A recent phase II randomized, double-blinded, placebo-controlled trial also reported that transient VEGF overexpression seems safe and showed improvement in regional wall motion in patients (Kastrup et al, 2005).

Despite the positive results, poor transduction efficiency is a problem when using the plasmid approach (Laitinen et al, 1997; Schmidt-Wolf et al, 2003; Yla-Herttuala et al, 2003). To overcome this problem, viral vectors carrying angiogenic gene were designed and tested for their safety and efficacy in animal models and human studies.

Viral vector: Pre-clinical

One of the earlier studies reporting the usefulness of using viral vectors encoding vascular growth factor gene was demonstrated by Mack and colleague (Mack et al, 1998). Using porcine myocardial ischemia model, they injected intramyocardially adenoviral vector carrying $VEGF_{121}$ (ad-$VEGF_{121}$). Ten injections in the left circumflex perfusion bed were performed with 10^8 plaque-forming units (pfu) per site. SPECT nuclear imaging revealed improvement in both myocardial perfusion and functional collateral vessel formation in ad-$VEGF_{121}$ treated animals at 4 weeks after treatment.

The same group then tested the toxic effects which might result from the intramyocardial injection of ad-$VEGF_{121}$ (Patel et al, 1999). The same experiment was repeated with animals receiving viral doses of either 10^8 or 10^9 pfu per injection site. Echocardiographic assessment, survival, blood analysis and myocardial and liver histology were examined 3 and 28 days after vector administration. Minimal inflammation and necrosis was observed in the myocardium of the ad-$VEGF_{121}$ treated animals but livers were normal. Even though inflammation and necrosis was minimal, it

was statistically significant and dose-related with increased degree in animals receiving 10^9 pfu per injection site. Viral vector administration had no deleterious effect on the basal regional function of the animals.

Lazarous and colleagues showed that injection of adenoviral vector carrying $VEGF_{165}$ (ad-$VEGF_{165}$) into canine pericardial cavity resulted in efficient gene expression of VEGF (Lazarous et al, 1999). Unfortunately, the level of expression was insufficient to promote collateral development and hence, improvement in myocardial blood flow in the canine model but the vascular permeability of over-expressed VEGF resulted in large pericardial effusion. Favourable results were obtained when using ad-$VEGF_{165}$ in rabbit model of myocardial ischemia which reported increased vascular density, improved heart ejection fraction and low myocardial ischemia (Tanaka et al, 2000).

One group did a comparitive study using adenoviral vector and plasmid carrying $VEGF_{165}$ and VEGF-D in porcine model using the NOGA system. Histological studies showed that administration of ad-$VEGF_{165}$ and ad-VEGF-D resulted in transmural angiogenesis with maximal effects in the epicardium. VEGF-D showed higher degree of angiogenesis as compared to $VEGF_{165}$ but surprisingly plasmid-$VEGF_{165}$ and plasmid-VEGF-D did not induce angiogenesis. The summary of pre-clinical studies using VEGF gene therapy for cardiac failure is listed in Table 3.

Viral vector: Clinical

The encouraging data from pre-clinical studies using ad-VEGF gene approach has prompted research groups to investigate the safety, efficacy and feasibility of using this approach in clinical patients. A phase I clinical trial using ad-$VEGF_{121}$ was performed in patients undergoing CABG surgery and also in patients as sole therapy (Rosengart et al,

Table 3: Pre-clinical studies using VEGF therapy for cardiac failure

Type of VEGF therapy	Animal model	Route of administration	References
Protein			
	Dog	Intra-coronary	Banai et al, 1994
	Dog	Intra-atrial	Lazarous et al, 1996
	Porcine		Harada et al, 1996
		Intra-coronary	Hariawala et al, 1996
		Intra-coronary	Lopez et al, 1998
			Hughes et al, 1999
		Intra-coronary and Intra-venous	Sato et al, 2001
			Hughes et al, 2004
Plasmid			
	Rat	Intra-myocardial	Kloner RA et al, 2000
		Intra-myocardial	Schwartz et al, 2000
	Porcine	Intra-myocardial	Sayeed-Shah et al, 1998
		Intra-myocardial	Tio et al, 1999
		Intra-myocardial	Crottogini et al, 2003
	Sheep		Vera et al, 2006
Adenoviral vector			
	Porcine	Intra-myocardial	Mack et al. 1998
		Intra-myocardial	Patel et al, 1999
		Intra-myocardial	Rutanen J et al, 2004
	Dog	Intra-coronary	Lazarous et al, 1999
	Rabbit	Intra-coronary	Tanaka et al, 2000

1999a). At day 30, all patients reported improvement in angina class and post-operative nuclear imaging suggested increased contractility in area where viral vector was injected but no significant improvement in myocardial perfusion. This data showed direct myocardial injection of ad-$VEGF_{121}$ appeared to be well-tolerated. A six-month follow-up on the study reported persistence of the therapy in patients and also confirmed the safety of using the vector (Rosengart et al, 1999b).

Hedman and colleagues carried out a randomized placebo-controlled double-blind phase II study using ad-VEGF for treatment of chronic myocardial ischemia in 103 patients (Hedman et al, 2003). No serious events were reported and myocardial perfusion was significantly improved after 5 months. This study also showed that gene transfer for coronary artery disease using adenoviral vector was feasible and well-tolerated. The summary of all clinical trials using VEGF gene therapy for cardiac failure is listed in Table 4.

1.6.2 Therapeutic angiogenesis and vasculogenesis: Cellular approach

Therapeutic angiogenesis and vasculogenesis aiming at restoring perfusion to chronically ischemic myocardial zones can also be achieved by transplantation of exogenous stem cells and differentiated cells and also by enhancing the mobilization of endogenous stem cells. These cells have natural capacity of participating in therapeutic angiogenesis and vasculogenesis by delivering angiogenic cytokines and growth factors in appropriate sequence and concentration and/or by incorporating into the newly generated blood vessels. Various cell types have been studied and major advances within the last several years have allowed the understanding of fundamental biology of these cells, their behavior properties *in vitro* and *in vivo* and their therapeutic potential. The

Table 4: Clinical studies using VEGF gene therapy

Type of VEGF therapy	Reference	Dose	No of patients	Study phase	Study design	Route of administration	End point of measurement	Results
Plasmid	Losordo et al, 1998	125µg	5	I	Feasibility and safety	Intra-myocardial	SPECT, Angiography	Perfusion scans showed fewer abnormally perfused segments and decreased segments with fixed defects. Coronary angiography showed improved blood flow. Significant reduction in angina.
	Symes et al, 1999	Low dose= 125µg High dose= 250µg	20	I	Safety and tolerability	Intra-myocardial	SPECT, Angiography	No peri-operative myocardial infarction or hemodynamic instability, one death 4 months after procedure. 16 patients reported reduction in angina after 90 days. 7 out of 10 patients reported reduction were free of angina after 6 months and 13 out of 17 showed reduction in ischemic defect.
	Sarkar et al, 2001	250µg	7	I	Safety and bioactivity, Open-labeled study	Intra-myocardial	SPECT, Angiography	Improved myocardial function was documented in all patients at 12 months. Improved collateralization was detected in four patients with coronary angiography.
	Vale et al, 2001	200µg	6	I	Randomized control	NOGA catheter-based	NOGA mapping, SPECT	Reduced ischemia and improved myocardial perfusion at 90 days

Type of VEGF therapy	Reference	Dose	No of patients	Study phase	Study design	Route of administration	End point of measurement	Results
Plasmid	Losordo et al, 2002	N=9, 200µg; N= 9, 800µG; N=1, 2000µG	19	I/II	Randomized, double-blinded, placebo-controlled	NOGA catheter-based	ETT, NOGA mapping, SPECT	Significant improvement in angina class, myocardial perfusion and ETT at 12 weeks
	Gyongyosi et al, 2005; Kastrup J et al 2005	N=40, 0.5mg of phVEGF-A165; N=40, placebo-plasmid	80	II	Randomized, double-blinded, placebo-controlled	NOGA catheter-based	NOGA mapping, SPECT	phVEGF-A165 plasmid injection improve, but do not normalize, the stress-induced perfusion abnormalities in 21 out of 40 VEGF-treated patients.
Adenoviral vector	Rosengart et al, 1999a and 1999b	Group A= 15, $4\times10^{8\text{-}10}$ pfu; Group B= 6, 4×10^{8}	21	I	Safety and Tolerability	Intra-myocardial	ETT, Echocardiography, Angiography, rest/stress SPECT	Group A had 2 deaths in 40 days and Group B had no death. Surviving patients reported improvement in angina class and post-operative nuclear imaging suggested increased contractility in area where viral vector was injected but no significant improvement in myocardial perfusion.
	Hedman et al, 2003	N=37,2× 10^{10}pfu; N= 28, 200µg	103	II	Feasibility, tolerability, Randomised placebo-controlled double blind	Intro-coronary	ETT, Angiography, SPECT	Myocardial perfusion significantly improved at 5 months

summary of both pre-clinical and clinical studies using various cell sources for induction of neovascularization in infarcted myocardium is listed in Table 5.

Adult mesenchymal stem cells

Mesenchymal stem cells constitute one of the stem cell populations in adult bone marrow. They are self-renewing clonal precursors of non hematopoietic tissue that provide the microenvironment for hematopoiesis. They can be induced to differentiate into cells of mesenchymal lineage such as fibroblasts, cartilage, bone, skeletal and cardiac muscle (Conget et al, 1999; Pittenger et al, 1999; Prockop 1997). Human mesenchymal stem cells do not express specific markers for EPCs and have never been reported to transdifferentiate into endothelial phenotype. However, it was reported recently that immortalized murine mesenchymal stem cells when treated in vitro with 5-azacytidine were able to differentiate to ECs, pericytes and smooth muscle cells (Gojo et al, 2003). Verfaille's group showed presence of multipotent adult progenitor cells, co-purified with mesenchymal stem cells that express VEGF receptor, Flk-1 and other endothelial lineage markers upon stimulation with VEGF (Verfaillie et al, 2003; Jiang et al, 2002). Paracrine action of transplanted mesenchymal stem cells on angiogenesis and cytoprotection in rodent model of MI was demonstrated in a study by Tang and collagues (Tang et al, 2005). The transplanted group showed an increase in angiogenic factors such as bFGF, VEGF and stem cell homing factor and a decrease in proapoptotic protein, Bax.

Several other studies also showed bone marrow stromal cells which contain the mesenchymal stem cells are capable of participating in angiogenesis (Tomita et al, 2002; Wang et al, 2001; Tomita et al, 1999). Capillary density was enhanced and presence of donor cells incorporating into the capillary endothelium was observed. However, most of

Table 5: Preclinical and clinical studies using cell therapy for myocardial revascularization

Cell source	Animal model	Route of administration	Results	Reference
PRE-CLINICAL				
Bone marrow derived	Rat Ligation model	Intra-myocardial injection after ligation	Angiogenesis was significant at 7 days after transplantation and 14 days later, specific markers for vascular endothelial cells were detected in the transplanted group.Transplanted group had upregulated expression of heat shock proteins indicating that bone marrow cells also conferred enhanced cytoprotection to the myocardium.	Zhang et al, 2003
Bone marrow derived mononuclear cells	Rat ligation model	Intra-myocardial injection after ligation	Increased capillary density, blood flow, angiopoietin-1 and VEGF expression at 2 months. Improvement of myocardial function.	Nishida M et al, 2003
Bone marrow derived mononuclear cells	Porcine ligation model	Intra-myocardial 4 weeks after ligation	Increased endothelial cell number, myocardial perfusion and myocardial function at 4 weeks	Fuchs S et al, 2001
Bone marrow derived mononuclear cells	Porcine ligation model	Trans coronary sinus injection 2 weeks after injury	Increased angiogenesis at 2 weeks	Vicario J et al, 2002
Bone marrow derived mononuclear cells	Porcine ligation model	Intra-myocardial injection 60 minutes after ligation	Increased capillary density, blood flow, angiographic collateral vessels and myocardial function at 3 weeks	Kamihata H et al, 2001
Endothelial cells	Rat cryoinjury model	Intra-myocardial	Increased vascular density and improved myocardial function and regional blood flow at 6 weeks	Kim E-JK et al, 2001
Peripheral-derived endothelial progenitor cells	Athymic nude rats ligation model	Intra-venous injection 3 hours after ligation	Increased capillary density with incorporation of human specific endothelial cells and improved myocardial function at 4 weeks	Kawamoto A et al, 2001

Peripheral-derived endothelial progenitor cells, CD34$^+$ cells	Athymic nude rats ligation model	Intra-venous injection 48 hours after ligation	Increased number of capillary of human and rat origin and improved myocardial function at 2 weeks	Kocher AA et al, 2001
Peripheral-derived endothelial progenitor cells	Porcine ligation model	Intra-myocardial injection 4 weeks after ligation	Increased angiographic collateral development and capillary density at 4 weeks	Kawamoto A et al, 2003
Umbilical cord blood derived endothelial progenitor cells, CD133$^+$ cells	Athymic nude rats ligation model	Intra-venous infusion 7 days after ligation	Improved myocardial function at 4 weeks. Donor-derived endothelial cells found in blood vessels	Leor J et al, 2005
Embryonic stem cells	Mouse ligation model	Intra-myocardial injection	Increased blood vessel density and improved myocardial function at 32 weeks.	Min JY et al, 2003
Embryonic stem cells	Mouse ligation model	Intra-myocardial injection	Donor-derived endothelial cells and smooth muscle cells and cardiomyocytes found in infarcted myocardium at 2 weeks. Improved myocardial function	Singla DK et al, 2006
Embryonic stem cells		Intra-venous injection on every other day for 6 days after infarction	Increased arteriole density, improved myocardial function and regional blood flow at 6 weeks	Min JY et al, 2006
Mesenchymal stem cells	Rat ligation model	Intra-myocardial injection	Increased capillary density and improved myocardial function at 8 weeks	Tang YL et al, 2005
Mesenchymal stem cells	Rat cryoinjury model	Intra-myocardial injection 3 weeks after cryoinjury	Increased capillary density and improved myocardial function at 8 weeks	Tomita S et al, 1999
Mesenchymal stem cells	Rat ligation model	Intra-aortic infusion 2 weeks after ligation	Presence of donor-derived endothelial cells, cardiomyocytes and fibroblasts in the myocardium at 4 weeks	Wang JS et al, 2001
Mesenchymal stem cells	Porcine ligation model	Intra-myocardial injection 4 weeks after ligation	Increased capillary density and improved myocardial function at 4 weeks	Tomita S et al, 2002

Mesenchymal stem cells	Uninjured Mouse	Intra-ventricular and Intra-myocardial injection	Increased capillary density with donor-derived endothelial cells at 1, 4,8 and 12 weeks	Gojo S et al, 2003
Hematopoietic stem cells	Mouse ligation model	Intra-myocardial injection 5 hours after ligation	Donor derived endothelial cells and smooth muscle cells present in de novo capillaries and arterioles at 9 days	Orlic D et al, 2001
$CD34^+$ cells from hematopoietic stem cells	Mouse ligation model	Bone marrow transplantation followed by 1 hour of artery occlusion after 10 weeks of transplantation	Donor derived endothelial cells and cardiomyocytes present at 2 and 4 weeks	Jackson KA et al, 2001
Smooth muscle cells	Rat cryoinjury model	Intra-myocardial injection 4 weeks after cryoinjury	Increased capillary density and improved myocardial function at 8 weeks	Li RK et al, 1999
Smooth muscle cells	Hamsters cryoinjury model	Intra-myocardial injection	Improved myocardial function at 4 weeks	Yoo KJ et al, 2000, 2002
CLINICAL				
Bone marrow derived mononuclear cells	Humans with acute myocardial infarction	Intra-coronary infusion after 5 to 9 days after acute myocardial infarction	Improved myocardial perfusion and function at 3 months	Strauer BD et al, 2002
Bone marrow derived mononuclear cells	Humans with severe ischemic heart disease	Intra-myocardial injection	Improved myocardial perfusion and function at 3 months	Tse HF et al, 2003
Bone marrow derived mononuclear cells	Humans with severe ischemic heart disease	Intra-myocardial injection	Improved myocardial perfusion and function at 2 months	Perin EC at al, 2003
Bone marrow derived mononuclear cells	Humans with severe ischemic heart disease	Intra-coronary injection	Improved myocardial perfusion and function at 6 months	Wollert KC et al, 2004
Bone marrow derived mononuclear cells	Humans with chronic artery disease	Intra-coronary injection	Reduced infarct size, improved myocardial function at 3 months	Strauer BE et al, 2005
Bone marrow derived	Humans with chronic	Intra-myocardial injection	4 out of 6 CABG patients showed	Stamm C et al, 2003

AC133+ cells	myocardial infarction		improved myocardial perfusion after 9 months post transplantation	
Highly enriched AC133+ cells	Humans with acute myocardial infarction	Intra-coronary injection	Improved myocardial perfusion and function at 4 months	Bartunek J et al, 2005
Bone marrow derived mononuclear cells and peripheral blood-derived endothelial progenitor cells	Humans with acute myocardial infarction	Intra-coronary infusion 5 days after acute myocardial infarction	Improved myocardial function, myocardial viability and coronary flow reserve at 4 months	Assmus B et al, 2002

the reported studies obtained mesenchymal stem cells from a non-purified plastic adherent cell fraction of bone marrow-derived mononuclear cells that also include hematopoietic stem cell population which are likely to participate in the neovascularization process. Furthermore, the success of mesenchymal stem cells transplantation in cardiac failure leading to reduced infarct scar and dilatation of the infarct region and improvements in contractile function are also due to the myogenic effect of these cells.

Smooth muscle cells

Smooth muscle cells are the major cell population of the arterial media and play a crucial role in the vascular tone. Under pathologic conditions, they can dedifferentiate, migrate, proliferate and secrete extracellular matrix to heal vascular injuries. They can also secrete bFGF and VEGF which are involved in angiogenic process (Ali et al, 1994; Stavri et al, 1995). A study by Li and colleagues successfully transplanted smooth muscle cells into cryoinjured myocardium of adult rats (Li et al, 1999). Results showed four to five fold increase in blood vessel formation and significant improvement in contractile function of the transplanted group. However, further investigation is required to assess if enhancement of angiogenesis by smooth muscle cell transplantation is due to their proliferation or by secretion of angiogenic growth factors. Similar results were shown by another group using hamster model of cryoinjured myocardium (Yoo et al, 2000). Smooth muscle transplantation prevented cardiac dilatation and improved ventricular function. It was even shown that smooth muscle cell was a better candidate for cardiac repair than cardiomyocytes (Yoo et al, 2002).

Hematopoietic stem cells and progenitor cells

Hematopoietic stem cell is another stem cell population found in adult bone marrow. These cells are known to participate in neovascularization as they are able to be mobilized by angiogenic growth factors such as VEGF and Ang-1 (Moore et al, 2001) and have a common precursor as the EPCs known as the hemangioblasts (Choi et al, 1998). A study by Jackson and colleagues transplanted highly enriched hematopoietic stem cells known as the side population (SP) into coronary artery occluded lethally irradiated mice (Jackson et al, 2001). This side population is characterized by $CD34^{-/low}$, c-Kit^{+}, Sca-1^{+} differentiated to ECs expressing Flt-1. Engraftment of these SP-derived ECs was predominantly found in newly formed capillaries in the "at-risk" myocardial tissue adjacent to the infarct zone. Transplantation of GFP-positive lin^{-} c-Kit^{+} bone marrow-derived mononuclear cells into the infarcted myocardium of mouse models showed the presence of GFP-positive endothelial and smooth muscle cells in developing capillaries and small arterioles in the infarct area (Orlic et al, 2001).

Endothelial progenitor and endothelial cells

EPCs are a group of cells that are known to differentiate and mature into ECs, play an important role in endothelium maintenance and participate in reendothelialization and neovascularization (Luttun et al, 2002; Szmitko et al, 2003). EPCs share a common precursor with hematopoietic stem cells known as the hemangioblasts (Choi et al, 1998b) and they can be isolated from bone marrow, peripheral blood and umbilical cord blood mononuclear cells. Their therapeutic potential in restoring tissue vascularization after ischemic events in limbs and myocardium has been shown in many studies.

Bone marrow-derived EPCs

Several animal studies have shown that transplantation of bone marrow cells contributes to neovascularization. Bone marrow cells contain many cell types including mesenchymal stem cells, hematopoietic stem cells and EPC stem cells. These cells have the capacity to home into different tissue, proliferate and acquire the phenotypes of the host organ. Many studies have evaluated the potential of unselected whole bone marrow cells for revascularization of ischemic organs in various animal models (Nishida et al, 2003; Yoshida et al; 2003; Vicario et al, 2002; Fuch et al, 2001). All these studies showed a significant increase in the capillary density together with improvement in myocardial function and higher limb salvage in the infarcted myocardium and ischemic hindlimb respectively when receiving bone marrow cells.

A study by Kamihata reported that 16% of the bone marrow-derived mononuclear cells were of endothelial lineage-cells and expressed bFGF, VEGF and Ang-1 (Kamihata et al, 2001). These bone marrow-derived mononuclear cells actively differentiated into ECs in vitro and formed network structure with human umbilical vein ECs. These cells incorporated into 31% of the neocapillaries and corresponded to approximately 8.7% of macrophages in the infarcted myocardium of the swine model. Autologous bone marrow mononuclear cells were also injected into the ischemic limb immediately following induction of ischemia and the cells were highly located in the capillary network of the myocardium. Similar work was perfomed in rat MI model and bone marrow mononuclear cells showed sustained improvement in cardiac function as assessed by left ventricle ejection fraction and fractional shortening (Zhang et al, 2003). Angiogenesis was induced to a significant degree at 7 days after transplantation and 14 days later, specific markers

for vascular ECs were detected in the transplanted bone marrow mononuclear cells. It was also shown that the transplanted group had upregulated expression of heat shock proteins in the infarcted myocardium indicating that bone marrow cells may also confer enhanced cytoprotection to the myocardium. Results from studies using bone marrow transplantation revealed that this may constitute a novel strategy for achieving optimal therapeutic angiogenesis by the natural ability of the bone marrow cells to secrete potent angiogenic ligands and cytokines as well as to be incorporated into the foci of neovascularization. ECs have also been used in cell therapy. One study reported increased vascular density when ECs were transplanted in cryoinjured rodent models (Kim et al, 2001).

The efficacy of clinical bone marrow stem cell therapy for cardiac revascularization has been assessed by various groups using various methods of delivery. Strauer and colleagues transplanted autologous bone marrow mononuclear cells into the infarcted and ischemic myocardial tissue via the intracoronary route using a balloon catheter in 10 acute MI patients (Strauer et al, 2002). Results were positive with significant decrease in the infarct region, improvement in stroke volume index, left ventricular end systolic volume and contractility and myocardial perfusion after 3 months post transplantation. In a randomized controlled clinical trial, Wollert and colleagues also reported enhanced left ventricular systolic function primarily in the myocardial segments adjacent to the infarcted area upon intracoronary transplantation of bone marrow cells (Wollert et al, 2004).

In another study, 8 patients with severe ischemic heart disease received autologous bone marrow mononuclear cells via intramyocardial injection using a NOGA

guiding system and at 3 months follow-up, they demonstrated significant increase in neovascularization and accompanied improvement in regional wall thickening (Tse et al, 2003). Autologous bone marrow mononuclear cells were also transplanted in 14 end-stage ischemic heart disease patients by transendocardial injection also using the NOGA guiding system in a non randomized, open-labeled study (Perin et al, 2003). At 2 and 4 months follow-up, there was a significant improvement in global left ventricular function. Electromechanical mapping revealed significant mechanical improvement of the injected segments of the myocardium after 4 months. A similar clinical trial done by Strauer and colleagues in 18 chronic heart patients further showed that metabolic regeneration of the infarcted and chronically avital myocardial tissue was realized upon cell transplantation (Strauer et al, 2005).

Significant improvement in myocardial perfusion was also observed in 4 out of 6 CABG patients who underwent autologous bone marrow-derived $AC133^{+}$ cell transplantation after 9 months post-transplantation. (Stamm et al, 2003). Another study performing intracoronary administration of highly enriched $CD133^{+}$ cells into 19 acute myocardial infarction patients showed favourable results with significant improvement in left ventricular performance but was associated with increased incidence of coronary events (Bartunek et al, 2005). Assmus and colleagues did a comparative study between bone marrow-derived and peripheral blood-derived progenitor cells in restoring revascularization after acute MI and found no significant difference between them (Assmus et al, 2002).

Even though clinical data revealed feasibility, safety and some benefits towards the use of bone marrow cell transplantation in post-myocardial and bypass surgery

patients, further studies involving large patient numbers, randomized, double-blinded, placebo-controlled are necessary before any definite conclusions of using such therapy is made. It is also necessary to note that in most of the studies, the effect of cell therapy alone is not analyzed since the patient population usually has undergone other types of treatment such as stenting, CABG and perfusion prior to cell transplantation.

Peripheral blood-derived EPCs

Circulating EPCs in peripheral blood is usually low during normal circumstances but can be increased by bone marrow stem cell mobilization with granulocyte colony stimulating factor (G-CSF), VEGF and HMG-CoA reductase inhibitors (Iwaguro et al, 2002; Vasa et al, 2001; Kalka et al, 2000; Peichev et al, 2000; Takahashi et al, 1999). These circulating EPCs are also upregulated in numbers in the circulation either after vascular injury or during tumor growth. Transplantation of EPCs into animal hindlimb ischemia models significantly improved blood flow recovery and capillary density. Kalka and colleagues demonstrated that ex vivo expanded human EPCs successfully promoted neovascularization of ischemic limb and the rate of limb loss was significantly reduced (Kalka et al, 2000).

Similar success was also obtained with EPC transplantation into MI models. Human EPCs derived from peripheral blood mononuclear cells injected in athymic nude rats showed increased number of capillaries of both human and rat origin at 2 weeks after transplantation (Kawamoto et al, 2001; Kocher et al, 2001). These cells were cultured and expanded ex vivo for 7 days in EC basal medium and then labeled as the ex-vivo expanded EPC-enriched fraction (Kawamoto et al, 2001). Reduction in cardiomyocyte apoptosis resulting in a lesser extent of scarring was also observed. Echocardiography

revealed ventricular dimensions that were significantly smaller and fractional shortening that was significantly greater in the transplanted group. Similar results were obtained by Kocher and colleagues who transplanted G-CSF mobilized $CD34^+$ human cells that contain both hematopoietic stem cells and EPCs (Kocher et al, 2001). Their results showed that while human-derived ECs were mainly located exclusively within the central infarct area, the rat-derived ECs were found in abundance in the peri-infarct area. These studies suggested that the transplanted EPCs are capable of differentiating in vivo into ECs to participate in vasculogenesis and angiogenesis in the rat myocardium and also secrete angiogenic factors that may be responsible for the mobilization, homing and differentiation of rat endogeneous stem cells. Transplantation of autologous EPCs from swine peripheral blood was also recently reported (Kawamoto et al, 2003). After 4 weeks post transplantation, increased angiographic collateral development, capillary density and myocardial function were observed.

Umbilical cord-derived EPCs

EPCs can usually be obtained in greater amounts from umbilical cord blood and they are of higher mitotic rate and have longer telomere as compared to bone marrow-derived cells (Forraz et al, 2002). Furthermore, the capability of bone marrow to produce effective EPCs usually decrease with aging, therefore making the use of umbilical cord blood to be more attractive (Rao et al, 2001). Human $CD133^+$ progenitor cells from cord blood had been shown to be effective in producing functional recovery in myocardial infarction models of athymic nude rats by preventing scar thinning and left ventricular systolic dilatation (Leor et al, 2005). These cells were found to be located in the newly formed vessel walls as ECs. Another study reported that $CD34^+/CD133^+$ cord blood cells

overexpressed Ang-1, Ang-2, VEGF and their receptor mRNA suggesting a role in regulating angiogenesis (Pomyje et al, 2003). In comparison, $CD34^+/CD133^+$ cells from bone marrow had lower Ang-1 and Tie-2 mRNA expression levels. Cord blood mononuclear cells upon culturing showed numerous cell clusters, spindle shaped adherent cells and cord-like structures. These cells and the cord-like structures were derived mainly from $CD34^+$ mononuclear cells. The adherent cells incorporated acetylated-LDL, released nitric oxide and expressed Flk-1, Ve-cadherin, CD31 and von Willebrand factor (Murohara et al, 2000). Upon transplantation of these cells into ischemic hind limb tissue of immunodeficient nude rats, these cells survived and participated in newly formed capillary networks. Similar studies were done with similar results showing that $CD34^+$ cells from the cord blood expressed endothelial markers and while these markers increased over time upon culturing, stem cells markers such as $CD133^+$ on these same cells disappeared (Fan et al, 2003; Yoo et al, 2003; Wada et al, 2003).

Embryonic stem cell-derived EPCs

EPCs have also been shown to be derived from embryonic stem cells (ESC). This will be discussed in greater lengths in the following segment of the Thesis.

1.7 Embryonic stem cells- a new era in therapeutic angiogenesis

The term ESC originated from the isolation of pluripotent stem cell cultures from mouse blastocysts in 1981 by Evans and Kaufman (Evans et al, 1981) and independently by Martin (Martin 1981). The ESCs were discovered to be capable of self-renewal and prolonged primitive undifferentiated proliferation in culture. They have also been shown

differentiate spontaneously into various cell lineages representative of all three embryonic germ layers which are the ectoderm, mesoderm and endoderm and also the germ cell line when incorporated into chimeras with intact mouse embryos (Bradley et al, 1984; Nagy et al, 1993). This initial isolation of murine ES cells in 1981 heralded a major breakthrough for developmental biology since it provided a simple model system to study the basic processes of early embryonic development and cellular differentiation. The large impact that these murine ES cell lines had on several research fields in the last 20 years had led to intensive efforts being invested into the derivation of human pluripotent stem cell lines.

Three pluripotent cell types have been established from human tissue. They are the human embryonic carcinoma cells (Finch et al, 1967; Andrews et al, 1980; Pera et al, 1989), human embryonic germ (EG) cells (Shamblott et al, 1998) and human embryonic stem cells (HESC) (Thomson et al, 1998; Reubinoff et al, 1998).

Human and murine embryonic carcinoma cell lines were the first pluripotent cell lines to be established. They were derived from the undifferentiated compartment of human and murine germ cell tumours. They can be expanded continuously in culture and can also differentiate into derivatives of all three embryonic germ layers either in vitro or through teratocarcinoma formation. However, these cells seem to have less differentiating capacity as compared to ESC and they are usually aneuploid, making them unsuitable for clinical applications. Pluripotent human and murine EG cell lines were derived from primordial germ cells in the genital ridges of the developing embryos, around 5 to 9 weeks after fertilization in humans.

HESCs are derived from the inner cell mass of human blastocysts which are produced via in vitro fertilization. The derivation procedure begins with the selective removal of the outer trophoblast layer of the blastocysts via immunosurgery. These outer trophoblast cells of the blastocysts usually give rise to extra-embryonic tissues. The inner cell mass cells were next isolated and cultured on a mitotically inactivated mouse embryonic fibroblasts (MEF) feeder layer. In order to obtain homogeneous colonies of ES cells, cells from the periphery of the colonies were mechanically isolated and recultured in similar fashion. These colonies were then selected, passaged and expanded for the creation of the ES cell lines. The HESCs can proliferate in culture under special conditions in its undifferentiated state for a prolonged period of time and have the capacity to form derivatives of all three germ layers. They also maintain a stable diploid karyotype and continuously express high level of telomerase activity during long term propagation in culture (Thomas et al, 1998; Amit et al, 2000).

HESCs show several important differences from murine ES cells in culture. They tend to proliferate slower and form flat colonies with distinct borders. Murine ES cell grow in spherical colonies with indistinct cell borders. HESCs are also more easily dissociated into single cells (Laslett et al, 2003). They require basic fibroblast growth factor in their culture medium to maintain their pluripotency instead of leukemia inhibitory factor (Thomas et al, 1998; Amit et al, 2000; Reubinoff et al, 2000). Murine and HESCs also differ in some of their antigenic phenotypes. While murine ES cells express embryonic self surface antigen SSEA-1 but not SSEA-3 and SSEA-4, HESCs express the opposite phenotype. Other antigens being expressed by HESCs include TRA-1-60 and TRA-1-81 and they also contain alkaline phosphatase activity.

Pluripotency of HESCs has been shown using two different approaches. The first approach is the demonstration that HESCs can differentiate into cells from the three germ layers in vivo. HESCs upon injecting into immunodeficient mice, develop into benign teratomas containing advanced differentiated tissue types representing all three germ layers (Thomas et al, 1998; Amit et al, 2000). The second approach involves demonstration of ES pluripotency during in vitro differentiation. When HESCs are removed from the MEF feeder layer and allowed to differentiate in suspension, they form 3-dimensional cell aggregates known as embryoid bodies (EBs). These EBs contain cell derivatives from ectodermal, endodermal and mesodermal origins (Itskovitz-Eldor et al, 2000).

1.7.1 In vitro differentiation of HESCs into endothelial progenitor cells and endothelial cells

HESC culture systems have shown that the formation of EBs and induction of cell differentiation results in 3-dimensional vessel-like structures within EBs in a pattern that resembles embryonic revascularization. The capillary areas in the EBs increased during subsequent maturation steps, starting from cell clusters that later sprout into capillary-like structure and eventually organize into a network-like arrangement (Gerecht-Nir et al, 2005; Levernberg et al, 2002). These vasculogenic $CD31^+$ cells when isolated from EBs and grown in culture, express endothelial markers and form vascular structures in vitro and in vivo (Levenberg et al, 2002). The time course of cell differentiation and development of extensive vascular structures within the EBs correlated with the RT-PCR analysis that demonstrated subsequent increase in RNA levels of endothelial genes such as CD31, CD34, Ve-cadherin and GATA-2, peaking at day 13-15. Large scale gene

expression analysis during EBs differentiation from 0 to 4 weeks using gene arrays and real time PCR further revealed that there were additional upregulated expression of vasculogenic growth factors; VEGF, Ang-1 and Ang-2 and PDGF-B, endothelial markers; VCAM-1, Flt-1 and -2 and transcription factors; GATA-1 and -3 (Gerecht-Nir et al, 2005). When direct HESC differentiation was performed by culturing HESCs directly on collagen IV, this resulted to two types of cell population which differ by size. When the small cells were filtered out, there was an upregulation of specific endothelial markers such as CD31, CD34, Tie-2 and GATA-2. When the filtrated cells on collagen IV were replated with VEGF supplementation, cord-like organization of the cells was observed. Addition of PDGF-B induced smooth muscle cells differentiation (Gerecht-Nir et al, 2003). Seeding of HESCs on stromal feeder cells consisting of bone marrow and yolk sac have been shown to induce differentiation into $CD34^+$ cells. About 50% of the $CD34^+$ cells also express endothelial marker, CD31 (Kaufman et al, 2001). However despite the enrichment step, these cells were present only at very low frequency and work is ongoing to increase the yield of the target cell type by modulating the composition of the culture medium.

1.7.2 Mechanisms by which EPCs and ECs induce neovascularization

1.7.2.1 Vasculogenesis

Vasculogenesis is the main process of blood vessel development during embryonic development (Conway et al, 2001; Yancopoulos et al, 2000; Risau et al, 1995). Vasculogenesis originates from primitive EPCs from angioblasts derived from pluripotent ESCs to form primitive vessel network. Blood vessel development first appears outside of the embryo proper, on the yolk sac known as blood islands which form

within the mesoderm adjacent to the extraembryonic endoderm. Here is where the mesodermal precursor known as the hemangioblasts reside and undergo their first critical steps of differentiation. Hemangioblast is the common precursor of both hematopoietic and ECs (Choi et al, 1998). Cells at the perimeter of blood islands give rise to EPCs and those cells at the centre constitute hematopoietic progenitor cells. Vasculogenesis occurs via migration of EPCs to the paraxial mesoderm, proliferation, subsequent differentiation into endothelial cells to form plexus with endothelial tubes and recruitment of other cell types such as pericytes and smooth muscle cells to complete the whole process of vascular formation.

Vasculogenesis was originally believed to be restricted to embryonic development. However, only in recent years, the discovery of circulating EPCs showed that a modified type of vasculogenesis does contribute to neovascularization in adults. In adults, EPCs originate from bone marrow, peripheral blood and umbilical cord (Szmitko et al; 2003; Walter et al, 2002; Asahara et al, 1999b; Isner et al, 1999). Circulating EPCs usually have high proliferation rate and home into sites of neovascularization postnatally via orchestrated signals of various growth factors and receptors (Lin et al, 2000).

1.7.2.2 Angiogenesis

Angiogenesis involves the extension of pre-existing primitive vasculature by the sprouting of new capillaries into the surrounding tissues through migration and proliferation of mature ECs (Madeddu 2005; Conway et al, 2001; Folkman et al, 1992). This process occurs spontaneously under a variety of stresses such as inflammation, wound healing, peripheral vascular disease, acute and chronic myocardial ischemia. The process begins with vasodilation, extravasation of plasma proteins so as to create a

temporary support structure for the migrating ECs and degradation of extracellular matrix by metalloproteinases. With the physical barriers no longer intact, ECs are free to migrate and assemble into solid cords. Finally, stabilization and remodeling of the newly formed vessels into 3-dimensional networks take place to complete the whole process (Risau 1997).

1.7.2.3 Arteriogenesis

Arteriogenesis refers to the maturation of capillary blood vessels into mature arteriolar blood vessels with recruitment of monocytes and macrophages which produce the cytokines and growth factors required for collateral growth and subsequent stimulation and recruitment of smooth muscle cells in the tunica media (Madeddu et al, 2005; Carmeliet 2003; Conway et al, 2001). These arterioles are normally enlarged in size and able to support high transportation capacity. These blood vessels are known to form true collateral blood vessels during ischemia.

1.8 Overall aim of the study

The overall aim of this study is to assess the efficacy of peptide therapy and cell-based therapy using HESC-derived EPCs in regulating inflammatory cytokines expression and forming therapeutic blood vessels via angiogenesis respectively for the treatment of heart failure. The following chapters will cover the two studies in greater detail.

1.9 Bibliography

Website

American Heart Association. Heart disease and stroke statistics- 2006 update. www.americanheart.org

Ministry of Health, Singapore. Health facts Singapore 2005. www.moh.gov.sg

World Health Organization. The World Health Report 2003. Geneva, Switzerland. www.who.int/whr/en/

Report

World Health Organization. .Preventing Chronic Diseases: a vital investment

Literature

Aikawa R, Nagai T, Tanaka M, Zou Y, Ishihara T, Takano H, Hasegawa H, Akazawa H, Mizukami M, Nagai R, Komuro I. Reactive oxygen species in mechanical stress-induced cardiac hypertrophy. Biochem Biophys Res Commun 2001; 289:901-907

Ali S, Becker MW, Davis MG, Dorn WG. Dissociation of vasoconstrictor-stimulated basic fibroblast growth factor expression from hypertrophic growth in cultured vascular smooth muscle cells. Relevant roles of protein kinase C. Circ Res 1994; 75: 836-843

Amit M, Carpenter MK, Inokuma MS, Chiu CP, Harris CP, Waknitz MA, Itskovitz-Eldor J, Thomson JA. Clonally derived human embryonic stem cell lines maintain pluripotency and proliferative potential for prolonged periods of culture. Dev Biol 2000; 227: 271-278

Andrews PW, Bronson DL, Benham F, Strickland S, Knowles BB. A comparative study of eight cell lines derived from human testicular teratocarcinoma. Int J Cancer 1980; 26: 269-280

Asahara T, Masuda H, Takahashi T, Kalka C, Pastore C, Silver M, Kearne M, Magner M, Isner JM. Bone marrow origin of endothelial progenitor cells responsible for postnatal vasculogenesis in physiological and pathological neovascularization. Circ Res 1999b; 85: 221-228

Asahara T, Takahashi T, Masuda H, Kalka C, Chen D, Iwaguro H, Inai Y, Silver M, Isner JM. VEGF contributes to postnatal neovascularization by mobilizing bone-marrow-derived endothelial progenitor cells. Embo J 1999; 18: 3964-3972

Assmus B, Schachinger V, Teupe C, Britten M, Lehmann R, Dobert N, Grunwald F, Aicher A, Urbich C, Martin H, Holezer D, Dimmeler S, Zeiher AM. Transplantation of

progenitor cells and regeneration enhancement in acute myocardial infarction (TOPCARE-AMI). Circulation 2002; 106: 3009-3017

Aukrust P, Ueland T, Lien E, Bendtzen K, Muller F, Andreassen AK, Norody I, Aass H, Espevik T, Simonsen S, Froland SS, Gullestad L. Cytokine network in congestive heart failure secondary to ischemic or idiopathic dilated cardiomyopathy. Am J Cardiol 1999; 83: 376-382

Ball SG. The sympathetic nervous system and converting enzyme inhibition. J Cardiovasc Pharmacol 1989; 13(3):S17-S21

Banai S, Jaklitsch MT, Shou M, Lazarous DF, Scheinowitz M, Biro S, Epstein SE, Unger EF. Angiogenic-induced enhancement of collateral blood flow to ischemic myocardium by vascular endothelial growth factor in dogs. Circulation 1994; 89(5):2183-2189

Banai S, Shweiki D, Pinson A, Chandra M, Lazarovici G, Keshat E. Upregulation of vascular endothelial growth factor expression induced by myocardial ischemia: implications for coronary angiogenesis. Cardiovasc Res 1994; 28: 1176-1179

Barleon B, Sozzani S, Zhou D, Weich HA, Mantovani A, Marme D. Migration of human monocytes in response to vascular endothelial growth factor (VEGF) is mediated via the VEGF receptor flt-1. Blood 1996; 87: 3336-3343

Bartunek J, Vanderheyden M, Vandekerckhove B, Mansour S, De Bruyne B, De Bondt P, Van Haute I, Lootens N, Heyndrickx G,Wijns W. Intracoronary injection of CD133-positive enriched bone marrow progenitor cells promotes cardiac recovery after recent myocardial infarction: feasibility and safety. Circulation 2005; 112: I178- I183

Baumgartner I, Rauh G, Pieczek A, Wuensch D, Magner M, Kearneny M, Schainfeld R, Isner JM. Lower-extremity edema associated with gene transfer of naked DNA vascular endothelial growth factor. Ann Int Med 2000; 132:880-884

Biswas SS, Hughes GC, Scarborough JE, Domkowski PW, Diodato L, Smith ML, Landolfo C, Lowe JE, Annex BH, Landolfo KP. Intramyocardial and intracoronary basic fibroblast growth factor in porcine hibernating myocardium: a comparative study. J Thorac Cardiovasc Surg. 2004; 127: 34-43

Blum A and Miller H. Pathophysiology role of cytokines in congestive heart failure. Ann Rev Med 2001; 52:15-27

Blum A and Miller H. Role of cytokines in heart failure. Am Heart J 1998; 135(2): 181-186

Bolger AP, Anker SD. Tumour necrosis factor in chronic heart failure: a peripheral view on pathogenesis, clinical manifestations and therapeutic implications. Drugs 2000; 60:1245-1257

Bozkurt B, Kribs S, Clubb Jr M, Michael LH, Didenko VV, Hornsby PJ, Seta Y, Oral H, Spinale FG, Mann DL. Pathophysiologically relevant concentrations of tumour necrosis factor –alpha promote progressive left ventricular dysfunction and remodeling in rats. Circulation 1998; 97: 1382-1391

Bradley A, Evans M, Kaufman MH, Robertson E. Formation of germ-line chimaeras from embryo-derived teratocarcinoma cell lines. Nature 1984; 309: 255-256

Bristow MR, Saxon LA, Boehmer J, Krueger S, Kass DA, Marco TD, Carson P, DiCarlo L, DeMets D, White BG, DeVries DW, Feldman AM. Cardiac-resynchronization therapy with or without an implantable defibrillator in advanced chronic heart failure. N Engl J Med 2004; 350:2140-2150

Brogi E, Wu T, Namiki A, Isner JM. Indirect angiogenic cytokines upregulate VEGF and bFGF gene expression in vascular smooth muscle cells, whereas hypoxia upregulates VEGF expression only. Circulation 1994; 90: 649-652

Bryant D, Becker L, Richardson J, Shelton J, Franco F, Peshock R, Thompson M, Giroir B. Cardiac failure in transgenic mice with myocardial expression of tumour necrosis factor-alpha. Circulation 1998; 97(14): 1375-1381

Byrne JA, Grieve DJ, Cave AC, Shah AM. Oxidative stress and heart failure. Arch Mal Coeur 2003; 96:214-221

Carmeliet P. Angiogenesis in health and disease. Nat Med 2003; 9: 653-660

Carmeliet P, Ferreira V, Breier G, Pollefeyt S, Kieckens L, Gertsenstein M, Fahrig M,Vandenhoeck A, Harpal K,Eberhardt C, Declercq C, Pawling J,Moons L, Collen D,Risau W, Nagy A. Abnormal blood vessel development and lethality in embryos lacking a single VEGF allele. Nature 1996; 380:435-439

Choi K. Hemangioblast development and regulation. Biochem Cell Biol 1998b; 76: 947-956

Choi K, Kennedy M, Kazarov A, Papadimitriou JC, Keller G. A common precursor for heamtopoietic and endothelial cells. Development 1998; 125: 725-732

Clauss M, Weich H, Breier G, Knies U**,** Röckl W**,** Waltenberger J, Risau W. The vascular endothelial growth factor receptor Flt-1 mediates biological activities. Implications for a functional role of placenta growth factor in monocyte activation and chemotaxis. J Biol Chem 1996;271: 17629-17634

Cleutjens JP, Kandala JC, Guarda E, Guntaka RV, Weber KT. Regulation of collagen degradation in the rat myocardium after infarction. J Mol Cell Cardiol 1995; 27:1281-1292

Cohen T, Nahari D, Cerem LW, Neufeld G, Levi BZ. Interleukin-6 induces the expression of vascular endothelial growth factor. J Biol Chem 1996; 271: 736-741

Cohn JN. Structural basis for heart failure. Ventricular remodeling and its pharmacological inhibition. Circulation 1995; 91: 2504-2507

Comstock KL, Krowne KA, Page MT, Martin D, Ho P, Pedraza M, Castro EN, Nakajima N, Glembotski CC, Quintana PJ, Sabbadini RA. LPS induced TNF alpha release from and apoptosis in rat cardiomyocytes: obligatory role for CD14 in mediating the LPS response. J Mol Cell Cardiol 1998; 30(12): 2761-2775

Conget PA, Minguell JJ. Phenotypical and functional properties of human bone marrow mesenchymal progenitor cells. J Cell Physiol 1999; 181: 67-73

Conway EM, Collen D, Carmeliet P. Molecular mechanisms of blood vessel growth. Cardiovasc Res 2001; 49: 507-521

Crottogini A, Meckert PC, Vera Janavel G, Lascano E, Negroni J, Del Valle H, Dulbecco E, Werba P, Cuniberti L, Martinez V, De Lorenzi A, Telayna J, Mele A, Fernandez JL, Marangunich L, Criscuolo M, Capogrossi MC, Laguens R. Arteriogenesis induced by intramyocardial vascular endothelial growth factor 165 gene transfer in chronically ischemic pigs. Hum Gene Ther. 2003;14: 1307-18.

Deten A, Volz HC, Briest W, Zimmer HG. Cardiac cytokine expression is upregulated in the acute phase after myocardial infarction. Experimental studies in rats. Cardiovasc Res 2002; 55: 329-340

Dor Y, Porat R, Keshet E. Vascular endothelial growth factor and vascular adjustments to perturbations in oxygen homeostasis. Am J Physiol 2001; 280:C1367-C1374

Dvorak HF, Brown LF, Detmar M, Dvorak AM. Vascular permeability factor/vascular endothelial growth factor, microvascular hyperpermeability and angiogenesis. Am J Pathol 1995; 146: 1029-1039

Esler M, Jennings G, Korner P, Willett I, Dudley F, Hasking G, Anderson W, Lambert G. Assessment of human sympathetic nervous system activity from measurements of norepinephrine turnover. Hypertension 1988; 11:3-20

Esser S, Lampugnani MG, Corada M, Dejana E, Risau W. Vascular endothelial growth factor induces VE-cadherin tyrosine phosphorylation in endothelial cells. J Cell Sci 1998; 282: 946-949

Evans MJ, Kaufman MH. Establishment in culture of pluripotential cells from mouse embryos. Nature 1981; 292: 154-156

Fan CL, Li Y, Gao PJ, Liu JJ, Zhang XJ, Zhu DL. Differentiation of endothelial progenitor cells from human umbilical cord blood CD34+ cells in vitro. Acta Pharmacol Sin 2003; 24: 212-218

Ferrara N, Davis-Smith T. The biology of vascular endothelial growth factor. Endocr Rev 1997; 18: 4-25

Ferrara N, Carver-Moore K, Chen H, Dowd M, Lu L, O'Shea KS, Powell-Braxton L, Hillan KJ, Moore MW. Heterozygous embryonic lethality induced by targeted inactivation of the VEGF gene. Nature 1996; 380:439-442

Ferrari R, Backett T, Confortini R, Opasich C, Febo O, Corti A, Cassani G, Visioli O. Tumour necrosis factor soluble receptors in patients with some various degrees of congestive heart failure. Circulation 1995; 92:1487-1493

Ferrari R. Tumour ncerosis factor in CHF: a double facet cytokine. Cardiovasc Res 1998; 37:554-559

Finch BW, Ephrussii B. Retention of multiple developmental potentialities by cells of a mouse testicular teratocarcinoma during prolonged culture in vitro and their extinction upon hybridization with cells of permanent lines. Proc Natl Acad Sci USA 1967; 57: 615-621

Fishbein MC, Maclean D, Maroko PR. The histopathologic evolution of myocardial infarction. Chest 1978; 73:843-849

Folkman J, Shing Y. Angiogenesis. J Biol Chem 1992; 267: 10931-10934

Forraz N, Pettengell R, Deglesne PA, McGuckin CP. $AC133^{+}$ umbilical cord blood progenitors demonstrate rapid self-renewal and low apoptosis. Br J Hematol 2002; 119: 516-524

Frangogiannis NG, Smith CW, Entman ML. The inflammatory response in myocardial infarction. Cardiovasc Res 2002. 53: 31-47

Frangogiannis NG, Youker KA, Rossen RD, Gwechenberger M, Lindsey MH, Mendoza LH, Michael LH, Ballantyne CM,Smith W, Entman ML. Cytokines and microcirculation in ischemia and reperfusion. J Mol Cell Cardiol 1998; 30: 2567-2576

Fuchs S, Baffour R, Zhou YF, Shou M, Pierre A, Tio FO, Weissman NJ, Leon MB, Epstein SE, Kornowski R. Transendocardial delivery of autologous bone marrow cell enhances collateral perfusion and regional function in pigs with chronic experimental myocardial ischemia. J Am Coll Cardiol 2001; 37: 1726-1732

Gerber HP, Dixit V, Ferrara N. Vascular endothelial growth factor induces expression of the antiapoptotic proteins Bcl-2 and A1 in vascular endothelial cells. J Biol Chem 1998a; 273: 13313-13316

Gerber HP, McMurtrey A, Kowalski J, Yan M, Keyt BA, Dixit V, Ferrara N. VEGF regulates endothelial cell survival by the PI3-kinase/Akt signal transduction pathway. Requirement for Flk-1/KDR activation. J Biol Chem 1998b; 273: 30366-30343

Gerecht-Nir S, Dazard JE, Golan-Mashiach M, Osenberg S, Botvinnik A, Amariglio N, Domany E, Rechavi G, Givol D, Itskovitz-Eldor J. Vascular gene expression and phenotypic correlation during differentiation of human embryonic stem cells. Dev Dyn 2005; 232: 487-497

Gerecht-Nir S, Ziskind A, Cohen S, Itskovitz-Eldor J. Human embryonic stem cells as an in vitro model for human vascular development and the induction of vascular differentiation. Lab Invest 2003; 83: 1811- 1820

Gilgenkrantz H, Duboc D, Juillard V, Couton D, Pavirani A, Guillet JG, Briand P, Khan A. Transient expression of genes transferred *in vivo* into heart using first-generation adenoviral vectors: Role of immune response. Hum Gene Ther 1995; 6:1265-1274

Glennon PE, Daddoura S, Sale EM, Sale GJ, Fuller SJ, Sugden PH. Depletion of mitogen-activated protein kinase using an antisense oligonucleotide approach downregulates the phenylalanine-induced hypertrophic response in rat cardiac myocytes. Circulation Research 1996; 78:954-961

Gojo S, Gojo N, Takeda Y, Mori T, Abe H, Kyo S, Hata J, Umezawa A. In vivo cardiovasculogenesis by direct injection of isolated adult mesenchymal stem cells. Exp Cell Res 2003; 288: 51-59

Grieve DJ, Byrne JA, Cave AC, Shah AM. Role of oxidative stress in cardiac remodeling after myocardial infarction. Heart, Lung and Circulation 2004; 13(2):132-138

Gurevitch J, Froklis I, Yuhas Y, Matsa M, Mohr R, Yakirevich V. Tumor necrosis factor –alpha is released from the isolated heart undergoing ischemia and reperfusion. J Am Coll Cardiol 1996; 28:247-252

Gwechenberger M, Mendoza LH, Youker KA, Frangogiannis NG, Smith CW, Michael LH, Entman ML. Cardiac myocytes produce interleukin-6 in culture and in viable border zone of reperfused infarctions. Circulation. 1999; 99(4):546-51

Gyongyosi M, Khorsand A, Zamini S, Sperker W, Strehblow C, Kastrup J, Forgensen E, Hesse B, Tagil K, Botker HE, Ruzlyyo W, Teresinska A, Dudek D, Hubalewska A, Ruck A, Nielsen SS, Graf S, Mundigler G, Novak J, Sochor H, Maurer G, Glogar D, Sylven C. NOGA-guided analysis of regional myocardial perfusion abnormalities treated with intramyocardial injections of plasmid encoding vascular endothelial growth factor A-165

in patients with chronic myocardial ischemia: subanalysis of the EUROINJECT-ONE multicenter double-blind randomized study. Circulation 2005; 112:I157-165

Habib FM, Springall DR, Davies GJ, Oakley CM, Yacub MH, Polak JM. Tumour necrosis factor and inducible nitric oxide synthase in dilated cardiomyopathy. Lancet 1996; 347: 1151-1153

Harada K, Friedman M, Lopez JJ, Wang SY, Li J, Prasad PV, Pearlman JD, Edelman ER, Sellke FW, Simons M. Vascular endothelial growth factor administration in chronic myocardial ischemia. Am J Physiol 1996; 270(5): H1791-H802

Hariawala MD, Horowitz JR, Esakof D, Sheriff DD, Walter DH, Keyt B, Isner JM, Symes JF. VEGF improves myocardial blood flow but produces EDRF-mediated hypotension in porcine hearts. J Surg Res 1996; 63(1): 77-82

Haywood GA, Tsao PS, von der Leyen HE, Mann MJ, Keeling PJ, Trindade PT, Lewis NP, Byrne CD, Rickenbacher PR, Bishopric NH, Cooke JP, McKenna WJ, Fowler MB. Expression of inducible nitric oxide synthase in human heart failure. Circulation 1996; 93:1087-94

Hedman M, Hartikainen J, Syvanne M, Stjernvall J, Hedman A, Kivela A, Vanninen E, Mussalo H, Kauppila E, Simula S, Narvanen O, Rantala A, Peuhkurinen K, Nieminen MS, Laakso M, Yla-Herttuala S. Safety and feasibility of catheter-based local intracoronary vascular endothelial growth factor gene transfer in the prevention of postangioplasty and in-stent restenosis and in the treatment of chronic myocardial ischemia: phase II results of the Kuopio Angiogenesis Trial (KAT). Circulation 2003; 107:2677-2683

Hendel RC, Henry TD, Rocha-Singh K, Isner JM, Kereiakes DJ, Giordano FJ, Simons M, Bonow RO. Effect of intracoronary recombinant human vascular endothelial growth factor in myocardial perfusion: evidence for a dose-dependent effect. Circulation 2000; 101: 118-121

Henry TD, Annex BH, McKendall GR, Azrin MA. Lopez JJ,Giordano FJ, Shah PK, Willerson JT, Benza RL, Berman DS, Gibson CM, Bajamonde A, Rundle AC, Fine J, Mc Cluskey ER; VIVA Investigators. The VIVA trial: Vascular endothelial growth factor in Ischemia for Vascular Angiogenesis. Circulation 2003; 107(10):1359-1365

Henry TD, Rocha-Singh K, Isner JM, Kereiakes DJ, Giordano FJ, Simons M, Losordo DW, Hendel RC, Bonow RO, Eppler SM, Zioncheck TF, Holmgren EB, McCluskey ER. Intracoronary administration of recombinant human vascular endothelial growth factor patients with coronary artery disease. Am J Heart 2001; 142(5):872-880

Hirota H, Yoshida K, Kishimoto T, Taga T. Continuous activation of gp130, a signaling-transdcuing receptors component for interleukin-6 related cytoines, causes myocardial hypertrophy in mice. Proc Natl Acad Sci USA 1995; 92: 4862-4866

Irwin MW, Mak S, Mann DL, Qu R, Penninger JM, Yan A, Dawood F, Wen WH, Shou Z, Liu P. Circulation 1999; 99: 1492-1498

Isner JM, Asahara T. Angiogenesis and vasculogenesis as therapeutic strategies for postnatal neovascularization. J Clin Invest 1999; 103: 1231-1236

Itzkovitz-Eldor J, Schuldiner M, Karsenti D, Eden A, Yanuka O, Amit M, Soreq H, Benvenisty N. Differentiation of human embryonic stem cells into embryoid bodies comprising the three embryonic germ layers. Mol Med 2000; 6: 88-95

Iwaguro H, Yamaguchi J, Kalka C, Murasawa S. Masuda H, Hayashi S, Silver M, Li T, Isner JM, Asahara T. Endothelial progenitor cell vascular endothelial growth factor gene transfer for vascular regeneration. Circulation 2002; 105: 732-738

Jackson KA, Majka SM, Wang H, Pocius J, Hartley CJ, Majesky MW, Entman ML, Michael LH, Hirschi KK, Goodell MA. Regeneration of ischemic cardiac muscle and vascular endothelium by adult stem cells. J Clin Invest 2001; 107: 1395-1402

Jiang Y, Jahagirder BN, Reinhardt RL, Schwartz RE, Keene CD, Ortiz-Gonzalez XR, Reyes M, Lenvik T, Lund T, Blackstad M, Du J, Aldrich S, Lisberg A, Low WC, Largaespada DA, Verfaillie CM. Pluripotency of mesenchymal stem cells derived from adult marrow. Nature 2002; 418: 41-49

Ju H, Zhao S, Tappia PS, Panagia V, Dixon IMC. Expression of Gq alpha and PLC-beta in scar and border tissue in heart failure due to myocardial infarction. Circulation 1998; 97: 892-899

Kalka C, Masuda H, Takahashi T, Kalka-Moll WM, Silver M, Kearney M, Li T, Isner JM, Asahara T. Transplantation of ex vivo expanded endothelial progenitor cells for therapeutic neovascularization. Proc Natl Acad Sci USA 2000; 28: 3422-3427

Kamihata H, Matsubara H, Nishiue T, Fujiyama s, Tsutsumi Y, Ozono R, Masaki H, Mori Y, Iba O, Tateishi E. Kosaki A, Shintani S, Murohara T, Imaizumi T, Iwasaka T. Implantation of bone marrow mononuclear cells into ischemic myocardium enhances collateral perfusion and regional function via side supply of angioblasts, angiogenic ligands and cytokines. Circulation 2001; 104: 1046-1052

Kapadia S, Torre-Amione G, Yokoyama T, Mann DL. Soluble TNF binding proteins modulate the negative inotropic effects of TNF-α in vitro. Am J Physiol 1995; 268(2 Pt 2): H517-525

Kapadia S, Lee J, Torre-Amione G, Birdsall HH, Ma TS, Mann DL. Tumour necrosis factor-α gene and protein expression in adult feline myocardium after endotoxin administration. J Clin Invest 1995a; 96(2):1042-1052

Karkkainen MJ, Makinen T, Alitalo K. Lymphatic endothelium: a new frontier of metastasis research. Nat Cell Biol 2002; E2-E5

Kastrup J, Jorgensen E, Ruck A, Tagil K, Glogar D, Ruzyllo W, Botker HE, Dudek D, Drvota V, Hesse B, Thuesen L, Blomberg P, Gyongyosi M, Sylven C: Euroinject One Group. Direct intramyocardial plasmid vascular endothelial growth factor-A165 gene therapy in patients with stable severe angina pectoris. A randomized double-blinded placebo-controlled study: the Euroinject One Trial. J Am Coll Cardiol 2005; 45:982-988

Katz SD, Rao R, Berman JW, Schwarz M, Demopoulos L, Bijou R, LeJemtel TH. Pathophysiological correlates of increased serum tumour necrosis factor in patients with congestive heart failure: relation to nitric oxide-dependent vasodilation in the forearm circulation. Circulation 1994; 90:12-16

Kaufman DS, Hanson ET, Lewis RL, Auerbach R, Thomson JA. Hematopoietic colony-forming cells derived from human embryonic stem cells. Proc Natl Acad Sci USA 2001; 98: 10716-10721

Kawamoto A, Tkebuchava T, Yamaguchi J, Nishimura H, Yoon YS, Milliken C, Uchida S, Masuo o, Iwaguro H, Ma H, Hanley A, Silver M, Kearney M, Losordo DW, Isner JM, Asahara T. Intramyocardial transplantation of autologous endothelial progenitor cells for therapeutic neovascularization of myocardial ischemia. Circulation 2003; 107: 461-468

Kawamoto A, Gwon HC, Iwaguro H, Yamaguchi JI, Uchida S, Masuda H, Silver M, Ma H, Kearney M, Isner JM, Asahara T. Therapeutic potential of ex vivo expanded endothelial progenitor cells for myocardial ischemia. Circulation 2001; 103: 634-637

Keck PJ, Hauser SD, Krivi G, Sanzo K, Warren T, Feder J, Connolly DT. Vascular permeability factor, an endothelial cell mitogen related to PDGF. Science 1989; 246: 1309-1312

Kelly RA, Smith TW. Cytokines and cardiac contractile function. Circulation 1997; 95: 778-781

Khan TA, Selke FW, Laham RJ. Gene therapy progress and prospects: Therapeutic angiogenesis for limb and myocardial ischemia. Gene Ther 2003; 10:285-291

Kim E-JK, Li RK, Weisel RD, Mickle DA, Jia ZQ, Tomita S, Sakai T,Yau TM. Angiogenesis by endothelial cell transplantation. J Thorac Cardiovasc Surg 122; 963-971

Kocher AA, Schuster MD, Szabolcs MJ, Takuma S, Burkhoff D, Wang J, Homma S, Edwrads NM, Itescu S. Neovascularization of ischemic myocardium by human bone marrow-derived angioblasts prevents cardiomyocytes apoptosis, reduces remodeling and improves cardiac function. Nature Med 2001; 7: 430-436

Kodoma H, Fukuda K, Pan J, Makino S, Baba A, Hori S, Ogawa S. Leukemia inbitory factor, a potent cardiac hypertrophic cytokine, activates the JAK/STAT pathways in rat cardiomyocytes. Circ Res 1997; 81: 656-663

Krijnen PAJ, Nijmeijer R, Meijer CJLM, Visser CA, Hack CE, Niessen HWM. Apoptosis in myocardial ischemia and infarction. J Clin Pathology 2002; 55:801-811

Krowne KA, Page MT, Nguyen C, Zechner D, Gutierrez V, Comstock KL, Glembotski CG, Quintana PJE, Sabbadini RA. Tumour necrosis factor alpha-induced apoptosis in cardiac myocytes: involvement of the sphingolipid signaling cascade in cardiac cell death. J Clin Invest 1996, 98: 2854-2865

Ku DD, Zaleski JK, Liu S, Brock TA. Vascular endothelial growth factor induces EDRF-dependednt relaxation in coronary arteries. Am J Physiol 1993; 265: H586-H592

Kubota T, McTiernan CH, Frye CS, Slawson SE, Lemster BH, Koretsky AP, Demetris AJ, Feldman AM. Dilated cardiomyopathy in transgenic mice with cardiac-specific overexpression of tumour necrosis factor-alpha. Circ Res 1997, 81:627-635

Kunisda K, Hirota H, Fujio Y, Matsui H, Tani Y, Yamauchi-Takihara K, Kishimoto T. Activation of JAK-STAT and MAP kinases by leukemia inhibitory factor through gp130 in cardiac myocytes. Circulation 1996; 94: 2626-2632

Laitinen M, Gene transfer into the carotid artery using an adventitial collar. Comparison of the effectiveness of plasmid-liposome complexes, retroviruses, pseudotyped retroviruses and adenoviruses. Hum Gene Ther 1997; 8:1645-1650

Laslett AL, Filipczyk AA, Pera MF. Characterization and culture of human embryonic stem cells. Trends Cardiovasc Med. 2003; 13: 295-301

Lazarous DF, Shou M, Stiber JA, Hodge E, Thirumurti V, Goncalves L, Unger EF. Adenoviral-mediated gene transfer induces sustained pericardial VEGF expression in dogs: effect on myocardial angiogenesis. Cardiovasc Res 1999; 44:294-302

Lazarous DF, Shou M, Scheinowitz M, Hodge E, Thirumurti V, Kitsiou AN, Stiber JA, Lobo AD, Hunsberger S, Guetta E, Epstein SE, Unger EF. Comparative effects of basic fibroblast growth factor and vascular endothelial growth factor on coronary collateral development and the arterial response to injury. Circulation 1996; 94(5):1974-1082

Leor J, Guetta E, Feinberg MS, Galski H, Bar I, Holbova R, Miller L, Zarin P, Castel D, Barbash IM, Nagler A. Human umbilical cord blood-derived $CD133^{+}$ cells enhance function and repair of the infarcted myocardium. Stem Cells 2005; 24:772-780

Levenberg S, Golub JS, Amit M, Itskovitz-Eldor J, Langer R. Endothelial cells derived from human embryonic stem cells. PNAS 2002; 99: 4391-4396

Levine B, Kalman J, Mayer L, Fillit HM, Packer M. Elevated circulating levels of tumor necrosis factor in congestive heart failure. N Eng J Med 1990; 236-241

Levy AP. Hypoxic regulation of VEGF MRNA stability by RNA-binding proteins. Trends Cardiovasc Med 1998; 8: 246-250

Lin Y, Weisdorf DJ, Solovey A, Hebbel RP. Origins of circulating endothelial cells and endothelial outgrowth from blood. J Clin Invest 2000; 105: 71-77

Li RK, Jia ZQ, Weisel RD, Merante F, Mickle DA. Smooth muscle cell transplantation into myocardial scar tissue improves heart function. J Mol Cell Cardiol 1999; 31: 513-522

Lopez JJ, Laham RJ, Stamler A, Pearlman JD, Bunting S, Kaplan A, Carrozza JP, Selke FW, Simons M. VEGF administration in chronic myocardial ischemia in pigs. Cardiovasc Res 1998; 40(2):272-281

Losordo DW, Vale PR, Hendel RC, Milliken CE, Fortuin FD, Cummings N, Schatz RA, Asahara T, Isner JM, Kuntz RE. Phase I/II placebo-controlled, double-blind, dose-escalating trial of myocardial vascular endothelial growth factor 2 gene transfer by catherter delivery in patients with chronic myocardial ischemia. Circulation 2002; 105:2012-2018

Losordo DW, Vale PR, Symes JF, Dunnington CH, Esakof DD, Maysky M, Ashare AB, Lathi K, Isner JM. Gene therapy for myocardial angiogenesis: initial clinical results with direct myocardial injection of phVEGF165 as sole therapy for myocardial ischemia. Circulation 1998; 98:2800-2804

Luttun A, Carmeliet G, Carmeliet P. Vascular progenitors: from biology to treatment. Trends Cardiovasc Med 2002; 12: 88-96

MacGowan GA, Mann DL, Kormos RL, Feldman AM, Murali S. Crculating interleukin-6 in severe heart failure. Am J Cardiol 1997; 79:1128-1131

Mack CA, Patel SR, Schwartz EA, Zanzonico P, Hahn RT, Ilercil A, Devereux RB, Goldsmith SJ, Christian TF, Sanborn TA, Kovesdi I, Hackett N, Isom OW, Crystal RG, Rosengart TK. Biologic bypass with the use of adenovirus-mediated gene transfer of the complementary deoxyribonucleic acid for vascular endothelial growth factor 121 improves perfusion and function in the ischemic porcine heart. J Thorac Cardiovasc Surg 1998; 115:168-176

Madeddu P. Therapeutic angiogenesis and vasculogenesis for tissue regeneration. Exp Physiol 2005; 90: 315-326

Majno G, Joris I. Apoptosis, oncosis, necrosis. An overview of cell death. Am J Pathol 1995; 146:3-15

Martin GR. Isolation of a pluripotent cell line from early mouse embryos cultured in medium conditioned by teratocarcinoma stem cells. Proc Natl Aca Sci USA 1981; 78: 7634-7638

Mayer NJ, Rubin SA. Molecular and cellular prospects for repair, augmentation and replacement of the failing heart. Am Heart J 1997; 134:577-586

Mazue G, Bertolero MG, Jacob F, Sarmientos P, Roncucci R. Preclinical and clinical studies with recombinant human basic fibroblast growth factor. Ann NY Acad Sci 1991; 638:329-340

Meldrum DR, Meng X, Dinarello CA, Ayala A, Cain BS, Shames BD, Ao L, Banarjee A, Harken AH. Human myocardial tissue TNF-α expression following acute global ischemia in vivo. J Mol Cell Cardiol 1998; 30:1683-1689

Melo LG, Pachori AS, Kong D, Gnecchi M, Wang K, Pratt RE, Dzau VJ. Gene and cell based therapies for heart disease. FASEB 2004; 18(6):648-663

Mie Lee Y, Kim SH, Kim HS, Jin Son M, Nakajima H, Jeong Kwon H, Kim KW. Inhibition of hypoxia-induced angiogenesis by FK228, a specific histone deacetylase inhibitor, via suppression of HIF-1alpha activity. Biochem Biophys Res Commun 2003; 300: 241-246

Millauer B, Wizigmann-Voos S, Schnurch H, Martinez R, Moller NP, Risau W, Ullrich A. High affinity VEGF binding and developmental expression suggest Flk-1 as a major regulator of vasculogenesis and angiogenesis. Cell 1993; 72: 835-846

Min JY, Huang X, Xiang M, Meissner A, Chen Y, Kaplan E, Rana JS, Oettgen P, Morgan JP. Homing of intravenously infused embryonic stem cell-derived cells to injured hearts after myocardial infarction. J Thorac Cardiovasc Surg. 2006; 131: 889-97.

Min JY, Yang Y, Sullivan MF, Ke Q, Converso KL, Chen Y, Morgan JP, Xiao YF. Long-term improvement of cardiac function in rats after infarction by transplantation of embryonic stem cells. J Thorac Cardiovasc Surg. 2003; 125: 361-9

Moore MAS, Hattori K, Heissig B, Shieh J-H, Dias S, Crystal RG, Rafii S. Mobilization of endothelial and hematopoietic stem and progenitor cells by adenovector-mediated of serum levels of SDF-1, VEGF and angiopoietin-1. Ann NY Acad Sci 2001; 938: 36-47

Murell AC, Francis M, Bromley L. Modulation of fibroblast proliferation by oxygen free radicals. Biochem J 1990; 265:659-665

Murohara T, Ikeda H, Duan J, Shintani S, Sasaki K, Eguchi H, Onitsuka I, Matsui K, Imaizumi T. Transplanted cord blood-derived endothelial precursor cells augment postnatal neovascularization. J Clin Invest 2000; 105: 1527-1536

Nagy A, Rossant J, Nagy R, Abramow-Newerly W, Roder JC. Derivation of completely cell culture-derived mice from early-passage embryonic stem cells. Proc Natl Acad Sci U S A. 1993; 90: 8424-8

Neufeld G, Cohen T, Gengrinovitch S, Poltorak Z. Vascular endothelial growth factor (VEGF) and its receptors. FASEB J 1999; 13: 9-22

Neumann FJ, Ott I, Gawaz M, Richardt G, Holzapfel H, Jochum M, Schomig A. Cardiac release of cytokines and inflammatory responses in acute myocardial infarction. Circulation 1995; 92:748-755

Nishida M, Li TS, Hirata K, Yano M, Matsuzaki M, Hamano K. Improvement of cardiac function by bone marrow cell implantation in a rat hypoperfusion heart model. Ann Thorac Surg 2003; 768-774

Olivetti G, Capasso JM, Sonnenblick EH, Anversa P. Side to side slippage of myocytes participates in ventricular wall remodeling acutely after myocardial infarction in rats. Circ Res 1990; 67:23-24

Oral H, Dorn GW, Mann DL. Sphingosine mediates the intermediate negative inotropic effects of tumour necrosis factor-α in the adult mammalian cardiac myocyte. J Biol Chem 1997; 272(8):4836-4842

Orlic D, Kajstura J, Chimenti S, Jakoniuk I, Anderson SM, Li P, Pickel J, McKay R, Nadal-Ginard B, Bodine DM, Leri A, Anversa P. Bone marrow cells regenerate infarcted myocardium. Nature 2001; 410: 701-705

Parissis JT, Adamopoulos S, Karas SM and Kremastinos DT. An overview of inflammatory cytokine cascade in chronic heart failure. Hellenic J Cardiol 2002; 43:18-28

Park JE, Keller HA, Ferrera N. The vascular endothelial growth factor isoforms (VEGF): differential deposition into the subepithelial extracellular matrix and bioactivity of extra cellular matrix-bound VEGF. Mol Cell Biol 1993; 4: 1317-1326

Patel SR, Lell LY, Mack CA, Polce DR, El-Sawy T, Hackett NR, Ilercil A, Jones EC, Hahn RT, Isom OW, Rosengart TK, Crystal RG. Safety of direct myocardial administration of an adenovirus vector encoding vascular endothelial growth factor 121. Hum Gene Ther 1999; 10:1331-1348

Peichev M, Naiyer AJ, Pereira D, Zhu Z, Lane WJ, Williams M, Oz MC, Hicklin DJ, Witte L, Moore MA, Rafii S. Expression of VEGFR-2 and AC133 by circulating human CD34(+) cells identifies a population of functional endothelial precursors. Blood 2000;95: 952-958

Pennica D, Shaw KJ, Swanson TA, Moore MW, Shelton DL, Zoncheck KA, Rosenthal A, Taga T, Paoni NF, Wood WI. Cardiotrophin-I. Biological activities and binding to the

leukemia inhibitory factor receptor/gp130-signaling complex. J Biol Chem 1995; 270: 10915-10922

Pera MF, Cooper S, Mills J, Parrington JM. Isolation and characterization of a multipotent clone of human embryonal carcinoma cells. Differentiation 1989; 42: 10-23

Perin EC, Dohmann HF, Borojevic R, Silva SA, Sousa AM, Mesquita CT, Rossi MI, Carvalho AC, Dutra HS, Dohmann HJ, Silva GV, Belem L, Vivacqua R, Rangel FO, Esporcatte R, Geng YJ, Vaughn WK, Assad JA, Mesquita ET, Willerson JT. Transendocardial autologous bone marrow cell transplantation for severe, chronic ischemic heart failure. Circulation 2003; 107: 2294-2302

Pfeffer MA, Braunwald E. Ventricular remodeling after myocardial infarction: experimental observations and clinical implications. Circulation, 1990;81:1167-1172

Pittenger MF, Mackay AM, Beck SC, Jaiswal RK, Douglas R, Mosca JD, Moorman RA, Simonetti DW, Craig S, Marshak DR. Multilineage potential of adult human mesenchymal stem cells. Science 1999; 284: 143-147

Plenz G, Song ZF, Tjan TDT, Koenig C, Baba HA, Erren M, Flesch M, Wichter T, Scheld HH, Deng MC. Activation of the cardiac interleukin-6 system in advanced heart failure. Eur J Heart Fail 2001; 3:415-421

Pomyje J, Zivny J, Sefc L, Plasilova M, Pytlik R, Necas E. Expression of genes regulating angiogenesis in human circulating hematopoietic cord blood $CD34^{+}/CD133^{+}$ cells. Eur J Haematol 2003; 77: 143-150

Prockop DJ. Marrow stromal cells as stem cells for nonhematopoietic tissues Science 1997; 276: 71-74
Pulkki KJ. Cytokines and cardiomyocyte death. Ann Med 1997; 29:339-343

Rao MS and Mattson MP. Stem cells and ageing: Expanding the possibilities. Mech Ageing Dev 2001; 122:713-734

Reubinoff BE, Pera MF, Fong C, Trounson A, Bongso A. Embryonic stem cell lines from human blastocysts: somatic differentiation in vitro. Nature Biotechnol 2000; 18: 399-404
Risau W, Flamme I: Vasculogenesis. Annual review of cell developmental biology 1995; 11: 73-91

Risau W. Mechanism of angiogenesis. Nature 1997; 386: 671-674

Rose EA, Geljins AC, Moskowitz AJ, Heitjan DF, Stevenson LW, Dembitsky W, Long JW, Ascheim DD, Tierney AR, Levitan RG, Watson JT, Meier P, Ronan NS, Shapiro PA, Lazar RM, Miller LW, Gupta L, Frazier OH, Desvigne-Nickens P, Oz MC, Poirier VL; Randomized Evaluation of Mechanical Assistance for the Treatment of Congestive Heart

Failure (REMATCH) Study Group. Long term mechanical left ventricular assistance for end stage heart failure. N Engl J Med 2001; 345:1435-1443

Rosengart TK, Lee LY, Patel SR, Sanborn TA, Parikh M, Bergman GW, Hachamovitch R, Szulc M, Kligfield PD, Okin PM, Hahn RT, Devereux RB, Post MR, Hackett NR, Foster T, Grasso TM, Lesser ML, Isom OW, Crystal RG. Angiogenesis gene therapy: phase I assessment of direct intramyocardial administration of an adenovirus vector expressing VEGF121 CDNA to individuals with clinically significant severe coronary artery disease. Circulation 1999a; 100:468-474

Rosengart TK, Lee LY, Patel SR, Kligfield PD, Okin PM, Hackett NR, Isom OW, Crystal RG. Six-month assessment of a phase I trial of angiogenic gene therapy for the treatment of coronary artery disease using direct intramyocardial administration of an adenovirus vector expressing the VEGF121 CDNA. Ann Surg 1999b; 230:466-470

Rutanen J, Rissanen TT, Markkanen JE, Gruchala M, Silvennoinen P, Kivela A, Hedman A, Hedman M, Heikura T, Orden MR, Stacker SA, Achen MG, Hartikainen J, Yla-Herttuala S. Adenoviral catheter-mediated intramyocardial gene transfer using the mature form of vascular endothelial growth factor-D induces transmural angiogenesis in porcine heart. Circulation 2004; 109:1029-1035

Ryan HE, Lo J, Johnson RS. HIF-1 alpha is required for solid tumour formation and embryonic vascularization. Embo J 1998; 17: 3005-3015

Sadoshima J, Izumo S. Molecular characterization of angiotensin II induced hypertrophy of cardiac myocytes and hyperplasia of cardiac fibroblasts: critical role of the AT1 receptor subtype. Circulation Research 1993; 73:413-423

Saraste A, Pulkki K. Morphologic and biochemical hallmarks of apoptosis. Cardiovasc Research 2000; 45:528-537

Sarkar N Ruck A, Kallner G, Y-Hassan S, Blomberg P, Islam KB, van der Linden J, Lindblom D, Nygren AT, Lind B, Brodin LA, Drvota V, Sylven C. Effects of intramyocardial injection of phVEGF-A165 as sole therapy in patients with refractory coronary artery disease- 12-month follow-up: angiogenic gene therapy. J Intern Med 2001; 250:373-381

Sato K, Wu T, Laham RJ, Johnson RB, Douglas P, Sellke FW, Bunting S, Simons M, Post MJ. Efficacy of intracoronary or intravenous VEGF165 in a pig model of chronic myocardial ischemia. J Am Coll Cardiol 2001; 37(2): 616-523

Sato Y, Kanno S, Oda N, Abe M, Ito M, Shitara K, Shibuya M. Properties of two VEGF receptors, Flt-1 and KDR in signal transduction. Ann NY Acad Sci 2000; 902: 201-205

Sayeed-Shah U, Mann MJ, Martin J, Grachev S, Reimold S, Laurence R, Dazu V, Cohn LH. Complete reversal of ischemic wall motion abnormalities by combined use of gene

therapy with transmyocardial laser revascularization. J Thorac Cardiovasc Surg 1998; 116: 763-769

Schmidt-Wolf GD & Schmidt-Wolf IG. Non viral and hybrid vectors in human gene therapy: an update. Trends Mol Med 2003; 9:67-72

Schwartz ER, Speakman MT, Patterson M, Hale SS, Isner JM, Kedes LH, Kloner RA. Evaluation of the effects of intramyocardial injection of DNA expressing encoding vascular endothelial growth factor (VEGF) in a myocardial infarction model in the rat-angiogenesis and angioma formation. J Am Coll Cardiol 2000; 35:1323-1330

Selke FW, Wang SY, Stamler A, Lopez JJ, Li J, Simons M. Enhanced microvascular relaxations to VEGF and bFGF in chronically ischemic porcine myocardium. Am J Physiol 1996; 271: H713-H720

Semenza G. Expression of hypoxia-inducible factor 1: mechanisms and consequencesBiochem Pharmacol 2000; 59: 47-53

Senger DR, Claffey KP, Benes JE, Perruzzi CA, Sergiou AP, Detmar M. Angiogenesis promoted by vascular endothelial growth factor: regulation through alpha1beta1 and alpha2beta1 integrins. Proc Natl Acad Sci, USA 1997; 94: 13612-13617

Shalaby F Rossant J, Yamaguchi TP, Gertsenstein M, Wu XF, Breitman ML, Schuh ACl. Failure of blood-island formation and vasculogenesis in Flk-1 deficient mice. Nature 1995; 376: 62-66

Shamblott MJ, Axelman J, Wang SP. Bugg EM, Littlefield JW, Donovan PJ, Blumenthal PD, Huggins GR, Gearhart JD. Derivation of pluripotent stem cells from cultured human primodial germ cells. Proc Natl Acad Sci USA 1998; 95: 13726-13731

Sheng Z, Knowlton K, Chen J, Hoshijima M, Brown JH, Chien KR. Cardiotrophin-I inhibition of cardiac myocyte apoptosis via a mitogen-activated protein kinase-dependent pathway. Divergence from downstream CT-1 signals for myocardial cell hypertrophy. J Biol Chem 1997; 272: 5783-5791

Shibuya M Yamaguchi S, Yamane A, Ikeda T, Tojo A, Matsushime H, Sato M. Nucleotide sequence and expression of a novel human receptor type tyrosine kinase (flt1) closely related to the fms family. Oncogene 1990; 8: 519-527

Shweiki D, Itin A, Soffer D, Keshat E. Vascular endothelial growth factor induced by hypoxia may mediate hypoxia-initiated angiogenesis. Nature 1992; 359: 843-845

Singla DK, Hacker TA, Ma L, Douglas PS, Sullivan R, Lyons GE, Kamp TJ. Transplantation of embryonic stem cells into infarcted mouse heart: formation of multiple cell types. J Mol Cell Cardiol 2006; 40: 195-200

Soker S, Takashima S, Miao HQ, Neufeld G, Klagsbrun M. Neuropilin-1 is expressed by endothelial and tumour cells as an isoform-specific receptor for vascular endothelial growth factor. Cell 1998; 92: 735-745

SOLVD Investigators. Effect of enalapril on survival in patients with reduced left ventricular ejection fractions and congestive heart failure. N Engl J Med 1991; 325: 293-302

Spinale FG. Matrix metalloproteinases: regulation and dysregulation in the failing heart. Circ Res, 2002; 90:520-530

Stamm C, Westphal B, Kleine HD, Petzsch M, Kittner C, Klinge H, Schumichen C, Nienaber CA, Freund N, Steinhoff G. Autologous bone marrow stem cell transplantation for myocardial regeneration. Lancet 2003; 361: 45-46 (AC133 positive cells)

Stavri GT, Zachay IC, Baskerville PA, Martin JF, Erusalimsky JD. Basic fibroblast growth factor upregulates the expression of vascular endothelial growth factor in vascular smooth muscle cells. Synergestic interaction with hypoxia. Circulation 1995; 92: 11-14

Stephanou A, Brar B, Heads R, Knight RD, Marber MS, Pennica D, Latchman DS. Cardiotrophin-I induces heat shock protein accumulation in cultured cardiac myocytes and protects them from stressful stimuli. J Mol Cell Cardiol 1998; 30:849-855

St John Sutton MG, Plappert T, Abraham ET, Smith AL, DeLurgio DB, Leon AR, Loh E, Kocovic DZ, Fisher WG, Ellestad M, Messenger J, Kruger K, Hilpisch KE, Hill MR; Multicenter InSync Randomized Clinical Evaluation (MIRACLE) Study Group. Effect of cardiac resynchronization therapy on left ventricular size and function in chronic heart failure. Circulation 2003; 107:1985-1990

Strauer BE, Brehm M, Zeus T, Bartsch T, Schwannwell C, Antke C, Sorg RV,Kogler G, Wermet P, Muller HW, Kostering M. Regeneration of human infarcted heart muscle by intracoronary autologous bone marrow cell transplantation in chronic artery disease: the IACT study. J Am Coll Cardiol 2005; 46: 1651-1658

Strauer BD, Brehm M, Zeus T, Kostering M, Hernandez A, Sorg RV, Kogler G, Wernet P. Repair of infarcted myocardium by autologous intracoronary mononuclear bone marrow cell transplantation in humans. Circulation 2002; 106: 1913-1918

Szmitko PE, Fedak PW, Weisel RD, Stewart DJ, Kutryk MJ, Verma S. Endothelial progenitor cells: New hope for a broken heart. Circulation 2003; 107: 3093-3100

Taga T, Kishimoto T. Gp130 and interleukin-6 family of cytokines. Annu Rev Immunol 1997; 15:797-819

Takahashi T, Kalka C, Masuda H, Chen D,Marcy S, Kearney M, MagNER m, Isner JM, Asahara T. Ischemia- and cytokine-induced mobilization of bone marrow-derived endothelial progenitor cells for neovascularization. Nat Med 1999; 5: 434-438

Tanaka E, Hattan N, Ando K, Ueno H, Sugio Y, Mohammed MU, Voltchikhina SA, Mori H. Ameriolation of microvascular myocardial ischemia by gene transfer of vascular endothelial growth factor in rabbits. J Thorac Cardiovasc Surg 2000; 120:720-728

Tang YL, Zhao Q, Qin X, Shen L, Cheng L, Phillips MI. Paracrine action enhances the effects of autologous mesenchymal stem cell transplantation on vascular regeneration in rat model of myocardial infarction. Ann Thorac Surg 2005; 80: 229-237

Terman BI, Dougher-Vermazen M, Carrion ME, Dimitrov D, Armellino DC, Gospodarowicz D, Bohlen P. Identification of the KDR tyrosine kinase as a receptor for vascular endothelial cell growth factor. Biochem Biophys REs Commun 1992; 187: 1579-1586

Terman BI, Carrion ME, Kovacs E, Rasmussen BA, Eddy RL, Shows TB. Identification of a new endothelial cell growth factor receptor tyrosine kinase. Oncogene 1991; 1677-1683

Thomas CV, Coker ML, Zellner JL, Handy JR, Crumbley JA III, Spinale FG. Increased matrix metalloproteinase activity and selective upregulation in LV myocardium from patients with end-stage heart failure. Circulation 1998; 97:1708-1715
Thomson JA, Itskovitz-Eldor J, Shapiro SS, Waknitz MA, Swiergiel JJ, Marshall VS, Jones JM. Embryonic stem cell lines derived from human blastocysts. Science 1998; 282: 1145-1147

Tio RA, Tkebuchava T, Scheuermann TH, Lebherz C, Magner M, Kearny M, Esakof DD, Isner JM, Symes JF. Intramyocardial gene therapy with naked DNA encoding vascular endothelial growth factor improves collateral flow to ischemic myocardium. Hum Gene Ther 1999; 10:2953-2960

Tischer E, Mitchell R, Hartman T, Silva M, Gospodarowicz D, Fiddes JC, Abraham JA. The human gene for vascular endothelial growth factor. Multiple protein forms are encoded through alternative exon splicing. J Biol Chem 1991; 266: 11947-11954

Tomita S, Mickle DA, Weisel RD, Jia ZQ, Tumiati LC, Allidina Y, Liu P, Li RK. Improved heart function with myogenesis and angiogenesis after autologous porcine bone marrow stromal cell transplantation. J Thorac Cardiovasc Surg 2002; 123: 1132-1140

Tomita S, Li RK, Weisel RD, Mickle DA, Kim EJ, Sakai T, Jia ZQ. Autologous transplantation of bone marrow cells improves damaged heart function. Circulation 1999; 100: II247-II256

Torre-Amione G, Kapadia S, Benedict C, Oral H, Young JB, Mann DL. Proinflammatory cytokine levels in patients with depressed left ventricular ejection fraction: a report from the studies of left ventricular dysfunction (SOLVD). J Am Coll Cardiol 1996a; 27:1201-1206

Torre-Amione G, Kapadia S, Lee J, Durand JB, Bies RD, Young JB, Mann DL. Tumour necrosis factor alpha and tumour necrosis factor receptors in the failing human heart. Circulation 1996b; 93: 704-711

Tse HF, Kwong YL, Chan JK, Lo G, Ho CL, Lau CP. Angiogenesis in ischaemic myocardium by intramyocardial autologous bone marrow mononuclear cell implantation. Lancet 2003; 361: 47-49

Vale PR, Losordo DW, Milliken CE, McDonald MC, Gravelin LM, Curry CM, Esakof DD, Maysky M, Symes JF, Isner JM. Randomized, single-blind, placebo-controlled pilot study of catheter-based myocardial gene transfer for therapeutic angiogenesis using left ventricular electromechanical mapping in patients with chronic myocardial ischemia. Circulation 2001; 13: 2138-2143

Vale PR, Losordo DW, Milliken CE, Maysky M, Esakof DD, Symes JF, Isner JM. Left ventricular electromechanical mapping to assess efficacy of phVEGF165 gene transfer for therapeutic angiogenesis in chronic myocardial ischemia. Circulation 2000; 102:965-974

Vasa M, Fichtlscherer S, Adler K, Aicher A, Martin H, Zelher AM, Dimmeler S. Increase in circulating endothelial progenitor cells by statin therapy in patients with stable coronary artery disease. Circulation 2001; 103: 2885-2890

Vassali P. The pathophysiology of tumor necrosis factor. Annu Rev Immunol 1992; 10:411-452

Vera Janavel G, Crottogini A, Cabeza Meckert P, Cuniberti L, Mele A, Papouchado M, Fernandez N, Bercovich A, Criscuolo M, Melo C, Laguens R.
Plasmid-mediated VEGF gene transfer induces cardiomyogenesis and reduces myocardial infarct size in sheep. Gene Ther. 2006; 13: 1133-42

Verfaillie CM, Scwartz R, Reyes M, Jiang Y. Unexpected potential of adult stem cells. Ann NY Acad Sci 2003; 996: 231-234

Vicario J, Piva J, Pierini A, Ortega HH, Canal A, Gerardo L, Pfeiffer H, Campos C, Fendrich I, Novero R, Monti A. Transcoronary sinus delivery of autologous bone marrow and angiogenesis in pig models with myocardial injury. Cardiovasc Radiat Med 2002; 3: 91-94

Wada M, Ebihara Y, Ma F, Yagasaki H, Ito M, Takahashi T, Mugishima H, Takahashi S, Tsuji K. Tunica interna endothelial cell kinase expression and hematopoietic and angiogenic potentials in cord blood $CD34^+$ cells. Int J Hematol 2003; 77: 245-252

Walter DH, Dimmeler S. Endothelial progenitor cells: regulation and contribution to adult neovascularization. Herz 2002; 27: 579-588

Wang H, Keiser JA. Vascular endothelial growth factor upregulates the expression of matrix metalloproteinases in vascular smooth muscle cells: role of flt-1. Circ Res 1998; 83:832-840

Wang JS, Shum-Tim D, Chedrawy E, Chiu RC. The coronary delivery of marrow stromal cells for myocardial regeneration: Pathophysiologic and therapeutic implications. J Thorac Cardiovasc Surg 2001; 122: 699-705

Webster KA, Discher DJ, Bishopric NH. Regulation of fos and jun immediate early genes by redox or metabolic stress in cardiac myocytes. Circ Res 1994; 74: 679-686

Wollert KC, Meyer GP, Lotz J, Ringes-Lichtenberg S, Lippolt P, Breidenbach C, Fichtner S, Korte T, Hornig B, Messinger D, Arseniev, L, Hertenstein B, Ganser A, Drexler H. Intracoronary autologous bone-marrow cell transfer after myocardial infarction: the BOOST randomized controlled clinical trial. Lancet 2004; 364: 141-148

Wollert KC, Drexler H. The role of interleukin-6 in the failing heart. Heart Fail Rev 2001; 6: 95-103

Wollert KC, Taga T, Saito M, Narazaki M, Kishimoto T, Glembotski CC, Vernallis AB, Heath JK, Pennica D, Wood WI, Chien KR. Cardiotrophin-1 activates a distinct form of cardiac muscle cell hypertrophy. Assembly of sarcomeric units in series VIA gp130/leukemia inhibitory factor receptor-dependent pathways J Biol Chem. 1996; 271: 9535-45

Yamazaki T, Komuro I, Kudoh S, Zou Y, Shiojima I, Mizuno T, Takano H, Hiroi Y, Ueki K, Tobe K, Kadowaki T, Nagai R, Yazaki Y. Angiotensin II partly mediates mechanical stress-induced cardiac hypertrophy. Circulation Research 1995; 77: 258-265

Yancopoulos GD, Davis S, Gale NW, Rudge JS, Wiegand SJ, Holash J. Vascular-specific growth factors and blood vessel formation. Nature 2000; 407: 242-248

Yla-Herttuala S & Alitalo K. Gene transfer as a tool to induce therapeutic vascular growth. Nature Medicine 2003; 9:694-701

Yokoyama T, Nakano M, Bednarczyk JL, McIntyre BW, Entman M, Mann DL. Tumour necrosis factor-alpha provokes a hypertrophic growth response in adult cardiac myocytes. Circulation 1997; 95:1247-1252

Yokoyama T, Vaca L, Rossen RD, Durante W, Hazarika P, Mann DL. Cellular basis for the negative inotropic effect of tumour necrosis factor-alpha in the adult mammalian heart. J Clin Invest 1993; 92:2303-2312

Yoo ES, Lee KE, Seo JW, Yoo EH, Lee MA, Im SA, Mun YC, Lee SN, Huh JW, Kim MJ, Jo DY, Ahn JY, Lee SM, Chung WS, Kim JH, Seong CM. Adherent cells generated during long-term culture of human umbilical cord blood CD34+ cells have characteristics of endothelial cells and beneficial effect on cord blood ex vivo expansion. Stem Cells 2003; 21: 228-235

Yoo KJ, Li RK, Weisel RD, Mickle DA, Tomita S, Ohno N, Fujii T. Smooth muscle cells transplantation is better than heart cells transplantation for improvement of heart function in dilated cardiomyopathy.Yonsei Med J 2002; 43: 296-303

Yoo KJ, Li RK, Weisel RD, Mickle DA, Li G, Yau TM. Autologous smooth muscle cell transplantation improved heart function in dilated cardiomyocpathy. Ann Thorac Surg 2000; 70: 859-865

Yoshida M, Horimoto H, Mieno S, Nomura Y, Okawa H, Nakahara K, Sasaki S. Intra-arterial bone marrow transplantation induces angiogenesis in rat hindlimb ischemia. Eur Surg Res 2003; 86-91

Zhang S, Zhang P, Guo J, Jia Z, Ma K, Liu Y, Zhou C, Li L. Enhanced cytoprotection and angiogenesis by bone marrow cell transplantation may contribute to improved ischemic myocardial function. Eur J Cardio-thorac Surg 2004; 25: 188-195

CHAPTER 2

DES-ASPARTATE-ANGIOTENSIN-I THERAPY FOR MYOCARDIAL INFARCTION

TABLE OF CONTENT

2.1 Abstract

We investigate the influence of des-Aspartate-angiotensin-I (DAA-I) on the cytokine expression profile in a rodent model of myocardial infarction. Myocardial infarction was created in female Wistar rats by coronary artery ligation. Animals were randomized to receive intravenously either a daily dose of 1.2μg DAA-1 /kg body weight (group-1; n=60) or saline (group-2; n=60) for 14-days after infarction. Heart function was assessed by echocardiography. Animals were euthanized at 1, 3, 7, 14 and 31-days. Morphometric analysis using tetrazolium chloride staining revealed that infarct size was reduced by 32.2% ($p<0.05$) in group-1 after 14 days of DAA-I treatment. Left ventricular ejection fraction in group-1 improved significantly (73.4%) as compared to group-2 (47.7%; $p<0.001$). Immunostaining for immune cells at the infarct size showed that $CD8^+$ lymphocytes infiltration at the infarct site declined in group-1 (15 ± 5 cells) as compared to group-2 (50 ± 6 cells; $p<0.001$). Infiltration of monocytes and macrophages remained significantly high at day 14 in group-2 (126 ± 40 cells) as compared to group-1 (49 ± 11 cells; $p=0.006$). Multiplex PCR was done for differential gene expression of various pro-inflammatory cytokines. IL-6, TNF-α, TGF-β and GM-CSF expression were significantly down-regulated in the infarct, peri-infarct and contra-lateral zones of the left ventricle in group-1 as compared to group-2. IL-6, TGF-β and GM-CSF expression started to decline from day 1 of DAA-I treatment whilst TNF-α expression was only reduced after 7-days of DAA-I treatment. It can be concluded that DAA-I prevented infarct expansion through suppression of inflammatory cytokines and immune cell infiltration in the infarct region.

2.2 Introduction

Des-aspartate angiotensin I (DAA-I) is a nona-peptide produced from cleavage of a deca-peptide through the action of an aminopeptidase (Blair-West et al, 1971), that has been demonstrated to significantly attenuate the experimentally induced cardiac hypertrophy in rats (Sim et al, 1998). Being an endogenous angiotensin peptide of the renin angiotensin cascade, it is capable of exerting cardioprotective actions in cardiovascular pathologies where angiotensin II is involved. These include attenuation of cardiac hypertrophy in rats with abdominal aortic coarctation, attenuation of neointima formation in balloon catheter-injured rat carotid artery and age-related vascular hypertrophy (Sim et al, 2004). DAA-I is also capable of counteracting the actions of angiotensin II (Sim et al, 1994). One example is the attenuation of angiotensin II-induced hypertrophy and hyperplasia in cardiomyocytes and vascular smooth muscle cells, respectively (Min et al, 2000). Anti-cardiac hypertrophic actions of DAA-I is mediated via the AT_1 receptors. However very high dosage of DAA-I diminished this anti-hypertrophic effects due to gradual loss of AT_1 receptors via the endocytic internalization process (Chen et al, 2004).

During myocardial ischemia, the renin-angiotensin cascade is activated and angiotensin II is implicated in ischemic damages of the heart (Santos et al, 1990; Dzau 2001). Angiotensin II elicits several responses that are either responsible for or exacerbate ischemia-reperfusion injury such as vasoconstriction, inflammation, remodeling and thrombosis. AT1 receptor antagonists and ACE inhibitors have been shown to be able to reduce infarct size in animal models of myocardial ischemic injury suggesting that deleterious actions of angiotensin II are mediated by AT1 receptors.

DAA-1 has also been shown to act via AT1 receptors to reduce the infarct size of ischemia-reperfusion injury rodent models (Wen et al, 2004).

The aim of this present study is to investigate the influence of DAA-I on the cytokine expression profile and its efficiency in reducing infarct size in a rodent model of MI. We hypothesized that DAA-1 may indirectly exert its cardioprotective effect via suppression of inflammatory cytokines that are implicated in the pathophysiology of heart failure.

2.3 Materials and Methods

2.3.1. Materials

2.3.1.1 Des-aspartate-angiotensin-I

DAA-I was kindly provided by our collaborator Associate Professor Sim Meng Kwoon, Department of Pharmacology, National University of Singapore.

2.3.1.2 Wistar rats

A total of 132 female Wistar rats (± 250g) were used for the creation of the rat myocardial infarction model. Wistar rats were purchased from Centre for Animal Resources, Lim Chu Kang, Singapore.

The materials used for this study is listed in Appendix 6.1.

2.3.2 Methods

2.3.2.1 Rat model of myocardial infarction

Rat ligation model of myocardial infarction was used for the *in vivo* studies. All animals received human care in compliance with the "Guide for the Care and Use of Laboratory Animals", published by the National Institute of Health, USA. Ethical approval was also obtained from International Animal Care And Use Committee (IACUC), National University of Singapore. All animals were monitored and maintained daily by the staff from Animal Holding Unit of National University of Singapore.

Creation of rat ligation model

Female Wistar rats weighing about 200 to 250g were anaesthetized with ketamine-xylazine mixure (ketamine 75mg/kg, xylazine 10mg/kg) by intraperitoneal injection. They were next intubated and mechanically maintained with room air. To ensure that the rats were properly anesthetized, their reaction to skin incision and toe

pinch were noted. The chests were then shaved and cleaned with 70% ethanol and iodine prior to exposing their hearts through a 2-cm left lateral thoracotomy. To ensure aseptic techniques, all surgical instruments were autoclaved before use and the area where the surgery was performed was cleaned with 70% ethanol. Sterile gloves, face mask and clean surgery lab coat were worn by the surgeon.

In order to locate the left anterior descending (LAD) coronary artery, the pericardium surrounding the left ventricle was carefully removed. Once the LAD artery was located, it was ligated proximally with a 6-0 prolene non-absorbable suture. Upon ligation, the area of infarction that was created would turn slightly pale. The muscle layer and skin incision were closed with 3-0 silk absorbable suture and rats were returned to their cages for recovery.

Animal groupings for DAA-I administration therapy

The animal groupings for DAA-I study were listed as follows:

1. Group-1a: DAA-I-treated day 1 ligation (n=12)
2. Group-1b: DAA-I-treated day 3 ligation (n=12)
3. Group-1c: DAA-I-treated day 7 ligation (n=12)
4. Group-1d: DAA-I-treated day 14 ligation (n=12)
5. Group-1e: DAA-I-treated day 31 ligation (n=12)
6. Group-2a: Saline-treated day 1 ligation (n=12)
7. Group-2b: Saline-treated day 3 ligation (n=12)
8. Group-2c: Saline-treated day 7 ligation (n=12)
9. Group-2d: Saline-treated day 14 ligation (n=12)
10. Group-2e: Saline-treated day 31 ligation (n=12)

11. Group-3: Sham-operated (n=12)

DAA-I administration

The rats were administered intravenously with 200µl of saline containing a daily dose of 1.2µg/kg of body weight of DAA-I. Optimal dose selection of DAA-I was based on previous studies. The rats were injected with DAA-I immediately after infarction was induced and this treatment regimen was continued daily till the time of animal sacrifice.

Post surgery care for the rat MI models

Analgesia (Buprenorphine; 0.1mg/kg) and antibiotics (Cefazolin; 40mg/kg) were injected subcutaneously into the rats for 5 days. Opsite spray and topical antibiotic powder were applied to the wound to prevent infection.

Euthanasia of the rats

The rats were euthanized by an overdose of sodium pentobarbital. Their chests were opened up and hearts harvested.

2.3.2.2 Functional studies

Rat heart function assessment using echocardiography

The assessment of the cardiac function were done 1, 3, 7, 14 and 31 days of DAA-I treatment. Left ventricular (LV) function assessment and dimension measurements were carried out by 2-dimensional (2D) echocardiography using a GE Vivid 5 ultrasound machine (GE Medical Systems) with a 10MHz phased array transducer**.** The transducer was covered with a surgical latex glove finger filled with ultrasound transmission gel to provide a standoff of 0.5-0.7cm to achieve optimum resolution. The rats were given very light anesthesia with low dosage of ketamine/xylazine mixture (ketamine 75mg/kg, xylazine 10mg/kg). Their chests were

shaved and they were placed in a left lateral position. A standard lead II electrocardiogram was recorded for heart rate measurement. After a 2-dimensional (2D) image was obtained in a para-sternal short axis view at the level close to the papillary muscles, a 2D guided M-mode trace crossing the anterior and posterior wall of the LV was recorded at a sweep speed of 100mm/s. Caution was taken not to apply excessive pressure over the chest which could cause bradycardia and deformation of the heart. Heart function parameters including LV internal end-diastolic (LVEDd) and end-systolic (LVESd) diameter were measured using M-mode tracings. The measurements were made using the leading edge method recommended by the American Society of Echocardiography. LV fractional shortening was calculated as FS%= [LVEDd-LVESd)/LVEDd]×100. Ejection fraction was calculated as LVEF= 1-[LVESd/LVEDd]^2 . All measurements were done by investigators blinded to the treatment groups. The measurements were averaged between three to five consecutive cardiac cycles.

2.3.2.3 Assessment of the effect of DAA-I on the infarction model

Morphometric analysis using tetrazolium chloride staining

After excision, the hearts were washed thoroughly with distilled water to remove any remaining blood. The heart were cut into 5 to 7 transverse slices and incubated in 1% triphenyltetrazolium prepared in 0.1M of sodium phosphate (NA_2PO_4) buffer; pH 7.4 for 20 minutes at 37°C. Tetrazolium chloride stained the viable tissue dark red leaving the necrotic tissue pink. The slices were fixed in 10% neutral buffered formalin solution for 20 minutes. Each slice was then carefully traced along the borders of the infarction area and the non-infarction area on a piece of paper and the corresponding areas were weighed out. The infarction area was calculated as the weight of the traced infarcted slice divided

by the total weight of both traced infarcted and non-infarcted slices multiplied by 100 percent.

$$\frac{\text{Infarcted area}}{\text{Infarcted and non infarcted areas}} \times 100\%$$

Multiplex PCR for inflammatory cytokines

MPCR was carried out for semi-quantitative analysis of rat inflammatory cytokines mRNA expression in DAA-I and saline-treated rat hearts using glyceraldehyde-3-phosphate dehydrogenase (GAPDH) as the internal control. The specific rat primer sequences and their sizes are summarized in Table 6. MPCR mixture (total volume of 50µl) contained 25µl of 2× MPCR buffer, 5µl of 10× MPCR primers, 0.5µl of 5U/µl Taq DNA Polymerase, 1.0µl of 10mM dNTPs, 5µl single stranded cDNA and sterile water. The mixture was transferred from ice to the thermal cycler using the following reaction conditions: Initial activation step: 96°C, 1 minute, 59°C, 4 minutes for 4 cycles, Denaturation step: 94°C, 1 minute and Annealing step: 59°C, 2 minutes for 30 cycles and Extension step: 70°C, 10 minutes. The PCR products were run on a 2% agarose gel and the relative density of GAPDH and the various inflammatory cytokines and growth factors bands were determined using a computerized densitometry system.

Immunohistochemical staining of cytokines

Immunohistochemistry was performed either on formalin-fixed paraffin-embedded tissue or snap-frozen tissue fixing medium-embedded cryosections. Both tissue preparations are mentioned in Appendix 6.2.3 and 6.2.4. The tissue sections were washed twice in 1× PBS for 5 minutes, fixed with -20°C methanol for 10 minutes and

Table 6: List of specific rat cytokines and growth factors primer sequences and their sizes

Cytokine	Primer Sequence	Product Size (bp)
GM-CSF	Forward= 5'- CTGAGCCTCCTAAATGACATG -3' Reverse= 5'- AAGGGTTGGAGGGCAGTTCG-3'	210
TGF-β	Forward= 5'- TATAGCAACAATTCCTGGCG -3' Reverse= 5'- AAGGTCGGTTCATGTCATGGA-3'	250
IL-1β	Forward= 5'-GATGTTCCCATTAGACAGCTG-3' Reverse= 5'-CTTTTCCATCTTCTTCTTTGGGTA-3'	294
TNF-α	Forward= 5'-CTACTGAACTTCGGGGTGATC-3' Reverse= 5'-CTGGTATGAAGTGGCAAATCG-3'	351
IL-6	Forward= 5'-CCAGTATATACCACTTCACAAG-3' Reverse= 5'-CAAGATGAGTTGGATGGTCTTGG-3'	453
GAPDH	Forward= 5'-GGGTGGTGCCAAAAG G- 3' Reverse= 5'-GGAGTTGCTGTTGAAGTC-3'	532

treated with 3% methanolic hydrogen peroxide solution (H_2O_2) for 15 minutes. After washing with 1× PBS, the tissue sections were blocked with Ultra V Block for 8 minutes followed by incubation with the respective primary antibodies at optimal dilution at room temperature (Table 7). After thorough washing with 1× PBS, they were incubated with the corresponding secondary antibody and washed using 1× PBS prior to the detection step. Depending on the secondary antibody used, the detection method used was either by fluorescent method or diaminobenzidine solution.

2.3.3 Statistical analysis

Statistical analysis was performed using SPSS (version 11.0). All data were presented as mean ± standard error mean (SEM) and compared by analysis of variance (ANOVA) between groups. Intra-group comparison was carried out using paired student t test. $P < 0.05$ was considered statistically significant.

Table 7: List of primary and secondary antibodies used for cytokine immunostaining

Primary Antibody	Dilution used	Secondary Antibody	Dilution used	Incubation time
Rabbit anti rat TNF-α	1:250	Goat anti-rabbit rhodamine conjugated	1:500	1 ½ hour
Goat anti-rat IL-6	1:100	Rabbit anti-goat FITC conjugated	1:700	1 ½ hour
Mouse anti-rat IL-1β	1:250	Rabbit anti-mouse rhodamine comjugated	1:500	1 ½ hour
Rabbit anti-rat TGF-β	1:200	Goat anti-rabbit rhodamine conjugated	1:500	1 ½ hour
Mouse anti-rat CD8a	1:20	Anti-mouse IgG-HRP conjugated	Ultravision kit	8 min
Mouse anti-rat ED1, monocytes and macrophages	1:20	Anti-mouse IgG-HRP conjugated	Ultravision kit	8 min

2.4 Results

There was no mortality in the treatment groups after DAA-I treatment thus reflecting the safety of DAA-I administration. All animals completed their respective designated time duration.

2.4.1 Effects of DAA-I on infarct size and heart function

Morphometric analysis revealed that infarct size was significantly reduced by 32.2% in DAA-1-treated group-1 animals (12% ±0.58%), as compared to the saline-treated group-2 animals (17.7%± 0.97; $p<0.05$) after 14 days of DAA-I treatment (Figure 2a). Echocardiographic assessment showed an associated improvement in left ventricular ejection fraction (LVEF) in group-1 as compared to group-2 (Figure 1b). However, a progressive deterioration in left ventricular performance was shown by the deterioration of ejection fraction in group-2. LVEF was maintained at an average of 73.4% after 14 days of DAA-I treatment in group-1 (range 69.2% to 75.9± 3.13%) which persisted until 31 days of observation as compared to group-2 which deteriorated (47.7%; $p<0.001$) from day 3 to day 31 of observation (range 38 to 51± 3.38%) (Figure 2b).

2.4.2 Immune cell filtration

Immunohistochemistry for monocytes, macrophages and $CD8^+$ cytotoxic T-lymphocytes surface markers showed that there was little infiltration of $CD8^+$ cytotoxic T-lymphocytes in both group-1 and group-2 as compared to monocytes and macrophages (Figures 3a & b and 4a & b). $CD8^+$ cells remained high in group-2 (50± 6 cells, at 300× magnification) until day 7 after infarction but dropped significantly by day 14 (10± 3 cells; $p<0.001$). DAA-I treatment was observed to suppress the number of these cytotoxic cells from day 3 after infarction. The mean number of $CD8^+$ cells in group-1 was 15± 5

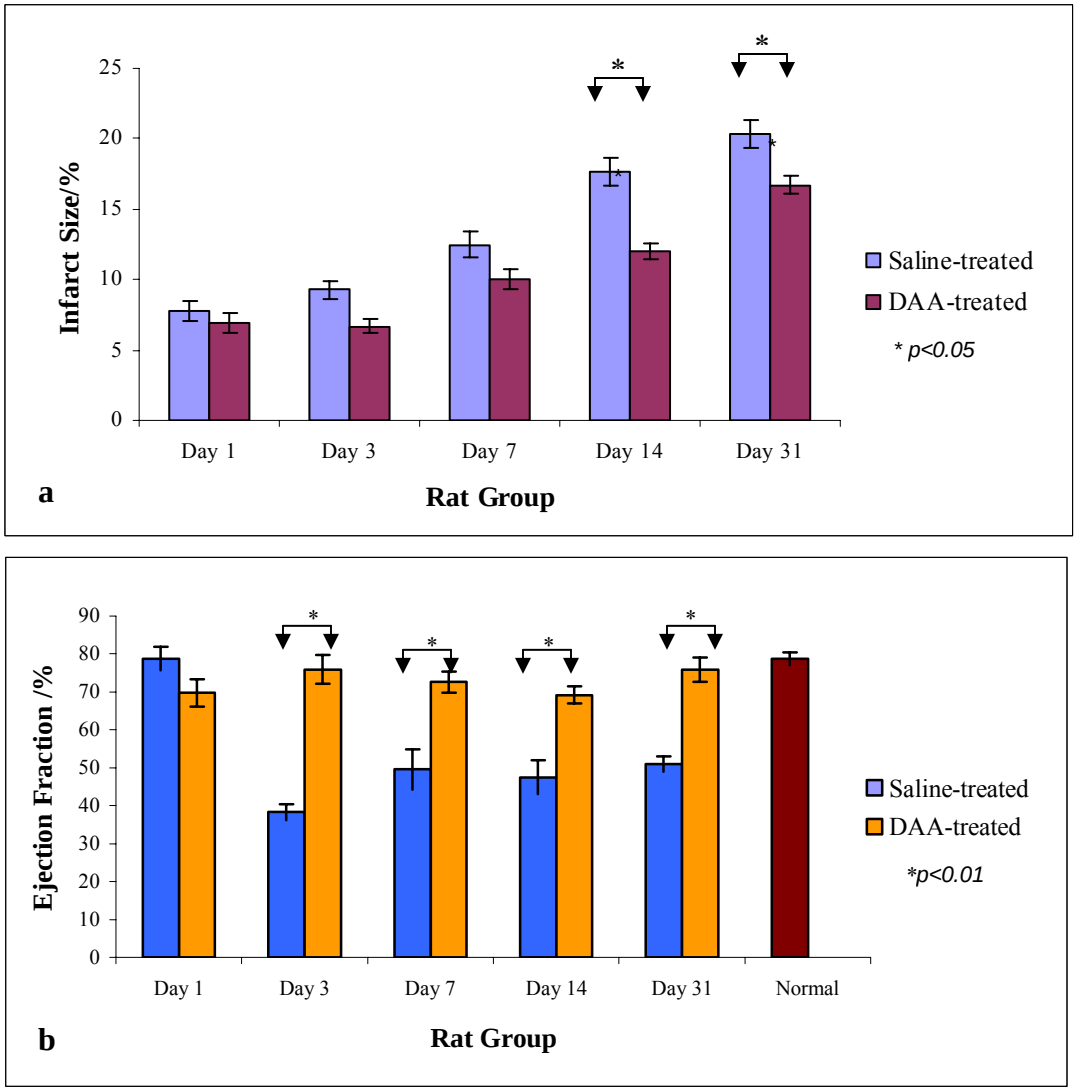

Figure 2: (a) **Effect of DAA-I treatment on infarct size.** Rats were treated intravenously with either saline (n=12 at each time point) or DAA-I (n=12 at each time point) daily for 14 days. Significant difference in the infarct size occurred at day 14 after treatment. The mean infarct sizes were 17.7% ± 0.97 for saline-treated rats and 12% ± 0.33 for DAA-I treated rats, (b) **Effect of DAA-I treatment on the ejection fraction of the heart.** Rats were subjected to echocardiographic studies before their hearts were explanted (n=12 at each time point). Significant improvement in ejection fraction was observed after 3 days of DAA-I treatment.

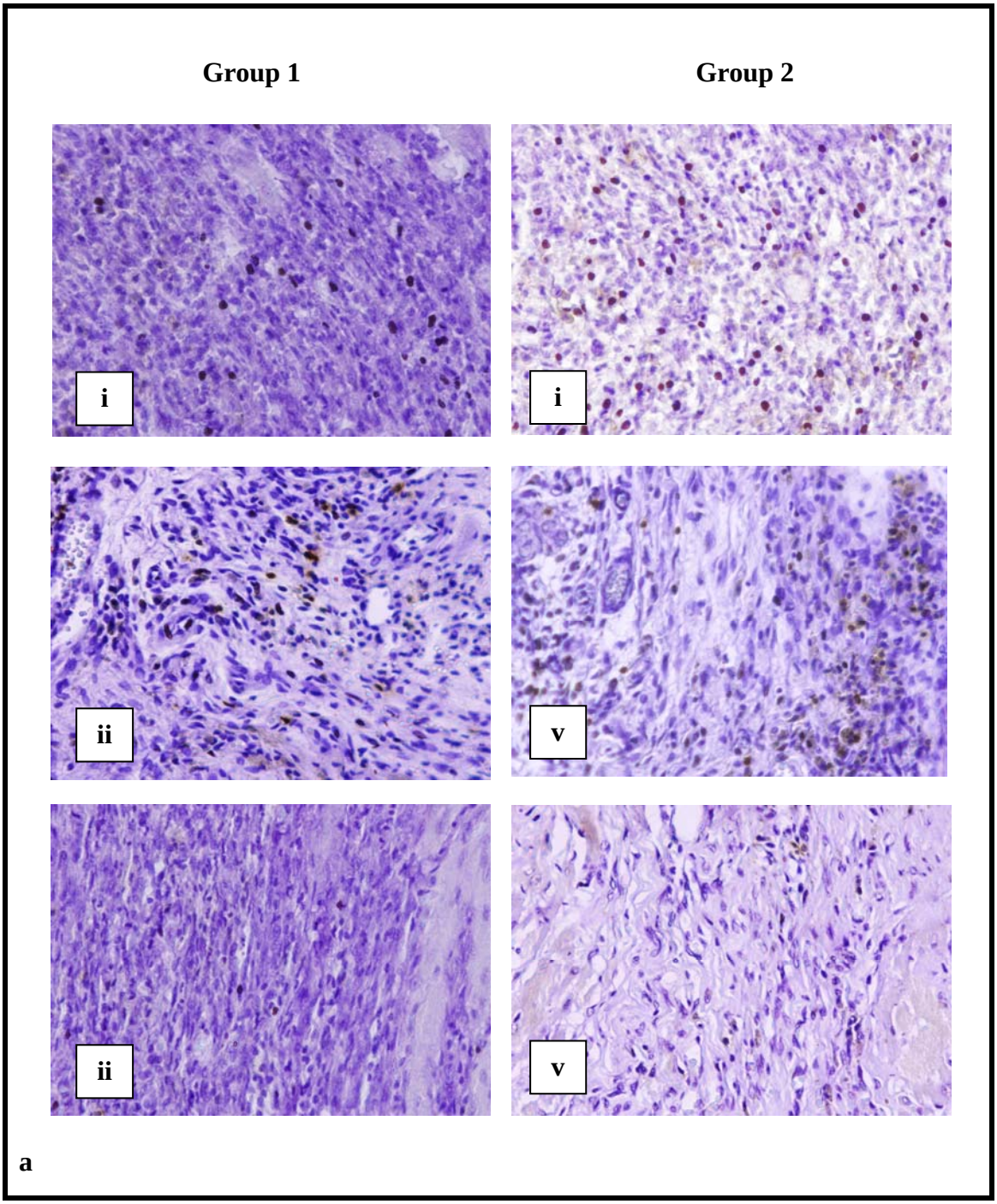

Figure 3: (a) **Immunostaining of CD8$^+$ T-lymphocytes on tissue sections from saline and DAA-treated rat hearts.** Positive cells staining brown as shown below, infiltrated in significantly higher numbers (48± 7 cells) in saline-treated animals at day 3 as compared to DAA-treated animals (15± 5 cells; *p=0.02*). However, the number of positive cells dropped to the same level in both groups of animals by day 14 (Magnification 300×)

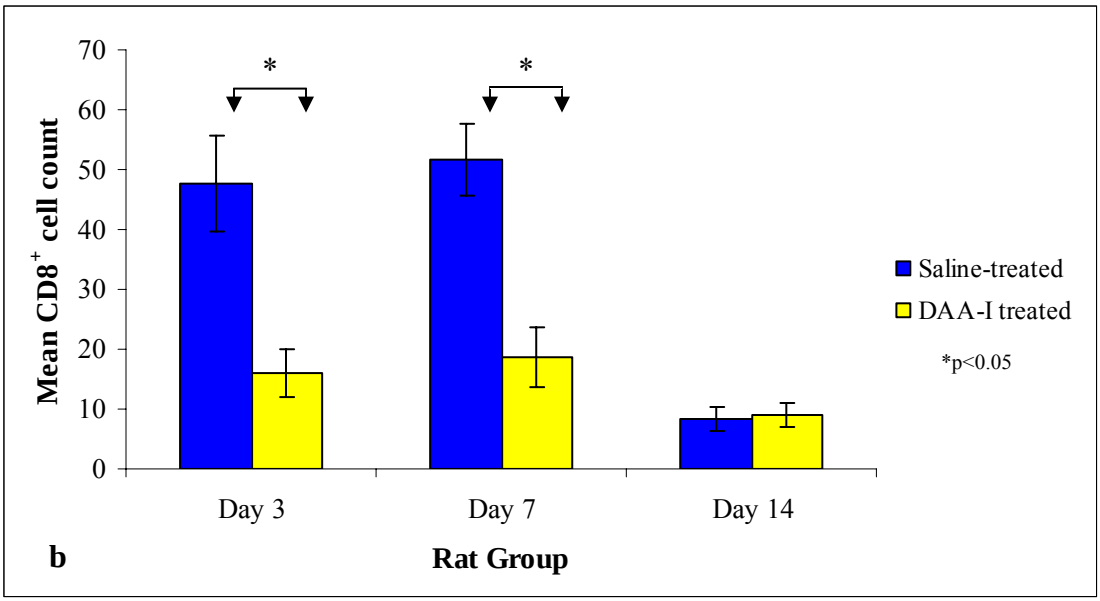

Figure 3: (b) **Graphical representation of the number of $CD8^+$ T-lymphocytes in the infarcted heart at various time points.**

cells until day 14. During the first 3 days after infarction, $CD8^+$ cells were widely and evenly distributed in the infarct area however, by day 14, the cells were only in certain regions of the infarct area.

Immunostaining for ED1 surface marker showed that the monocytes and macrophages continued to decline from day 3 post-infarction until day 14 of observation, in both group-1 and group-2 animals (Figure 4a & b). Both monocytes and macrophages were found widely distributed in the infarct area. Upon quantification, mean number of monocytes and macrophages was initially high (220± 38 cells at 300× magnification) during the first 3 days after infarction in group-2. However a significant drop was observed (126± 40 cells; *p=0.002*) by day 14. On the other hand, mean number of monocytes and macrophages showed more significant reduction in group-1 (49± 11 cells; p=*0.006*) by day 14 as compared to group-2.

2.4.3 Effect of DAA-I on cytokine gene expression

Expression of inflammatory cytokines was analyzed in the infarcted myocardium with and without intravenous DAA-I treatment. Changes in expression of the cytokine genes in the infarct, per-infarct and contra-lateral regions of the rat heart tissue as a function of time are illustrated in Figures 5-9.

2.4.3.1 IL-6

In the infarct area, IL-6 expression in group-2 remained high from day 1 to day 7 while its expression slowly increased until day 7 in group-1, however remaining at lower level as compared to group-2 (0.75-fold vs 1.0-fold) and dropping significantly in both groups at day 14 (0.28-fold). In the peri-infarct area, IL-6 expression was low at day 1 but peaked at days 3 and 7 in group-1. In contrast, IL-6 expression in group-1 was

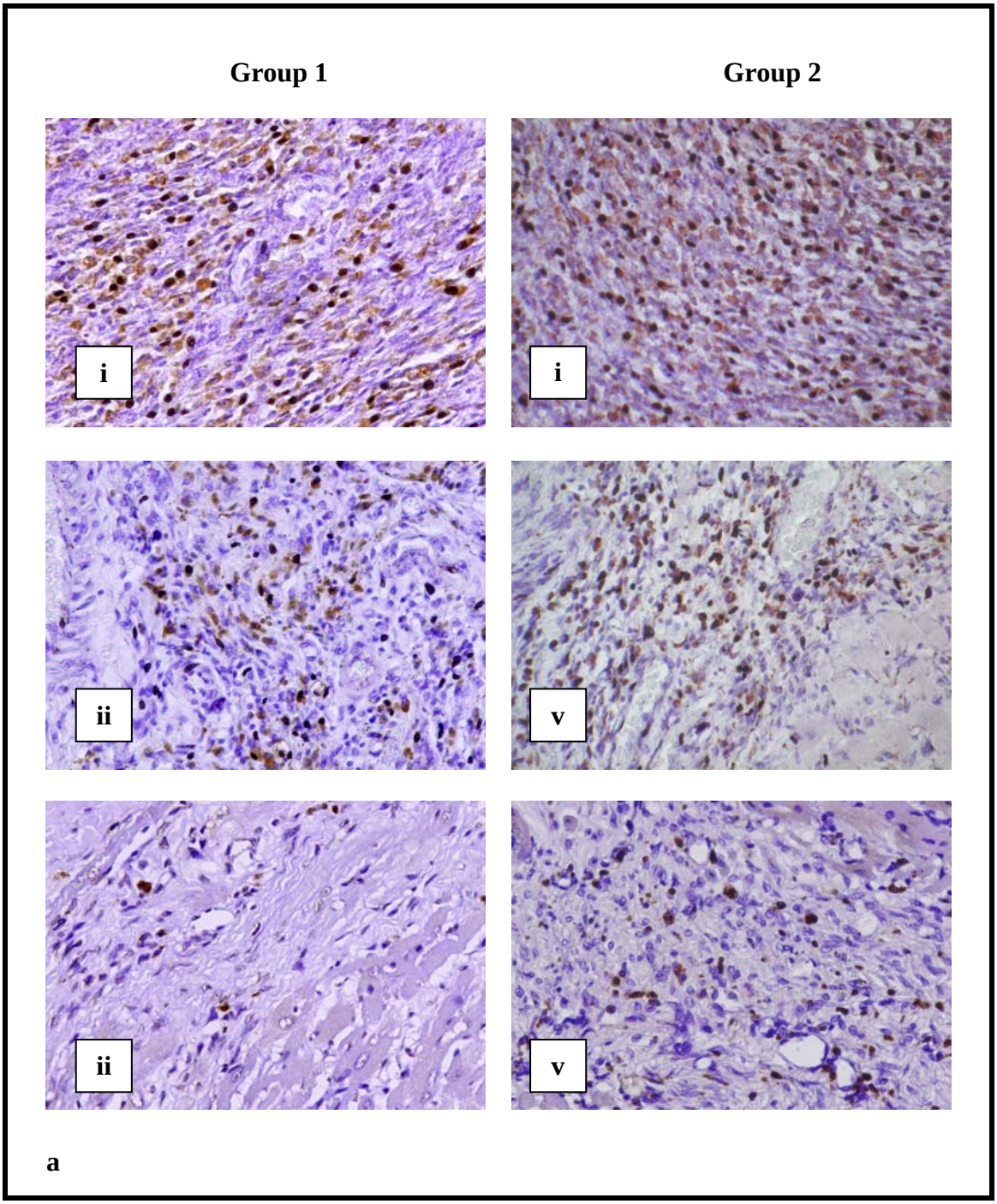

Figure 4: (a) **Immunostaining of monocytes and macrophages on tissue sections from saline and DAA-treated rat hearts**. Positive cells staining brown as shown below. The number of monocytes and macrophages infiltrating into the infarct area was very high in both groups of animals at day 3. No significant difference was seen until day 7. However by day 14, their number was much lower in DAA-treated animals (50± 9 cells) as compared to the saline-treated animals (130± 24 cells) (Magnification 300×)

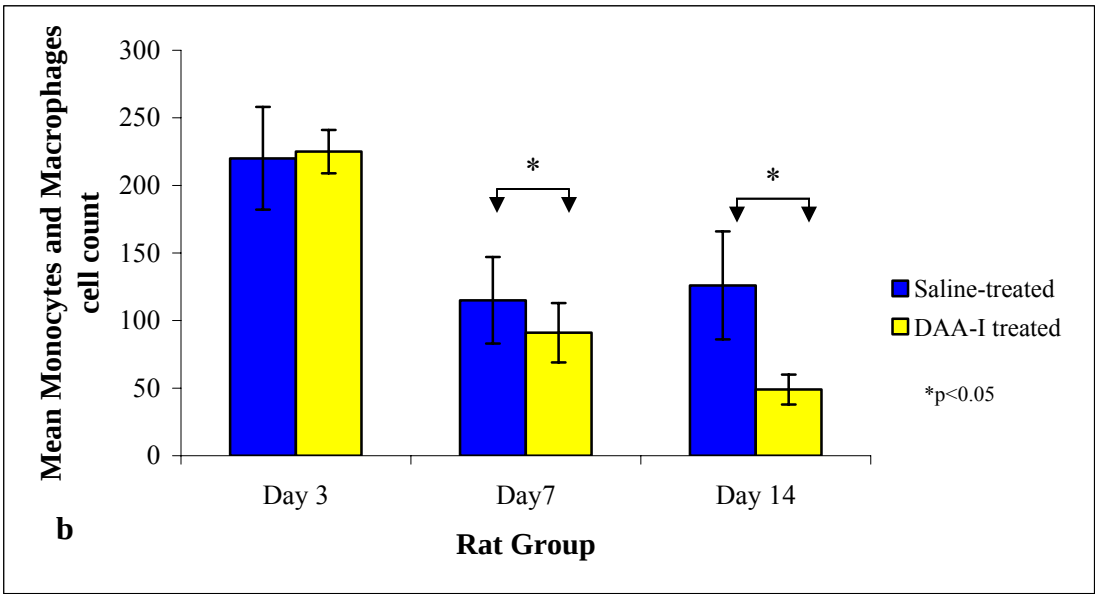

Figure 4: (b) **Graphical representation of the number of monocytes and macrophages in the infarcted heart at various time points.**

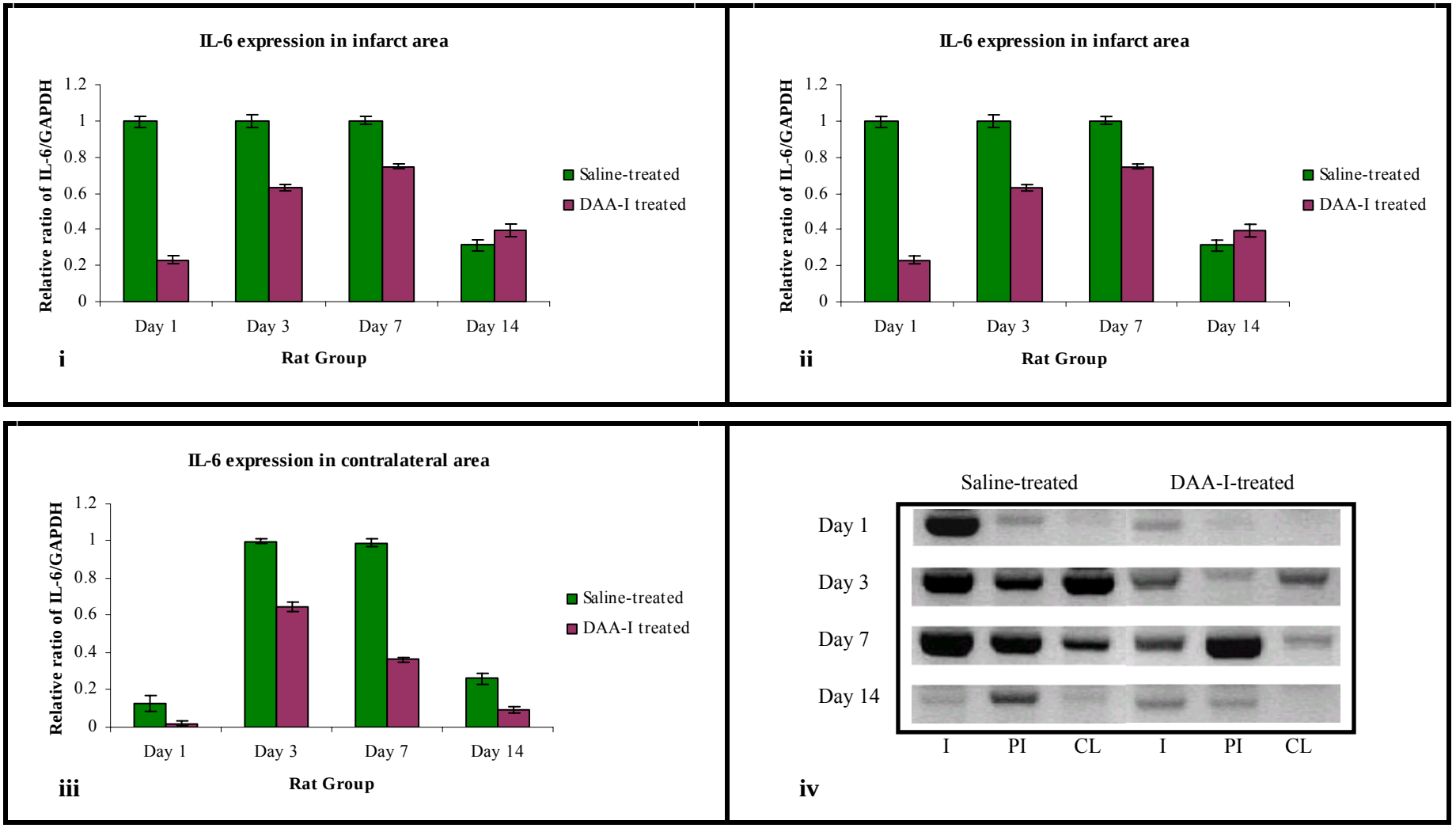

Figure 5: (i-iii) **Densitometric quantification of RT-PCR products of IL-6** in (i) infarct, (ii) peri-infarct, (iii) contra-lateral areas of saline and DAA-I treated rat heart tissue samples, (iv) **RT-PCR products of IL-6**, fractionated by electrophoresis through a 2% agarose gel and visualized by ethidium bromide staining.

significantly lower than group-2 from day 1 to day 3 (0.05-fold vs 0.35-fold and 0.25-fold vs 1-fold, respectively). IL-6 expression in both groups dropped significantly by day 14 (0.32-fold for group-1 and 0.76-fold for group-2). The same kind of trend was observed in the contra-lateral area (Figures. 5a-d).

2.4.3.2 IL-1β

IL-1β expression in the infarct area remained high in both groups from day 1 to day 14 (0.8- to 1-fold). In the peri-infarct area, IL-1β expression still remained quite high but in group-1, the expression at day 14 dropped by half. IL-1β expression in contra-lateral areas only peaked at days 3 and 7 for group-2 (1-fold) as compared to group-1 where the expression peaked at day 3 (1-fold) and reduced significantly after that (0.47-fold) (Figures. 6a-d).

2.4.3.3 GM-CSF

GM-CSF expression in the infarct area in group-2 showed gradual but constant decline, starting from 0.52-fold at day 1 to 0.2-fold at day 14. Compared to group-1, GM-CSF expression was low at day 1 (0.2-fold) and remained fairly low throughout until day 14 (0.1-fold). In the peri-infarct area of group-2, the expression was lower as compared to the infarct area. The expression also remained the same throughout the different time-points (average of 0.17-fold). Similar trend was observed in group-1 but the expression level was very low (average of 0.04-fold). The expression however, was slightly higher in the contra-lateral area. It peaked at days 3 and 7 for both groups (0.23-fold and 0.14-fold for group-2 and group-1, respectively) (Figures. 7a-d).

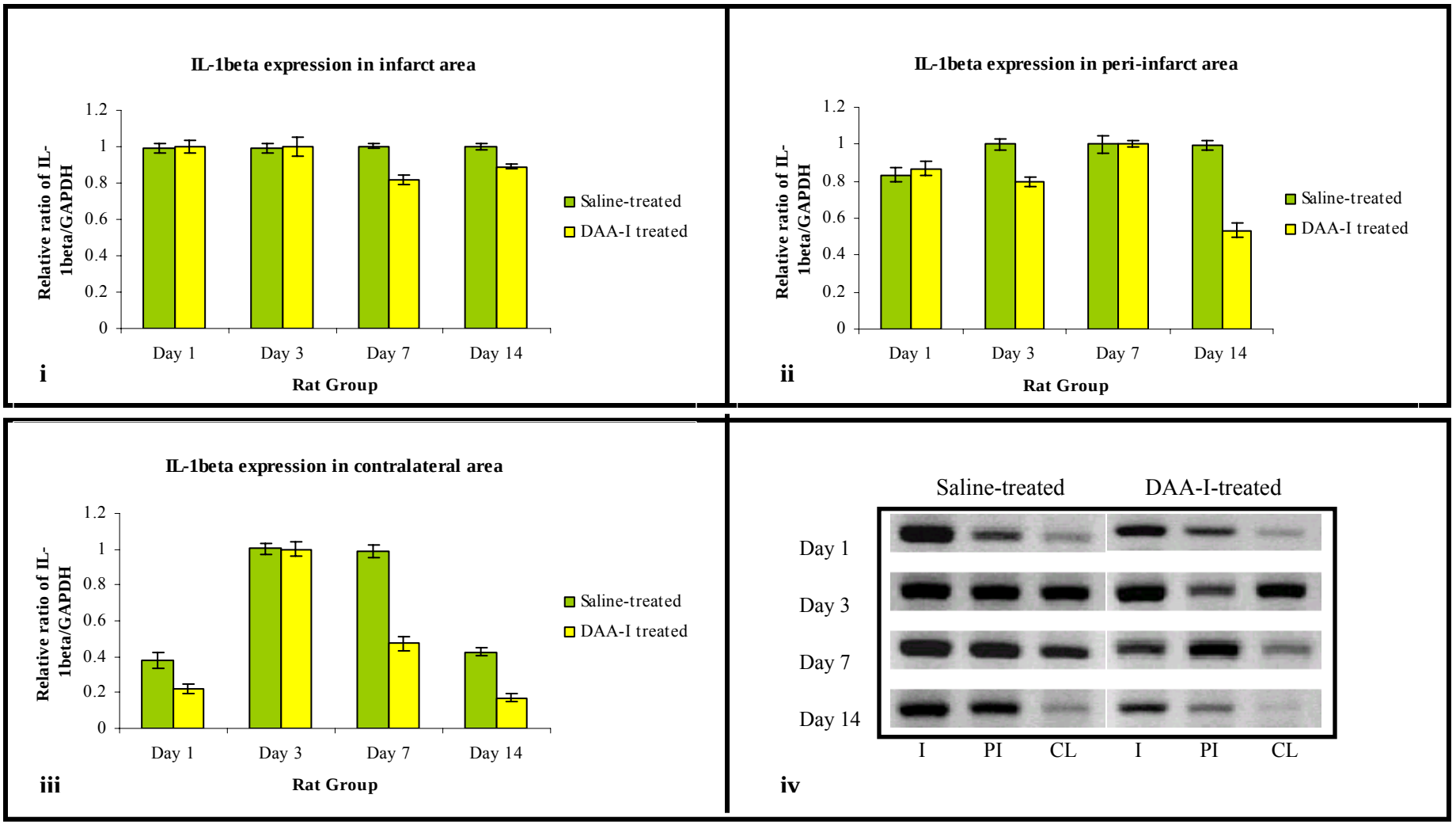

Figure 6: (i-iii) **Densitometric quantification of RT-PCR products of IL-1β** in (i) infarct, (ii) peri-infarct, (iii) contra-lateral areas of saline and DAA-I treated rat heart tissue samples, (iv) **RT-PCR products of IL-1β**, fractionated by electrophoresis through a 2% agarose gel and visualized by ethidium bromide staining.

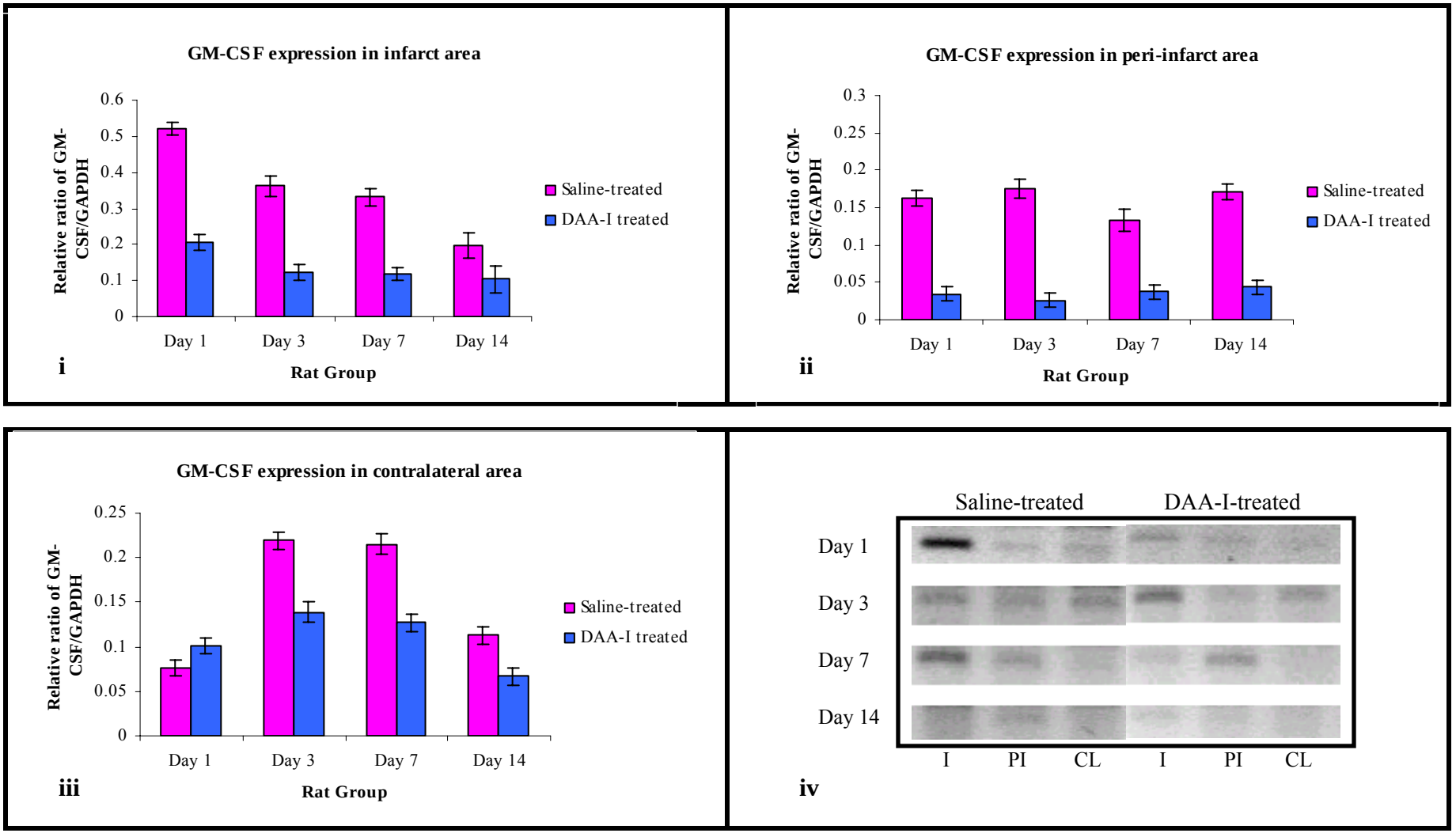

Figure 7: (i-iii) **Densitometric quantification of RT-PCR products of GM-CSF** in (i) infarct, (ii) peri-infarct, (iii) contra-lateral areas of saline and DAA-I treated rat heart tissue samples, (iv) **RT-PCR products of GM-CSF,** fractionated by electrophoresis through a 2% agarose gel and visualized by ethidium bromide staining.

2.4.3.4 TNF-α

TNF-α expression in the infarct and contra-lateral areas in group-1 peaked at day 3 (0.76-fold and 0.61-fold respectively) but reduced significantly by day 14 (0.2-fold and 0.13-fold respectively). In group-2, TNF-α expression in the infarct area remained high throughout the 14 days (average of 0.7-fold) as compared to the peri-infarct and contra-lateral areas (average of 0.4-fold and 0.3-fold respectively). DAA-I treatment globally suppressed the expression of TNF-α at most time points (Figure 8a-d).

2.4.3.5 TGF-β

TGF-β expression in the infarct area of group-2 was the highest at day 1 (1.0-fold) and the lowest at day 7 (0.35-fold) after infarction. Moderate expression was seen at day 3 and day 14 (0.6-fold). Upon treatment with DAA-I, the expression remained lower throughout, ranging from 0.25- to 0.42-fold. In the peri-infarct area, expression was highest at day 3, with 0.68-fold. DAA-I treatment also resulted in significant reduction of TGF-β throughout the 14 days, with the highest also being at day 7 with 0.48-fold. Approximately the same level and trend of expression was observed in the contra-lateral area for both group-1 and group-2 (Figures 9a-d).

2.4.4 Immunohistochemical staining of cytokines

To determine whether the change in cytokine mRNA transcript levels resulted in change in cytokine protein production, immunohistochemical staining of cytokine was done using respective antibodies (Figures 10-13). The results were consistent with the results obtained from multiplex PCR.

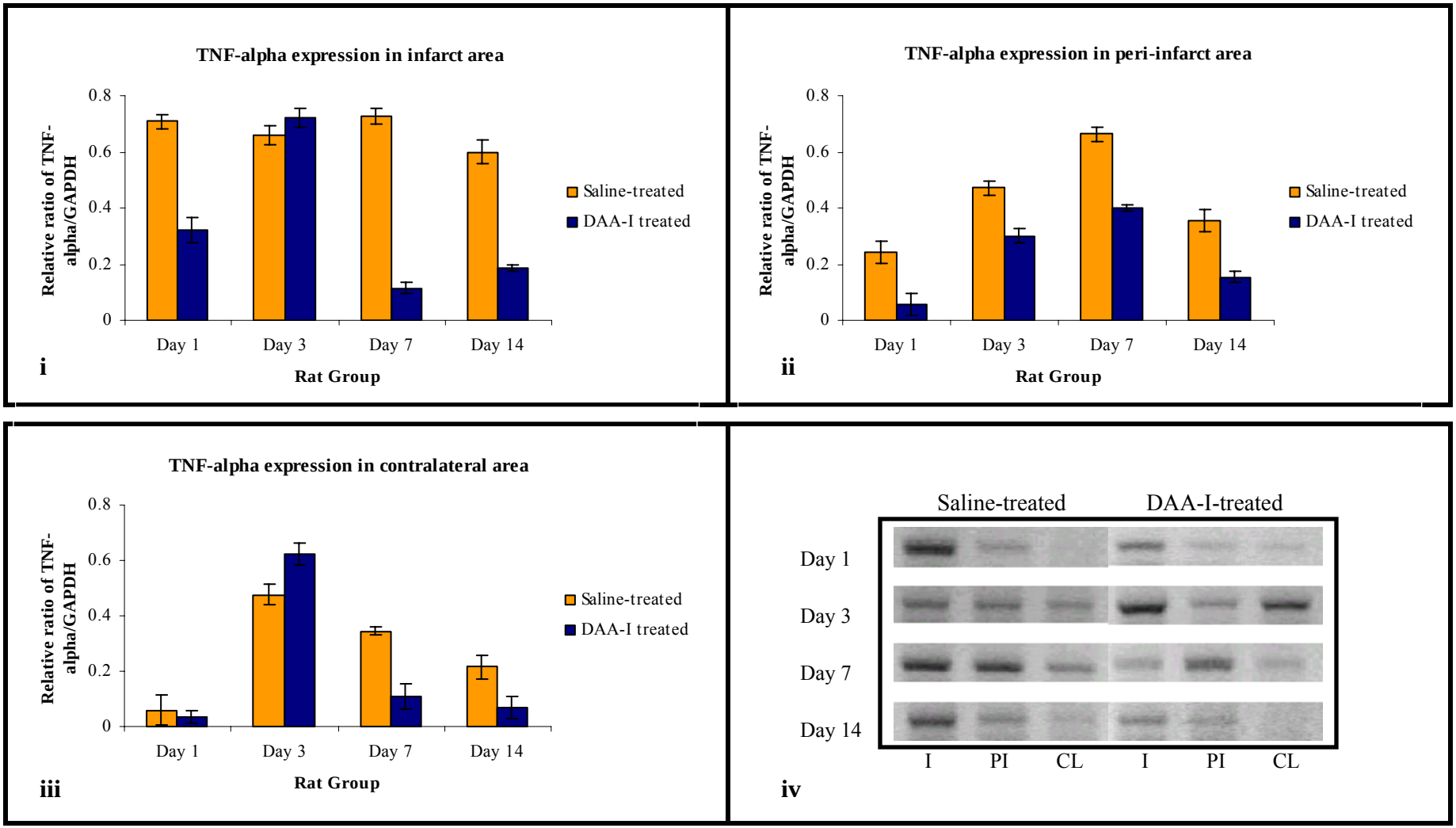

Figure 8: (i-iii) **Densitometric quantification of RT-PCR products of TNF-α** in (i) infarct, (ii) peri-infarct, (iii) contra-lateral areas of saline and DAA-I treated rat heart tissue samples, (iv) **RT-PCR products of TNF-α,** fractionated by electrophoresis through a 2% agarose gel and visualized by ethidium bromide staining.

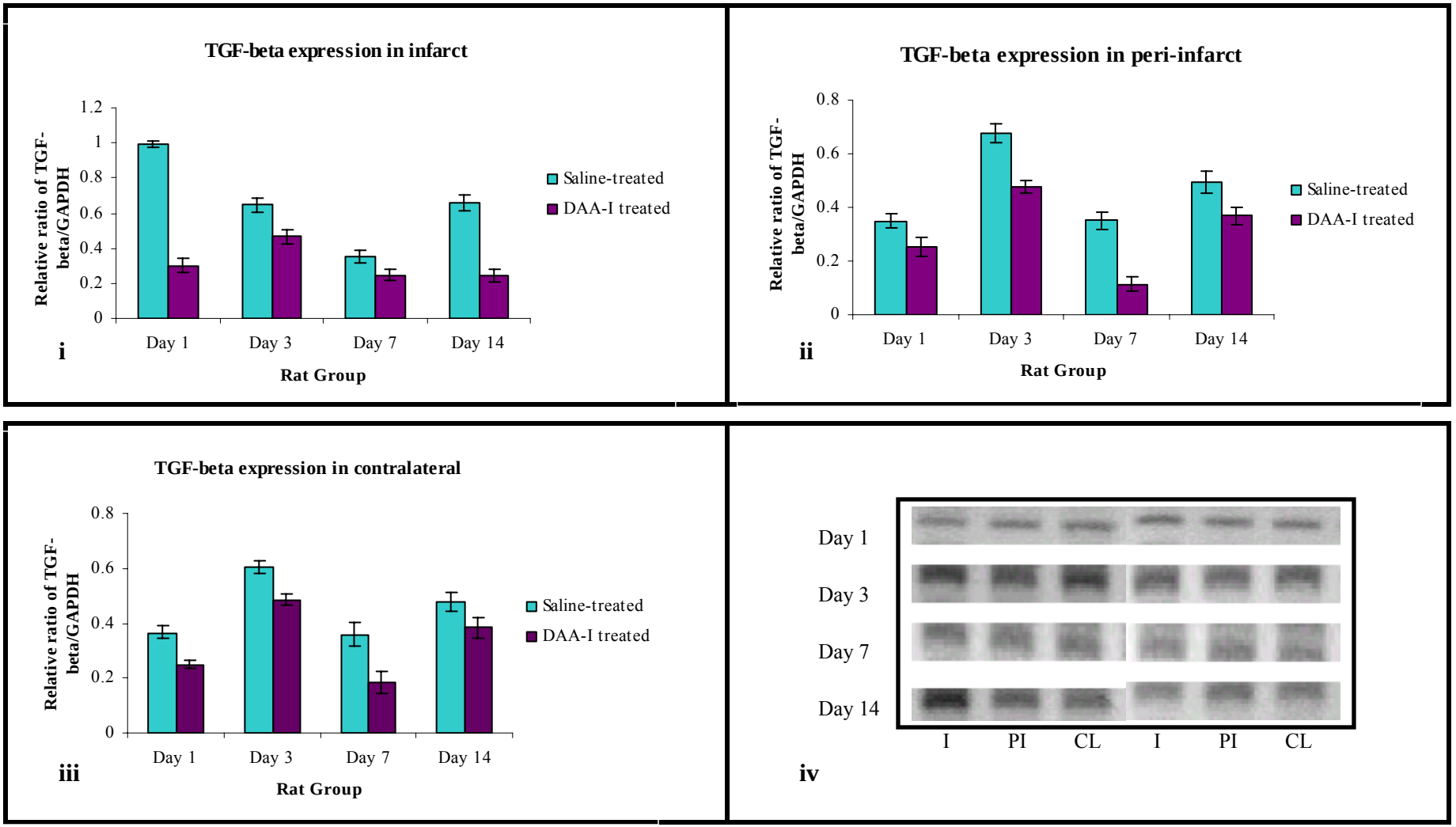

Figure 9: (i-iii) **Densitometric quantification of RT-PCR products of TGF-β** in (i) infarct, (ii) peri-infarct, (iii) contra-lateral areas of saline and DAA-I treated rat heart tissue samples, (iv) **RT-PCR products of TGF-β,** fractionated by electrophoresis through a 2% agarose gel and visualized by ethidium bromide staining.

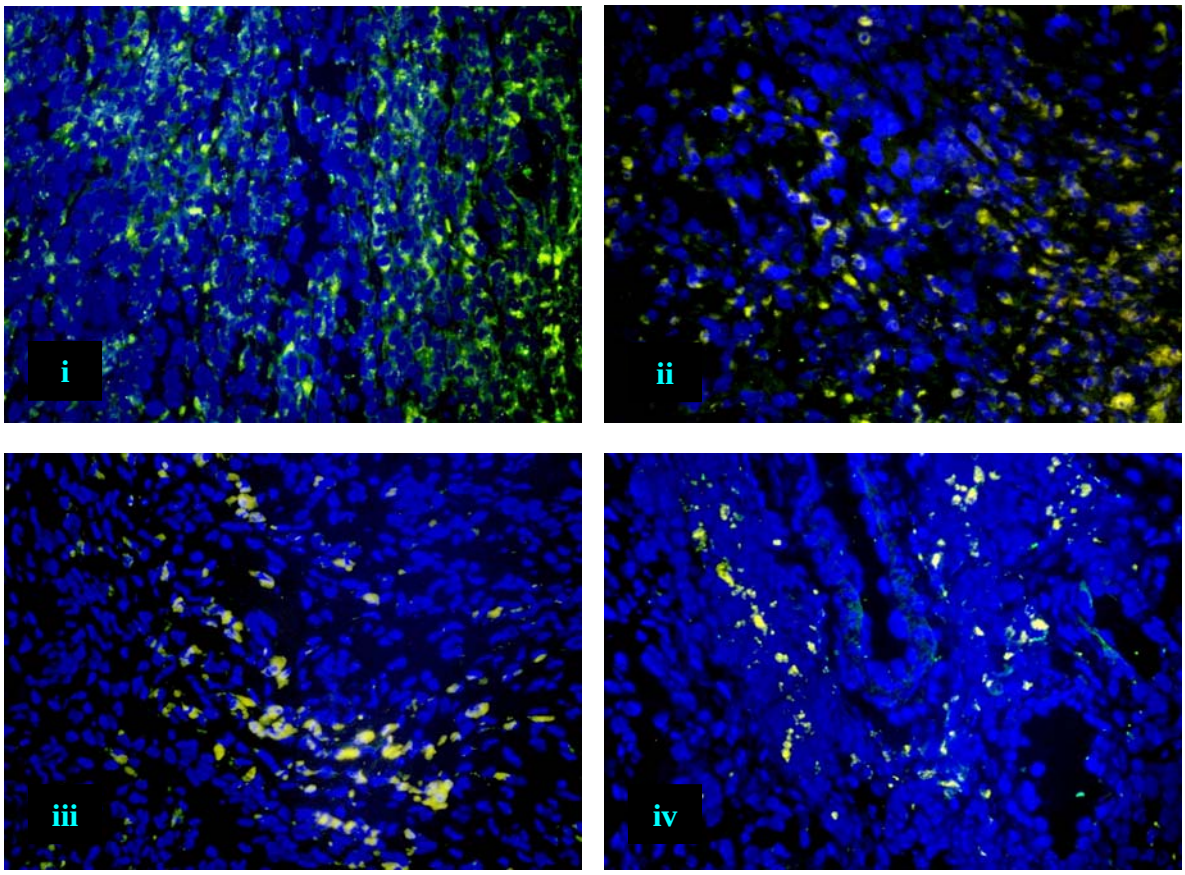

Figure 10: **Immunofluorescent staining of IL-6 using FITC (green fluorescence) in saline and DAA-I treated rat hearts showing its expression in the infarct region.** (a) heart section from 3-day saline-treated rat, (ii) heart section from 3-day DAA-I-treated rat, (iii) heart section from 2-week saline-treated rat, (iv) heart section from 2-week DAA-I-treated rat. Expression of IL-6 was much higher during the first 3 days after infarction but reduced significantly at 2 weeks after infarction. IL-6 expression was lower in DAA-treated animals compared to saline-treated animals. (Magnification 200×)

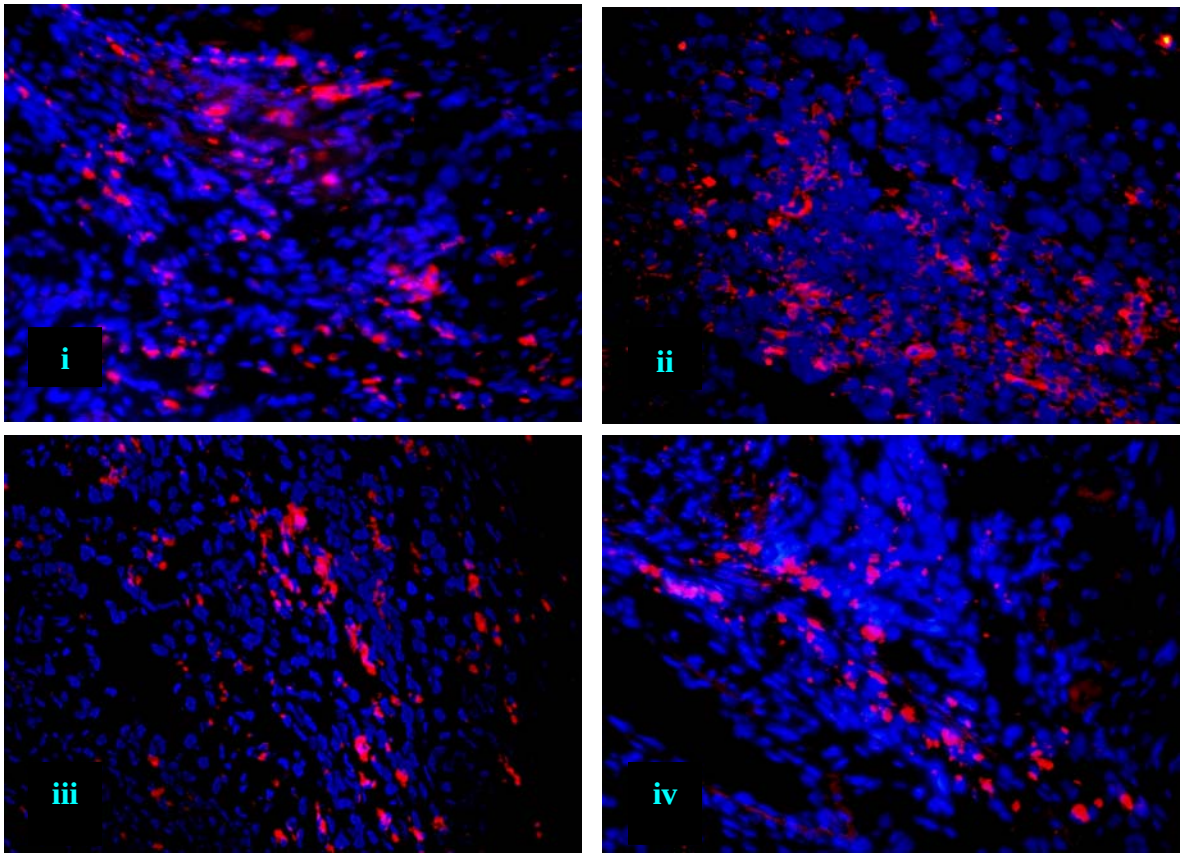

Figure 11: **Immunofluorescent staining of IL-1β using TRITC (red fluorescence) in saline and DAA-I treated rat hearts showing its expression in the infarct region.** (i) heart section from 3-day saline-treated rat, (ii) heart section from 3-day DAA-I-treated rat, (iii) heart section from 2-week saline-treated rat, (iv) heart section from 2-week DAA-I-treated rat. Expression of IL-1β was approximately about the same throughout from day 3 to day 14 in both DAA-treated animals and saline-treated animals. (Magnification 200×)

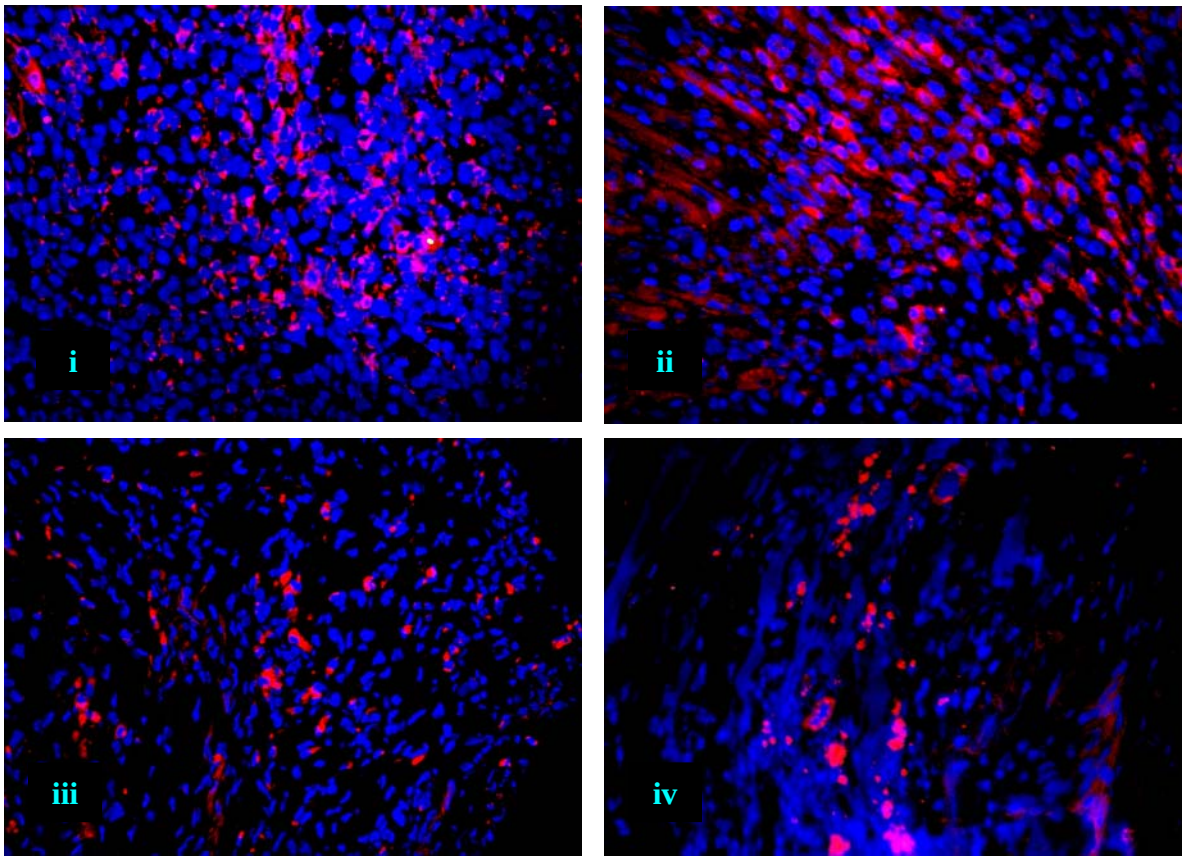

Figure 12: **Immunofluorescent staining of TNF-α using TRITC (red fluorescence) in saline and DAA-I treated rat hearts showing its expression in the infarct region.** (i) heart section from 3-day saline-treated rat, (ii) heart section from 3-day DAA-I-treated rat, (iii) heart section from 2-week saline-treated rat, (iv) heart section from 2-week DAA-I-treated rat. Expression of TNF-α was much higher during the first 3 days after infarction but reduced significantly at 2 weeks after infarction. Its expression was much lower in the DAA-I treated than saline-treated animals. (Magnification 200×)

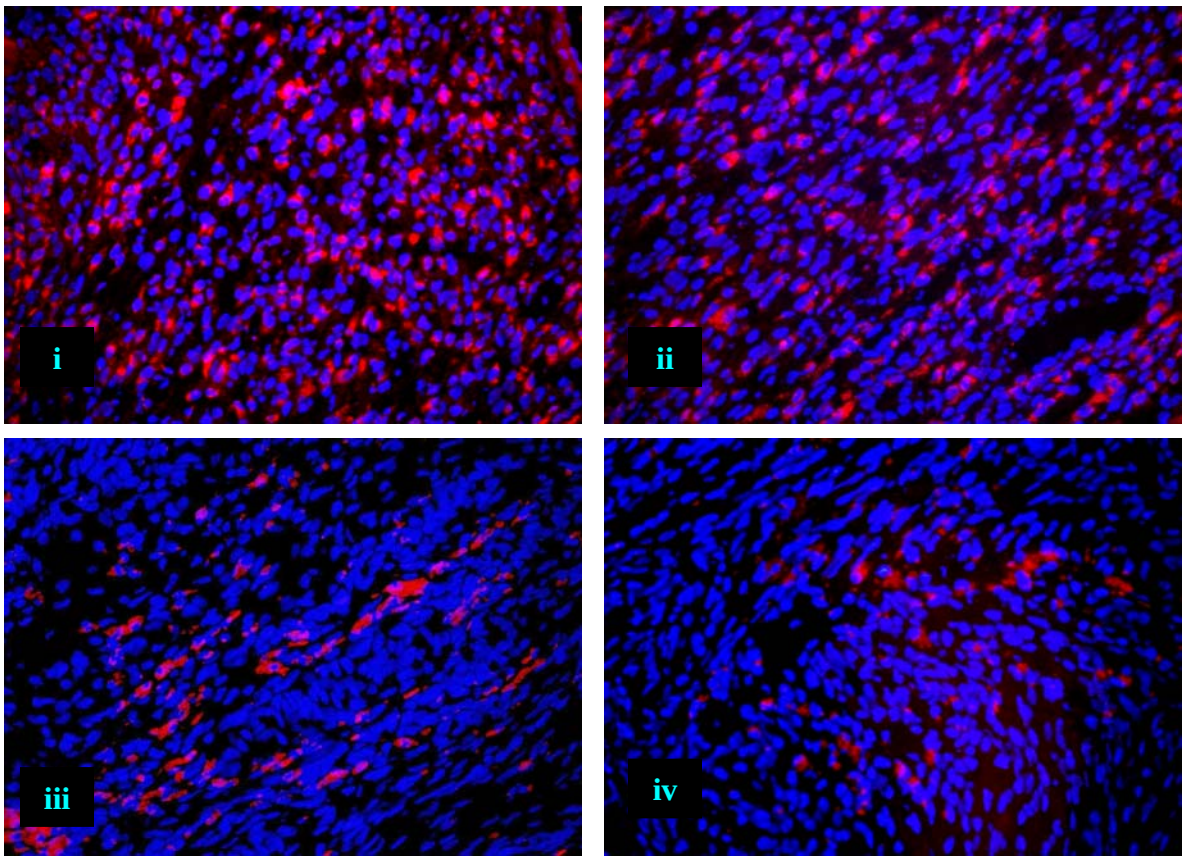

Figure 13: **Immunofluorescent staining of TGF-β using TRITC (red fluorescence) in saline and DAA-I treated rat hearts showing its expression in the infarct region.** (i) heart section from 3-day saline-treated rat, (ii) heart section from 3-day DAA-I-treated rat, (iii) heart section from 2-week saline-treated rat, (iv) heart section from 2-week DAA-I-treated rat. TGF-β expression was much stronger in saline-treated animals than the DAA-I treated animals, being highly expressed at day 3 and reduced significantly at day 14. (Magnification 200×)

2.5 Discussion

In the present study, we showed that 14-day DAA-I treatment of rats subjected to permanent ligation of the LAD artery significantly reduced infarct size. This reduction in infarct size correlated with improved heart function. The infarct size measured at 14 days of DAA-I treatment was 32.2% smaller as compared to saline-treated group-2. LVEF in saline-treated group-2 was significantly higher improved in DAA-I treated group-1, from 48% to 69%. The cardioprotective effect of DAA-I was maintained over 31 days of observation, while LVEF of group-1 remaining significantly higher than that of group-2 and the infarct size was significantly reduced even though the significance was lower as compared to the 14-day time point.

During the acute MI phase, a very high number of mononuclear immune cells infiltrated into the infarcted area. These cells released various cytotoxic compounds such as the complement, reactive oxygen species, inflammatory cytokines and chemokines that led to damage of the ischemic myocardium. The acute immune response plays a strong role in myocardial damage. Hence, various pharmacological approaches have been designed to protect the myocardium during this crucial phase. Most experimental studies showing reduction of infarct size after myocardial infarction by pharmacological drugs are concluded within 24 hours after injury. In our study, we extended the experiments until 31 days to see if the cardioprotective effect exerted by DAA-I during acute phase will be translated to a better morphology and/or function of the injured myocardium after a longer period of time.

The reduction in infarct size after 14 days of DAA-I treatment is multifactorial and may be a combined effect of several processes. Reduced infiltration of immune cells

into the infarcted area might have led to reduced cardiac tissue damage. DAA-I treatment significantly reduced infiltration of $CD8^+$ cytotoxic T-lymphocytes into the infarcted area during 3 to 7 days after infarction (Figures 3a & b). Even though the number of $CD8^+$ cells in both groups was the same at the end of 14 days of treatment (8± 2 cells), the initial number of infiltrating cells salvaging the cardiac muscle during the acute phase is crucial in determining the extent of damaged cardiac muscle. Monocytes and macrophages, the main source of various inflammatory cytokines, were only significantly reduced at day 7 after DAA-I treatment (220 to 115 cells in group-2 and 225 to 91 cells in group-1) (Figures 4a & b).

Inflammatory cytokines have attracted considerable attention as important players in the pathological cascade implicated in the developmental and progression of heart failure; therefore it would be prudent to evaluate the effects of DAA-I on the myocardium at the molecular level. The present study profiles the LV gene expression of several inflammatory cytokines including IL-6, IL-1β, TNF-α, TGF-β and GM-CSF starting from day 1 to day 14, with and without DAA-I treatment. The results showed up-regulated expression of the proinflammatory cytokines and growth factors in rats with MI in the absence of DAA-I treatment (Figures 5-9). These findings were consistent with the already documented studies in literature which showed elevated cardiac expression of mRNA transcripts encoding for these cytokines in both acute as well as chronic phase of MI (Ono et al, 1998; Irwin et al, 1999; Deten et al, 2002). Moreover, clinical and experimental studies have shown that the inflammatory response to MI is associated with the induction of cytokines such as TNF-α, IL-1β and IL-6, which acts in a cascade fashion (Cesari et al, 2003; Chin et al 2003; Torre-Amione et a1, 1996).

DAA-I treatment significantly reduced the expression of IL-6, TNF-α, TGF-β and GM-CSF in the infarct, peri-infarct and contra-lateral areas of the left ventricle (Figures 5, 8-9). Reduction in expression was observed after 3 days of DAA-I treatment. For IL-1β expression, differences were seen after 7 days of DAA-I treatment and only in the peri-infarct and contra-lateral areas (Figures 6b & c). Activation of the inflammatory cytokine cascade has been shown to exert a direct negative inotropic effect mediated through myocardial nitric oxide synthase. This phenomenon results in abnormal cardiac contractile performance and promotes maladaptive left ventricular remodeling (Finkel et al, 1992). The inhibitory effect of DAA-I on expression of the proinflammatory cytokines and growth factors seen in this study thus may have contributed, in part to improvement of cardiac function in group-1 (Figure 2b). This inhibitory action of DAA-I on inflammatory cytokine expression is probably due to its antagonizing action on angiotensin II (Sim et al, 1994). Angiotensin II is known for stimulating and activating cytokine production which in turn leads to inducible nitric oxide synthase and oxy-radical formation (Han et al, 1999; Nakamura et al, 1999; Sadoshima 2000: Ruiz-Ortega et al, 2001). Furthermore, angiotensin II has also been reported to play a role in modulating mononuclear cell chemo-attractant protein-1 (MCP-1) activity. MCP-1 functions by establishing a chemical gradient to attract adherent monocytes and T-lymphocytes to the injury site (Ruiz-Ortega et al, 1998).

In conclusion, we showed that administration of DAA-I for 14 days following acute MI resulted in significant reduction in infarct size and preservation of left ventricular function. The beneficial effect of DAA-I was accompanied by reduced

immune cell infiltration into the infarcted area and suppressed proinflammatory cytokines and growth factors gene expression.

2.6 Bibliography

Blair-West JR, Coghlan JP, Denton DA, Funder JW, Scoggins BA, Wright RD. The effect of the heptapeptide (2-8) and hexapeptide (3-8) fragments of angiotensin II on aldosterone secretion. J Clin Endocrinol Metab 1971; 32: 575-578

Cesari M, Penninx BWJH, Newman AB, Kritchevsky SB, Nicklas BJ, Sutton-Tyrell K, Tracy RP, Rubin SM, Harris TB, Pahor M. Inflammatory markers and cardiovascular diseases (The Health, Aging and Body Composition [Health ABC] Study). Am J Cardiol 2003; 92: 522-528

Chen WS, Sim MK. Effects of des-aspartate-angiotensin I on the expression of angiotensin AT_1 and AT_2 receptors in ventricles of hypertrophic rat hearts. Regul Pept 2004; 117: 207-212

Chin B.S.P.; Blann A.D.; Gibbs C.R.; Chung N.A.Y.; Conway D.G.; Lip G.Y.H. Prognostic value of interleukin-6, plasma viscosity, fibrinogen, von Willebrand factor, tissue factor and vascular endothelial growth factor levels in congestive heart failure**.** Eur J Clin Invest 2003; 33: 941-948

Deten A, Volz HC, Briest W, Zimmer HG. Cardiac cytokine expression is upregulated in the acute phase after myocardial infarction. Experimental studies in rats. Cardiovasc Res 2002; 55: 329-340

Dzau JV. Tissue angiotensin and pathobiology of vascular diseases: a unifying hypothesis. Hypertension 2001; 37:1047-1052

Finkel MS, Oddis CV, Jacob TD, Watkins SG, Hattler BG, Simmons RL. Negative inotropic effects of cytokines on the heart mediated by nitric oxide. Science 1992; 257: 387-389

Han Y, Runge MS, Brasier AR. Angiotensin II induces IL-6 transcription in vascular smooth muscle cells through pleiotropic activation of NF-κB transcription factors. Cicr Res 1999; 84: 695-703

Irwin MW, Mak S, Mann DL, Qu R, Penninger JM, Yan A, Dawood F, Wen WH, Shou Z, Liu P. Tissue expression and immunolocalization of tumour necrosis factor-α in post-infarction dysfunctional myocardium. Circulation 1999; 99: 1492-1498

Min L, Sim MK, Xu XG. Effects of des-aspartate-angiotensin I on angiotensin II-induced incorporation of phenylalanine and thymidine in cultured rat cardiomyocytes and aortic smooth muscle cells. Regul Pept 2000; 95: 93-97

Nakamura A, Johnson EJ, Imaizumi A, Yanagawa Y, Kohsaka T. Effect of β2-adrenoreceptor activation and angiotensin II on tumour necrosis factor and interleukin 6 gene transcription in the rat renal resident macrophage cells. Cytokine 1999; 11: 759-765

Ono K, Matsumori A, Shioi T, Furukawa Y, Sasayama S. Cytokine gene expression after myocardial infarction in rat hearts. Possible implication in left ventricular remodeling. Circulation 1999; 98: 149-156

Ruiz-Ortega M, Lorenzo O, Suzuki Y, Ruperez M, Egido J. Proinflammatory actions of angiotensins. Curr Opin Nephrol Hypertension 2001; 10: 321-329

Ruiz-Ortega M, Bustos C, Hernandez-Presa MA, Lorenzo O, Plaza JJ, Egido J. Angiotensin II participates in mononuclear cell recruitment in experimental immune complex nephritis through nuclear factor-kappa B activation and monocyte chemoattractant parotein-I synthesis. J Immunol 1998; 161: 430-439

Sadoshima J. Cytokine actions of angiotensin II. Circ Res 2000; 86: 1187-1189

Santos RA, Brum JM, Brosnihan KB, Ferrario CM. The renin-angiotensin system during acute myocardial ischemia in dogs. Hypertension 1990; 15 (Suppl I): I-121

Sim MK, Tang FR, Xu XG. Effects of des-aspartate-angiotensin I on neointima growth and cardiovascular hypertrophy. Regul Pept 2004: 117: 213-217

Sim MK, Min L. Effects of des-Aspartate-angiotensin I on experimentally-induced cardiac hypertrophy in rats. Int J Cardiol 1998; 63: 223-227

Sim MK and Radhakrishnan R. Novel central action of des-Asp-angiotensin I. Eur J Pharmacol 1994; 257: R1-R3

Torre-Amione G, Kapadia S, Benedict C, Oral H, Young JB, Mann DL. Proinflammatory cytokine levels in patients with depressed left ventricular ejection fraction: a report from the studies of left ventricular dysfunctional (SOLVD). J Am Col Cardiol 1996; 27: 1201-1206

Wen Q, Sim MK, Tang FR. Reduction of infarct size by orally-administered des-aspartate-angiotensin I in the ischemic reperfused rat heart.

CHAPTER 3

Endothelial lineage differentiation of human embryonic stem cells - *in vitro* studies

TABLE OF CONTENT

3.1 Abstract

The ability of HESCs to differentiate into specific somatic lineages is expected to have far reaching therapeutic applications in cell and gene therapy. Realization of this potential depends on the development of efficient and reliable protocols for directed differentiation *in vitro* which will significantly increase the number of specific differentiated cell type of interest and ultimately generate pure cultures of that particular lineage.

In this study, we demonstrated that the transduction of adenoviral vector expressing human $VEGF_{165}$ (ad-$hVEGF_{165}$) gene into differentiating HESCs can enhance the efficiency of endothelial lineage differentiation. EPCs and ECs play an important role in blood vessel formation via vasculogenesis and angiogenesis.

HESC line, H1 was induced to form EBs by culturing them in low attachment plates for 7 days, trypsinized into single cells and transduced with ad-$hVEGF_{165}$ under optimized transduction condition. Assessment of mature ECs and putative EPCs was achieved through immunostaining of markers such as CD31, Ve-cadherin, von-Willebrand factor; semi-quantitative and quantitative PCR of various vascular-related transcription factors, growth factors and their receptors gene markers and flow cytometric analysis. ELISA was performed to measure the $hVEGF_{165}$ protein expression and the biological activity of the secreted $hVEGF_{165}$ was assessed using a HUVEC proliferation assay.

Optimal transduction efficiency with high cell viability was achieved by 4-hour exposure of the cells to viral particles at a ratio of 1:500 for 3 consecutive days. ELISA results showed that ad-$hVEGF_{165}$ transduced cells secreted hVEGF for more than 30 days

post-transduction, peaking at day 8 (27.5 ± 7ng/ml). The conditioned medium from the ad-hVEGF$_{165}$ transduced cells resulted in extensive proliferation of HUVEC as compared to other conditioned media (≈2-fold). Upregulation of VEGF, Ang-1, Flt-1, Tie-2, CD34, CD3, CD133 and Flk-1 gene expressions were observed in ad-hVEGF$_{165}$ transduced cells. Real time PCR also showed the gradual increase of CD133 and Flk-1 gene transcripts over a regular time period after transduction. Further flow cytometric analysis of CD133 cell surface marker revealed an approximately 5-fold increase of CD133 marker expression in ad-hVEGF$_{165}$ transduced cells.

These findings suggest that ad-hVEGF$_{165}$ transduction of differentiating HESCs facilitates expression of the VEGF transgene which is able to significantly enhance endothelial-lineage differentiation in HESCs.

3.2 Introduction

HESCs isolated from the inner cell mass of blastocyst stage embryos are pluripotent cells that can be propagated indefinitely in the undifferentiated state in vitro (Reubinoff et al, 2000; Thomson et al, 1998). The successful establishment of several HESC lines in recent years, together with increasing knowledge of their unique properties has led to many attempts at exploiting their therapeutic potential. Differentiation of HESCs into various differentiated somatic lineages such as neurons (Reubinoff et al, 2001; Carpenter et al, 2001; Schuldiner et al, 2000), hematopoietic cells (Kaufman et al, 2001; Schuldiner et al, 2000), cardiomyocytes (Mummery et al, 2002; Kehat et al, 2001) and ECs (Gerecht-Nir et al, 2003; Levenberg et al 2002) have been reported, and subsequent accompanying studies in animal models have demonstrated much potential in cellular transplantation therapy for the treatment of various human diseases. This pluripotential ability of HESCs to differentiate into various cell types holds immense potential for therapeutic use in cell and gene therapy and realization of this potential depends very much on efficient and optimized protocols for genetic manipulation of these cells.

While most of the reported studies use growth factor cocktails to direct differentiation of HESCs, an alternative genetic approach is currently under development based on the hypothesis that HESCs differentiation can be controlled or triggered after gene transfer with specific regulatory genes in order to stimulate or inhibit differentiation of specific lineages. In this context, several research groups have focused on optimization of efficient gene transfer technologies for HESCs and its derivatives.

Several methods are available to achieve introduction of foreign DNA that carries a gene of interest for ectopic expression in HESCs. Electroporation has been shown to generate transient yet stable transfected HESCs (Zwaka et al, 2003). However, it was not a feasible tool because of poor cell survival due to the voltage shock. Modification by performing electroporation of HESCs in clumps suspended in isotonic, protein-rice solution significantly improved cell survival but transfection efficiency was still very low; around 6%. The transfection efficiency was increased to about 66% using nucleofection method (Siemen et al, 2005; Lakshmipathy et al, 2004). Chemical transfection using various lipofection-based reagents including Lipofectamine (Invitrogen), Fugene (Boehringer Mannheim) and ExGen 500 (Fermentas) have also been used in HESCs. A more efficient strategy to stably introduce exogenous DNA into cells is based on the use of viral vectors. Various studies have successfully reported the use of adenovirus, adeno-associated virus and lentivirus to overexpress genes in HESCs (Smith-Africa et al, 2003; Gropp et al, 2003; Ma et al, 2003) and showed encouraging results with either transient or sustained and stable expression of the transgenes depending on the viral vector used.

In this study the focus is on derivation of human EPCs from HESCs. Human EPCs are important for the development of blood vessels which takes place in situ via vasculogenesis and angiogenesis (Carmeliet 2000; Risau 1997; Risau et al, 1995). Both vasculogenesis and angiogenesis take place in functional vascular development both within the developing embryo, as well as in postnatal neovascularization (Asahara T et al, 1999; Flamme I et al, 1997). In vasculogenesis, EPCs or angioblasts differentiate into ECs and assemble into tube-like vascular structures that form a primitive vascular

network. On the other hand, angiogenesis involves the sprouting of new capillaries from pre-existing blood vessels.

Cell-based therapy using EPCs or ECs is one of the more recent advances in the field of regenerative medicine. These cells can either be utilized for the tissue engineering of new blood vessels *in vitro* with implantable scaffolds, or can be transplanted directly into ischemic tissues to augment blood vessel growth, so as to prevent further cellular necrosis within the ischemic microenvironment.

Previous studies have reported endothelial differentiation of HESCs either spontaneously or under the influence of various supplemented exogenous growth factors within the culture milieu i.e. VEGF (Gerecht-Nir et al, 2003; Levenberg et al 2002). VEGF, a heparin-binding glycoprotein is a potent vascular EC-specific mitogen that stimulates EC proliferation, function and survival, microvascular permeability, vasodilation and angiogenesis (Ferrara et al, 1997). VEGF has not only been proven to be a specific and critical growth factor for blood vessel formation, but has also been shown to improve EC function and survival *in vitro*, as well as vascular reactivity *in vivo* (Ferrara et al, 2003; Gerber et al, 1998a & 1998b). It is one of the best studied vascular related growth factor with positively demonstrated therapeutic ability in both animal models and human clinical trials (Haider et al, 2004; Makinen et al, 2002; Street et al, 2002; Henry et al, 2001; Vale et al, 2000; Ferrara et al, 1999).

In this study, we described the use of ad-hVEGF$_{165}$, for enhancing EPC differentiation in HESCs characterized by CD133 marker expression. Adenoviral vectors can be produced at high titers and do not integrate into the host cell genome therefore providing a transient expression of the transgene (Tatsis et al, 2004). Here, we report that

adenoviral type 5 (Ad5) is capable of infecting differentiated HESCs and the transient expression of $VEGF_{165}$ enhances endothelial differentiation. Extensive formation of vascular tube-like structures within transduced cells was observed and the secreted VEGF protein from the differentiating cells was biologically functional. Real-time PCR and immunohistochemical analysis also showed upregulated expression of various vascular genes and markers upon transduction.

3.3 Materials and Methods

3.3.1 Materials

3.3.1.1 Cell lines

Human embryonic stem cells, H1 cell line

Cells were purchased with license agreement from Wicell Research Institute, Inc.

Mouse embryonic fibroblasts

Cells were obtained from mice of CF-1 strain at 13 to 14 days of gestation.

3.3.1.2 Animals

CF-1 mice

A total of 10 female CF-1 mice (13 to 14 days of gestation) were used for obtaining mouse embryonic fibroblasts (MEF) used as feeder layers during human embryonic stem cell culture. CF-1 mice were purchased from Charles Rivers Laboratories.

The materials used for this study is listed in Appendix 6.1.

3.3.2 Methods

3.3.2.1 Cell culture

Human embryonic stem cell culture

HESCs (H1 cell line, Wicell Research Institute Inc, Madison, WI, USA, passage 35 to 70) were grown on a feeder layer of mitotically-inactivated MEF, plated on 0.1% gelatin-coated wells of a 6-well cell culture plate. Each well contained 2×10^5 MEF cells. The H1 cell line used in the present study is one of the National Institutes of Health-approved human ES cell clones.

The culture medium used for HESC culture consisted of 80% DMEM:F-12 media (GIBCO/BRL) supplemented with 20% knockout serum replacement (GIBCO/BRL), 2mM L-glutamine (GIBCO/BRL), 0.1mM β-mercaptoethanol (Sigma), 1% non-essential amino acid stock (GIBCO/BRL) and 4ng/ml bFGF (Invitrogen). All HESC cultures were carried out in a humidified 37^{o}C incubator with a 5% CO_2 atmosphere and were routinely passaged every 5 to 7 days after disaggregation with 1mg/ml collagenase type IV (GIBCO/BRL). HESCs were incubated with collagenase for 5 to 10 minutes at 37°C and scraped off using a cell scraper, washed by centrifugation at 200g/min and replated onto inactivated MEF.

Human umbilical vein endothelial cell culture

HUVEC were cultured in F-12K medium supplemented with 10% (v/v) FBS, 1% penicillin/streptomycin, 20 IU/ml of heparin and 20ng/ml α-FGF. The cells are grown at 37°C in humidified, 5% CO_2 incubator.

Human embryonic kidney 293 cell culture

HEK293 cells were cultured in DMEM supplemented with 10% (v/v) FBS at 37°C in humidified, 5% CO_2 incubator.

3.3.2.2 Derivation, culture, propagation and inactivation of MEF

Derivation of MEF

Fetuses were obtained from CF-1 mouse strain at 13 to 14 days of gestation. CF-1 mouse strain was purchased from Charles River Laboratories. The mice were intraperitoneally injected with 0.01ml/g of mice anesthesia working solution consisting of ketamine:medetomidine mixture in the ratio 1:4. Once the mice were anesthetized, cervical dislocation was performed. The mice were placed belly up in a sterile tissue

culture hood and the abdomen was sterilized with 70% alcohol. Using sterilized instruments, the skin was cut and the peritoneum was exposed. The peritoneal wall was cut to expose the uterine horns. The uterine horns were removed and washed three times with 1× PBS. The embryonic sacs were cut open and embryos were released. The visceral tissue was separated from the embryos. The embryos were then washed three times with 1× PBS and counted. The tissue was minced for 5 to 10 minutes with trypsin dissecting scissors into grain sized pieces and then incubated for 20 to 30 minutes in a 37°C incubator. The minced tissue mixture was vigorously pipetted up and down until it had a sludgy consistency. MEF derivation culture media was added and the mixture was equally divided into the T75 flasks, each containing 3 embryos. MEF derivation culture medium was made up of DMEM supplemented with 10% FBS, 2mM L-glutamine, 1% non-essential amino acids solution and 1× penicillin-streptomycin solution. The flasks were incubated overnight in 37°C incubator. Once 90% of the flask surface was covered with a cell layer, the cells were trypsinized for 5 minutes and scraped with a cell scraper. MEF culture medium was then added to neutralize the trypsin and the mixture was pipetted vigorously up and down to break up the cell chunks. MEF culture medium consisted of DMEM supplemented with 10% FBS, 2mM L-glutamine and 1% non-essential amino acids solution. The mixture was allowed to settle, supernatant was then removed, leaving the large cell chunks behind. The mixtures were centrifuged at 200g for 5 minutes. The cell pellet was resuspended in equal volume of fresh MEF culture medium and cryopreservation medium. Cryopreservation medium consisted of DMEM supplemented with 0.2% FBS and 0.2% dimethyl sulphoxide (DMSO) (Sigma). The cell suspension was dispensed into 1.5ml cryovials and stored in isopropanol freezing

container overnight at -80°C freezer. The cryovials were then transferred to liquid nitrogen racks for permanent storage.

MEF culture, propagation and inactivation

MEF was cultured in MEF culture medium in a 37°C incubator. When 80 to 90% confluency was reached, the cells were passaged using 1× trypsin for 5 minutes at 37°C. Mitotic inactivation of the MEF was achieved through pre-treatment with 10μg/ml mitomycin-C for 2 hours at 37°C. For preparation of human embryonic stem cells, 2×10^5 inactivated MEF cells were seeded per well of a 6-well plate.

3.3.2.3 In vitro characterization of human embryonic stem cells

Immunofluorescent staining of pluripotency markers of human embryonic stem cells

The HESC was grown in a 24-well cell culture plate. They were washed with 1× PBS and fixed with 4% paraformaldehyde for 20 minutes at room temperature. After washing, the cells, they were permeabilized with 0.1% Triton X-100 and blocked with 1% bovine serum albumin (BSA), 10% normal donkey serum in 1×PBS for 45 minutes. For staining of SSEA-4, permeabilization with Triton X-100 was omitted. The cells were then incubated with one of the following antibodies (Table 8) at a concentration of 10ug/ml overnight at 2 to 8°C. The cells were washed three times with 1× PBS containing 1% BSA for 5 minutes and then incubated with the respective diluted secondary antibodies for 60 minutes at room temperature in the dark. After washing three times with 1× PBS containing 1% BSA, the cells were covered with a Vectashield mounting medium with DAPI and visualized with a fluorescent microscope.

Table 8: Primary and secondary antibodies used for immunostaining of pluripotency markers

Name of primary antibody	Name of secondary antibody
Goat anti-Nanog	Donkey anti goat IgG-FITC
Goat anti-Oct3/4	Donkey anti goat IgG-FITC
Mouse anti-SSEA-4	Donkey anti mouse IgG-TRITC
Mouse anti human Tra-1-60	Donkey anti mouse IgG-TRITC
Mouse anti human Tra-1-81	Donkey anti mouse IgG-TRITC

Table 9: PCR cycling programme

Initial activation step	15 min	95°C
3-step cycling: Denaturation	1 min	94°C
Annealing	1 min	*refer to table 10 and 12 for respective primers
Extension	1 min	72°C
Number of cycles	*refer to table 10 and 12 for respective primers	
Final extension	10 min	72°C

Table 10: List of primer sequences for pluripotency markers

Gene	Sequence	Number of Cycle
Oct-4 (247bp)(55°C)	Forward= 5'-CGTGAAGCTGGAGAAGGAGAAGCTG-3' Reverse= 5'-AAGGGCCGCAGCTTACACATGTTC-3'	30
Sox-2 (370bp)(55°C)	Forward= 5'-CCGCATGTACAACATGATGG-3' Reverse= 5'- CTTCTTCATGAGCGTCTTGG-3'	30

Table 11: List of primary and secondary antibodies used for immunostaining of various vascular markers

Primary antibody	Dilution used	Secondary antibody	Dilution used
Mouse anti human VEGF	1:100	Goat anti mouse IgG-FITC	1:500
Mouse anti human CD31	1:100	Rabbit anti mouse IgG-TRITC	1:500
Rabbit anti human Ve-cad	1:200	Goat anti rabbit IgG-TRITC	1:500
Rabbit anti human vWF	1:500	Mouse anti rabbit IgG-FITC	1:500

RT-PCR analysis for pluripotency gene markers expression for human embryonic stem cells

HESCs, ad-hVEGF$_{165}$ and ad-null transduced differentiating cells were analyzed by RT-PCR for expression of pluripotency markers. Total RNA was isolated using Total RNA extraction kit (Qiagen) according to manufacture's instruction that is outlined in 6.2.1.

Total RNA was reverse transcribed into cDNA using oligo(dT)$_{20}$ and resuspended in ddH_2O. Briefly, 10μg of RNA was added to a mixture containing 1μg of oligo(dT)$_{20}$ and incubated for 5 minutes at 70°C. The RNA and oligo(dT)$_{20}$ mixture was mixed with 1× RT buffer-reaction buffer, 1mM of dNTPs, 65U of RNase inhibitor, 250U of Moloney murine leukemia virus reverse transcriptase. Distilled water was added to a final volume 50μl. The sample mixture was incubated at 37°C for 1 hour and then at 95°C for 10 minutes before quickly chilling it on ice.

Reverse transcription polymerase chain reaction (RT-PCR) was performed using a HotStarTaq PCR kit. One PCR reaction mixture consisted of 1× PCR buffer containing 1.5mM Mg^{2+}, 200μm of dNTPs, 2.5U of HotStarTaq DNA polymerase and 0.5μm of forward and reverse primers, 500ng of template cDNA. Distilled water was added to give a final volume of 25μl. The PCR cycling program used is outlined below in Table 9. The annealing temperature and the cycling times were optimized for each gene target. The details of each primer sets that were used are listed in Table 10. GAPDH was used as the internal control for the PCR reactions. The amplified PCR products were run on a 2% agarose gel with ethidium bromide. The mean pixel intensities of each gene band was measured and normalized to mean pixel intensities of the GAPDH band. The intensities

were determined using a computerized densitometry system (Olympus Micro Image, Maryland, USA).

3.3.2.4 Embryoid body-derived cells transduction with ad-hVEGF$_{165}$

EB formation

To induce differentiation through EB formation, a confluent six-well plate of undifferentiated HESC colonies was used. The HESC colonies were removed from the feeder layers by digestion with 1mg/ml collagenase type IV for 5 minutes at 37°C. They were then dissociated into small clumps by using 1,000ul pipette tips and transferred to low attachment plates. EBs were grown in medium consisting 80% DMEM:F-12 media supplemented with 20% knockout serum replacement, 2mM L-glutamine, 0.1mM β-mercaptoethanol and 1% non-essential amino acids solution. EBs were cultured in suspension for 5 to 21 days.

Dissociation of EBs into single cells

The EBs were incubated in 2mg/ml collagenase IV for 15 minutes at 37°C. They were centrifuged at 200rpm/min for 5 minutes and were next incubated in a mixture containing cell dissociation buffer and 0.1% trypsin at a ratio of 2:1 for 20 minutes at 37°C. They were washed by centrifugation at 200rpm/min for 5 minutes and filtered using a 40μ cell strainer before being used in further designated experiments.

Monocistronic ad-hVEGF$_{165}$

The monocistronic adenoviral vector carrying human VEGF$_{165}$ gene was kindly provided by Associate Professor Ge Ruowen from Department of Biological Sciences, National University of Singapore. The replication deficient adenoviral vector carrying human VEGF$_{165}$ gene was driven by immediate early human cytomegalovirus promoter

which was rescued into the E1 region of the pJMK17 Ad5 genomic plasmid by cotransfection into HEK-293 cells. The virus was plaqued purified thrice before propagation.

Adenoviral vector propagation

Ad-hVEGF$_{165}$ was propagated in HEK-293 cells. These cells were cultured in 75mm^2 tissue culture flask at a density of 1×10^6 cells using DMEM supplemented with 10% FBS. When 80 to 90% confluence was reached, the cells were transfected with ad-hVEGF$_{165}$. Following full cytopathic effect (CPE) development, the supernatant from the HEK-293 cells were removed. The cells were lysed and centrifuged to remove the debris. The virus was purified by cesium chloride gradient ultra centrifugation and used for transduction of the differentiating embryonic stem cells from EBs.

Adenoviral vector titer

Adenoviral vector titration was performed using an endpoint assay as described by Quantum Biotechnology, USA. About 1×10^4 HEK 293 cells were plated in each well of a 96-well tissue culture plate in 100µl of 2% DMEM on the day of the experiment. This was followed by adding 100µl of 2% DMEM containing purified viral stock with dilution ranging from 10^{-3} to 10^{-15} per ml. Each dilution was applied to 10 wells and another 16 wells were added with 2% DMEM as negative controls. Cells were incubated for 10 days at 37°C and observed daily for CPE development. At the end of the incubation, the tissue culture dose-50 (TC_{ID50}) was calculated using the following formula: $TC_{ID50}/ml=10^{[1+d\ (S-0.5)]}$, where d = Log 10 of the dilution (=1 for a 10 fold dilution) and S = the sum of the ratios (always starting from the first 10^{-1} dilution). PFU

per ml was also calculated by subtracting the TC_{ID50} /ml from 0.7 log. Assays were repeated three times to get the average viral titer.

Optimization of EBs transduction with adenoviral vector

1×10^5 cells/cm^2 were cultured in each well of a 12-well plate (3.8cm^2). The cells were exposed to either ad-$hVEGF_{165}$ or null adenoviral vector (ad-Null) at various titers ranging from 50pfu/cell to 2000pfu/cell. The supernatant containing the adenoviral vector was filtered through 0.22μm filter into each well and incubated at 37°C in 5%CO2 incubator for 4 hours. The viral transduction medium was replaced after 4 hours with normal 10% DMEM:F12 for 24 hours. The transduction procedure was repeated on three consecutive days to achieve optimum transduction efficiency.

3.3.2.5 In vitro characterization of differentiating cells from embryoid bodies transduced with ad-$hVEGF_{165}$

Immunofluorescent staining for vascular markers; VEGF, CD31, Ve-cadherin and von-Willebrand factor

$1\times\ 10^5$ ad-$hVEGF_{165}$ transduced cells were seeded and grown on each glass chamber slides. Ad-null transduced cells were used as the negative control. Cells were fixed with 4% paraformaldehyde for 20 minutes at room temperature. After washing with 1× PBS twice for 5 minutes each, the cells were incubated with 3% methanolic hydrogen peroxide for 15 minutes to reduce the non specific background staining from endogenous peroxidase. The non specific binding sites were blocked by Ultra V block (Ultravision detection system) for 8 minutes at room temperature followed by incubation with the respective primary antibodies at optimal dilution at room temperature overnight (Table 11). The cells were washed thrice with 1× PBS on the following and then incubated with

the respective diluted secondary antibodies for 90 minutes at room temperature in the dark. After further washing, the cells were air dried in the dark. They were then covered with a Vectashield mounting medium with DAPI and visualized with a fluorescent microscope. The FITC or TRITC positive cells were calculated by counting 6 microscopic fields on stained and unstained cells on 6 slides.

RT-PCR analysis for vascular growth factors and their receptors, transcription factors, surface markers

Ad-hVEGF$_{165}$ and ad-Null transduced differentiating cells were analyzed by RT-PCR for expression of various vascular growth factors and their receptors, transcription factors and EPC cell markers. The PCR cycling program used is outlined in Table 9. The details of each primer sets that were used are listed in Table 12.

Real time PCR quantitative analysis for endothelial progenitor cell markers; CD133 and Flk-1

TaqMan Universal PCR Master Mix and Assays-on-Demand Gene Expression Probes (Applied Biosystems) for CD133, Flk-1 and GAPDH were used according to the manufacturer's instructions. The TaqMan PCR step was performed using an Applied Biosystems Fast 7500 Fast Real Time PCR System. The relative expression of CD133 and Flk-1 was normalized to the amount of GAPDH in the same cDNA by using the standard curve method described by the manufacturer. The relative standard curve method was used to calculate amplification differences between HESCs and the ad-hVEGF$_{165}$ transduced differentiating cells. The average values of the experiments were obtained and graphed with standard deviations.

Table 12: List of primer sequences for endothelial-related gene markers

Gene	Sequence	Number of cycles
Flt-1 (554bp)(60°C)	F= 5'-GTCATTCCCTGCCGGGTTAC-3' R= 5'-CGATGTTTCACAAGTGATGAAT-3'	30
VEGF (576bp) (64°C)	Forward= 5'-ATGAACTTTCTGCTGTCTTGGGTG-3' Reverse= 5'-TCACCGCCTCGGCTTGTCACA-3'	35
CD34 (420bp)(60°C)	Forward= 5'-TGACTCAGGGCATCTGCCTG-3' Reverse= 5'-CTTTCTCCTGTGGGGCTCCA-3'	35
CD31 (700bp)(60°C)	Forward= 5'-GCTGTTGGTGGAAGGAGTGC-3 Reverse= 5'-GAAGTTGGCTGGAGGTGCTC-3'	35
Tie-2 (250bp)(55°C)	Forward= 5'-CCTTAGTGACATTCTTCC-3' Reverse= 5'-GCAAAAATGTCCACCTGG-3'	31
Ang-1 (378bp)(64°C)	Forward= 5'-CGGTGAATATTGGCTGGGGAATGAG-3' Reverse= 5'-GTAGTGCCACTTTATCCCATTCAG-3'	35
GATA-2 (480bp)(60°C)	Forward= 5'-CCCTAAGCAGCGCAGCAAGAC-3' Reverse= 5'-TGACTTCTCCTGCATGCACT-3'	31
GATA-3 (790bp)(60°C)	Forward= 5'-ACCCCACTGTGGCGGCGAGAT-3' Reverse= 5'-CACAGCACTAGAGACC-3'	31
Flk-1 (450bp)(55°C)	Forward=ACCACAGTCCATGCCATCAC-3' Reverse= 5'-TTCACCACCCTGTTGCTGTA-3'	30
CD133 (200bp)(58°C)	Forward= 5'-CAGTCTGACCAGCGTGAAAA-3' Reverse= 5'-GCCATCCAAATCTGTCCTA-3'	27
GAPDH (800bp)(60°C)	Forward= 5'-CGGATTTGGTCGTATTGGGCG-3' Reverse= 5'-GTGGAGGAGTGGGTGTCGCTG-3'	35

Enzyme Linked Immunoabsorbent Sandwich Assay for $hVEGF_{165}$

$hVEGF_{165}$ protein secreted by ad-$hVEGF_{165}$ and ad-Null transduced differentiating cells were detected using human VEGF Quantikine Sandwich enzyme-linked immunoabsorbent assay (ELISA) kit. The cells were grown in 6-well plates at a density of 2×10^5 cells per well.

The supernatant from each well was collected at regular time intervals from day 1 to day 30 at 2-day intervals. The samples were kept frozen at -80°C until they were used for the assay. The assay was performed according to the supplier's instructions. Briefly 200µl of sample or $hVEGF_{165}$ standards were coated into each designated well in triplicate, incubated for 2 hours at room temperature. After washing three times with washing buffer, 200µl horseradish peroxidase conjugated polyclonal antibody against hVEGF was then dispensed into each well. The plate was incubated at room temperature for 2 hours, washed with a wash buffer and incubated at room temperature for 20 minutes with colour substrate solution containing hydrogen peroxide and chromogen (tetramethylbenzidine) for detection of the presence of primary antibody. Absorbance was determined at 540nm by using an ELISA plate reader.

Flow cytometry for CD133 positive cells

To determine the percentage of $CD133^+$ cells from ad-$hVEGF_{165}$ and ad-null transduced differentiating cells, the cells were incubated with 10µl of phycoerythrin-labeled anti-CD133 monoclonal antibody for 30 minutes in the dark at 4°C. For isotype control, the cells are incubated with phycoerythrin-labeled mouse IgG1. Flow cytometric analysis was perfomed using Beckman Coulter Epics Altra Hypersort system and WinMDI software. Each analysis included ≥10 000 events.

3.3.2.6 Biological activity assessment of hVEGF$_{165}$ secreted by the transduced EB-derived cells

HUVEC proliferation assay

HUVEC cells were cultured in F-12K medium supplemented with 10% (v/v) FBS, 1% penicillin/streptomycin, 20 IU/ml heparin and 20ng/ml α-FGF. For cell proliferation assay, 2×10^4 cells/well was cultured in a 6-well cell culture plate in triplicate for each sample. After culturing for 24 hours with DMEM supplemented with 2% (v/v) FBS, the cells were washed once with PBS and conditioned medium from ad-hVEGF$_{165}$ transduced cells, untransduced cells and ad-Null transduced cells were applied to the designated wells. The cells are grown at 37°C in humidified, 5% CO_2 incubator for 96 hours.

3.3.3 Statistical analysis

Statistical analysis was performed using SPSS (version 11.0). All data were presented as mean ± standard error mean (SEM) and analyzed by analysis of variance (ANOVA) between groups. Intra-group comparison was carried out using paired student t test. $P< 0.05$ was considered statistically significant.

3.4 Results

3.4.1 Characterization of HESCs grown on mouse feeder layer

HESCs were grown on mouse feeder layer to maintain its undifferentiated state. The morphology of human embryonic stem cells grown on mouse feeder layer is as shown in Figure 14. They grew in very compact, round-shaped colonies with defined borders. They were highly proliferative and confluency was reached by 5 days post-passage.

HESCs expressed cell surface markers that characterized their undifferentiated state and pluripotential capability (Figure 15). They expressed stage-specific embryonic antigen-4 (SSEA-4), glycoprotein; tumour rejection antigen-1-60 (TRA-1-60) and TRA-1-81. They were also positive for immunostaining of transcription factors controlling pluripotency such as Oct-4 and Nanog.

3.4.2 Morphology of EBs formed in suspension and on gelatin coated plate

In order to induce differentiation in human embryonic stem cells, they had to be grown in suspension as aggregates. They were cultured in human embryonic stem cell medium without bFGF in low attachment plates. Under these conditions, human embryonic stem cells consistently aggregated and formed simple embryoid bodies (EBs) (Figure 16). Simple EBs generally consisted of densely packed human embryonic stem cells. Over time, differentiation of a columnar epithelium with a basal lamina and formation of central cavity occurred creating cystic EBs (Figure 16).

When the EBs were seeded on gelatin coated plates, random differentiation occurred, resulting in the appearance of a heterogenous population of mesodermal, endodermal and ectodermal cell types (Figure 17).

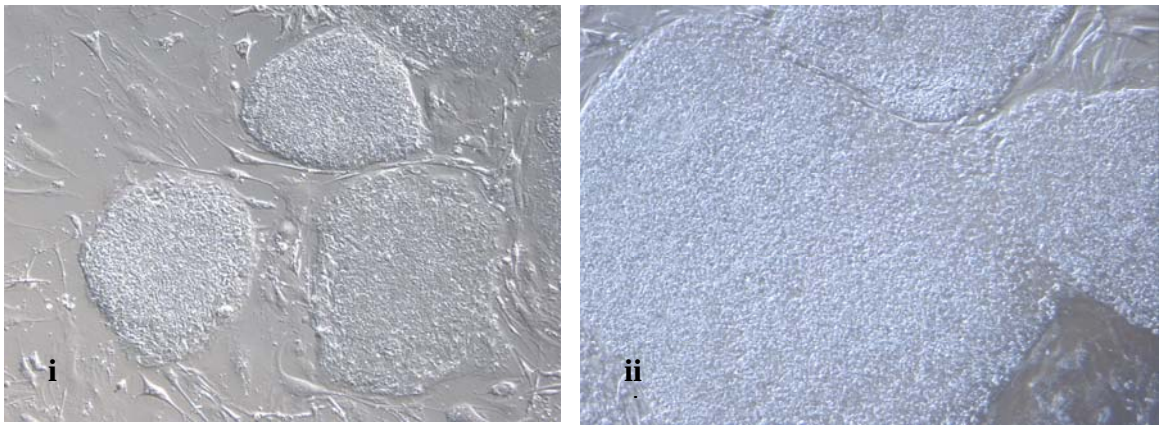

Figure 14: **Human embryonic stem cells cultured on mouse fibroblast feeder layer.** (i) day 3, (ii) day 5. (Magnification 200×)

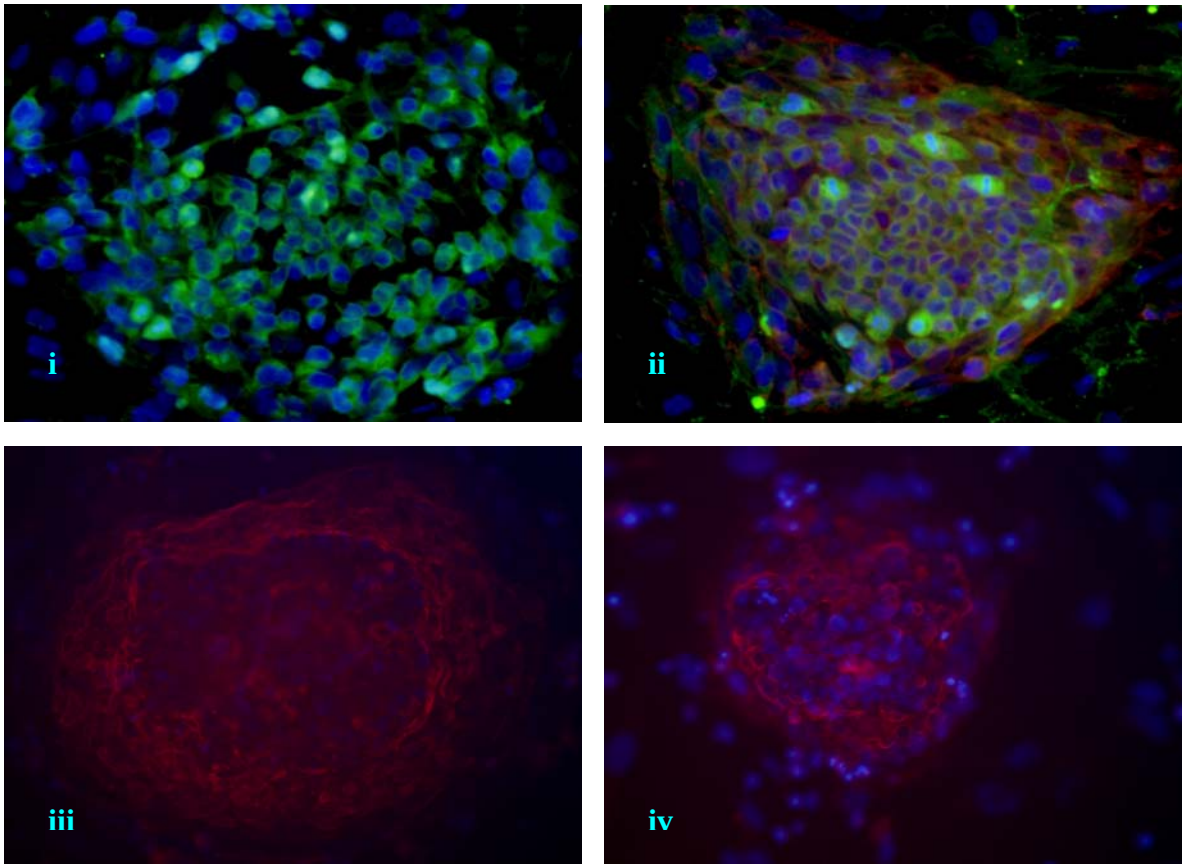

Figure 15: **Immunofluorescent staining of human embryonic stem cell pluripotent markers.** (i) Oct-4- green FITC fluorescence, (ii) SSEA-4 and Nanog- red TRITC fluorescence and gree FITC fluorescence respectively, (iii) TRA-1-60- red TRITC fluorescence, (iv) TRA-1-81-red TRITC fluorescence. Nuclei were stained with blue DAPI fluorescence. (Magnification 200×)

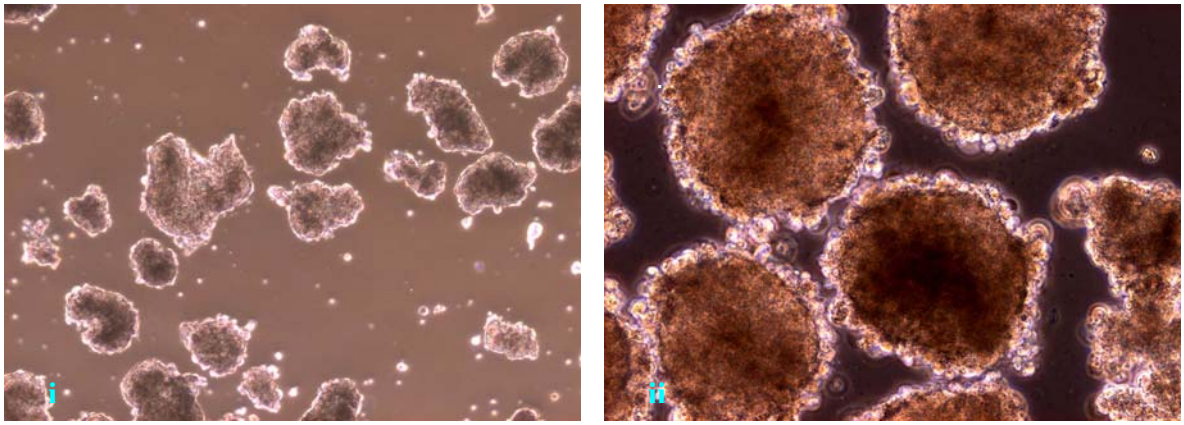

Figure 16: **Embryoid body formation. EBs cultured in suspension in low attachment wells.** (i) day 0, (ii) day 5. Magnification 100×. EBs differentiating once plated in gelatin coated wells. a) day 2 after plating, b) day 8 after plating. (Magnification 200×)

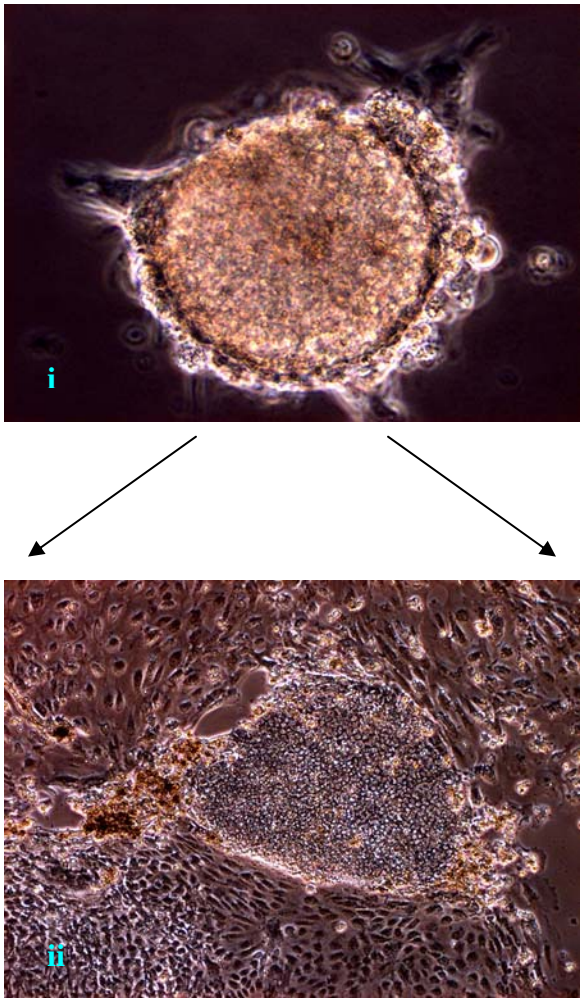

Figure 17: **Random differentiation of EBs plated on gelatin-coated plate wells.** (i) day 2 after plating, (ii) day 8 after plating. (Magnification 200×)

3.4.3 Expression of pluripotency genes in HESCs, EBs and transduced EB-derived cells

Expression of pluripotency gene markers, Oct-4 and Sox-2 were significantly expressed in HESCs. These pluripotent gene markers were significantly downregulated when embryonic stem cells started to differentiate. These were observed in the EBs and the transduced EB-derived cells (Figure 18).

3.4.4 Adenoviral vector titer

The adenoviral vector titer determined by end point assay revealed that the viral titer was ~8× 10^8 pfu/ml for ad-null and ~7× 10^6 pfu/ml for ad-hVEGF$_{165}$. Both viral vectors were found to be replication deficient when tested for replication competence.

3.4.5 Optimization of transduction condition and extent of apoptotic cell death upon transduction in EB-derived cells

The transduction efficiency as assessed by hVEGF$_{165}$ ELISA revealed a dose-dependent relationship between the number of viral particles and the number of 7 day EB-derived cells. Transduction efficiency increased with higher viral titer with highest VEGF expression level achieved at 1:500 cell/viral particles ratio (Figure 19). While transduction efficiency increased with increasing viral titer, this was accompanied with increased extent of cell death (Figure 20). Approximately 23% of the cells died upon transduction at 1:500 cell/viral particles ratio and as the ratio reached to 1:2000, almost 80% of the cells died. The optimal condition used in this study was transduction at 1:500 cell/viral particles ratio for 4 hours three times at an interval of 24 hours after every transduction. The cell viability was about 80% as shown by dye exclusion method using Trypan Blue staining after transduction.

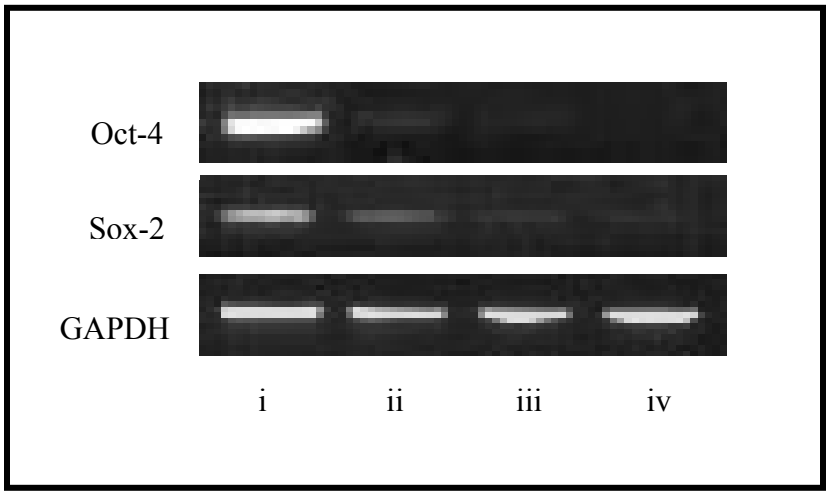

Figure 18: **Gene expression of pluripotency markers Oct-4 and Sox-2** in (i) undifferentiated human embryonic stem cells, (ii) 7-day EBs, (iii) ad-null transduced 7-day EB-derived cells and (iv) ad-hVEGF$_{165}$ transduced 7-day EB-derived cells.

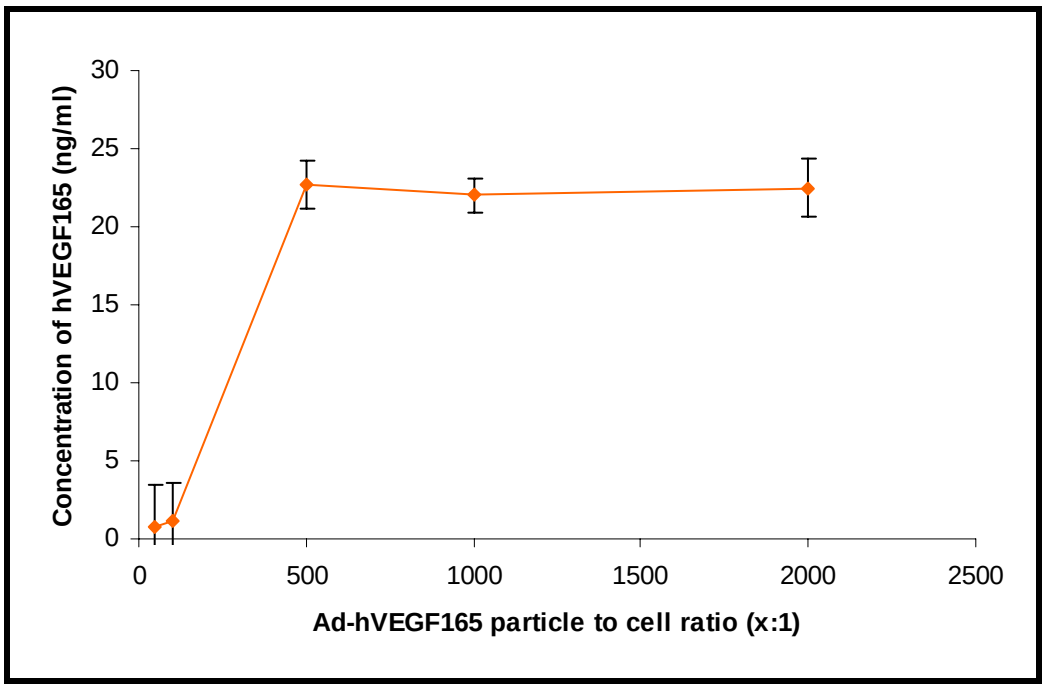

Figure 19: **Optimization of transduction conditions for EB-derived cells.** Transduction efficiency as a function of the ratio between ad-hVEGF$_{165}$ particles and 7 day EB-derived cells. The transduction efficiency was maximum at 1 cell: 500 pfu ratio.

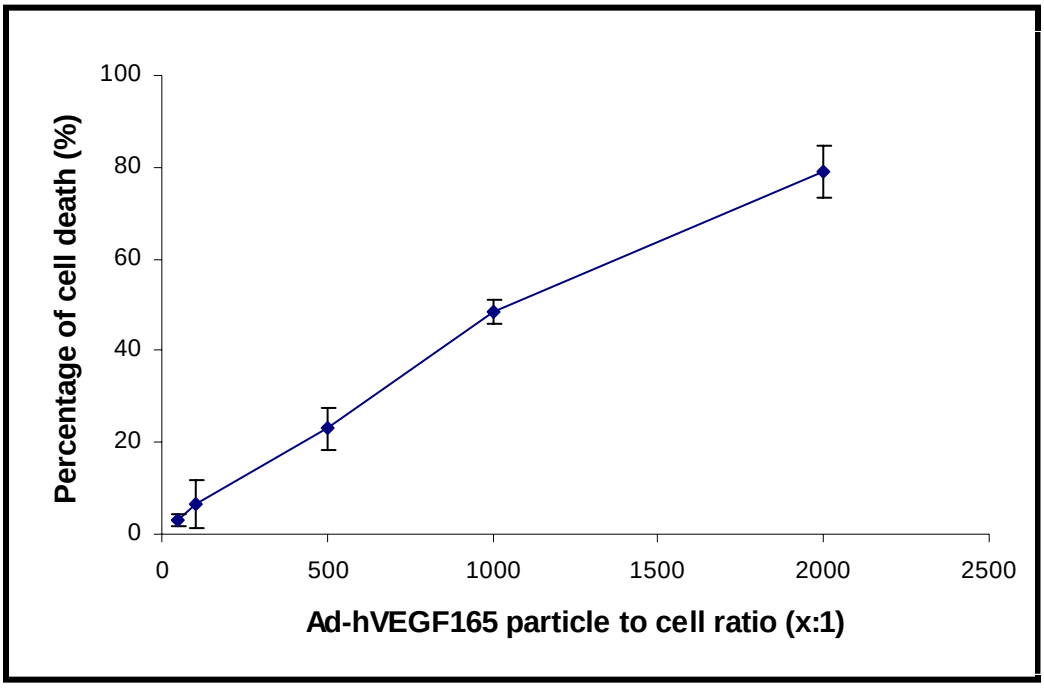

Figure 20: **Apoptotic cell death upon transduction of ad-hVEGF$_{165}$ to the EB-derived cells.** Trypan blue exclusion dye was performed to count the number of dead cells at various cell to viral particle ratios.

3.4.6 VEGF expression from transduced EB-derived cells

ELISA results showed that ad-hVEGF$_{165}$ transduced cells secreted hVEGF for more than 30 days post-transduction, peaking at day 8 (27.5 ± 7ng/ml) (Figure 21). This level of expression was significantly higher ($p<0.01$) than the untransduced and ad-Null transduced cells. Untransduced and ad-Null viral transduced cells showed very low levels of hVEGF expression, with an average value of 0.15± 3 ng/ml throughout the 30 days with no increase in expression levels.

Fluorescent immunostaining also showed high transduction efficiency of about 90% for HVEGF in ad-hVEGF$_{165}$ transduced cells (Figure 22).

3.4.7 Biological activity of the secreted VEGF$_{165}$

The biological activity of the VEGF$_{165}$ secreted by ad-hVEGF$_{165}$ transduced cells was assessed by its capability to induce HUVEC proliferation. VEGF is known to promote endothelial proliferation and triggers DNA synthesis in ECs. Beginning at 2 $\times 10^4$ cells, HUVEC showed significantly higher proliferation rate after culturing with conditioned medium from ad-hVEGF$_{165}$ transduced cells after 5 days of observation (4.1 ± 0.3 $\times 10^3$, $p<0.01$) as compared with conditioned medium from untransduced and null-ad transduced cells ($2.2 \pm 0.04 \times 10^5$ and $2.1 \pm 0.04 \times 10^5$ respectively). Incubation of the conditioned medium from ad-hVEGF$_{165}$ transduced cells with anti-hVEGF$_{165}$ antibody inhibited this effect (Figure 23).

3.4.8 Characterization of endothelial cells upon ad-hVEGF$_{165}$ transduction

The efficiency of endothelial cell differentiation in ad-hVEGF$_{165}$ transduced cells was assessed by fluorescent immunostaining and standard PCR.

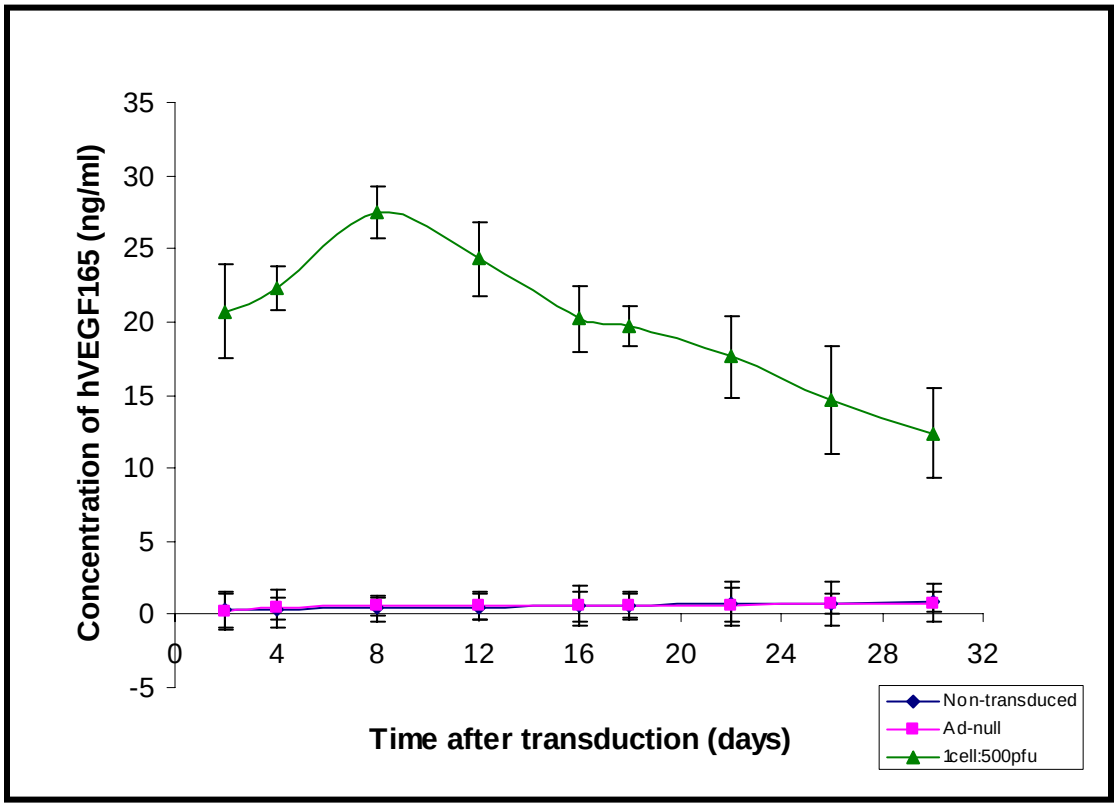

Figure 21: **Time course of hVEGF protein secretion from ad-hVEGF$_{165}$ transduced cells (transduced at 1:500 cell to viral particle ratio).** The secretion of hVEGF protein from the cells in cell culture supernatant was measured at a regular time interval of 2 days for up to 30 days after transduction.

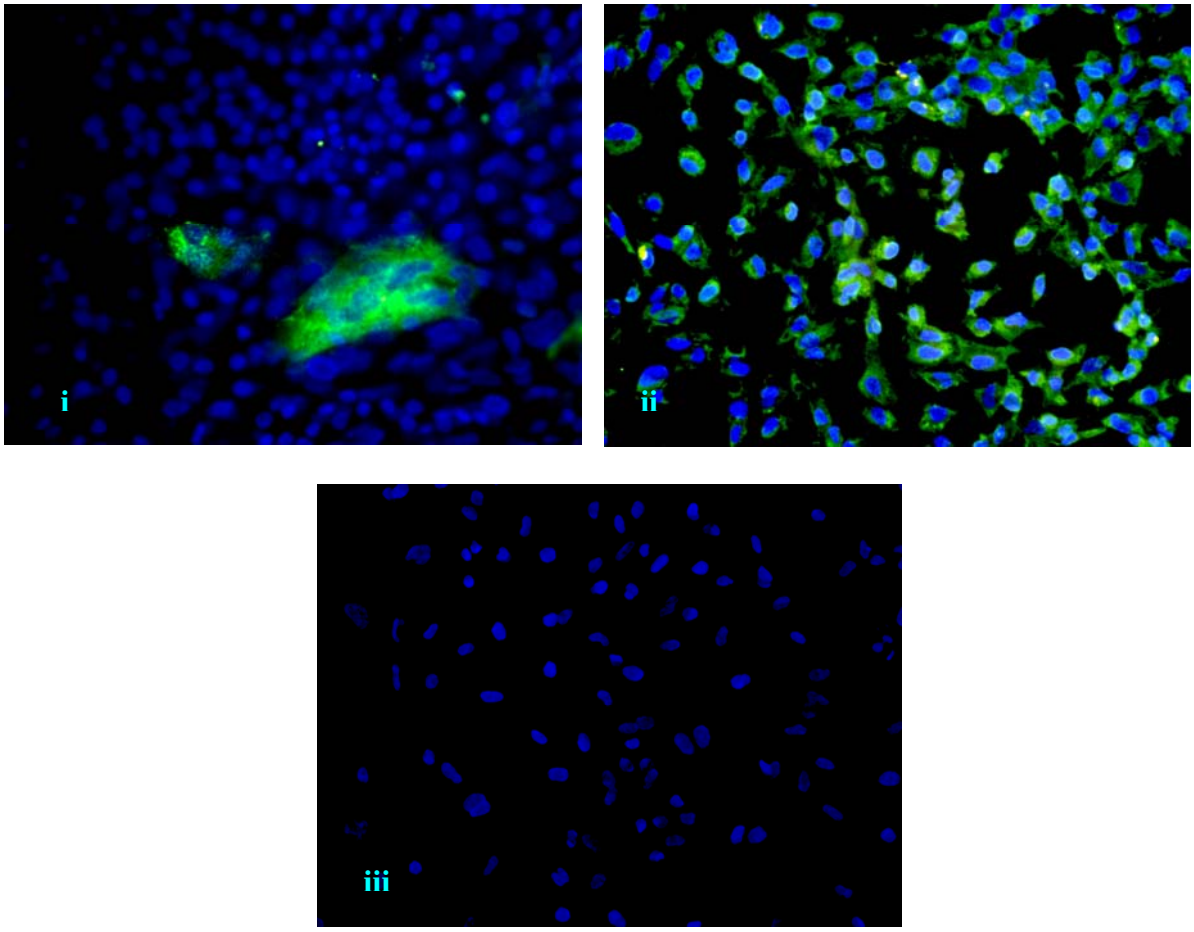

Figure 22: **Immunofluorescent staining for VEGF expression.** VEGF expression seen as green fluorescent (FITC) in (i) ad-Null transduced cells and (ii) ad-hVEGF$_{165}$ transduced cells, (iii) negative control incubated without VEGF primary antibody. Cell nuclei were stained with DAPI (blue fluorescence). (Magnification= 200×)

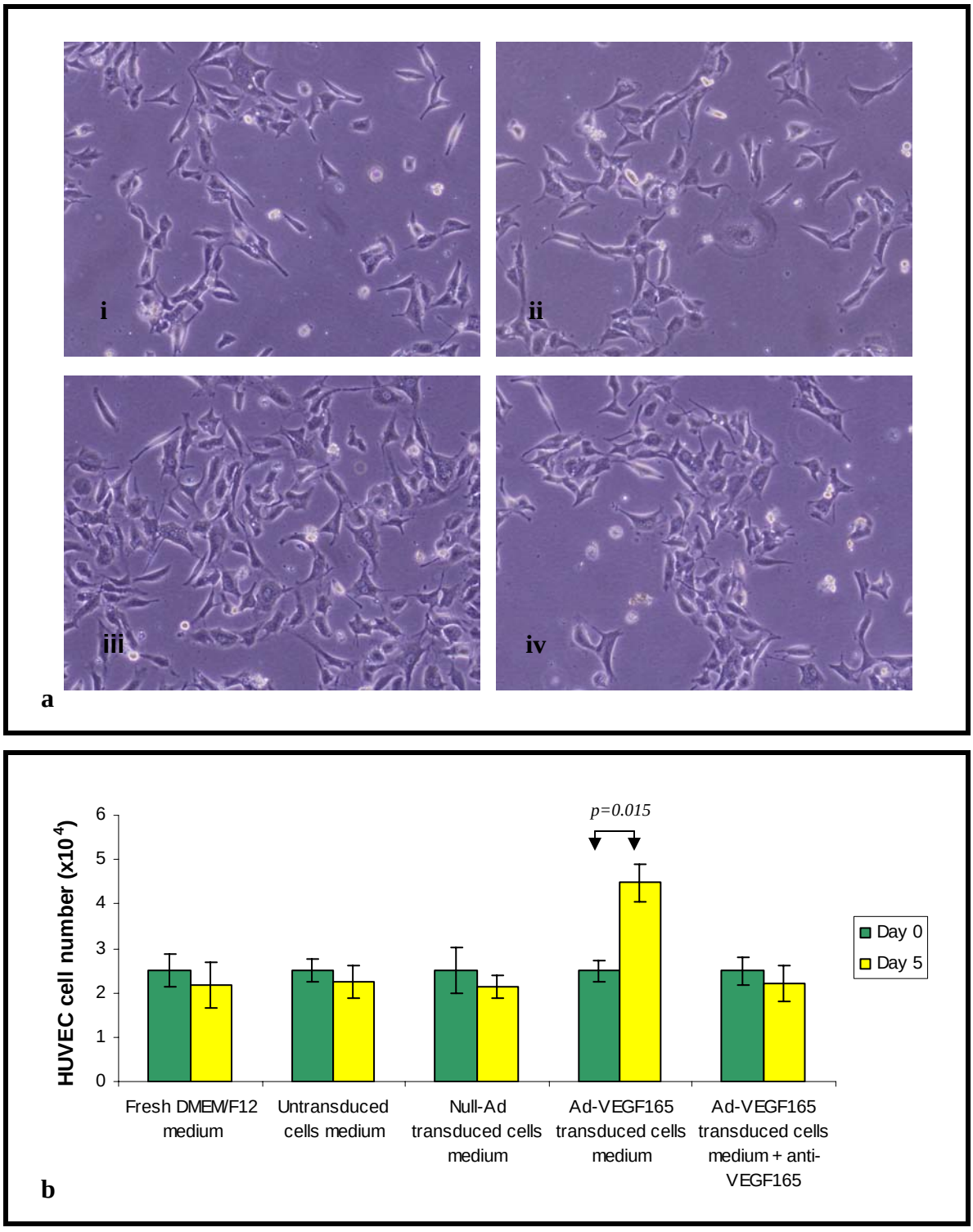

Figure 23: (a & b) **HUVEC proliferation assay to assess the biological activity of $hVEGF_{165}$ secreted from the transduced differentiating embryonic stem cells.** (i) Conditioned medium (CM) from non-transduced cells, (ii) CM from ad-Null transduced cells, (iii) CM from ad-$hVEGF_{165}$ transduced cells, (iv) CM from ad-$hVEGF_{165}$ transduced cells pretreated with anti-$VEGF_{165}$ antibody.

Fluorescent immunostaining

Flurorescent immunostaining of several endothelial markers such as CD31, Ve-cadherin, and von Willebrand Factor (vWF) was carried out. The percentages and the staining patterns of cells expressing the markers are shown in Table 13 and Figures 24-26. CD31 and Ve-cadherin are cell surface antigens while vWF is a cytosolic protein. The data revealed that transduction of EB-derived cells successfully enhanced endothelial differentiation as determined by the increased number of positively immunostained cells for the various endothelial markers. However, this efficiency decreased with increasing age of the EBs (Table 13).

Standard PCR for gene expression analysis

Standard semi-quantitative PCR was performed to study the various endothelial-related transcription factors, surface markers, growth factors and their related receptors (Figure 27). The genes analyzed in this study were transcription factors, GATA-2 and GATA-3, surface markers, CD31 and CD34, VEGF with its receptor, Flt-1 and Ang-1 and its receptor, Tie-2. VEGF, Ang-1 and CD34 gene expressions showed significant upregulation of more than 5-fold with reference to the spontaneously differentiated cells from 7-day EBs. Flt-1, Tie-2 and CD31 gene expressions showed moderate upregulation of one to 3-fold with reference to the spontaneously differentiated cells from 7-day EBs. No significant change was observed for GATA-2 and GATA-3 gene expression in ad-h$VEGF_{165}$ transduced cells.

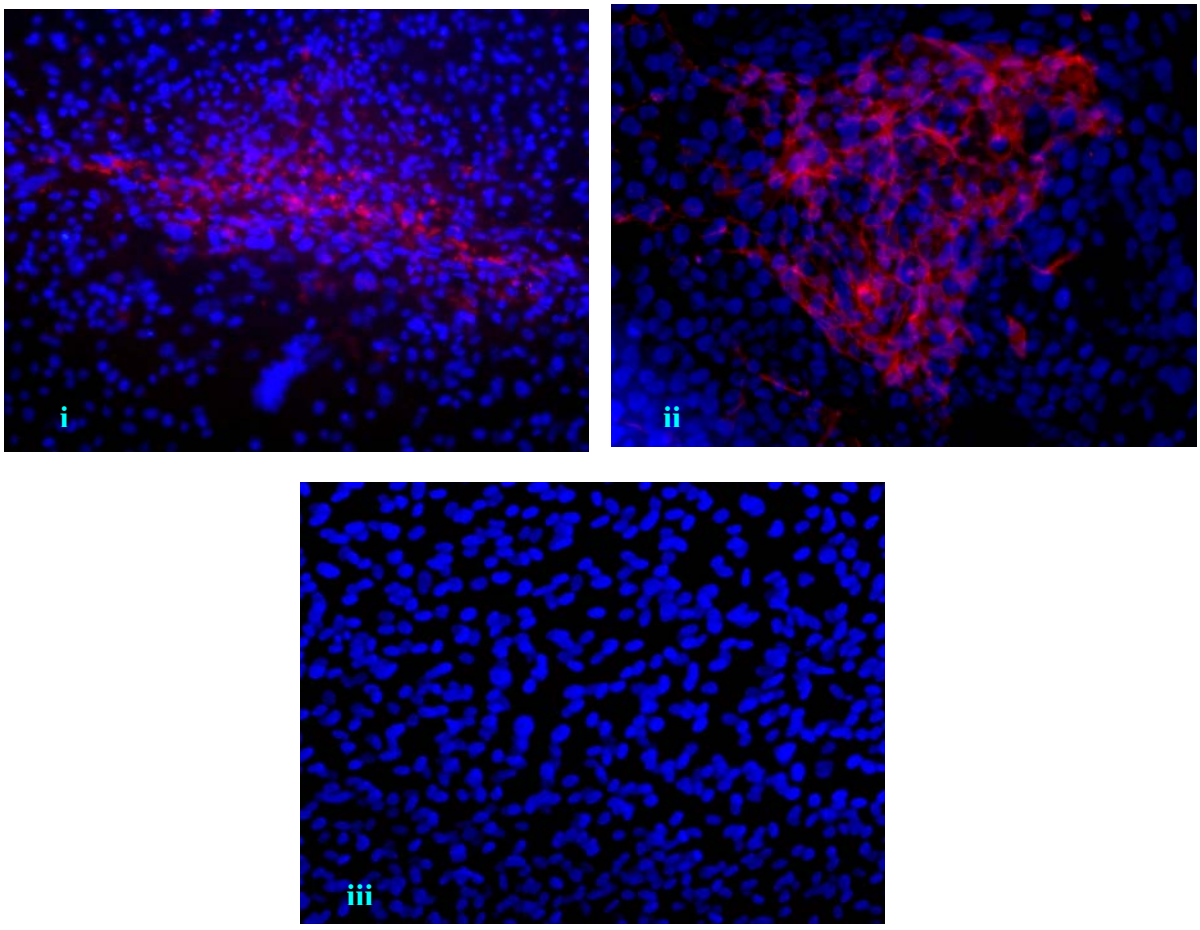

Figure 24: **Immunofluorescent staining for CD31 expression.** CD31 expression seen as red fluorescent (TRITC) in (i) ad-Null transduced cells and (ii) ad-hVEGF$_{165}$ transduced cells, (iii) negative control incubated without CD31 primary antibody. Cell nuclei were stained with DAPI (blue fluorescence). (Magnification= 200×)

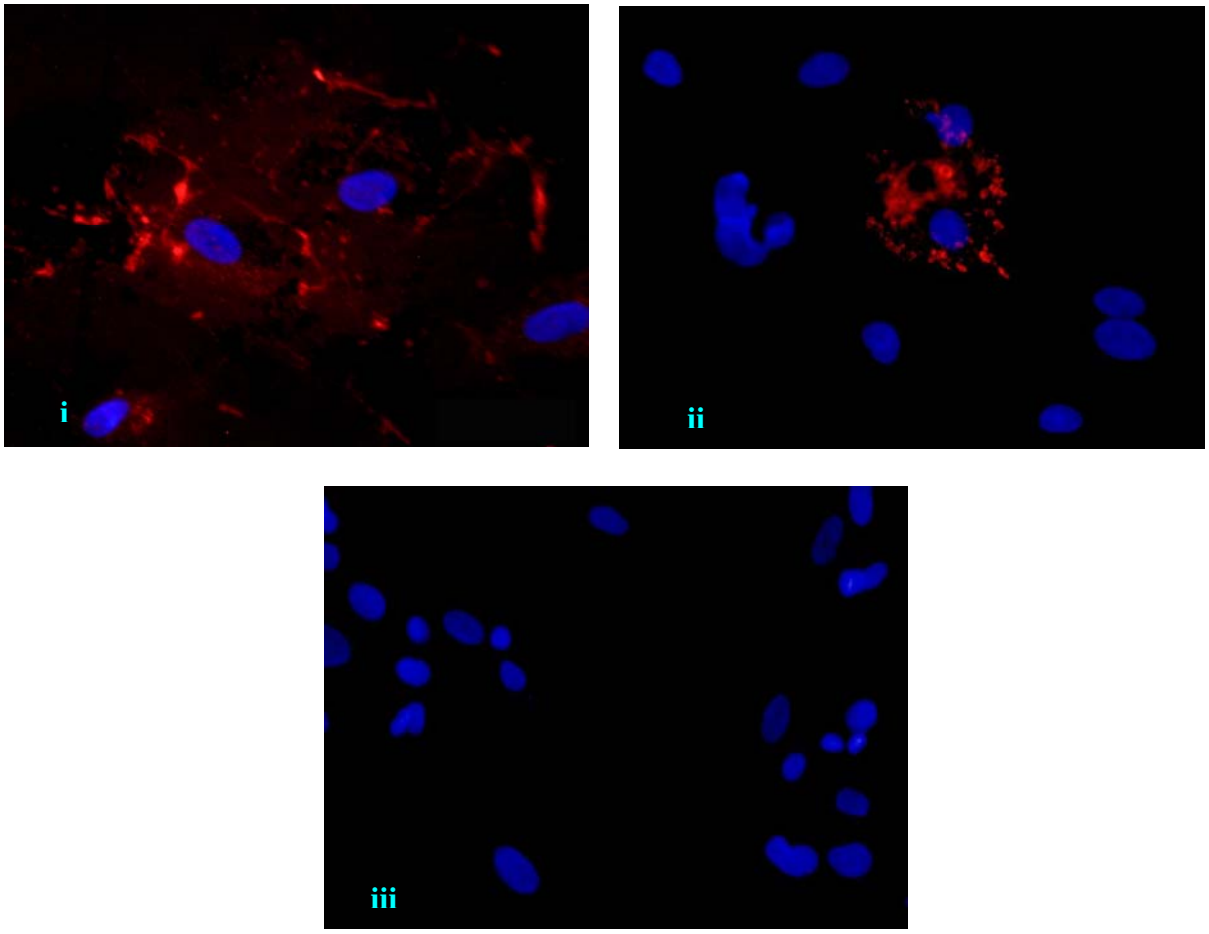

Figure 25: **Immunofluorescent staining for Ve-cadherin expression.** Ve-cadherin expression seen as red fluorescent (TRITC) in (i) ad-Null transduced cells and (ii) ad-hVEGF$_{165}$ transduced cells, (iii) Negative control incubated without Ve-cadherin primary antibody . Cell nuclei were stained with DAPI (blue fluorescence). (Magnification= 300×)

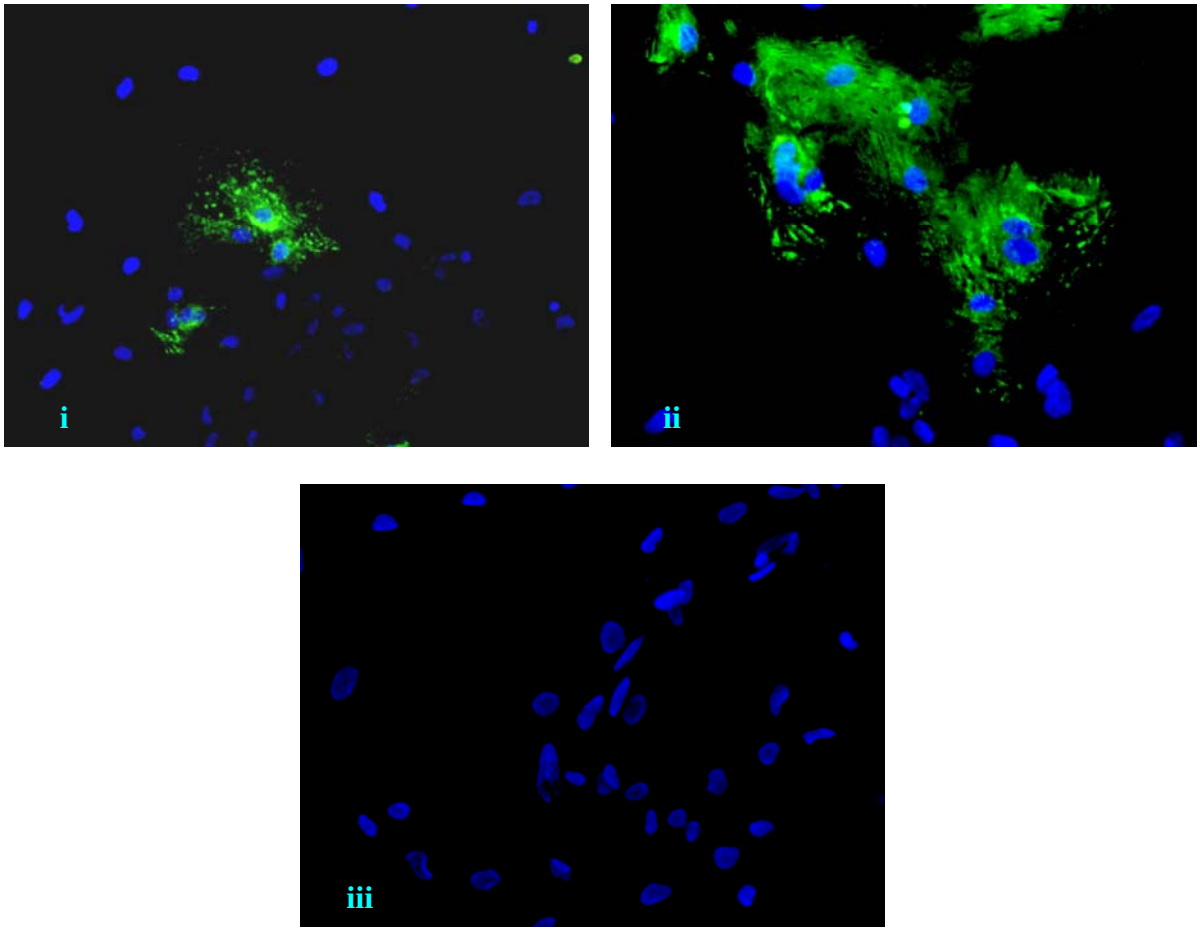

Figure 26: **Immunofluorescent staining for von-Willebrand factor expression.** Von-Willebrand factor expression seen as green fluorescent (FITC) in (i) ad-Null transduced cells and (ii) ad-hVEGF$_{165}$ transduced cells, (iii) Negative control incubated without von-Willebrand factor primary antibody. Cell nuclei were stained with DAPI (blue fluorescence). (Magnification= 300×)

Table 13: Phenotype of ad-hVEGF$_{165}$ transduced and ad-null transduced EB-derived cells grown in culture for 15 days.

		Phenotype/%		
		CD31	**Ve-cad**	**vWF**
ad-null transduced				
	7d EB	5.4	7.1	8.1
	14d EB	9.3	13.4	15.2
	21d EB	18.7	15.2	23.8
ad-hVEGF$_{165}$ transduced				
	7d EB	52.1	42.6	56.3
	14d EB	46.1	39.5	34.7
	21d EB	34.7	30.4	27.2

Percentage of positive cells in the ad-hVEGF$_{165}$ transduced and ad-null transduced cells after 15 days in culture. The percentage of positive cells was obtained by calculating the number of positive cells per number of total cells counted multiply by 100.

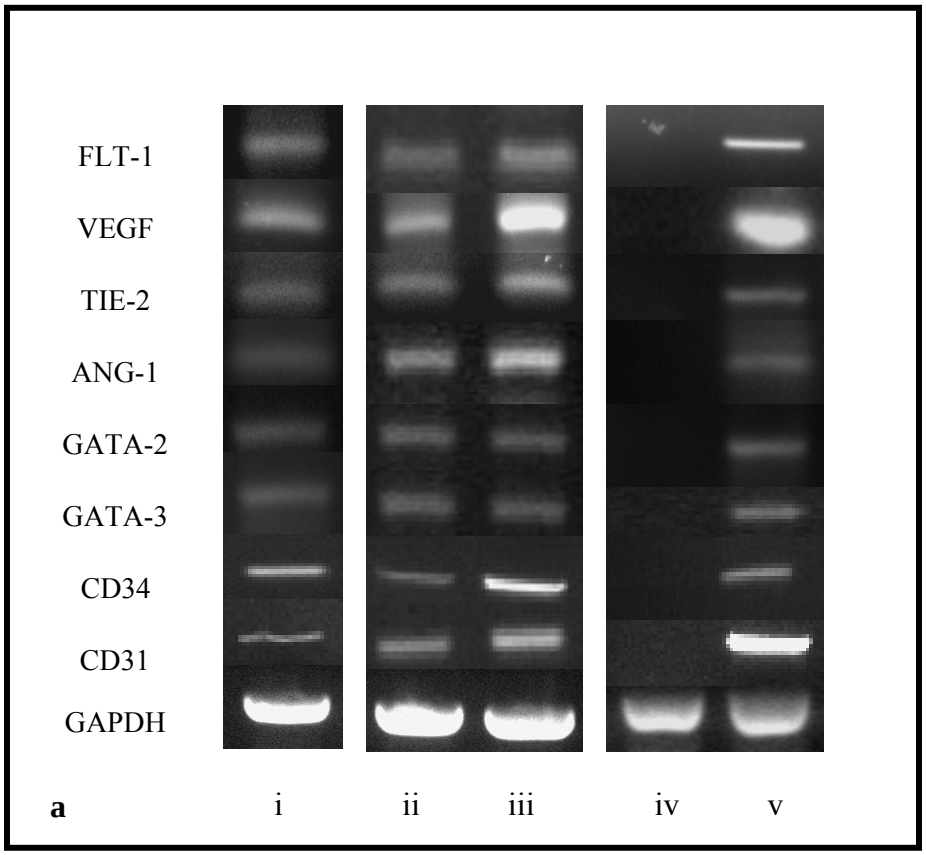

Figure 27: **Gene expression studies of endothelial markers.** (a) The expression of several vasculogenic surface markers, growth factors, receptors and transcription markers was assessed by RT-PCR on (i) 7-day EB-derived cells, (ii) ad-Null transduced cells, (iii) ad-hVEGF$_{165}$ transduced cells, (iv) MEF (negative control) and (v) HUVEC (positive control).

3.4.9 Characterization of putative EPCs upon ad-hVEGF$_{165}$ transduction

The efficiency of putative EPC differentiation in ad-hVEGF$_{165}$ transduced cells was assessed by standard and real time PCR and flow cytometry.

Standard and Real Time quantitative PCR for gene expression analysis

Standard RT-PCR and real time quantitative RT-PCR were performed for two markers, CD133^{+} and Flk-1^{+} used to characterize the population of EPCs in this study. Both CD133 and Flk-1 gene expressions were upregulated in ad-hVEGF$_{165}$ transduced cells (Figures 28a & b). They showed constant upregulation in expression from day 0 to day 12 post-transduction. By day 12 post-transduction, CD133 and Flk-1 expressions had increased significantly by approximately 20-fold and 27-fold respectively (Figure 28b).

Flow cytometric analysis of cell surface marker expression CD133

Phenotypic flow cytometry analysis revealed that 40.23 ± 5.6% of the ad-hVEGF$_{165}$ transduced cells was CD133^{+} as compared to 8.48 ± 1.7% ($p<0.01$) in ad-Null transduced cells (Figure 29).

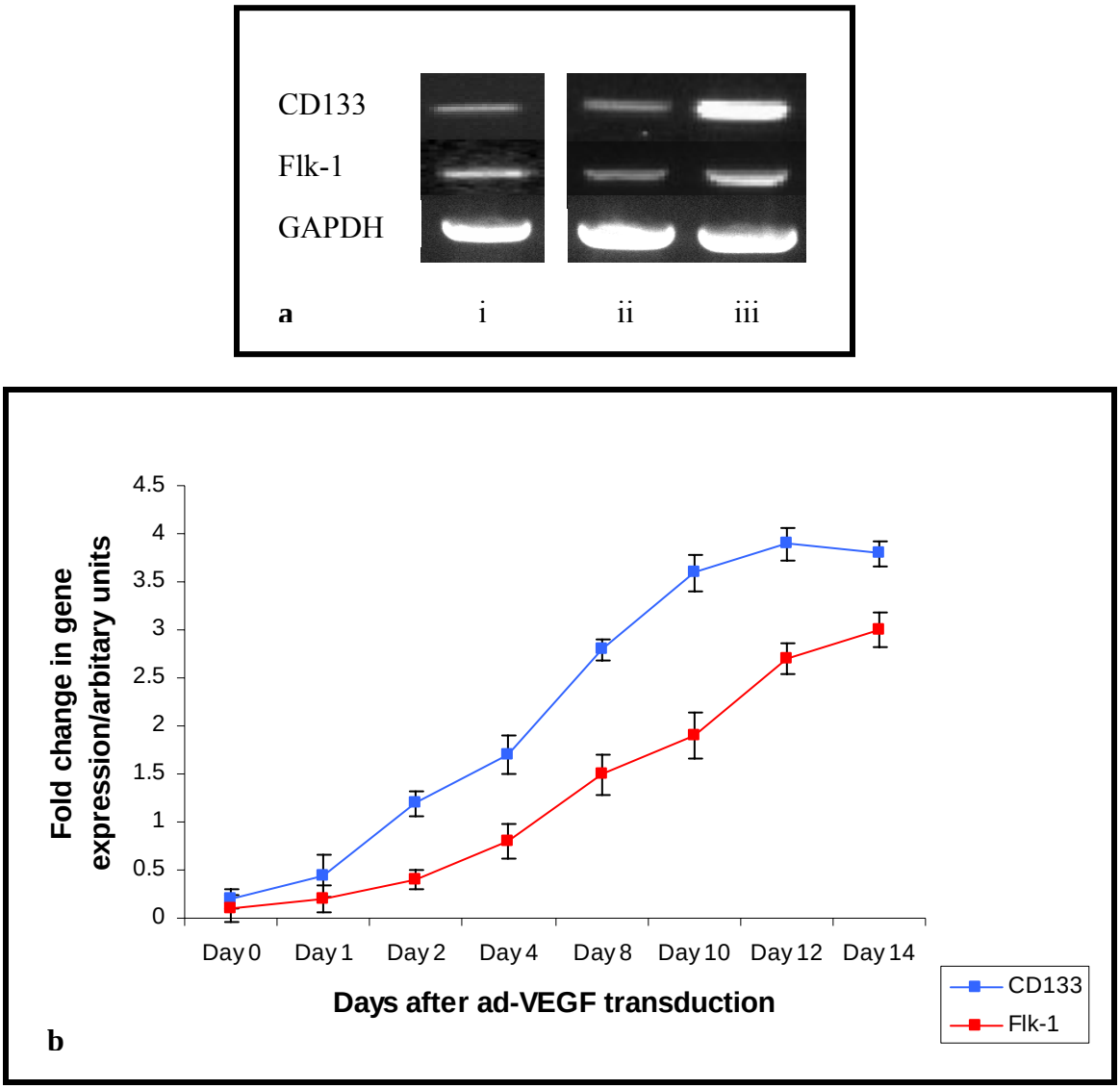

Figure 28: **Gene expression studies of EPCs.** (a) Gene expression of EPCs as assessed by CD133 and Flk-1 markers using RT-PCR on (i) 7-day EB-derived cells, (ii) ad-Null transduced cells, (iii) ad-hVEGF$_{165}$ transduced cells, (b) Real-time PCR studies for expression of CD133 and Flk-1 in ad-hVEGF$_{165}$ transduced cells as a function of time after transduction.

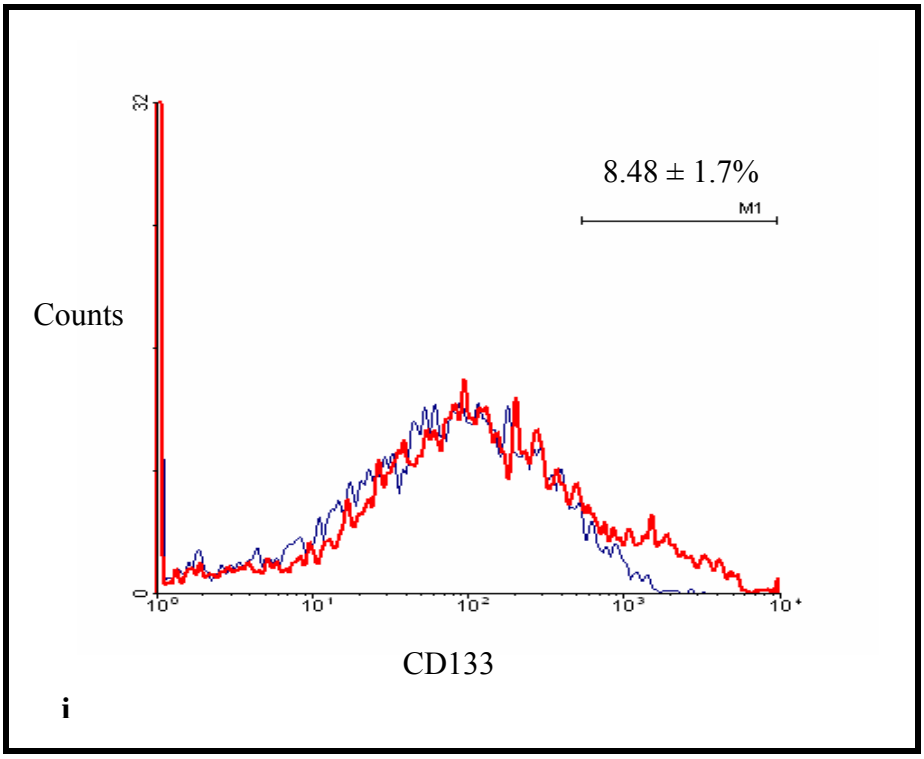

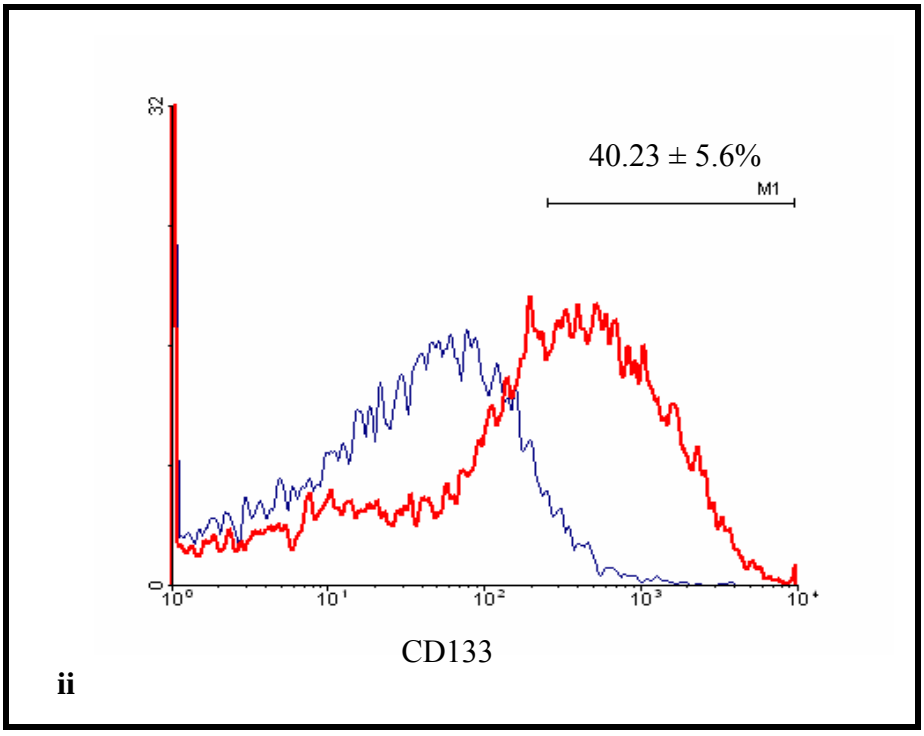

Figure 29: **Flow cytometric analysis of cell surface marker expression of CD133** on (i) ad-Null transduced cells and (ii) ad-hVEGF$_{165}$ transduced cells. Positively stained cells outlined in red were determined based on isotype controls which were outlined in blue.

3.5 Discussion

Previous approaches in directing endothelial lineage differentiation in HESCs had always focused on the use of angiogenic growth factors in the culture medium. However, the procedures were tedious with limited numbers of endothelial cells obtained, ranging from 2 to 20% (Gerecht-Nir et al, 2003; Levenberg et al, 2002). This low efficiency of endothelial differentiation using angiogenic growth factors in the culture medium may be due to the weak stimulatory effect exerted by the diluted growth factors within the culture medium. The non-specific pleiotropic effects exerted by various cytokines and growth factors in culture medium also make this a relatively inefficient approach in directing endothelial differentiation. Another possible reason could be the relatively short active half-life of the supplemented proteins within the culture medium.

In this study, we examined the ability of transient expression of VEGF in differentiating HESCs via transduction of ad-hVEGF$_{165}$ gene in enhancing the efficiency of endothelial-lineage differentiation of human embryonic stem cells. Adenoviral vectors are among the most utilized vectors in gene therapy studies. They possess the advantage of excellent gene expression, high viral titers and infection efficiency (Wang et al, 2000; Benihoud et al, 1999). They are able to infect a wide range of both dividing and non-dividing cells. Furthermore, adenoviral vectors do not integrate into the target cell genome and therefore, survive only transiently within the target cell (Schwarz et al, 2000; Springer et al, 1998). This unique property ensures that only transient expression of the introduced gene takes place, therefore, alleviating the danger of an unnecessarily prolonged expression with possible deleterious effects.

To date, this is the first study reporting the use of an adenoviral vector expressing $VEGF_{165}$ in the differentiating HESC system. We assessed the efficacy of adenoviral vector in transducing differentiating HESC and the efficiency of delivering the human VEGF gene into differentiating HESCs, with the aim of enhancing endothelial-lineage differentiation.

Our results demonstrated that adenoviral vector is an efficient tool in genetic modification of differentiating HESCs. Transduction efficiency was near to 90% as seen from VEGF immunofluorescent staining of the transduced cells (Figure 22). Expression of VEGF was stable and sustained over a period of 30 days in the transduced cells with a peak level at about day 8. The ad-$hVEGF_{165}$ transduced cells secreted significantly higher amounts of VEGF as compared to ad-Null and untransduced cells (27.5 ± 7ng/ml versus 0.15 ± 3ng/ml). The optimal transduction efficiency was obtained at a ratio of 1:500 cell/viral particles for 4 hours in three consecutive days. This resulted in highest VEGF expression and highest percentage of cell viability of 80% upon transduction (Figures 19 and 20). Very high viral titers were accompanied with an increased extent of cell death due to the toxicity effect of the virus on the cells. The secreted VEGF by ad-$hVEGF_{165}$ transduced differentiating cells was biologically active since it was capable of supporting HUVEC proliferation (Figure 23). VEGF triggers DNA synthesis and proliferation of ECs.

Immunostaining of endothelial markers showed significant increase in the number of CD31, Ve-cadherin and von-Willebrand factor positive cells in ad-$hVEGF_{165}$ transduced cells (52.1% ± 12.5%, 42.6% ± 9.8% and 56.3% ± 14.2% respectively) (Figures 24 to 26 and Table 13). The number of endothelial-positive cells decreased as

the age of the EBs that the cells were derived from increased. This showed that transduction of cells derived from younger EBs was more efficient since most of the cells had not yet committed to any particular lineage which makes them more amendable to manipulation.

Gene expression studies revealed upregulation of VEGF, Ang-1, Flt-1, Tie-2, CD31 and CD34 in ad-hVEGF$_{165}$ transduced cells. Upregulation of Ang-1 was noteworthy as this indicated a possible role of VEGF in regulating Ang-1 expression, which is known to play a prominent role in the maturation and stabilization of new blood vessel formation. This is especially useful in cell transplantation studies *in vivo* where balanced expression of both angiogenic growth factors is necessary for formation of functional blood vessels.

Upregulation of endothelial progenitor markers such as CD133 and Flk-1 were also observed in ad-hVEGF$_{165}$ transduced cells. Real time PCR data showed the gradual increase of these markers over regular time points after ad-hVEGF$_{165}$ transduction (Figure 28). CD133 and Flk-1 are surface markers that are used to characterize functionally early putative endothelial progenitor cells (Hristov et al, 2003, Gehling et al, 2000, Peichev et al, 2000, Yamashita et al, 2000). CD133 marker expression has been reported to be lost upon terminal differentiation of EPCs into mature ECs. (Hristov et al, 2003; Peichev et al, 2000). This is then followed by the expression of endothelial markers such CD31 and von-Willebrand factor. However, the CD133^{+} cell population is believed also to include some hematopoietic stem cells to a minimal extent. As endothelial and hematopoietic cells are derived from a common bipotent mesodermal precursor; putatively known as hemangioblasts (Wang et al, 2004), analysis of defined antigenic

determinants of endothelial and hematopoietic progenitor cells can be complicated since they tend to overlap. The number of $CD133^+$ cells increased significantly by 5-fold in the ad-$hVEGF_{165}$ transduced cells as revealed in flow cytometric analysis.

Gene transfer is a better approach in obtaining a higher degree of homogeneous differentiation than using growth factors in culture medium and our results demonstrated that introducing angiogenic VEGF gene into the differentiating HESCs was successful and effective in increasing the efficiency of endothelial-lineage differentiation. This is due to the ability of ad-$hVEGF_{165}$ transduced cells to continually produce VEGF on their own and endothelial-lineage differentiation is no longer hindered by the relatively short active half-life of exogenous VEGF supplemented into the culture medium. The gene transfer approach is also considered to be more economical, because there is no longer any need to supplement highly-expensive cytokines/growth factors within the culture milieu.

Despite the ethical and immunological concerns revolving around the use of HESCs, it still represents one of the best source of donor cells for regenerative therapy due to its unique characteristics; in particular its high proliferative capacity and multi-lineage differentiation potential. However, clinical application of these HESC-derived EPCs or mature ECs can only be established if they can be purified from the heterogeneous population and if they can be immunologically tolerated upon transplanted *in vivo*. These cells have numerous potential applications including their use in various tissue regenerative therapeutic approaches such as transplantation into infarcted hearts for myocardial regeneration, engineering of new blood vessels or induction of angiogenesis for treatment of regional ischemia.

We conclude that adenoviral vector carrying the human $VEGF_{165}$ gene is capable of efficient delivery and stable expression of VEGF into differentiating HESCs which in turn is effective in directing endothelial-lineage differentiation. Genetic modification by the adenoviral vector may offer new avenues for this study and for the use of HESCs in basic and applied scientific research.

3.6 Bibliography

Asahara T, Takahashi T, Masuda H, Kalka C, Ghen D, Iwaguro H, Inai Y, Silver M and Isner JM. VEGF contributes to postnatal neovascularization by mobilizing bone-marrow derived endothelial progenitor cells. EMBO J 1999; 18: 3964-3972

Benihoud K, Yeh P, Perricaudet M. Adenovirus vectors for gene delivery. Curr Opin Biotechnol 1999; 10: 440-447

Carmeliet P. Mechanisms of angiogenesis and arteriogenesis. Nat Med 2000; 6: 389-395
Flamme I, Frolich T and Risau W. Molecular mechanisms of vasculogenesis and embryonic angiogenesis. J Cell Physiol 1997; 173: 206-210

Carpenter MK, Inokuma MS, Denham J, Mujtaba T, Chiu CP and Rao MS. Enrichment of neurons and neural precursors from human embryonic stem cells. Exp Neurol 2001; 172: 383-397

Ferrara N, Gerber HP and LeCouter J. The biology of VEGF and its receptors. Nat Med 2003; 9: 669-676

Ferrara N and Alitalo K. Clinical applications of angiogenic growth factors and their inhibitors. Nat Med 1999; 5: 1359-1364

Ferrara N and Davis-Smith T.The biology of vascular endothelial growth factor. Endocr Rev 1997; 18: 4-25

Gehling UM, Ergun Suleyman, Schumacher U, Wagener C, Pantel K, Otte M, Schuch G, Schafhausen P, Mende T, Kilic N, Kluge K, Schafer B, Hossfeld DK, Fiedler W. In vitro differentiation of endothelail cells from AC133-positive progenitor cells. Blood 2000; 95: 3106-3112

Gerber HP, Dixit V and Ferrara N. Vascular endothelial growth factor induces expression of the anti-apoptotic proteins Bcl-2 and A1 in vascular endothelial cells. J Biol Chem 1998a; 273: 13313-13316

Gerber HP, McMurtrey A, Kowalski J, Yan M, Keyt BA, Dixit V, Ferrara N. VEGF regulates endothelial cell survival by the PI3-kinase/Akt signal transduction pathway. Requirement for Flk-1/KDR activation. J Biol Chem 1998b; 273: 30366-30343

Gerecht-Nir S, Ziskind A, Cohen S, Itskovitz-Eldor J. Human embryonic stem cells as an in vitro model for human vascular development and the induction of vascular differentiation. Lab Invest 2003; 83: 1811-1820

Gropp M, Itsykson P, Singer O, Ben-Hur T, Reinhartz E, Galun E, Reubinoff BE. Stable genetic modification of human embryonic stem cells by lentiviral vectors. Mol Ther 2003;7: 281-287

Haider KH, Ye L, Jiang S, Ge R, Law PK, Chua T, Wong P and Sim EK. Angiomyogensis for cardiac repair using human myoblasts as carriers of human vascular endothelial growth factor. J Mol Med 2004; 82: 485-487

Henry TD, Rocha-Sing K, Isner JM, Kereiakes DJ, Giordano FJ, Simons M, Losordo DW, Hendel RC, Bonow RO, Eppler SM, Zioncheck TF, Holmgren EB and McCluskey ER. Intracoronary administration of recombinant human vascular endothelial growth factor (rhVEGF) to patients with coronary artery disease. Am Heart J 2001; 142: 872-880

Hristov M, Erl W, Weber PC. Endothelial progenitor cells- mobilization, differentiation and homing. Arterioscle Thromb Vasc Biol 2003; 23:1185-1189

Kaufman DS, Hanson ET, Lewis RL, Auerbach R and Thompson JA. Hematopoietic colony-forming cells derived from human embryonic stem cells. Proc Natl Acad Sci USA 2001; 98: 10716-10721

Kehat I, Kenyagin-Karsetin D, Snir M, Segev H, Amit M, Gepstein A, Livne E, Binah O, Itskovitz-Eldor J and Gepstein L. Human embryonic stem cells can differentiate into myocytes with structural and functional properties of cardiomyocytes. J Clin Invest 2001;108: 407-414

Lakshmipathy U, Pelacho B, Sudo K, Linehan JL, Coucouvanis E, Kaufman DS, Verfaillie CM. Efficient transfection of embryonic and adult stem cells. Stem Cells 2004; 22: 531-543

Levenberg S, Golub JS, Amit M, Itskovitz-Eldor J, Langer R. Endothelial cells derived from human embryonic stem cells. Proc Natl Acad Sci USA 2002; 99: 4391-4396

Makinen K, Manninen H, Hedman M, Matsi P, Mussalo H, Alhava E, Yla-Herttuala S . Increased vascularity detected by digital subtraction angiography after VEGF gene transfer to human lower limb artery: a randomized, placebo-controlled, double-blinded phase II study. Mol Ther 2002; 6: 127-133

Mummery C, Ward D, van den Brink CE, Doevendans PA, Opthof T, Brutel de la Riviere A, Tertoolen L, van der Heyden M, Pera M. Cardiomyocytes differentiation of mouse and human embryonic stem cells. J Anat 2002; 200: 233-242

Peichev M, Naiyer AJ, Pereira D, Zhu Z, Lane WJ, Williams M, Oz MC, Hicklin DJ, Witte L, Moore RA, Rafii S. Expression of VEGFR-2 and AC133 by circulating human CD34+ cells identifies a population of functional endothelial precursors. Blood 2000; 95: 952-958

Reubinoff BE, Itsykson P,Turetsky T, Pera MF, Reinhartz E, Itzik A and Ben-Hur T. Neural progenitors from human embryonic stem cells. Nat Biotechnol 2001; 10: 1134-1140

Reubinoff BE, Pera MF, Fong CY, Trounsen A and Bongso A. Embryonic stem cell lines from human blastocysts: somatic differentiation in vitro. Nat Biotechnol 2000; 18: 399-404

Risau W. Mechanisms of angiogenesis. Nature 1997; 386: 671-674

Risau W and Flamme I. Vasculogenesis. Annu Rev Cell Dev Biol 1995; 11: 73-91

Siemen H, Nix M, Endl E, Koch P, Itskovitz-Eldor J, Brustle O. Nucleofection of human embryonic stem cells. Stem Cells Dev 2005;14: 378-383

Schuldiner M, Yanuka O, Itskovitz-Eldor J, Melton DA and Benvenisty N. Effects of eight growth factors on the differentiation of cells derived from human embryonic stem cells. Proc Natl Acad Sci USA 2000; 97: 11307-11312

Schwarz ER, Speakman MT, Patterson M, Hale SS, Isner JM, Kedes LH, Kloner R. Evaluation of the effects of intramyocardial injection of DNA expressing vascular endothelial growth factor (VEGF) in a myocardial infarction model in the rat angiogenesis and angioma formation. J Am Coll Cardiol 2000; 35: 1323-1330

Springer ML, Chen AS, Kraft PE, Bednarski M, Blau HM. VEGF gene delivery to muscle: potential role of vasculogenesis in adults. Mol Cell 1998; 2: 549-558

Street J, Bao M, deGuzman L, Bunting S, Peale FV Jr, Ferrara N, Steinmetz H, Hoeffel J, Cleland JL, Daugherty A, van Bruggen N, Redmond HP, Carano RA, Filvaroff EH. Vascular endothelial growth factor stimulates bone repair by promoting angiogenesis and bone turnover. Proc Natl Acad Sci USA 2002; 99: 9656-9661

Tatsis N,Ertl HC. Adenoviruses as vaccine vectors. Mol Ther. 2004;10: 616-29

Thomson JA, Itskovitz-Eldor J, Shapino SS, Waknitz MA, Swiergiel JJ, Marshall VS and Jones JM. Embryonic stem cell lines derived from human blastocysts. Science 1998; 282: 1145-1147.

Vale PR, Losordo DW Milliken CE, Maysky M, Esakof DD, Symes JF and Isner JM (2000). Left ventricular electromechanical mapping to assess efficacy of phVEGF(165) gene transfer for therapeutic angiogenesis in chronic myocardial ischemia. Circulation 102: 965-974

Wang I and Huang I. Adenovirus technology for gene manipulation and functional studies. Drug Discov Today 2000; 5: 10-16

Wang L, Menendez P, Cerdan C, Menendez P, Martin T, Rouleau A, Bhatia M. Endothelial and hematopoietic cell fate of human embryonic stem cells originates from primitive endothelium with hemangioblastic properties. Immunity 2004; 31-41

Yamashita J, Itoh H, Hirashima M, Ogawa M, Nishikawa S, Yurugi T, Naito M, Nakao K, Nisihikawa S. Flk1-positive cells derived from embryonic stem cells serves as vascular progenitors. Nature 2000; 408: 92-96

Zwaka TP, Thomson JA. Homologous recombination in human embryonic stem cells. Nat Biotechnol. 2003; 21: 319-321

CHAPTER 4

Endothelial lineage differentiation of human embryonic stem cells - *in vivo* studies

TABLE OF CONTENT

4.1 Abstract

The present study investigated the functionality of $CD133^+$ EPCs differentiated from HESCs by ad-$hVEGF_{165}$ transduction. Their ability to survive, differentiate and integrate in an ischemic environment was assessed by transplanting them into a rat MI model. Two weeks after MI was created by ligation of the LAD artery, Wistar rats were randomly allotted to receive either an injection of $CD133^+$ EPCs derived from differentiating HESCs transduced with ad-$hVEGF_{165}$, ad-Null transduced differentiating HESCs or just culture medium. 6 weeks after treatment, the degree of neovascularization and apoptotic activity in the infarct and peri-infarct areas was evaluated by histology and immunohistochemical staining. Echocardiography was performed for cardiac function assessment and fluorescent microsphere analysis was carried out to assess the regional blood flow.

Transplanted $CD133^+$ EPCs survived and participated actively and passively in the regeneration of the infarcted myocardium by differentiating into endothelial and smooth muscle cells that incorporate into the newly formed blood vessels; as well as by secretion of angiogenic growth factors such as VEGF and Ang-1 into the infarcted myocardium that are responsible for the process of vasculogenesis and angiogenesis. Mature blood vessel density was 23.62 ± 2.36 in the $CD133^+$ EPC transplanted group as compared to 2.41 ± 1.17 in medium-injected group, which was a significant 10-fold increase.

$CD133^+$ EPC transplantation significantly reduced infarct size to (28% ± 6.2%) as compared to the medium-injected group (76% ± 4.3%, $p<0.001$). Regional blood flow analysis showed improvement in the $CD133^+$ EPC transplantation group (2.86 ± 0.278

ml/min/g) as compared to the medium-injected group (0.8 ± 0.156 ml/min/g, *p=0.05*). Echocardiography assessments at 6 weeks post-transplantation revealed that the left ventricle ejection fraction was significantly higher in the $CD133^+$ EPC transplanted group than in the medium-injected group (72.85% ± 9.7% vs 38.22 ± 5.4%, *p=0.023*) and similar observation was seen for fractional shortening (54.8% ± 7.4% vs 27.2% ± 1.85%, *p=0.028*).

In conclusion, HESC derived $CD133^+$ EPC transplantation holds promise to be a novel and effective means of heart regeneration therapy with much potential for clinical applications in the future.

4.2 Introduction

Animal studies and preliminary results in human clinical trials have suggested that the lower extremity of myocardial ischemia can be reduced effectively by treatment with angiogenic cytokines. The resident population of ECs which respond to the level of various angiogenic growth factors after infarction is usually a limiting factor in the extent of tissue neovascularization upon cytokine supplementation. More recently, EPCs have been investigated as therapeutic agents, which have the ability to participate actively in therapeutic angiogenesis, supplementing the contribution of resident ECs in the vasculature that migrate, proliferate and remodel in response to angiogenic cues. Additionally, the transplanted cells can also exert a passive effect by supplying various angiogenic growth factors to the tissue environment.

Therapeutic angiogenesis is one of the key factors for myocardial regeneration since it helps to create a favourable environment by ensuring the availability of sufficient amount of oxygen and nutrients to promote survival of either the hibernating or ischemic cardiomyocytes or the transplanted cells used in cellular cardiomyoplasty. In a normal heart, there is a capillary next to almost every cardiomyocyte and endothelial cells outnumber cardiomyocytes by ≈3: 1 (Brutsaert 2003). Mediating this endothelial-myocardial interaction is therefore a key strategy for myocardial regeneration.

Accordingly, EPCs differentiated from ad-hVEGF$_{165}$ transduced differentiating HESCs were investigated for their ability to survive, differentiate and integrate within an ischemic environment by transplanting them in a rat model of myocardial infarction. We hypothesized that these progenitor cells characterized by the expression of CD133 are able to differentiate *in vivo* and augment blood vessel growth via vasculogenesis and

angiogenesis, hence improving blood perfusion and reducing infarct expansion by preventing further death of cardiomyocytes. This would be followed by reduction in left ventricular remodeling and improved cardiac performance.

4.3 Materials and Methods

4.3.1 Materials

4.3.1.1 Cell line

Human embryonic stem cells, H1 cell line

Cells were purchased with license agreement from Wicell Research Institute, Inc.

4.3.1.2 Animal

Wistar rats

A total of 100 female Wistar rats (± 250g) were used for the creation of the rat MI model. Wistar rats were purchased from Centre for Animal Resources, Lim Chu Kang, Singapore.

The materials used for this study is listed in Appendix 6.1.

4.3.2 Methods

4.3.2.1 Preparation of transplanted cells

Magnetic cell sorting for CD133 positive cells

Enrichment of $CD133^+$ cells from ad-$hVEGF_{165}$ transduced differentiating cells was performed using immunomagnetic separation using magnetic activated cell sorting (MACS) with the use of anti-CD133-conjugated superparamagnetic microbeads following the manufacturer's recommendations. Briefly, the transduced cells were incubated with for 30min at 4°C with FcR blocking reagent and CD133 microbeads. After washing with 0.5% bovine serum albumin in PBS, the labeled cells were loaded onto a column installed in a strong magnetic field. The trapped cells were eluted after the column was removed from the magnet.

Labeling of cells with DAPI

The transplanted cells were labelled with DAPI. The cells were incubated in 1× DAPI solution diluted in DMEM:F12 medium for 30 minutes at 37°C. The cells were washed three times in Hanks Balanced Salt solution to remove the excess DAPI. The cells were then resuspended in 150µl DMEM:F12 medium and stored in ice until transplantation into the myocardium.

4.3.2.2 Rat model of myocardial infarction

Creation of rat ligation model

Please refer to 2.3.2.1 for the procedure to create a rat model of MI by ligation of the LAD artery.

Animal groupings for cell transplantation

The animal groupings for cell transplantation study were as the following:

1. Group-1: Sham-operated (n=25)
2. Group-2: DMEM/F12 medium injection (n=25)
3. Group-3: Ad-Null transduced cells transplantation (n=25)
4. Group-4: $CD133^+$ purified from ad-$hVEGF_{165}$ transduced cells tranplantation (n=25)

Transplantation of the EPCs into the rat heart

For the cell transplantation procedure, the rats were subjected to a second surgerical operation similar to that mentioned earlier. Cell suspension of about 150µl containing of approximately 5×10^6 cells was directly injected into the infarcted and around infarcted region by using an insulin syringe 2 weeks post-infarction. After

transplantation, the muscle layer and skin incision will be closed with 3-0 silk absorbable suture.

Post surgery care for the rat MI models

Please refer to 2.3.2.1 for the post surgery care for the animal models.

Once the rats were transplanted with the cells, they were also given daily intraperitoneal injection of an immunosuppresive agent, cyclosporin daily for the next 6 weeks.

Euthanasia of the rats

Please refer to 2.3.2.1 for the euthanasia procedure of the animal models.

4.3.2.3 Functional studies

Rat heart function assessment using echocardiography

Please refer to 2.3.2.2 for the echocardiography procedure for heart function assessment.

Regional blood flow study using fluorescent microspheres

For assessment of the regional blood flow, the rats were subjected to fluorescent microsphere study 2 weeks after ligation and 6 weeks after treatment. After anaesthesia and intubation, the rats were placed in a dorsal decubitus position. After the chest was cut opened, the right or left carotid artery was isolated and a catheter were inserted until it reached the left ventricle. At the same time, the right or left superficial femoral artery was isolated and a needle attached to a 5ml-syringe were inserted into it so as to collect the blood sample. Microsphere solution (1.4×10^4 microspheres/kg body weight) was injected through the catheter into the left ventricle during the second ten seconds of a

minute while 2ml blood samples were drawn within the same minute. The left ventricle of the rat hearts were weighed out.

The micropsheres in the tissue and blood samples were recovered by digestion and negative filtration procedure. The blood samples were incubated in a digestion solution containing 89.2% potassium hydroxide (KOH) and 2% of Tween-80 while the heart samples were incubated in a digestion solution containing 22.4% KOH and 2% Tween-80. Digestion was allowed to take place overnight at 37°C.

The fluorescent dye was extracted by ethoxyethyl acetate from the microspheres and measured by a Luminescence Spectrophotometer at 505/515nm for yellow-green flourescence. Regional blood flow was calculated using the following equation:

$$Q\ (ml/min/g) = \frac{FI_{tissue}}{FI_{blood}} \times R\ (ml/minute)/g$$

FI_{tissue} is the fluorescent reading for the tissue sample; FI_{blood} is the fluorescent reading for the blood sample and R is the withdrawal rate of the reference blood flow.

4.3.2.4 Assessment of the effect of EPC transplantation on the infarction model

Morphometric analysis using tetrazolium chloride staining

Please refer to 2.3.2.3 for tetrazolium chloride staining for infarct size measurement.

Survival of the cells in the rat heart

Tissue sections were viewed under fluorescent microscope to evaluate transplanted DAPI-labeled cell survival and incorporation into the ischemic myocardium. PCR analysis for human Y chromosome was also performed. Total DNA was isolated

using DNeasy Tissue kit following the manufacturer's instruction. Primer sequence for human Y chromosome is listed in Table 14. The PCR condition is as shown in Table 15.

Quantitative assessment of capillary density

The tissue sections were washed twice in 1× PBS for 5 minutes, fixed with -20°C methanol for 10 minutes and treated with 3% methanolic hydrogen peroxide solution (H_2O_2) for 15 minutes. After washing with 1× PBS, the tissue sections were blocked with Ultra V Block for 8 minutes followed by overnight incubation with primary antibodies; rabbit anti human von-Willebrand factor and mouse anti human smooth muscle actin at dilution factor 1:500 and 1:400 respectively. The tissue sections were washed thoroughly on the following day and then incubated for 90 minutes with secondary antibodies; goat anti-rabbit FITC (for von-Willebrand factor) and goat anti-mouse TRITC (for smooth muscle actin) at dilution factor of 1:500 each. The slides were observed under a fluorescent microscope after thorough washing and air drying.

A total of 20 slides from each group were used to assess the capillary density based on von-Willebrand factor and smooth muscle actin fluorescent immunostaining. Five random images of the peri-infarct region were captured from each slide. The capillary density was calculated based on the number of FITC-positive (for von-Willebrand factor) and TRITC-positive (for smooth muscle actin) cells.

TUNEL assay for assessment of cardiomyocyte death

Parafinized tissue sections were deparafinized, digested with Proteinase K and incubated with TdT and fluorescein-labeled dUTP in a humidified atmosphere at 37°C for 60 minutes. After thorough washing, the tissue sections were incubated with an antibody specific for fluorescein-conjugated alkaline phosphatase for 30 minutes. The

Table 14: Primer sequence for human Y chromosome

Primer	Sequence
Human Y chromosome	Forward= 5'-CATGAACGCATTCATCGTGTG GTC-3' Reverse= 5'-CTGCGGGAAGCAAACTGCAATTCTT-3'

Table 15: PCR condition for Y chromosome gene

Initial activation step	15 min	95°C
3-step cycling: Denaturation	1 min	94°C
Annealing	1 min	63°C
Extension	1 min	72°C
Number of cycles	30	
Final extension	10 min	72°C

TUNEL stain was visualized with a substrate system in which nuclei with DNA fragmentation were stained green (BCIP/NBT substrate system). In order to determine the proportion of apoptotic cardiomyocytes, the tissue sections were counterstained with Nuclear Fast Red and viewed under fluorescent microscope. A total of 15 slides from each group were used to assess the percentage of apoptotic cardiomyocytes. Five random images were captured from each slide.

RT-PCR and ELISA for analysis of human VEGF and Ang-1 RNA and protein expression

The details of each primer sets that were used are listed in Table 12 (page 128) and the PCR cycling program used is outlined in Table 9 (page 123). ELISA procedure for both proteins is similar to the protocol mentioned under section 3.3.2.5.

4.3.3 Statistical analysis

Statistical analysis was performed using SPSS (version 11.0). All data were presented as mean ± standard error mean (SEM) and analyzed by analysis of variance (ANOVA) between groups. Intra-group comparison was carried out using paired student t test. $P < 0.05$ was considered statistically significant.

4.4 Results

4.4.1 Improvement of left ventricular function after human CD133$^+$ EPCs transplantation

Echocardiographic assessments revealed that the LVEF was higher in the cell-injected rats than in the medium-injected rats. However, rats receiving the enriched population of CD133$^+$ cells showed a significantly higher LVEF when compared to rats receiving ad-null transduced cells (72.85% ± 9.7% vs 51.16% ± 6.5%, *p=0.036*) (Figure 30a).

The left ventricular fractional shortening at baseline was not significantly different among the four groups. 6 weeks after cell transplantation, significant improvement in the left ventricular fractional shortening was observed in the CD133$^+$ cells transplanted myocardium whereas there was decrease with left ventricular fractional shortening in the control group (54.8% ± 7.4% vs 27.2% ± 5.8%, *p=0.028*) (Figure 30b). Improved mobility of the anterior wall in the CD133$^+$ cells transplanted rats versus the medium-injected rats at 6 weeks after transplantation was also observed. Moreover, less left ventricular dilatation was found in the CD133$^+$ cells transplanted group rats compared with the medium-injected rats.

4.4.2 Survival of human CD133$^+$ transplanted cells in the infarcted rat myocardium

Frozen sections prepared from infarct and peri-infarct sites of cell-transplanted groups at 6 weeks after cell transplantation showed DAPI-positive cells under fluorescent microscope (Figure 31). In contrast, sections from the sham-operated or medium-injected group had no such DAPI-positive cells. RT-PCR showed the presence of human Y chromosome in the rat hearts from week 1 to week 6 after cell transplantation. The

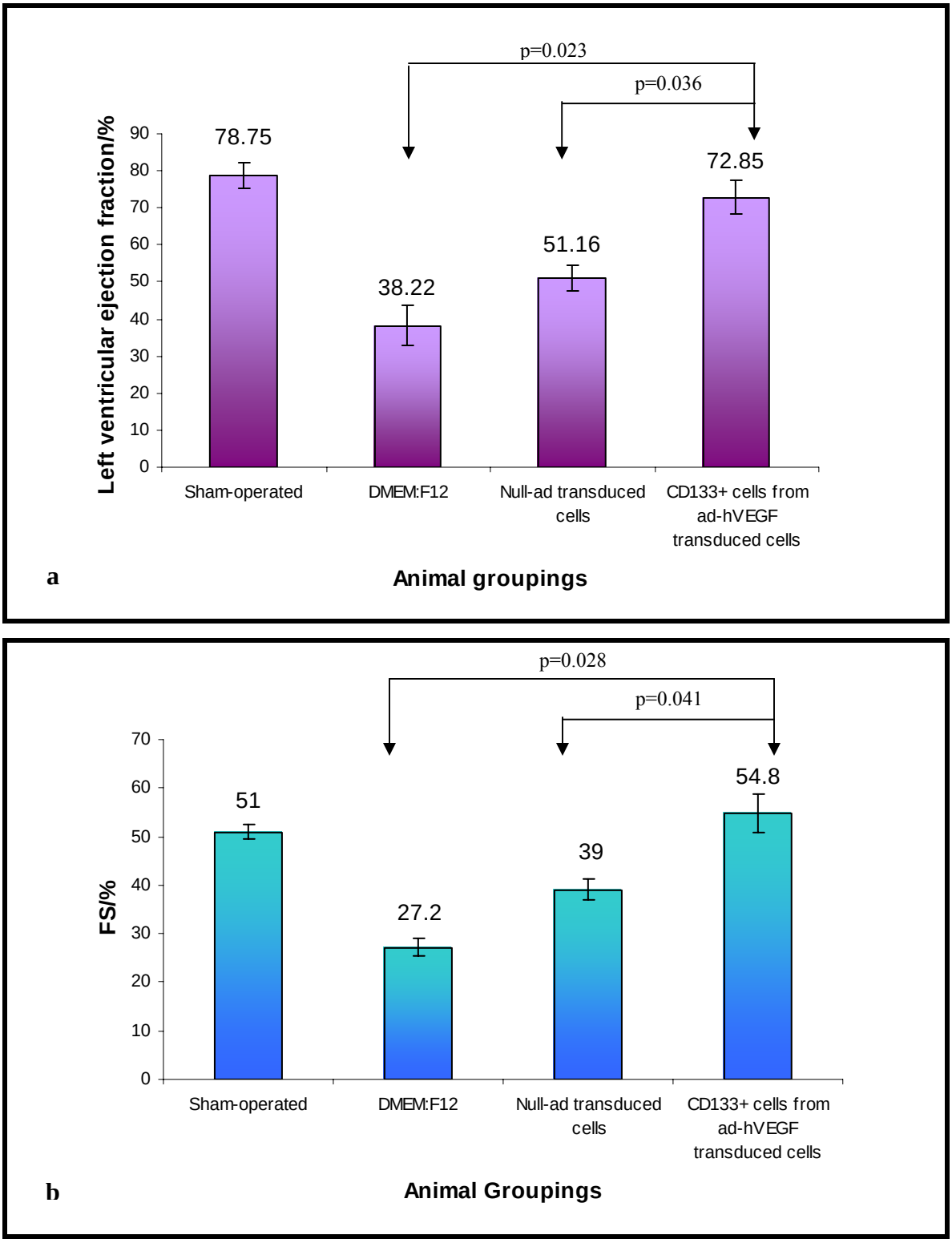

Figure 30: **Assessment of cardiac function using echocardiography.** (a) Left ventricular ejection fraction measured for the 4 animal groups. (b) Fractional shortening measured for the 4 animal groups.

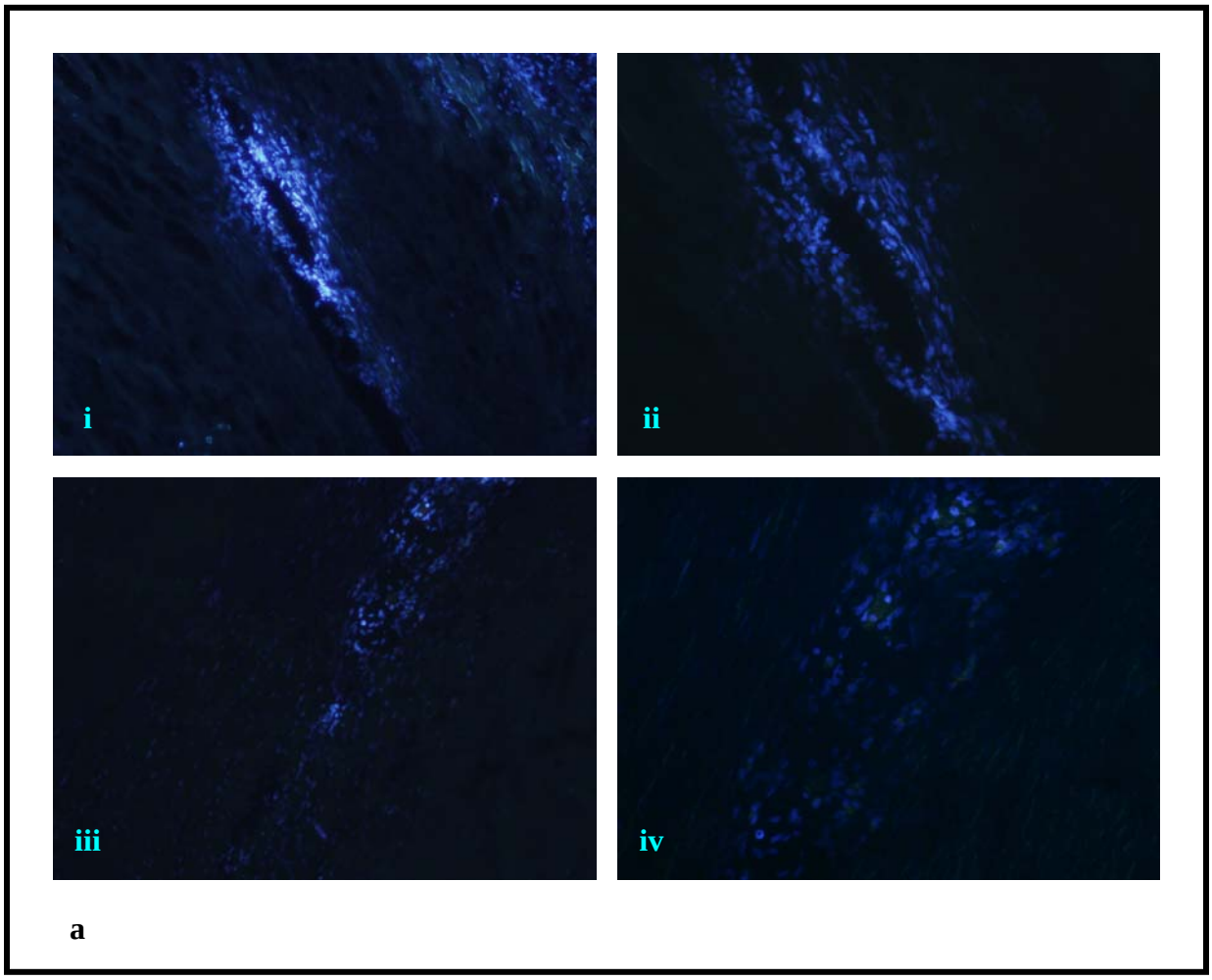

Figure 31: (a) **Survival of transplanted CD133^{+} derived cells in the rat heart.** (Magnification: i & iii= 100×, ii & iv= 200×), (b) **PCR for human Y chromosome in rat heart tissue after CD133^{+} cell transplantation at various weeks after cell transplantation**

presence of human Y chromosome DNA demonstrated the survival of human $CD133^+$ cells in the rat heart at 6 months post-transplantation.

4.4.3 Extent of injury upon MI

Gradual loss of cardiomyocytes by necrosis was observed within the first 7 days post-infarction. Accompanying this was the significant increase in the number of inflammatory immune cells infiltrating into the myocardium within the first 7 days post-infarction. By day 14 post-infarction, the number of infiltrating immune cells has significantly decreased. The degree of infarct expansion was rapid and by day 31 post-infarction, there was significant loss of viable myocardium (Figure 32). Accelerated fibrosis and collagen deposition also occurred resulting in significant formation of collagen scar in the myocardium by day 31 post-infarction (Figure 33).

4.4.4 Endogenous blood vessel density analysis in the infarcted rat myocardium

Endogenous blood vessels formed after myocardial infarction was analyzed over a period of two weeks. The number of blood vessels increased till week 2 after infarction (Figure 34). Non-stabilized or non-perfused nascent blood vessels consisting of only ECs slowly regressed over time by the end of week 4, leaving only the mature blood vessels.

4.4.5 Blood vessel density upon human $CD133^+$ EPCs transplantation

Blood vessel density was quantified using fluorescent immunostaining of von-Willebrand factor expression in capillaries found in the infarct and peri-infarct area at high power field magnification (200×). Results were compared among groups. $CD133^+$ EPCs transplantation resulted in high blood vessel density at 6 weeks post-transplantation (29.35 ± 1.02). This was significantly higher when compared to medium-injected controls (5.25 ± 0.73, $p<0.001$), the ad-Null transduced cells transplanted group (15.36 ± 1.42,

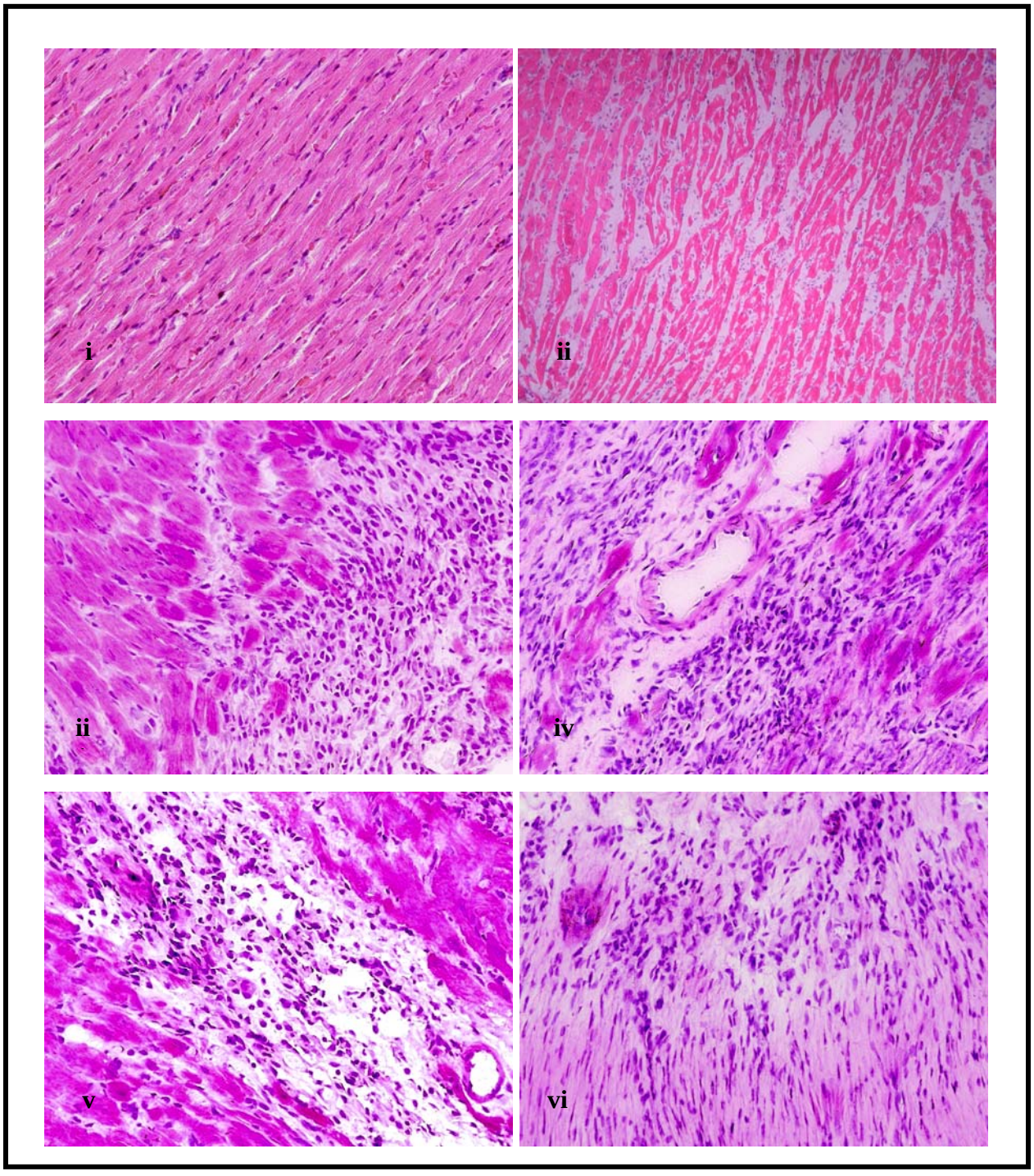

Figure 32: **Hematoxylin and eosin staining of the rat heart upon infarction**. (i) normal, (ii) 1 day, (iii) 3 days, (iv) 7 days, (v) 14 days, (vi) 31 days after infarction. (Magnification= 200×)

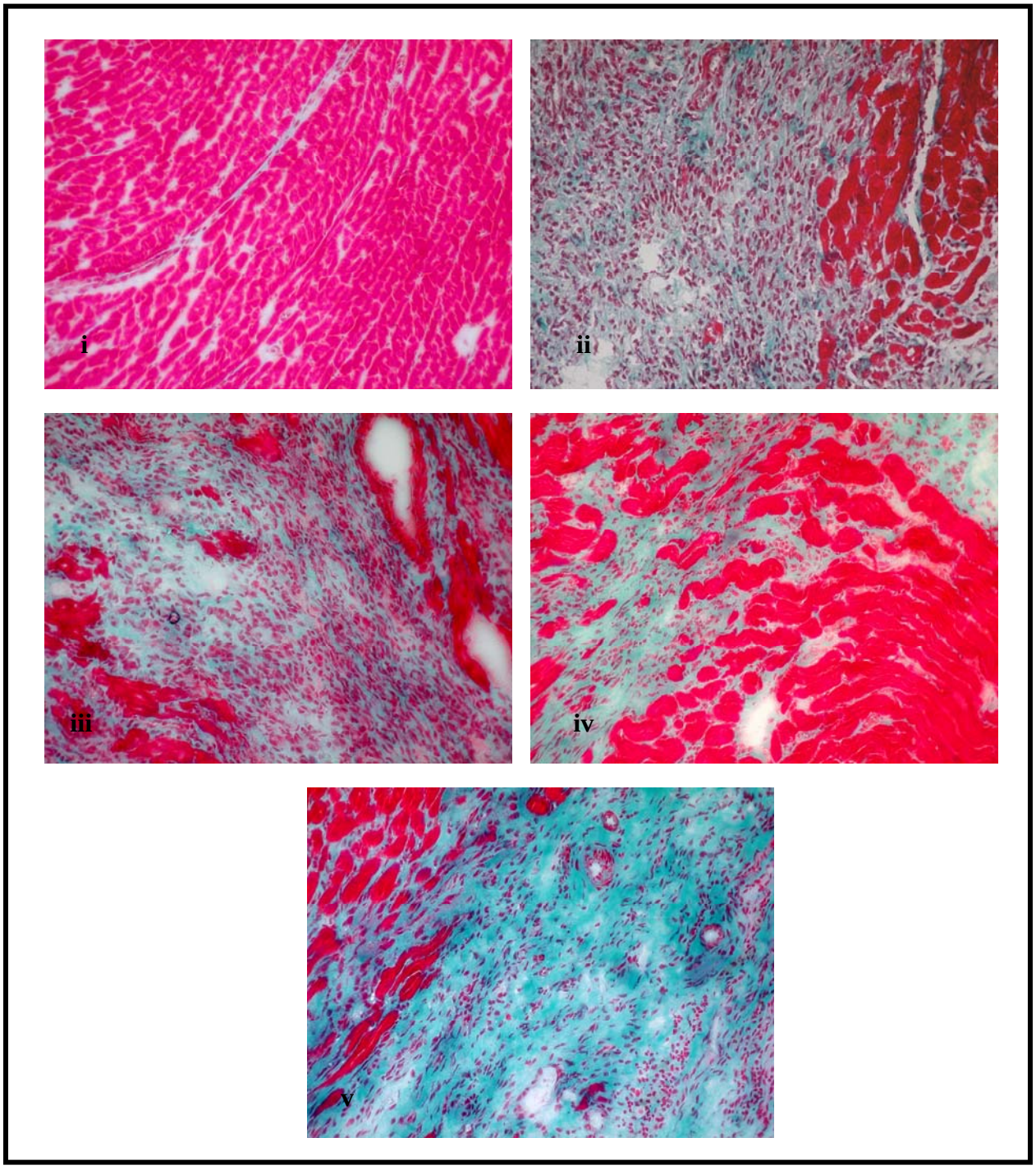

Figure 33: **Masson Trichrome staining of the rat heart upon infarction.** (i) normal, (ii) 3 days, (iii) 7 days, (iv) 14 days and (v) 31 days after infarction.(Magnification= 200×)

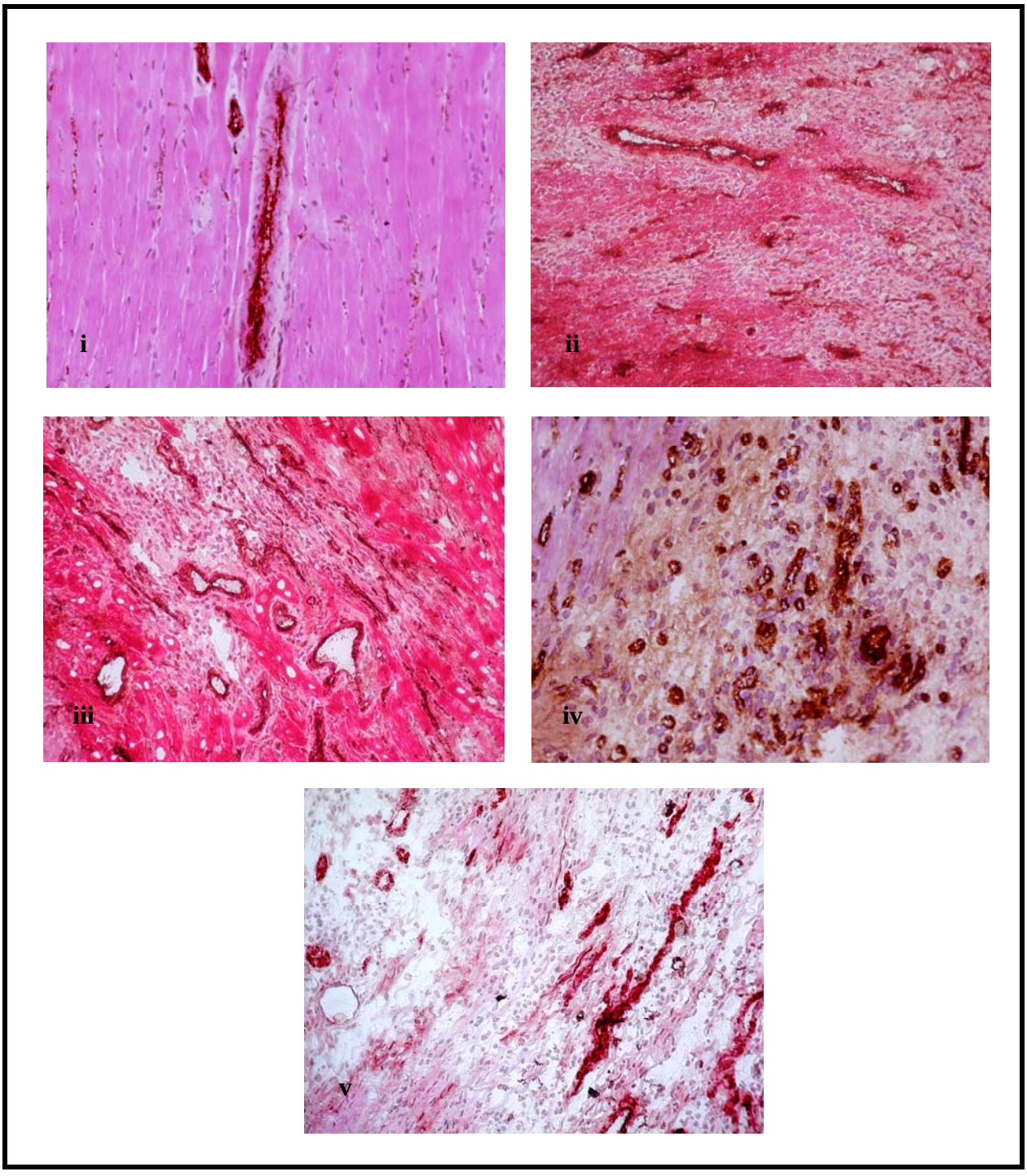

Figure 34: **von-Willebrand factor staining for endogenous blood vessels in the rat heart**. (i) normal, (ii) 3 days, (iii) 7days, (iv) 14 days, (v) 31 days after infarction (Magnification= 200×)

p<0.001) and the sham-operated group (4.34 ± 2.35, *p<0.001*) (Figure 35). DAPI-labelled $CD133^+$ derived cells were dispersed around the ischemic myocardium, indicating that some of the cells were engrafted within newly-formed blood vessels.

4.4.6 Mature blood vessel density upon human $CD133^+$ EPCs transplantation

Using smooth muscle cells as an indicator of the maturity of the blood vessels, mature blood vessels were quantified by counting blood vessels that were positive for both von-Willebrand factor and smooth muscle actin. They were counted at high power field magnification (200×). The number of mature blood vessels was highest in the $CD133^+$ EPC transplanted group (23.62 ± 2.36), followed by ad-Null transduced cells transplanted group (8.82 ± 0.89, *p<0.001*), medium-injected group (2.41 ± 1.17, *p<0.001*) and sham-operated group (2.73 ± 1.47, *p<0.001*) (Figure 35).

4.4.7 Improvement in regional myocardial perfusion after human $CD133^+$ EPC transplantation

The perfusion defect was reduced in both cell transplanted groups. However, significant increase in regional blood perfusion was observed in $CD133^+$ EPC transplantation group (2.86 ± 0.278 ml/min/g) as compared to ad-Null transduced cells transplanted group (1.48 ± 0.227 ml/min/g, *p=0.026*), medium-injected group (0.8 ± 0.156 ml/min/g, *p=0.05*) and sham-operated group (1.13 ± 0.234 ml/min/g) at 6 weeks post-transplantation (Figure 36).

4.4.8 Reduction of infarct size after human $CD133^+$ EPC transplantation

Tetrazolium chloride staining showed a marked reduction of infarct size in the cell transplanted groups compared to the medium-injected group in the infarcted myocardium (Figure 37). The extent of reduction of the infarct size was higher in the

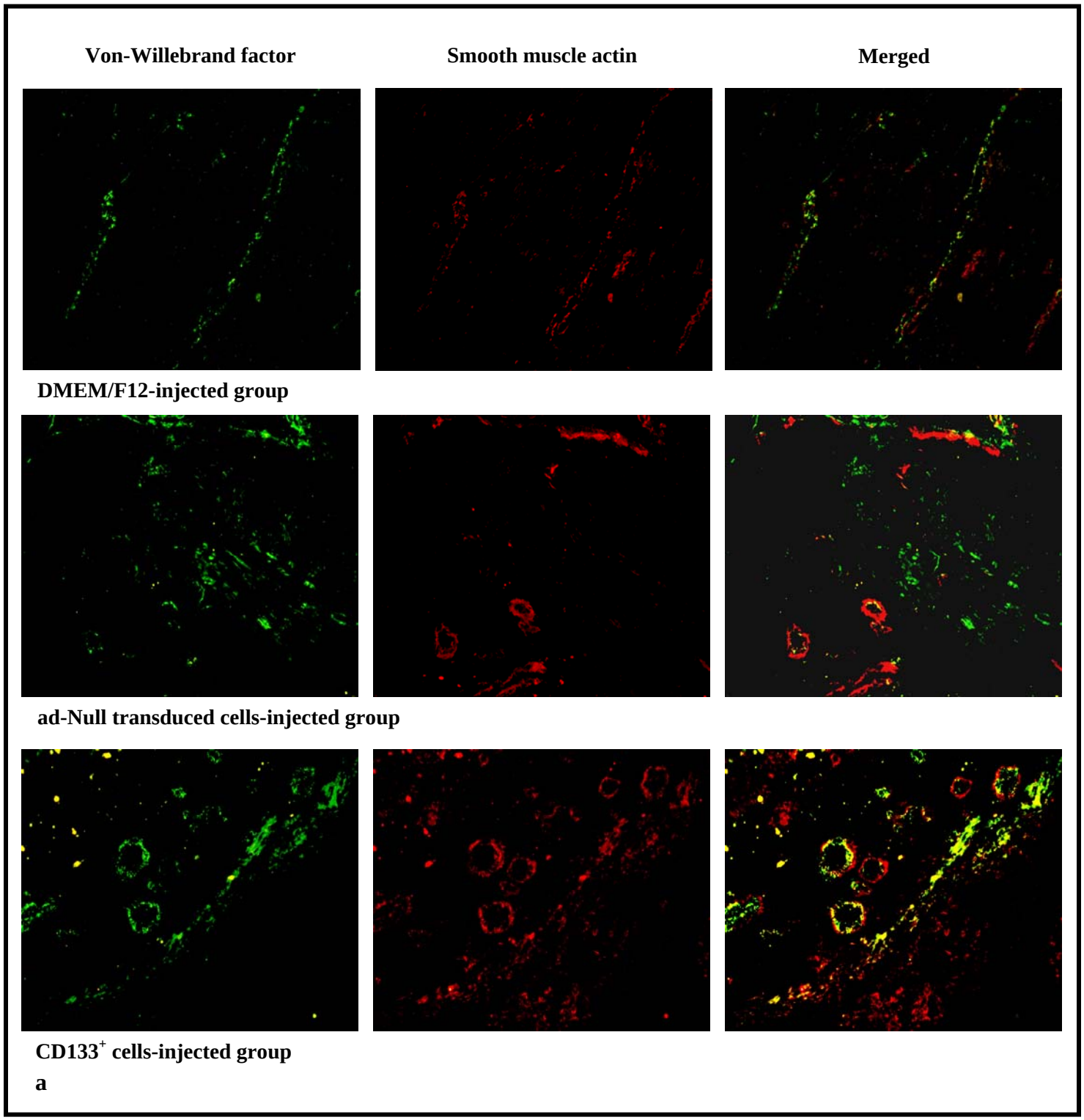
Von-Willebrand factor
Smooth muscle actin
Merged
DMEM/F12-injected group
ad-Null transduced cells-injected group
CD133+ cells-injected group

a

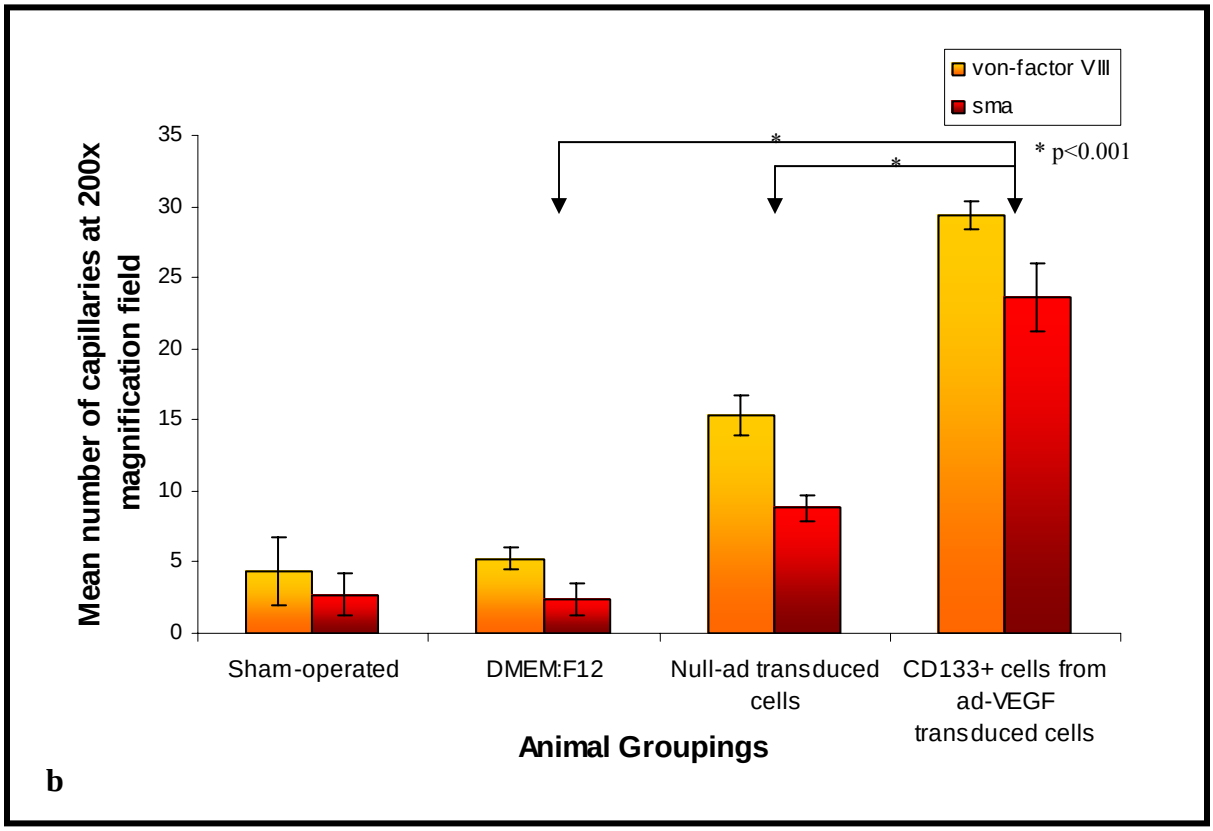

Figure 35: (a) **Blood vessel density in the ischemic myocardium at high 200× magnification at 6 weeks after cell transplantation.** Double fluorescent immunostaining for von-Willebrand factor (green fluorescence- FITC) and smooth muscle actin (red-fluorescence-TRITC) was performed to visualize the blood vessels, (b) **Graphical representation of the blood vessel density in the 4 animal groupings.**

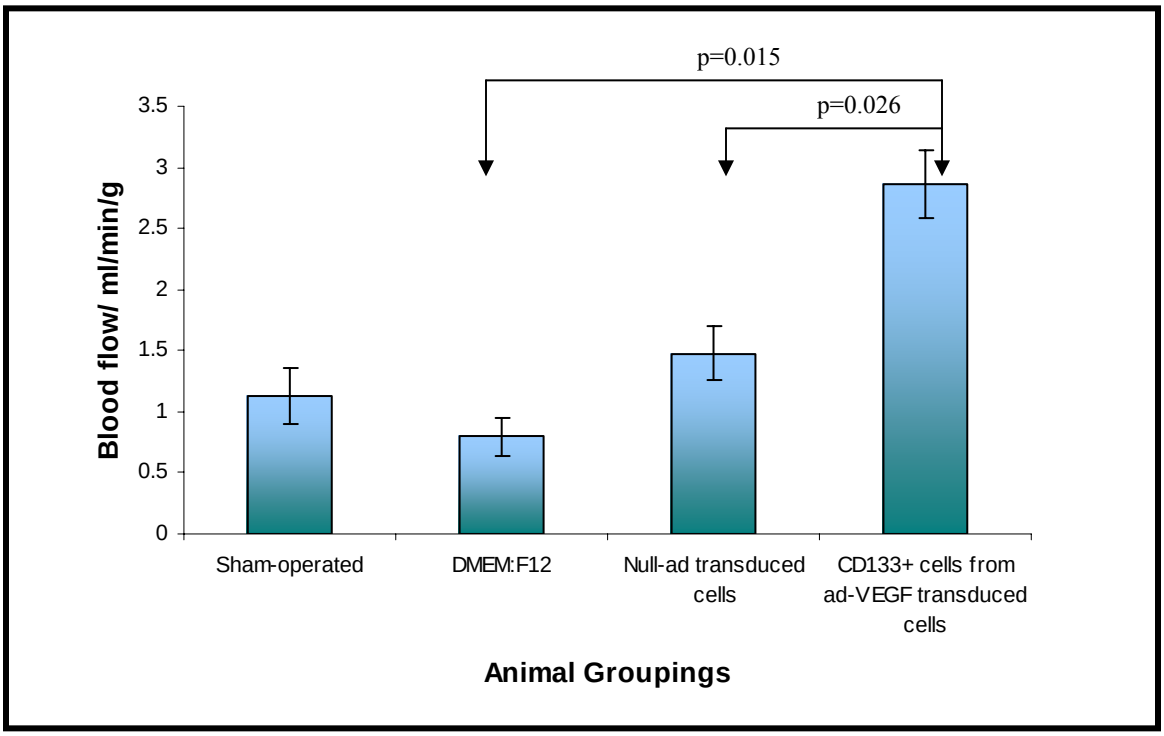

Figure 36: **Regional myocardial flow assessment in between CD133^{+} cell transplanted group and medium-injected group**

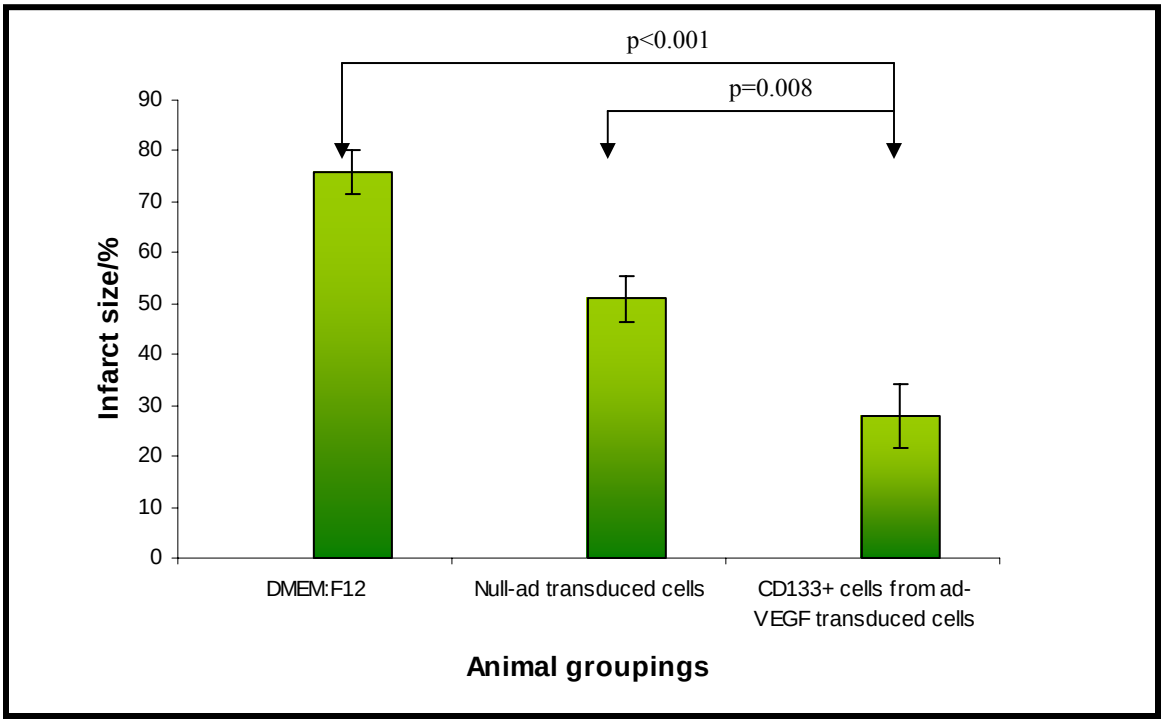

Figure 37: **Infarct size assessment a between CD133^{+} cell transplanted group and medium-injected group**

$CD133^+$ EPC transplanted group (28% ± 6.2%) when compared to the ad-Null transduced cells transplanted group (51% ± 4.5%, *p=0.008*) and medium-injected group (76% ± 4.3%, *p<0.001*) at 6 weeks post-transplantation. Interestingly, most of the myocardial structure in the border zone was intact and accompanied by many new blood vessels in the cell transplanted rats whereas the myocardial structure was chaotic in the medium-injected group, indicating that cell engraftment attenuated left ventricular remodeling after infarction.

4.4.9 Reduction in number of apoptotic cells in the infarcted hearts transplanted with human $CD133^+$ EPCs

The number of apoptotic cells in the infarct and peri-infarct areas of the myocardium was assessed by TUNEL assay. The number of TUNEL-positive cells in $CD133^+$ EPC transplanted group was significantly lower than in the ad-Null transduced cell transplanted group and medium-injected group (Figure 38).

4.4.10 Incorporation of human $CD133^+$ derived cells into foci of myocardial neovascularization

Co-localization of von-Willebrand factor with smooth muscle actin with DAPI fluorescence documented that the transplanted population of DAPI-labeled cells incorporated into the neovascular foci (Figure 39). Review of 15 sections retrieved from the infarcted myocardium of $CD133^+$ EPC transplanted group identified labeled $CD133^+$ derived cells in up to 72% (± 4.2%) of the total blood vessels under high power magnification field (200×).

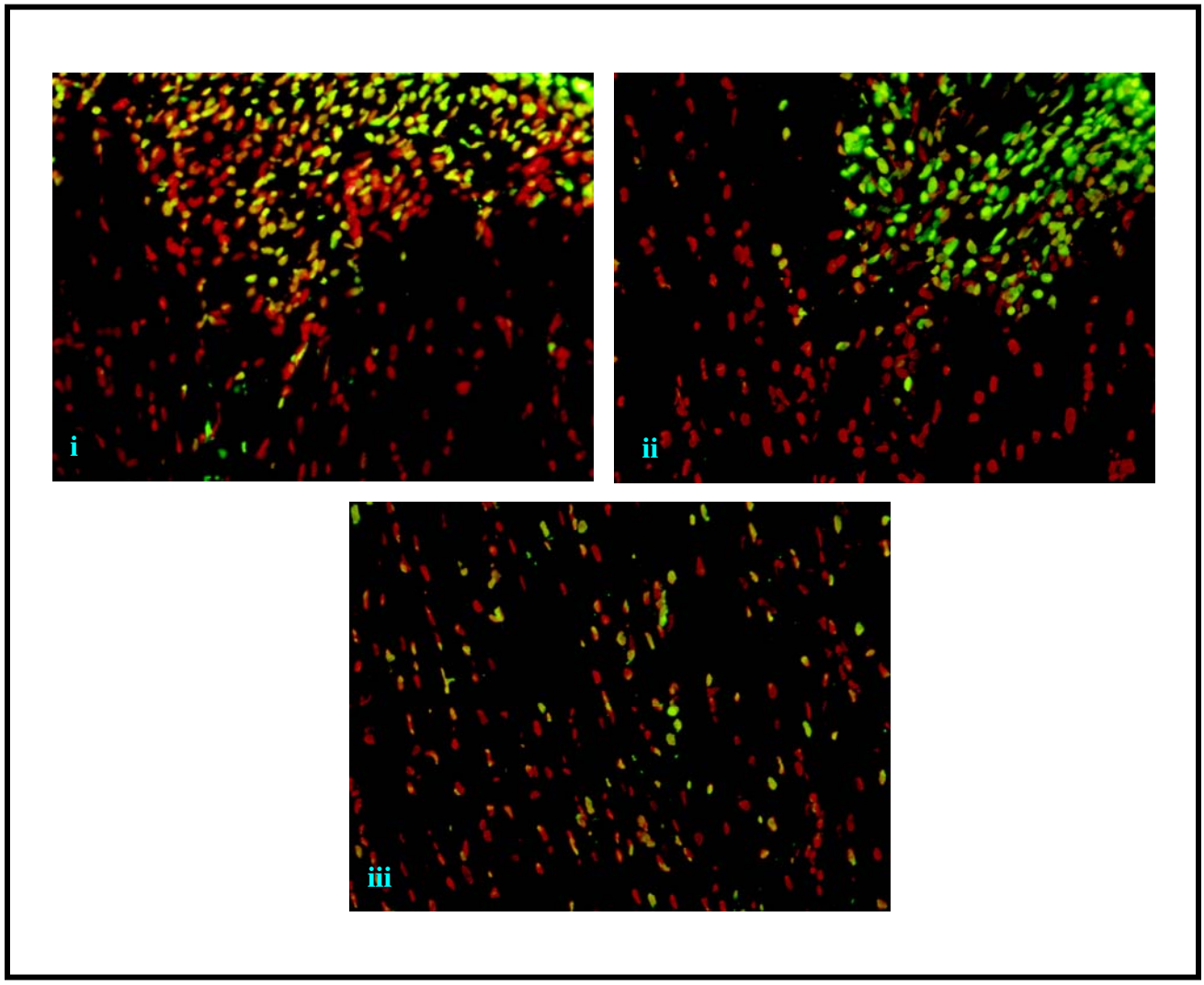

Figure 38: **TUNEL assay for assessment of the apoptotic cells in the infarct and peri-infarct areas of the ischemic myocardium.** TUNEL positive cells are visualized as green fluorescence and cell nuclei are visualized as red fluorescence using propidium iodide. Tissue sections from (i) DMEM/F12 medium injected animals, (ii) ad-Null transduced cells transplanted animals, (iii) $CD133^{+}$ cells from ad-$hVEGF_{165}$ transduced cells transplanted animals (Magnification= 200×)

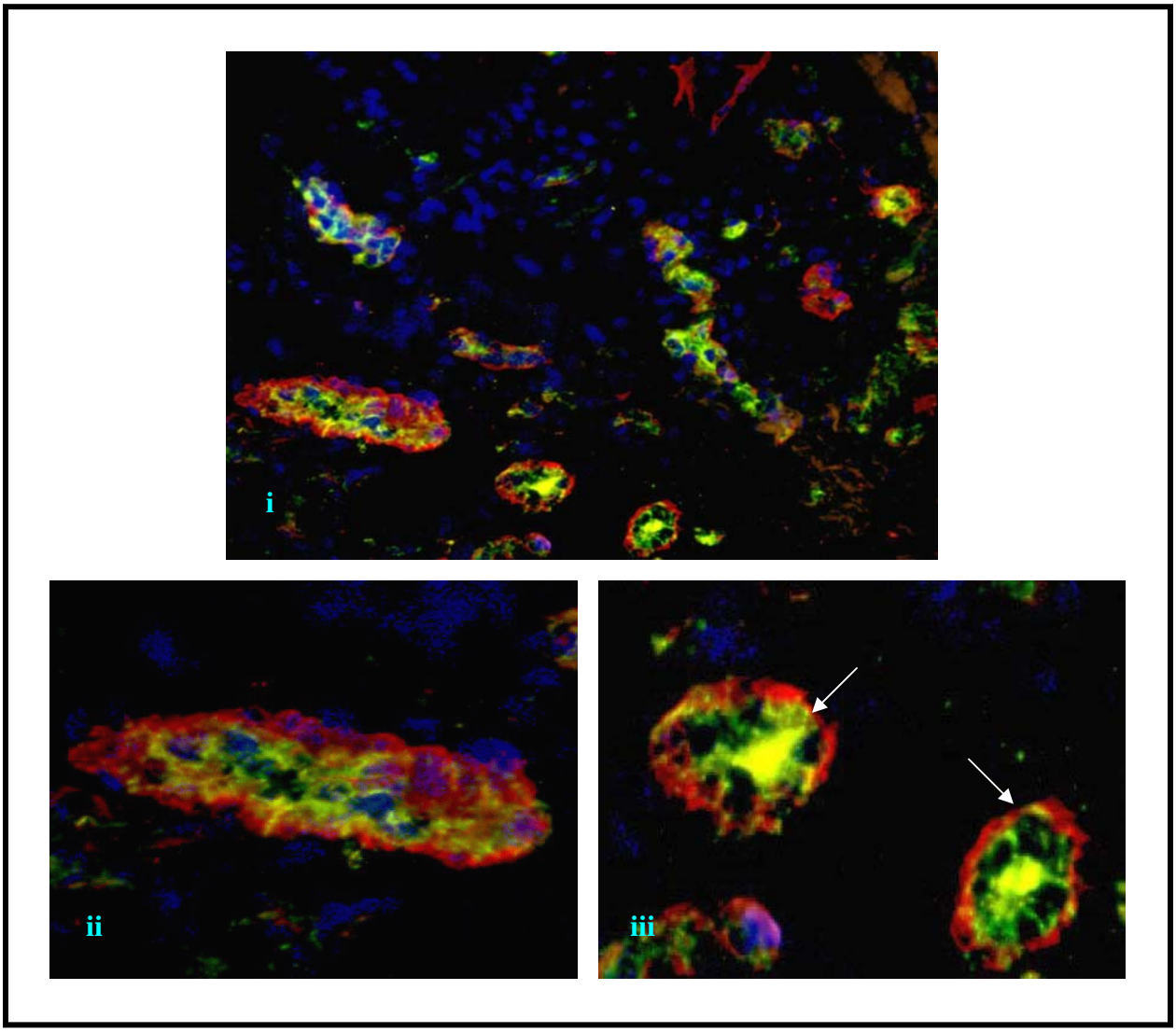

Figure 39: **Effects of CD133^{+} cell transplantation on neovascularization in the rat ischemic myocardium. (**i) Presence of newly formed blood vessels in the infarcted and peri-infarct areas, (ii) Incorporation of CD133^{+} derived cells into newly formed blood capillaries, iii) Endogenous blood capillaries formed by the rat vascular-related cells. (i: Magnification= 200×, ii & iii: Magnification= 400×)

The cells were found mainly in the infarct and peri-infarct areas of the myocardium. Other than the ischemic areas of the myocardium, $CD133^+$-derived cells were detected neither in contra-lateral non-ischemic myocardium nor the other organs.

Enhanced neovascularization in CD133+ EPC transplanted group led to important biological preservation of myocardium as observed from the infarct size assessment of the infarcted myocardium.

4.4.11 Angiogenic cytokines supply by transplanted $CD133^+$ EPCs to the infarcted rat myocardium

Cardiac mRNA and protein expression of VEGF and Ang-1 were higher in the $CD133^+$ EPCs transplanted group than the medium-injected group (Figure 40a & b). VEGF mRNA and protein expression in medium-injected group remained at a low level from day 1 up till 6 weeks after medium injection. In $CD133^+$ EPC transplanted group, VEGF mRNA and protein expression significantly increased 5 to 8 days post-transplantation and slowly decreased till 6 weeks post-transplantation. Ang-1 mRNA and protein expression in medium-injected group were high from day 1 to day 8 after medium injection but started to decline from day 14 onwards. In $CD133^+$ EPC transplanted group, Ang-1 mRNA and protein expression increased gradually and peaked at day 8 and day 14 post-transplantation. At 6 weeks, both VEGF and Ang-1 mRNA and protein expressions were higher in the $CD133^+$ EPC transplanted group than the medium-injected group.

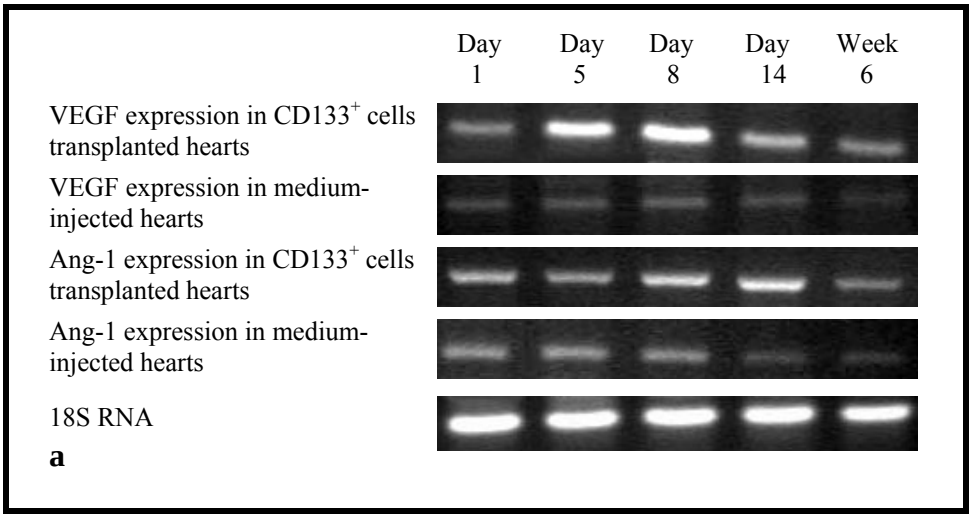

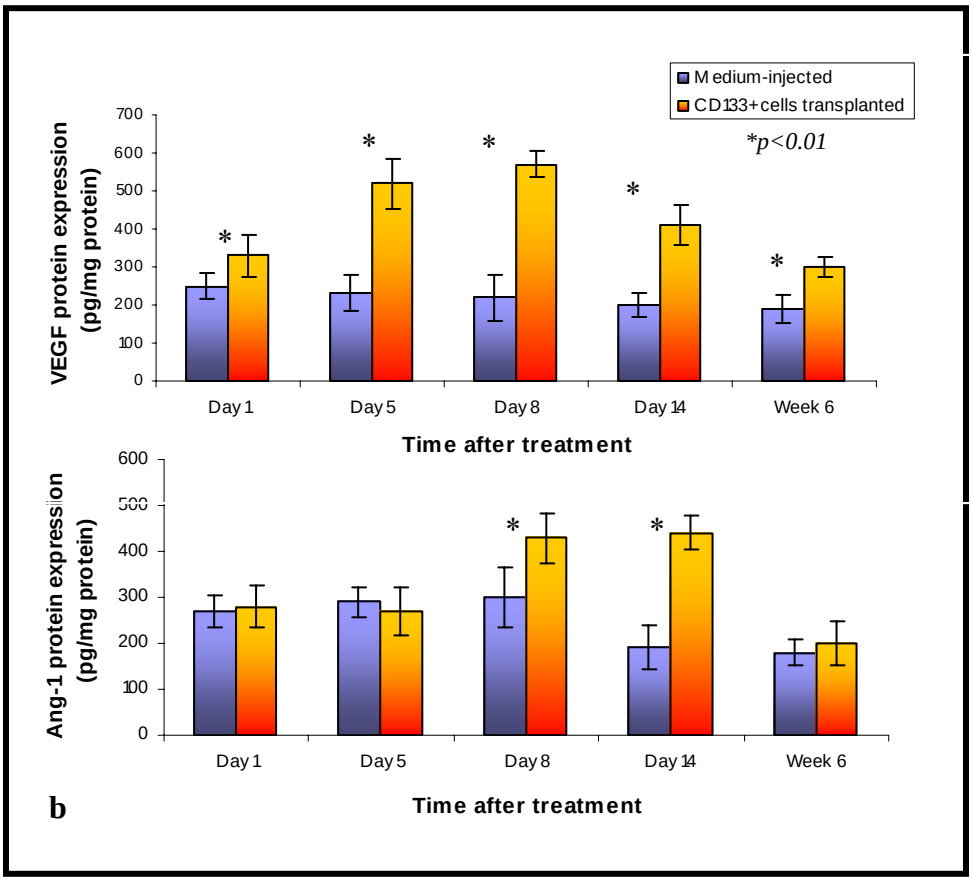

Figure 40: **VEGF and Ang-1 expression in rat myocardium at various time points after treatment.** (a) RT-PCR showing VEGF and Ang-1 mRNA expression in rat myocardium at day 1, day 5, day 8 and week 6 after treatment, (b) VEGF and Ang-1 protein expression in rat myocardium at day 1, day 5, day 8 and week 6 after treatment as measured by ELISA.

4.5 Discussion

Following an infarction, the viable myocardial tissue bordering the infarct area is significantly hypertrophied (Braunwald et al, 1991; Olivetti et al, 1991). Although endogenous angiogenesis within the infarcted area appears to be a crucial component of the left ventricle remodeling process, under normal circumstances, the capillary network is unable to keep pace with tissue growth and support the greater demands of the hypertrophied but viable myocardium which subsequently undergoes apoptosis due to inadequate oxygenation and nutrition (Cheng et al, 1996; Narula et al, 1996). Findings that indicated circulating EPCs from the bone marrow may home to sites of neovascularization and differentiate into ECs in situ is consistent with the vasculogenesis, the establishment of vascular network in the embryo (Shi et al, 1998). This suggested that growth and development of blood vessels in the adult is not restricted only to angiogenesis but also to embryonic vasculogenesis. Therefore, a novel strategy of EPC transplantation to supplement resident fully differentiated ECs in promoting neovascularization of the infarct and peri-infarct areas is potentially beneficial.

The main findings of this study demonstrated that (i) HESC derived $CD133^+$ EPCs using VEGF adenoviral transduction is safe upon transplantation, (ii) $CD133^+$ EPCs can successfully survive in the infarcted myocardium for 6 weeks post-transplantation, (iii) $CD133^+$ EPCs are able to differentiate into endothelial and smooth muscle cells *in vivo* within the ischemic environment, (iv) $CD133^+$ derived cells incorporate into the blood vessel walls, (v) $CD133^+$ EPC transplantation resulted in improvement of regional blood flow and cardiac function, (vi) $CD133^+$ EPC

transplantation limits the extent of infarct expansion and (vii) $CD133^+$ derived cells supplied angiogenic cytokines such as VEGF and Ang-1.

This pre-clinical study demonstrated that $CD133^+$ EPC transplantation can effectively and safely induces neovascularization in ischemic myocardium by differentiating into vascular-related cells and supplying angiogenic factors. This has important biological consequences as the transplantation augmented the naturally impaired neovascularization and improved blood flow recovery. Additionally, LVEF and fractional shortening also improved by 2-fold in comparison between rats receiving $CD133^+$ EPCs and rats receiving medium injection, reaching values as good as sham-operated rats (Figure 30). The same strategy but using different markers for identifying population of EPCs have also been used successfully to enhance myocardial function after infarction and limb ischemia in experimental animal models (Kawamoto et al, 2003; Kawamoto et al, 2001; Kocher et al, 2001; Kalka et al, 2000).

Despite the promising potential of EPCs for regenerative applications, the fundamental scarcity of their population in the bone marrow and peripheral blood combined with their possible functional impairment due to age-related factors and other human phenotypes such as diabetes and hypercholesterolemia constitute a potential liability of therapeutic vasculogenesis and angiogenesis via primary EPC transplantation (Cosentino et al, 1998; Drexler et al, 1991). HESCs on the other hand, represent one of the best source of donor cells for regenerative therapy as compared to bone marrow and peripheral blood since they are highly proliferative, hence providing a potentially unlimited reservoir of cells for induction of EPC differentiation.

In this study, cell transplantation was delayed until 2 weeks post-infarction to reduce the extent of transplanted cell loss during the post-necrosis inflammatory process. The significant decrease in the number of infiltrating immune cells into the myocardium and the moderate amount of collagen scar in the myocardium at 2 weeks post-infarction made the microenvironment conducive for the survival of the transplanted $CD133^+$ cells (Figure 32 & 33). $CD133^+$ EPCs in the infarcted myocardium could survive for 6 weeks post-transplantation in an immunosuppressed animal. RT-PCR of human Y chromosome was used to assess the extent of the presence of the transplanted cells in the rat myocardium (Figure 31a & b). The Y-chromosome expression level decreased up till week 3 post-transplantation before increasing slowly by week 6. This data supported the fact that the surviving transplanted cells proliferated in the rat infarcted myocardium. Besides cell loss due to physical strain during and after injection, direct cell injection into the infarcted rats may also helped to reduce the degree of cell loss. This is because the injected cells have more difficulty in escaping beyond the fibrous capsule through vascular or lymphatic channels.

Even though myocardial infarction was a stimulus to induce endogenous neovascularization in the rat heart, this was insufficient to provide beneficial revascularization in order to salvage the damaged heart tissue (Figure 34). $CD133^+$ EPC transplantation resulted in significantly higher degree of neovascularization, identified by fluorescent immunohistochemical staining for von-Willebrand factor and smooth muscle actin, evaluated by blood capillary density and regional blood flow by microspehere injection as compared to controls receiving medium injection and null-ad transduced cells that have significantly lower amount of EPCs (Figure 35 and 36). Blood vessel and

mature blood vessel density were approximately 6- and 8-fold respectively greater in $CD133^+$ EPC transplanted rats than in medium-injected rats, while regional blood flow increased by 3-fold. The enhanced neovascularization also resulted in a lower degree of left ventricle infarct expansion, possibly due to the lower degree of apoptotic death of the cardiomyocytes shown in the TUNEL assay (Figure 37 and 38). The salvage of the cardiomyocyte death especially at the peri-infarct area is critical as it prevents the decrease in ventricular wall thickness which according to Laplace's law, will reduce left ventricular stress and prevent infarct expansion, left ventricular dilatation and deterioration of function (Mann, 1999). Furthermore, it has been reported that cell apoptosis from the activation of pro-apoptotic signal transduction pathways accounts for at least half of the total cell destruction during myocardial infarction (Takashi et al, 2000; Kajstura et al, 1996).

Most of the surviving cells were found to be incorporated into the foci of myocardial neovascularization. Potential mechanisms by which neovascularization may be induced after $CD133^+$ EPC transplantation include (i) formation of blood vessels by the transplanted $CD133^+$ cells and (ii) stimulation of angiogenic growth factors expressed or stimulated by the transplanted $CD133^+$ cells. This study showed that $CD133^+$ cells played a structural role in induction of neovascularization as many DAPI-labeled $CD133^+$ derived cells were found to be incorporated into the newly formed blood vessels, differentiated into both endothelial and smooth muscle cells, hence enhancing the mature vascularization in both infarct and peri-infarct areas 6 weeks post-transplantation (Figure 35 & 39). This result was consistent with the finding of a study by Gehling which showed

the ability of $CD133^+$ EPCs purified from peripheral blood differentiate into ECs both *in vitro* and *in vivo* (Gehling et al, 2000).

The results showed that there were differences in the VEGF and Ang-1 cardiac mRNA and protein expression levels between the $CD133^+$ EPC transplanted and medium-injected rats (Figure 40a & b). RT-PCR and ELISA showed that cardiac mRNA and protein expression of VEGF in $CD133^+$ EPC transplanted rats were highly expressed after day 1 post-transplantation, peaked by day 5 and day 8. Following that, VEGF expression slowly decreased but was still detectable at 6 weeks post-transplantation whereas VEGF expression in medium-injected rats remained low throughout the various time points after medium injection. RT-PCR and ELISA showed that cardiac mRNA and protein expression of Ang-1 which plays a role in the maturation and stability of the blood vessels were seen to be upregulated later than VEGF. In the $CD133^+$ EPC transplanted group, Ang-1 was only highly expressed at day 8 to day 14 post-transplantation. Ang-1 expression slowly declined and reached a low level at 6 weeks post-transplantation. Endogenous expression of angiogenic cytokines and their increased expression upon cell transplantation have also been reported in other studies using other cell types such as mesenchymal stem cells and bone marrow cells (Tang et al, 2005; Zhang et al, 2004; Heba et al, 2001; Kamihata et al, 2001).

Overall, the present study adds to the number of investigations pointing to the potential utility of embryonic stem cells in the heart regeneration therapy. The difference of this present study from the other previous work is that this study focused on the use of differentiated derivative from embryonic stem cells which in this case is EPCs unlike other studies that focused on undifferentiated embryonic stem cells that may differentiate

into various cell types in the myocardium. $CD133^{+}$ EPCs derived from ad-$VEGF_{165}$ transduced differentiating HESCs were effective and safe for heart regeneration in a rat model of myocardial infarction. However, important barriers such as adequate source of pathogen-free HESC lines, immune rejection and tumorigenesis must be overcome before HESCs can finally reach clinical applications.

4.6 Bibliography

Brutsaert DL. Cardiac endothelial-myocardial signaling: its role in cardiac growth, contractile performance and rhythmicity. Physiol Rev 2003; 83: 59-115

Cheng W,Kajstura J,Nitahara JA, Li B, Reiss K, Liu Y, Clark WA, Krajewski S, Reed JC, Olivetti G, Anversa P. Programmed myocyte cell death affects the viable myocardium after infarction in rats. Exp Cell Res 1996; 226: 316-327

Cosentino F, Luscher TF. Endothelial dysfunction in diabetes mellitus. J Cardiovasc Pharmacol 1998; 32: S54-S61

Drexler H, Zeiher AM, Meinzer K, Just H. Correction of endothelial dysfunction in coronary microcirculation of hypercholesterolemic patients by L-arginine. Lancet 1991; 338: 1546-1550

Gehling UM, Ergun Suleyman, Schumacher U, Wagener C, Pantel K, Otte M, Schuch G, Schafhausen P, Mende T, Kilic N, Kluge K, Schafer B, Hossfeld DK, Fiedler W. In vitro differentiation of endothelail cells from AC133-positive progenitor cells. Blood 2000; 95: 3106-3112

Heba G, Krzeminski T, Pore M, Grzyb J, Ratajska A, Dembinska-Kiec A. The time course of tumour necrosis factor-alpha, inducible nitric oxide synthase and vascular endothelial growth factor expression in an experimental model of chronic myocardial infarction in rats. J Vasc Res 2001; 38: 288-300

Kajstura J, Cheng W, Reiss K, Clark WA,Sonnenblick EH, Krajewski S, Reed JC, Olivetti G, Anversa P. Apoptotic and necrotic myocyte cell deaths are independent contributing variables of infarct size in rats. Lab Invest 1996; 74: 86-107

Kalka C, Masuda H, Takahashi T, Kalka-Moll WM, Silver M, Kearney M, Li T, Isner JM, Asahara T. Transplantation of ex vivo expanded endothelial progenitor cells for therapeutic neovascularization. Proc Natl Acad Sci USA 2000; 28: 3422-3427

Kamihata H, Matsubara H, Nishiue T, Fujiyama s, Tsutsumi Y, Ozono R, Masaki H, Mori Y, Iba O, Tateishi E. Kosaki A, Shintani S, Murohara T, Imaizumi T, Iwasaka T. Implantation of bone marrow mononuclear cells into ischemic myocardium enhances collateral perfusion and regional function via side supply of angioblasts, angiogenic ligands and cytokines. Circulation 2001; 104: 1046-1052

Kawamoto A, Tkebuchava T, Yamaguchi J, Nishimura H, Yoon YS, Milliken C, Uchida S, Masuo o, Iwaguro H, Ma H, Hanley A, Silver M, Kearney M, Losordo DW, Isner JM, Asahara T. Intramyocardial transplantation of autologous endothelial progenitor cells for therapeutic neovascularization of myocardial ischemia. Circulation 2003; 107: 461-468

Kawamoto A, Gwon HC, Iwaguro H, Yamaguchi JI, Uchida S, Masuda H, Silver M, Ma H, Kearney M, Isner JM, Asahara T. Therapeutic potential of ex vivo expanded endothelial progenitor cells for myocardial ischemia. Circulation 2001; 103: 634-637

Kocher AA, Schuster MD, Szabolcs MJ, Takuma S, Burkhoff D, Wang J, Homma S, Edwrads NM, Itescu S. Neovascularization of ischemic myocardium by human bone marrow-derived angioblasts prevents cardiomyocytes apoptosis, reduces remodeling and improves cardiac function. Nature Med 2001; 7: 430-436

Mann DL. Mechanisms and models in heart failure: a combinatorial approach. Circulation 1999; 100: 999–1008

Narula J, Haider N, Virmani R, DiSalvo TG, Kolodgie FD, Hajjar RJ, Schmidt U, Semigran MJ, Dec GW, Khaw BA. Apoptosis in myocytes in end-stage heart failure. N Eng J Med 1996; 335: 1182-1189

Shi Q, Rafii S, Wu MH, Wijelath ES, Yu C, Ishida A, Fujita Y, Kothari S, Mohle R, Sauvage LR, Moore MA, Storb RF, Hammond WP. Evidence for circulating bone marrow-derived endothelial cells. Blood 1998; 92: 362-367

Takashi E, Ashraf M. Pathologic assessment of myocardial necrosis and apoptosis after ischemia and reperfusion with molecular and morphological markers. J Mol Cell Cardiol 2000: 32: 209-224

Tang YL, Zhao Q, Qin X, Shen L, Cheng L, Phillips MI. Paracrine action enhances the effects of autologous mesenchymal stem cell transplantation on vascular regeneration in rat model of myocardial infarction. Ann Thorac Surg 2005; 80: 229-237

Zhang S, Zhang P, Guo J, Jia Z, Ma K, Liu Y, Zhou C, Li L. Enhanced cytoprotection and angiogenesis by bone marrow cell transplantation may contribute to improved ischemic myocardial function. Eur J Cardio-thorac Surg 2004; 25: 188-195

CHAPTER 5

GENERAL CONCLUSION AND FUTURE DIRECTIONS

Left ventricular remodeling can be considered as a critical therapeutic target for heart failure as it is not only a consequence of heart failure but also contribute to its progression. This raises the interesting possibility that therapeutic strategies specifically designed to prevent and/or antagonizing left ventricular remodeling may be beneficial to the prognosis of heart failure. However, the complexity of the disease makes it uncertain as to which myriad of cellular and molecular mechanisms that contribute to left ventricular remodeling should be therapeutic targets. It is not possible to antagonize all of the biologically active systems that become activated in the setting of heart failure.

This study has chosen to focus on preservation of cardiomyocytes and maintenance of ventricle integrity via studying the influence of a novel peptide on expression of pro-inflammatory cytokines and HESC-derived $CD133^+$ cell transplantation for enhanced neovascularization in the ischemic myocardium. Both studies showed their positive effect in controlling the size of the myocardial infarct and improving cardiac function.

DAA-I therapy revealed downregulation of critical pro-inflammatory cytokines that are known to play important role in the pathophysiology of heart failure. It also resulted in significant downregulation of the number of infiltrating immune cells into the infarct area. These immune cells and pro-inflammatory cytokines are responsible for initiating necrotic and apoptotic death of the cardiomyocytes through the inflammation process upon infarction.

Transplantation of HESC-derived $CD133^+$ cells into the infarcted myocardium led to significant increase in the number of functional blood vessels which either consisted of donor or host-origin vascular cells. This stable collateral enhancement improved the

microvascular network which led to improved perfusion and hence provision of oxygen and nutrients to the starved cardiomyocytes. This is critical in the salvaging of the cardiomyocytes especially in the peri-infarct area. With this mechanism, $CD133^+$ EPC transplantation therapy is successful in reducing infarct area leading to improved cardiac function.

Despite the encouraging results obtained from the two studies, additional work is still required to further elucidate the mechanisms, safety and beneficial effects exerted by both therapies. DAA-I is a functional angiotensin peptide of the renin-angiotensin system implicated in the pathophysiology of the cardiovascular system. It has been reported to exert its protective actions on cardiovascular pathologies, in which angiotensin II is implicated, by counteracting the actions of angiotensin II via the AT1 receptor. With this knowledge, it would be helpful to clarify the mechanism on how regulation of inflammatory cytokine expression by des-asparate-angiotensin-I upon MI occurs via the angiotensin II receptor pathway.

Therapeutic angiogenesis represents an exciting new avenue in the treatment of ischemic heart disease. Various angiogenic proteins and gene therapies in pre-clinical and clinical trials have been reported for the past decade and now cell-based therapy is the latest strategy being intensively studied. An array of donor cell types including the bone marrow cells, mesenchymal stem cells and EPCs have been studied for their effectiveness in regenerating the infarcted myocardium. The recent derivation of several pluripotent HESC lines has led to their application in pre-clinical myocardial regeneration therapy. However, despite the exciting advances in HESC research, much basic work is still

required and several obstacles remain to be overcome before this technology can enter any serious clinical trials.

It is of utmost importance to develop efficient, controlled and stable strategies and selection protocols that are able to yield 100% pure population of a specific lineage such as cardiomyocytes or vascular cells from HESC differentiation. It is crucial to avoid transplanting undifferentiated cells or inappropriate cell lineages due to the risk of teratoma formation or unwanted disturbance of the diseased tissue function. Currently, modulating composition of cell culture medium to significantly increase the yield of a target cell type has not been very successful. An alternative approach is the gene transfer method, introducing relevant gene constructs into the HESCs with either viral or non-viral vectors such as immunoliposomes. While our study using ad-hVEGF$_{165}$ demonstrated significant increase of CD133^{+} EPCs from 8% to 40% within the heterogenous population of EB-derived cells, it would be more attractive to obtain purified population of CD133^{+} EPCs directly from HESCs without EB formation. Future work can be focused on genetic modification of HESCs by designing and introducing gene construct containing a marker gene under the control of a vascular tissue-specific promoter or enhancer which can direct vascular differentiation within HESCs themselves. The vascular cells can then be selected by the marker to allow for their preferential selection. Another approach would be designing vectors with forced expression of transcriptional factors that can direct differentiation of HESCs into vascular cells.

Our study showed that HESC derived CD133^{+} cells had good survival rate in the infarcted rat myocardium due to cyclosporine, an immunosuppressive agent that was administered to the rats. Even the study showed that the immunogenicity of the

transplanted cells can be contained through the use of immunosuppressive drug, unpleasant side effects may occur as the host receiving the cells may become extremely susceptible to infection. Long-term maintenance immunosuppresive therapy would thus limit successful clinical application. Immediate future work on this can focus on generating genetically engineered immunologically-priviledged HESC lines that can be used as a universal transplant. This can be achieved via either inserting immunosuppressive molecules or deleting immunoreactive molecules by immunoliposomes or RNA interference methodology. More ambitiously, another approach to increase the immunocompatibility of the cells is to replace the foreign major histocompatibilty complex (MHC) genes could be replaced with the recipient's MHC genes.

Genetic modification using adenoviral vector may have far-reaching applications but it is also noteworthy to consider the potential of immunologic complications that are attached to the use of adenoviral vectors. In this study, ex vivo transduction strategy was used and this precludes the exposure of the adenovirus to the recipient's immune system. Nevertheless, it is always good to be cautious and further studies are essential to examine the safety and clinical efficacy of using these HESC-derived $CD133^{+}$ cells that are generated from adenoviral-mediated delivery of the $VEGF_{165}$ gene.

In the recent years, there has been rapid development of novel myocardial imaging techniques in small animals such as mice and rats. This is necessary for improving the accuracy for myocardial infarct measurement based on the gold standard staining procedure such as Evans Blue dye or triphenyltetrazolium chloride (TTC) staining. A variety of techniques have been recently reported for assessment of the

myocardial infarct size. These include nuclear imaging with positron emission tomography (PET) or single photon emission tomography (SPECT) and contrast-enhanced magnetic resonance imaging (MRI). The advantage of using these non-invasive techniques is the ability to visualize the scar tissue directly in vivo and quantitate the infarct size in real time.

Interest in the use of SPECT to determine rat myocardial infarct size has been growing. Measurement of the myocardial perfusion defect by injection of perfusion agents such as ^{99m}Tc-sestamibi during coronary occlusion indicates the amount of myocardium at risk while injection of ^{99m}Tc-sestamibi after coronary occlusion measures the infarct size. When these measurements are obtained through high resolution imaging of small animals, they can be used to investigate metabolism, revascularization therapy, gene and cell therapy and new radiopharmaceuticals for diagnosing

High resolution ^{99m}Tc-sestamibi pinhole SPECT has been reported to be used for quantitative analysis of myocardial infarct in rats (Acton PD et al, 2006; Maskali F et al, 2006; Liu Z et al, 2002). This imaging technique is capable of accurate quantification of the size of perfusion deficit which in return correlate to the myocardial infarct size. While TTC staining indicates non-viable myocardium; the infarcted region, ^{99m}Tc-sestamibi signal indicates the viable (maybe stunned) and perfused region. However, the calculated size of the perfusion deficit measured using ^{99m}Tc-sestamibi SPECT compared very favourably with the TTC staining especially in within the threshold value range of 50 to 70%. This strong correlation demonstrates that the non-invasive ^{99m}Tc-sestamibi SPECT can serve as a surrogate for quantification of the infarct size.

The most accurate non-invasive technique up to date that has been reported is the

contrast-enhanced MRI. MRI allows precise detection of scar tissue and currently the only technique discriminating between subendocardial and transmural infarction (Wagner A et al, 2003). This method has been used to measure the LV volumes and mass, myocardial infarct size and cardiac output of rat and mouse infarction models (Yang Z et al, 2004; Nahrendorf M et al, 2003; Watzinger N et al, 2002; Nahrendorf M et al, 2000).

Both SPECT and MRI have an edge over Evans dye and TTC staining. They allow serial measurements to be made and use computed 3-dimensional display which allows absolute infarct volume to be measured more reliably. These up to date techniques are to be considered to be used in future studies so as to obtain new insights into the remodeling process before and after treatment of the infarction.

The idea of using drug and cell-based therapies as an adjunctive to and/or possible synergist with existing heart failure strategies can potentially be useful but whether this combinatorial approach will really ever encompass the whole truth about heart failure remains unknown for the present, but represents a potentially important area of theoretical and therapeutic discovery in the coming millennium.

Bibliography

Acton PD, Thomas D, Zhou R. Quantitative imaging of myocardial infarct in rats with high resolution pinhole SPECT. Int J Cardiovasc Imaging. 2006;22(3-4):429-34

Liu Z, Kastis GA, Stevenson GD, Barrett HH, Furenlid LR, Kupinski MA, Patton DD, Wilson DW. Quantitative analysis of acute myocardial infarct in rat hearts with ischemia-reperfusion using a high-resolution stationary SPECT system. J Nucl Med. 2002 Jul;43(7):933-9

Maskali F, Franken PR, Poussier S, Tran N, Vanhove C, Boutley H, Le Gall H, Karcher G, Zannad F, Lacolley P, Marie PY. Initial infarct size predicts subsequent cardiac remodeling in the rat infarct model: an in vivo serial pinhole gated SPECT study. J Nucl Med. 2006;47(2):337-44

Nahrendorf M, Wiesmann F, Hiller KH, Han H, Hu K, Waller C, Ruff J, Haase A, Ertl G, Bauer WR. In vivo assessment of cardiac remodeling after myocardial infarction in rats by cine-magnetic resonance imaging. J Cardiovasc Magn Reson. 2000;2(3):171-80

Nahrendorf M, Hiller KH, Hu K, Ertl G, Haase A, Bauer WR. Cardiac magnetic resonance imaging in small animal models of human heart failure. Med Image Anal. 2003 Sep;7(3):369-75

Watzinger N, Lund GK, Higgins CB, Wendland MF, Weinmann HJ, Saeed M. The potential of contrast-enhanced magnetic resonance imaging for predicting left ventricular remodeling. J Magn Reson Imaging. 2002;16(6):633-40

Yang Z, Berr SS, Gilson WD, Toufektsian MC, French BA. Simultaneous evaluation of infarct size and cardiac function in intact mice by contrast-enhanced cardiac magnetic resonance imaging reveals contractile dysfunction in noninfarcted regions early after myocardial infarction. Circulation. 2004 Mar 9;109(9):1161-7

CHAPTER 6

APPENDICES

TABLE OF CONTENT

6.1 Materials

6.1.1 Cell lines

Human embryonic kidney 293 cells

Cells were kindly given by Associate Professor Ge Ruowen, Department of Biological Sciences, Faculty of Science, National University of Singapore

Human umbilical vein endothelial cells

Cells were kindly given by Associate Professor Ge Ruowen, Department of Biological Sciences, Faculty of Science, National University of Singapore

6.1.2 Cell culture products

Dulbecco's Modified Eagle's Medium (DMEM)	Sigma, USA
Fetal Bovine Serum	Hyclone, USA
DEM: F12 Medium	GIBCO-Invitrogen, USA
Knockout Serum	GIBCO-Invitrogen, USA
Matrigel Basement Membrane Matrix	Becton Dickinson, USA

6.1.3 Chemicals

Agarose (molecular biology grade)	Bio-Rad, USA
Dimethyl sulphoxide (DMSO)	Sigma, USA
Bouin's Solution	Sigma, USA
L-glutamine solution	GIBCO-Invitrogen, USA
Non-essential amino acids	GIBCO-Invitrogen, USA
Penicillin/Streptomycin	Sigma, USA
Phosphate buffered saline (PBS)	NUMI, Singapore
Trypsin EDTA solution	Invitrogen, USA
Collagenase IV	GIBCO-Invitrogen, USA
2-Mercaptoethanol	Sigma, USA
Bovine serum albumin	ICN Biomedicals Inc, USA
Gelatin	Sigma, USA
Absolute alcohol	Hayman, England
Cyclosporin A	Novartis, Germany
Cesium chloride	Sigma, USA
4, 6-diamidino-2-phenylindole	Sigma, USA
Ethidium Bromide	BioRad, USA
Eosin Y	Sigma, USA
Ethanol	Sino Chemical. Singapore
Fluospheres yellow-green polystyrene Microspheres (505/515), 15μm	Molecular Probes, USA
Formalin (37%)	Sigma, USA

Paraformaldehyde	Sigma, USA
Tissue freezing medium	Leica, Germany
Gluteraldehyde (25%)	Sigma, USA
Hematoxylin	Sigma, USA
Heparin	Leo Pharma, Denmark
Histowax	Leica, Switzerland
Hydrogen Peroxide	Analar, UK
Isopentane	Acros Organic, USA
Methanol	Fischer Scientific, UK
Ketamine/Xylazine	APEX Laboratories, Italy
Mounting medium	Shandon, USA
Paraffin wax	Leica, Switzerland
Polyoxyethylenesorbitan mono oleate (Tween 80)	Sigma, USA
Potassium hydroxide	Merck, Germany
RNAlater RNA stabilizing reagent	Qiagen, Germany
Sodium chloride (0.9%)	NUMI, Singapore
Xylene	Merck, Germany
Trypan blue	Sigma, USA
Triton-X 100	BioRad, USA
2,3,5-Triphenyltetrazolium chloride	Sigma, USA
Permount/Poly-mount xylene	Polysciences Inc, PA, USA
Propidium Iodide	Sigma, USA
Hank's Balanced Solution	Sigma, USA

6.1.4 Proteins, antibodies and kits

Recombinant alpha fibroblast growth factor (αFGF)	Invitrogen, USA
Recombinant basic fibroblast growth factor (bFGF)	Invitrogen, USA
Recombinant human $VEGF_{165}$	Chemicon, USA

Primary antibodies

Mouse anti human VEGF	RnD systems, USA
Mouse anti human CD31	RnD systems, USA
Rabbit anti ve-cadherin	Sigma, USA
Mouse anti α-smooth muscle actin	Sigma, USA
Mouse anti human CD133-PE	Militenyl Biotech, USA
Rabbit anti vWF-VIII	Dako, Germany
Mouse anti human Tra-1-60	Chemicon, USA
Mouse anti human Tra-1-81	Chemicon, USA
Goat anti-Nanog	RnD systems, USA
Goat anti-Oct4	RnD systems, USA
Mouse anti-SSEA-4	RnD systems, USA
Mouse anti-alkaline phosphatase	RnD systems, USA

Secondary antibodies

Goat anti mouse IgG-FITC	Sigma, USA
Goat anti rabbit IgG-TRITC	Sigma, USA
Mouse anti rabbit IgG-FITC	Sigma, USA
Rabbit anti goat IgG-FITC	US Biological, USA
Rabbit anti mouse IgG-TRITC	Chemicon, USA
Anti mouse IgG-HRP	Lab Vision, USA
Donkey anti goat IgG-FITC	Chemicon, USA
Donkey anti mouse IgG-TRITC	Chemicon, USA

Kits

Human VEGF ELISA kit	RnD systems, USA
Human Ang-1 ELISA kit	RnD systems, USA
Qiagen Hot Start PCR kit	Qiagen, Germany
Qiagen RNeasy Midi kit	Qiagen, Germany
Ultravision Detection system	Lab Vision, USA
Taqman PCR Universal Master Mix	Applied Biosystems, USA
Human embryonic stem cell marker antibody panel	RnD systems, USA
Taqman Reverse Transcription Reagentst	Applied Biosystems, USA
TaqMan Gene Expression Assays- CD133 and Flk-1	Applied Biosystems, USA
CD133 Cell isolation kit	Militenyl Biotech, USA
In situ cell death detection kit, Fluorescein	Roche Applied Science, USA
DNeasy isolation kit	Qiagen, Germany
Accustain Trichrome Stain kit	Sigma, USA

6.1.5 Apparatus

Normal culture flasks (25 and 75cm^2)	NUNC, Denmark
Microfilter (0.22μm)	Millex, USA
Chamber slides	BD Pharmingen, USA
Sterile pipette	Costar, USA
Power supply (200V, 500mA)	Bio-Rad, USA
Polylysine coated glass slides	Esco, USA
Tissue culture plates (6-, 12- and 24- well plates)	NUNC, Denmark
Pipettor	Finnpipette, USA

6.1.6 Surgical Instruments

Prolene Suture	Johnson & Johnson, Belgium
Scissors	Aesclulap, USA
Scalpel blade	Aesclulap, USA
Forceps	Aesclulap, USA
Retractor	Aesclulap, USA
Rodent ventilator	Harvard Apparatus, USA

Gauze	Lozon (S) Pte Ltd, Singapore
Catheter	Terumo Corporation, USA

6.1.7 Equipments

12mHZ echocardiographic probe	Agilent Technologies, USA
Aquasonic 100 Ultrasound transmission gel	Agilent Technologies, USA
Regulatable CO_2 cell culture incubator	Heraeus Hera Cell, Germany
Gel electrophoresis system	Bio-Rad, USA
Electronic pipettor	Drummond, USA
ELISA plate reader	Bio-Tek Instruments, USA
Fluorescent microscope	Olympus, Japan
Inverted phase contrast microscope	Olympus, Japan
Flow Cytometry	Beckman Coulter Epics Altra, USA
-20°C freezer	Sanyo, Japan
-80°C freezer	Forma Scientific Inc, USA
Hematocytometer	Sigma, USA
Tissue homogenizer	Polytron, USA
Cell culture work station (BS II)	Nuaire, USA
Cryostat	Leica, Switzerland
Microtome	Leica, Switzerland
Liquid nitrogen facility	CBS, France
Spectrophotometer	Beckman, USA
Microcentrifuge	Hettich, UK
Centrifuge	Sorvall, Germany
Microwave Oven	Sanyo, Japan
Minigel apparatus	BioRad, USA
Paraffin Tissue Processor	Leica, Switzerland
Peltier Thermal Cycler	MJ Research, USA
pH meter	IQ Scientific Instruments, USA
Vingmed Vivid 5 ultrasound machine	General Electric, USA
Vacuum Pump	Goldbell, China/Japan
Waterbath	Memmert, Germany
Weighing balance	Goldbell, China/ Japan

6.1.8 Computer software

Microsoft Office 2000	Microsoft, USA
Olympic Micro Image	Olympus, Germany
Quantity One (version 4.2.1)	BioRad, USA
SPSS statistics software (version 11)	SPSS, USA
WinMDI (version 2.8)	Scripps Res Institute, USA

6.2 General Protocols

6.2.1 RNA extraction

Total RNA from cell samples were extracted using Qiagen RNeasy mini column kit (Qiagen, California, USA). The extraction was performed according to the supplier's instructions. The RNA was finally eluted in in diethylpyrocarbonate-treated distilled water (ddH_2O). RNA quality and quantity is assessed by relative absorbance at 260nm versus 280nm.

Total RNA from heart tissue samples were also extracted using Qiagen RNeasy mini column kit (Qiagen, California, USA) according to the supplier's instructions. However the tissue samples were subjected to proteinase K (20mg/ml) digest treatment for 10 minutes at 55°C before RNA extraction. This was to remove the highly abundant contractile proteins, connective tissue and collagen in the heart tissues that makes RNA isolation difficult.

6.2.2 Complementary DNA (cDNA) synthesis

Total RNA was reverse transcribed into cDNA using oligo$(dT)_{20}$ and resuspended in ddH_2O. Briefly 10ug of RNA was added to a mixture containing 1μg of oligo$(dT)_{20}$ and incubated for 5 minutes at 70°C. The RNA and oligo$(dT)_{20}$ mixture was mixed with 1× RT buffer-reaction buffer, 1mM of dNTPs, 65U of RNase inhibitor, 250U of Moloney murine leukemia virus reverse transcriptase (MMLVRT). Distilled water was added to a final volume 50μl. The sample mixture was incubated at 37°C for 1 hour and then at 95°C for 10 minutes before quickly chilling it on ice.

6.2.3 Preparation of frozen tissues for cryosectioning procedure

Fresh left ventricle samples from the heart tissues were first rinsed in 1× PBS and then dried before being carefully placed in a self-made embedding mold made of aluminum foil containing a small amount of the tissue freezing medium. The mold was then filled with tissue freezing medium until the whole tissue samples were fully immersed in the matrix. The mold was then rapidly submerged into isopentane which was earlier been cooled with liquid nitrogen. Once the tissue samples had frozen up, they were wrapped with aluminum foil and store in -20°C freezer. Tissue sections of 4 to 7μm were cut using a cryostat. The sections were mounted on poly-L-lysine coated slides and stored in -20°C. Immediately prior to processing for immunohistochemistry, the slides were removed from the freezer and allowed to warm to room temperature and air-dried. They were then rinsed in 1× PBS twice for 5 minutes each and fixed in 100% cold methanol in -20°C for 10 minutes.

6.2.4 Fixation and processing of tissue for paraffin sections

Fresh left ventricle samples from heart tissues were cut into small pieces of about 3 to 5 mm in thickness and placed into 10% neutral buffered formalin for 24 hours at room temperature. The tissues were then subjected to a 9-hour processing schedule outlined below:

Station Number	Time taken	Tissue treatment
1	45 min	50% alcohol
2	45 min	70% alcohol
3	45 min	95% alcohol
4	45 min	100% alcohol
5	45 min	100% alcohol
6	45 min	100% alcohol
7	45 min	Clearing reagent
8	45 min	Clearing reagent
9	45 min	Clearing reagent
10	1 hour	Paraffin
11	1 hour	Paraffin

Following infiltration of the tissue samples with paraffin, the heart tissue samples were then embedded into paraffin blocks for storage until microtome sectioning. The whole procedure was performed using specialized automated tissue processing system. 5 to 8μm thick paraffin-embedded sections were cut using a rotary microtome. The sections were floated in a 56°C water bath until they were straightened out. They were then

mounted onto histological poly-L-lysine coated slides. The slides were dried overnight at room temperature.

To prepare the sections for immunohistochemistry, they had to be deparaffinized and rehydrated using the following standard procedure outlined below:

Xylene	3 changes, 5 minutes each
100% alcohol	2 changes, 3 minutes each
95% alcohol	2 changes, 3 minutes each
70% alcohol	2 change, 3 minutes each
1× PBS	2 changes, 3 minutes each

6.2.5 Hematoxylin and eosin staining

The tissue sections were stained with hematoxyin solution for 5 minutes followed by rinsing under running tap water. The sections were then stained with Eosin Y for 1 minute and rinsed under running water.

6.2.6 Masson Trichrome staining

The tissue sections were rinsed with water and mordant in Bouin's solution for 15 minutes. The sections were then washed in running tap water to remove the picric acid or until the yellow colour disappear. The sections were next stained with Weigert's Iron Hematoxylin Solution for 5 minutes, washed under running tap water and rinsed with distilled water. The sections were then stained with Biebrich Scarlet-Acid Fuchsin for 5 minutes and rinsed with distilled water. This was followed by staining with Phosphomolybdic/Phosphotungstic Acid Solution for 5-10 minutes and rinsing in 2% acetic acid for 10 dips and distilled water. The sections were transferred into 2% light green for 10 dips and rinsed in 2% acetic acid for 10 dips followed by distilled water.